Spring 2000

Rational design and syntheses of 4-phosphino-catechol hybrid ligands for mixed -metal clusters

Xiankai Sun
University of New Hampshire, Durham

INFORMATION TO USERS

This manuscript has been reproduced from the microfilm master. UMI films the text directly from the original or copy submitted. Thus, some thesis and dissertation copies are in typewriter face, while others may be from any type of computer printer.

The quality of this reproduction is dependent upon the quality of the copy submitted. Broken or indistinct print, colored or poor quality illustrations and photographs, print bleedthrough, substandard margins, and improper alignment can adversely affect reproduction.

In the unlikely event that the author did not send UMI a complete manuscript and there are missing pages, these will be noted. Also, if unauthorized copyright material had to be removed, a note will indicate the deletion.

Oversize materials (e.g., maps, drawings, charts) are reproduced by sectioning the original, beginning at the upper left-hand corner and continuing from left to right in equal sections with small overlaps.

Photographs included in the original manuscript have been reproduced xerographically in this copy. Higher quality 6" x 9" black and white photographic prints are available for any photographs or illustrations appearing in this copy for an additional charge. Contact UMI directly to order.

RATIONAL DESIGN AND SYNTHESES OF
4-PHOSPHINO-CATECHOL HYBRID LIGANDS
FOR MIXED-METAL CLUSTERS

BY

XIANKAI SUN

B. S., WUHAN UNIVERSITY, 1986
M. S., CHINESE ACADEMY OF SCIENCES, 1989

DISSERTATION

Submitted to the University of New Hampshire
In Partial Fulfillment of
the Requirements for the Degree of

Doctor of Philosophy

in

Chemistry

MAY 2000

UMI®
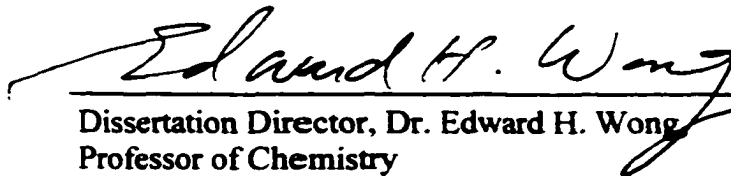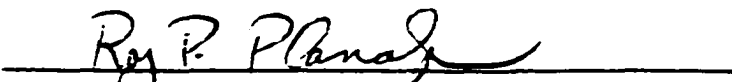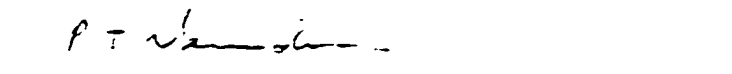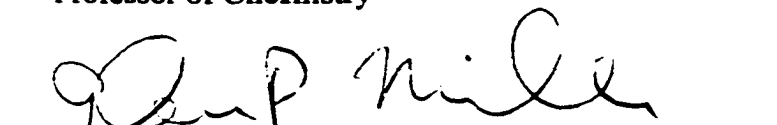
This dissertation has been examined and approved.
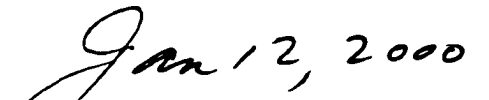
Dissertation Director, Dr. Edward H. Wong
Professor of Chemistry

Dr. Roy P. Planalp,
Associate Professor of Chemistry

Dr. Palligarnai T. Vasudevan
Associate Professor of Chemical Engineering

Dr. Richard P. Johnson,
Professor of Chemistry

Dr. Glen P. Miller
Assistant Professor of Chemistry

Date: January 12, 2000

DEDICATION

To the memory of my grandparents

Zengqi Sun and *Qingzhen Zhang*

for their love

To my parents Xianji Sun and Jiaxiu Pi,

my parents-in-law Gengsheng Pan and Youyun Xiao,

my wife Fang Pan, and my son Eric Xiangwei Sun

for their love and support

iii

ACKNOWLEDGEMENTS

I would like to give my heartfelt thanks and deepest appreciation to my academic advisor, Dr. Edward H. Wong, for his professional guidance, innovative ideas, encouragement, patience and support, as well as for his invaluable help in the preparation of this dissertation. I am grateful to Kathleen S. Gallagher for her professional instruction in the use of NMR instruments and friendship. Thanks to John Wilderman, Bill Dotchin, and Nancy Cherim at the UNH Instrumentation Center for their constant technical assistance and analyzing samples for elemental analysis. I would also like to thank our collaborators in Dr. Kenneth Raymond's group at the University of California at Berkeley, Dana Caulder and Daren Johnson, for their excellent work in solving the X-ray structures of our mixed-metal clusters; I also benefited a lot from many helpful discussions with them. My gratitude goes to Dr. Roy Planalp, Dr. Gary Weisman and Dr. Glenn Miller for their professional teaching and patient instruction during my course studies. The encouragement and understanding of Neng Ye, Megan Tran and Gyungse Park during some difficult times are very much appreciated. Also, thanks to Cindi Rohwer, Peg Torch, Sabrina Kirwan and Bob Constantine for their enthusiastic help. My special thanks go to my wife for her love, understanding, patience and support throughout these years.

iv

TABLE OF CONTENTS

.

.

LIST OF TABLES

LIST OF SCHEMES

LIST OF FIGURES

xviii

ABSTRACT

RATIONAL DESIGN AND SYNTHESES OF 4-PHOSPHINO-CATECHOL HYBRID LIGANDS FOR MIXED-METAL CLUSTERS

BY

XIANKAI SUN

University of New Hampshire, MAY, 2000

Based on the concepts of *Incommensurate Symmetry-Driven Cluster Formation*, an approach to mixed-metal cluster formation has been proposed and realized by using the *incommensurate symmetry* requirements at two different metal centers bridged by a hybrid ligand. Critical to this strategy is the proper design and synthesis of hybrid ligands with coordination sites selective towards each metal. 4-Phosphino-Catechol hybrid ligands with both hard catecholate and soft phosphine donor sites have been shown to serve such a role. Three new ligands; 4-PPh$_2$-Catechol (H$_2$L), 4-PH$_2$-Catechol (H$_2$2) and 4-P(CH$_2$OH)$_2$-Catechol (H$_3$3) as well as their precursors 4-PPh$_2$-Veratrole and 4-PH$_2$-Veratrole have been synthesized and characterized. Several phosphine-coordinated soft-metal [Pd(II), Pt(II), Ru(II), Cr(0)] complexes of 4-PPh$_2$-Veratrole and 4-PH$_2$-Veratrole have been synthesized and spectrally characterized to have 2-fold, 3-fold or 4-fold symmetry. The 3:1 catecholate complexes of H$_2$L, H$_2$2 and H$_3$3 with several trivalent and tetravalent metal cations [M(III) = Fe, Ga; M(IV) = Ti, Sn] have also been prepared and characterized as potential precursors with C_3 symmetry for the stepwise *aufbau* of

heterometallic clusters. While the X-ray structure of the Cs_2TiL_3 salt revealed a C_1-*mer*-configuration in the solid-state, room temperature and variable-temperature solution NMR studies of this and other complexes are consistent with either exclusive formation of the C_3-*fac*-isomer with all phosphine donor sites *syn* to each other, or facile *fac/mer* isomerization. While attempts to synthesize mixed-metal clusters from ligand 4-PH$_2$-Catechol (H$_2$2) and 4-P(CH$_2$OH)$_2$-Catechol (H$_2$3) via either *aufbau* or self-assembly processes failed because of side reactions and/or the poor solubility of intermediates (or products), *aufbau* of pentametallic $[M_2L_6Pd_3Br_6]^{4-}$ (M = Ti, Sn) clusters have been successful through coordination of the $[M^{IV}L_3]^{2-}$ (M = Ti, Sn) metalla-ligands via their soft P donor sites to C_2-symmetric PdBr$_2$ units. These clusters have been fully characterized by spectral and X-ray structural data to be C_{3h} mesocates with Cs$^+$ or protonated 1,4-diazabicyclo[2.2.2]octane (DABCO-H$^+$) cations incorporated into deep molecular clefts. In addition to this *aufbau* approach, self-assembly of several of these $[M_2L_6Pd_3Br_6]^{4-}$ (M = Ti, Sn) clusters from their eleven components (two M(IV), three PdBr$_2$, six L) can also be accomplished under appropriate reaction conditions. Exclusive formation of this type of supramolecular species is sensitive to the nature of counterions. Alkali cations like Li$^+$, K$^+$, Rb$^+$, and Cs$^+$ led to high-yield formation of the respective clusters while other countercations such as tetramethylammonium (TMA$^+$), tetraphenylphosphonium (Ph$_4$P$^+$), and *bis*(triphenylphosphoranylidene)ammonium (PPN$^+$) gave either a mixture of products or insoluble precipitates. Extension of the *aufbau* assembly to produce related $[M_2L_6Pd_3Cl_6]^{4-}$, $[M_2L_6Pd_3I_6]^{4-}$, $CsSn_2L_6Ag_3$ and $[M_2L_6Cr_3(CO)_{12}]^{4-}$ clusters has also been realized.

Chapter I

Introduction

In the recent decade, modern supramolecular chemistry has been dominated by studies of non-covalent assemblies, although it emerged from studies of certain covalent systems, such as cyclophanes, crown ethers, calixarenes and cryptands.[1] Non-covalent interactions have been regarded as major bonding forces that operate within the entire man-made or biological supramolecules. In biological systems, non-covalent interactions include electrostatic interactions, hydrogen bonding, van der Waals forces, hydrophobic interactions, etc., while they can also refer to metal-ligand interactions in the "unnatural" assemblies. To form a supramolecular cluster instead of an oligomer or polymer, the interactions between each individual subunit must be thermodynamically stable, yet kinetically labile to allow the self-rearrangement of the subunits within the entire structure, thereby enabling the self-correction of initial kinetic defects. Thus, non-covalent interactions which are both thermodynamically stable and kinetically labile are exploited by nature to form numerous biological clusters, like apoferritin,[2] human rhinovirus,[3, 4] ribosomes, mitochondria, chromosomes[5-7] and others.[8, 9] To achieve the synthesis of highly-ordered assemblages, transition metal-ligand interactions have been used by supramolecular chemists. It is well-known that the transition metal-ligand interactions are strong and directional, and they are also non-covalent. Being strong, fewer metal-ligand interactions may be used in place of many weak interactions between the subunits in biological systems to simplify the formation of "artificial" supramolecular

1

clusters. Being directional, metal-ligand interactions may also facilitate the building of supramolecular clusters with extensive and well-defined variations in their shapes and sizes. [10, 11]

Even though supramolecular coordination chemistry is still at a relatively early age, [1, 10, 12] there are now numerous examples of supramolecular assemblies based on metal-ligand interactions. Among these, triple bimetallic helical and tetrahedral four-metal clusters have been extensively studied, partly because they are among the simplest supramolecular coordination clusters. Many such assemblies have been synthesized serendipitously, while others have been the result of systematic variations of metal and ligand components. Until recently, a rational methodology for the synthesis of metal-ligand coordination clusters is rare. In 1996, Raymond and coworkers proposed an approach they named *Incommensurate Symmetry-Driven Cluster Formation*. [13] Through its successful development in recent years, it has become a powerful methodology in the field of supramolecular coordination chemistry. [12, 13, 14]

1. Concepts of the *Incommensurate Symmetry-Driven Cluster Formation*

The basic idea for Raymond's methodology is: the *Incommensurate Symmetry* involved in the interactions of subunits is the driving force for cluster formation. [13] This idea was generated from the symmetrical molecular clusters in nature. As is well-known, there are many non-covalently linked supramolecular clusters in nature of stunning symmetry and beauty. Apoferritin 24-mer and human rhinovirus 60-mer are just two examples of such clusters (Figure 1.1).

2
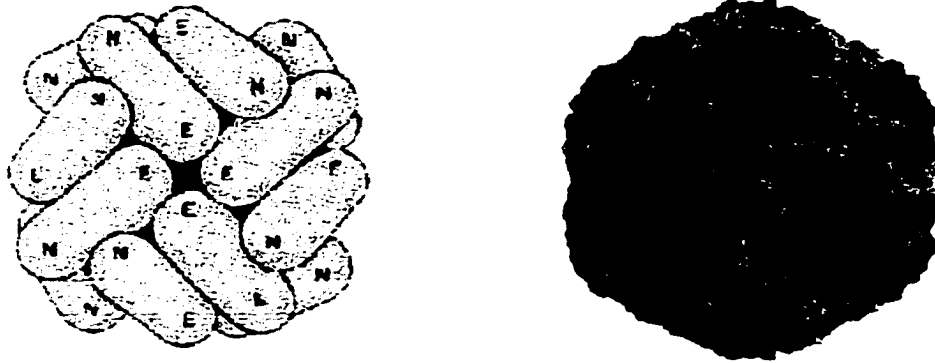
Figure 1.1 Models of the apoferritin 24-mer (left) and human rhinovirus 60-mer (right). The view of ferritin is down one of the C_4 axes, the other two C_4 axes of the octahedral cluster are horizontal and vertical, respectively. Along the body diagonal (between three of ellipsoid ends marked N) lies the C_3 axes of the octahedral cluster. The view of the virus is down the C_3 axis, and the regions related by symmetry through the C_2 axis and the C_5 axis are shown in green and blue, respectively.
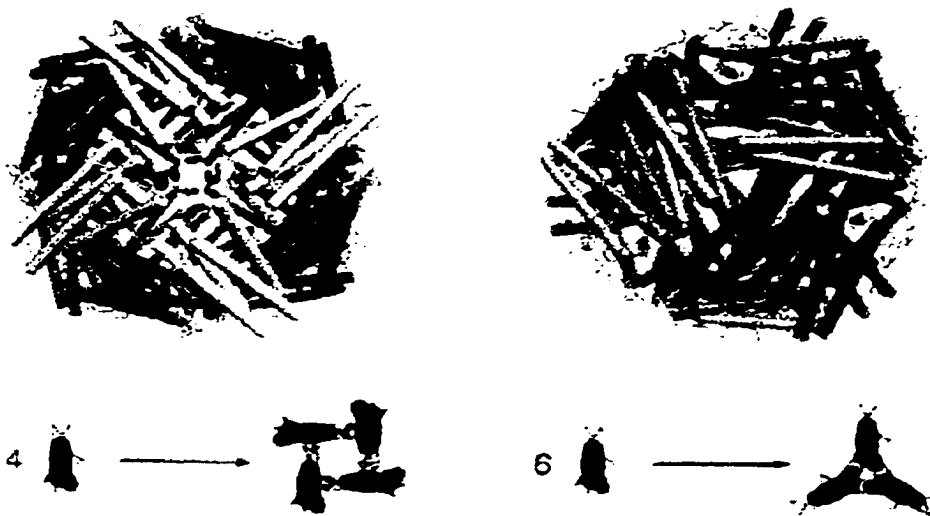
Figure 1.2 Based on the crystal structure of human H chain ferritin,[1] the octahedral 24-subunit iron storage protein as viewed down the four-fold (left) and three-fold (right) axes. The four helix bundle protein subunits that directly interact at these symmetry axes are highlighted in yellow and blue, respectively. The interaction at the four-fold axis, in which the lock and key are 90° apart, requires the formation of tetramers. Similarly, the interaction at the three-fold axis, in which the lock and key are 60° apart, requires the formation of trimers.

3

The iron storage protein apoferritin [15, 16] is composed of 24 non-covalently linked protein subunits which assemble to form a hollow protein shell of octahedral symmetry. The shell is capable of encapsulating up to 4,500 iron atoms in the form of a hydrous ferric oxide mineral core. In effect, ferritin operates to keep iron in solution as a small particle of rust by stopping the growth of the iron oxide particle before it reaches a size that would result in precipitation. When the apoprotein is dissociated into the individual subunits and then allowed to reassemble, only this highly symmetrical 24-mer of apoferritin forms. [17] Intermediate assemblies of less than the full 24 complement are only transiently stable. Something similar happens with many viruses in which non-covalently linked assemblies of protein subunits are used to protect the viral nucleic acid. The protein cluster coat of the human rhinovirus contains 60 protein subunits, which simultaneously assemble to give an icosahedral capsid (symmetry group I). It is generally true that dissociation and reassembly of the protein coat does not give a random polymeric assembly, instead only this highly symmetrical 60-mer forms.[3, 4] Viral coats of this stoichiometry and the ferritin cluster correspond to the pure rotation groups I and O with 60 and 24 symmetry elements, respectively. That is, each of the protein subunits constitutes an asymmetric unit of the respective rotation groups. [18]

Based on the analysis of *Incommensurate Symmetry* interactions involved in the formation of biological supramolecules, Raymond and coworkers proposed a model of the lock-key interactions to illustrate the assembly of apoferritin and viral protein coats in 1996.[13, 14]

The model they used to show the formation of the apoferritin and its octahedral symmetry is shown in Figure 1.2. The top left schematic structure is a view down a C_4

4

axis of the apoferritin where the interactions between the protein subunits can be considered as the so-called lock-and-key interactions. The lock and key (yellow) of an individual protein subunit are 90° apart as seen in Figure 1.2 (bottom left). The right angle of the lock-and-key interaction requires four protein subunits to form a tetramer.

So, the interaction around the four-fold axis is both a symmetry and stoichiometry requirement. The top right schematic structure is a view down a C_3 axis of the apoferritin where the interactions between the protein subunits can be also regarded as lock-and-key interactions. The lock and key (blue) of an individual protein subunit here are 60° apart as seen in the Figure 1.2 (bottom right). This angle of the lock-and-key interaction requires three protein subunits to form a trimer. Therefore, the interaction around the three-fold axis is also both a symmetry and stoichiometry requirement. *Simultaneous satisfaction of these two incommensurate four-fold and three-fold symmetry axes can only be satisfied by formation of a cluster with an octahedral symmetry.* The formation of the human rhinovirus 60-mer (an icosahedral cluster) can be rationalized in a similar way through the combination of incommensurate lock-and-key interactions with five-fold, three-fold, and two-fold symmetries.

The term "incommensurate" is used in the same sense as applied to incommensurate lattices. As occurs with some natural silicates, the superposition of one layer upon another which has a slightly different lattice spacing results in a mismatch of the unit cells due to the incommensurate lattice spacing.[19] The two spacings can be only kept in register by curling them (Figure 1.3). Similarly, two incommensurate coordination numbers can coexist only by a curvature of the surface lattice of the molecular array.

5
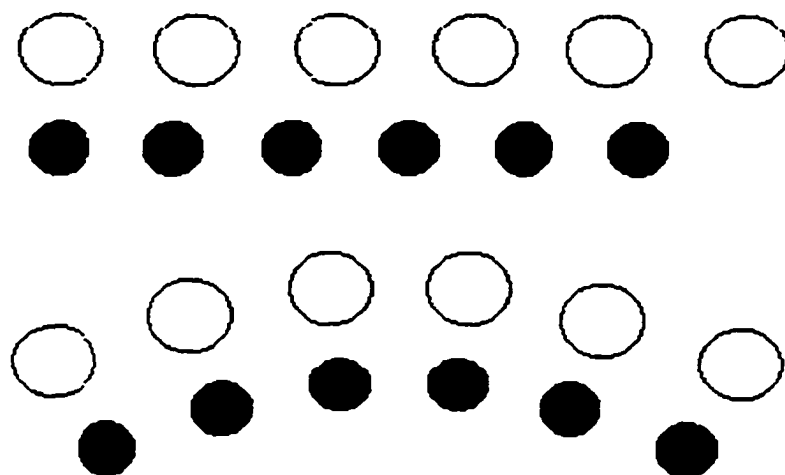
Figure 1.3 Lattice 1 (yellow) and 2 (blue) shown schematically have incommensurate repeat distances (top). If stacked together the lattices must curl in order to remain in register (bottom)

The "lock-and-key" concept of steric fit was first used in 1894 by Emil Fisher to enunciate the notion of selective binding, which implied geometrical complementarity. [20] The idea of coordination introduced by Alfred Werner in 1893 can be also applied to the selective binding and affinity between the subunits.[21] By using these traditional terms and concepts creatively, Raymond and coworkers have developed a totally new methodology for supramolecular chemistry which can be regarded as a generalization of coordination chemistry. Now supramolecular chemistry has extended into organic chemistry and the synthetic procedures for molecular construction, into coordination chemistry and metal ion-ligand complexes.

In accord with the concepts of *Incommensurate Symmetry-Driven Cluster Formation*, the formation of clusters of any symmetry should be possible.[12] Illustrated here are two examples of simplest clusters: a tetrahedron and a triple helicate. As we

6

know, a tetrahedron has all the symmetry elements of the T point groups, while a triple helicate has all the symmetry elements of a D_3 point group.

As shown in Figure 1.4, a triple helicate has two types of symmetry axes, C_2 and C_3, whose positions are perpendicular to one another. In order to design a triple helicate with D_3 symmetry, both the symmetry axes of the point group D_3 and their orientations
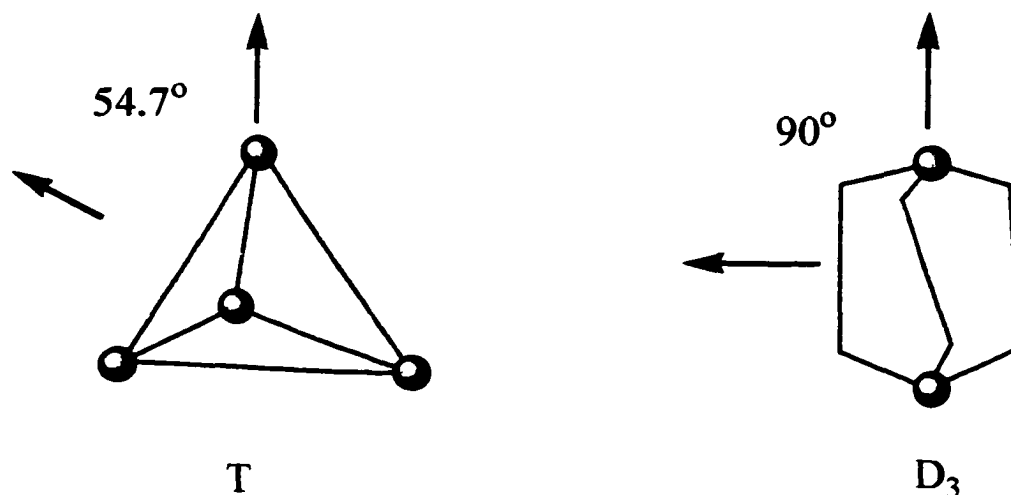
Figure 1.4 The symmetry elements of a tetrahedron (T) and a triple helicate (D_3) and their positions (gray spheres represent metal atoms, while red curves between metal atoms represent ligands).

must be taken into consideration; a C_2-symmetric bis(bidentate) ligand can provide the 2-fold axis, while a metal ion with pseudo-octahedral coordination by three bidentate chelators can provide the 3-fold axis. If these symmetry axes are oriented 90° to one another, they lead to the formation of a triple helicate M_2L_3 (Figure 1.4). As for the design of a cluster with T symmetry, the same combination of symmetry elements can be used, but the C_2 and C_3 axes must now be oriented 54.7° from one another to drive the formation of a tetrahedral M_4L_6.

7

As discussed above, to design a supramolecular cluster with a particular symmetry is to design a ligand which may provide the desired metal coordination geometry (symmetry elements) and orientation of the interaction sites (specific angles between symmetry elements). In this sense, supramolecular chemistry can be called a molecular information science. [22, 23]

2. Design Strategies for Metal-ligand Coordination Supramolecular Clusters

The formation of a proposed cluster can be realized by a specifically-designed ligand by which the metal coordination geometry and the orientation of the interaction sites are determined. To ensure the successful assembly of desired supramolecular clusters based on metal-ligand interactions, three important factors must be taken into consideration: (1) as a result of the chelate effect, multi-branched chelating ligands should be preferably chosen, because of their increased preorganization and stronger binding. [24] (2) the backbone of the designed ligand must be rigid to maintain the right stoichiometries and correct geometries. (3) the metal-ligand coordination bonds involved in the synthetic process of supramolecular clusters should be labile to enable a self-correction process which can convert intermediates or byproducts to the desired clusters, namely, the whole formation process of a supramolecular cluster should be under thermodynamical control.

8

Definitions Three terms have been defined by Raymond and coworkers in their methodology of *Incommensurate Symmetry-Driven Cluster Formation* to describe the relevant geometric relationships: *Coordination Vector*, *Chelate Plane* and *Approach Angle*.

The *Coordination Vector* represents the interaction direction between a ligand and metal (Figure 1.5). If the ligand is monodentate, the coordination vector is the vector from the coordinating atom of the ligand directed towards the metal center. In case of a bidentate ligand, the coordinate vector is the vector that bisects the chelating group and is directed towards the metal ion.

The *Chelate Plane* is the plane orthogonal to the major symmetry axis of a metal complex when using chelating ligands. All of the coordination vectors of the chelating ligands lie in the chelate plane (Figure 1.6).
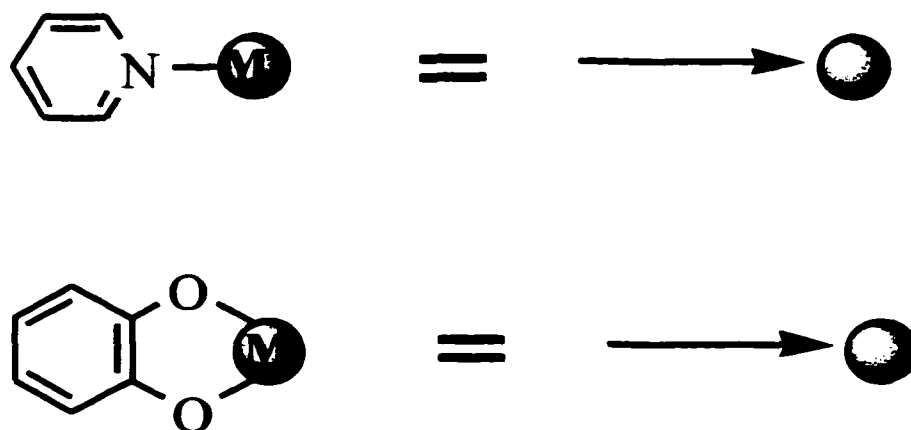
Figure 1.5 The definition of *Coordinate Vector*
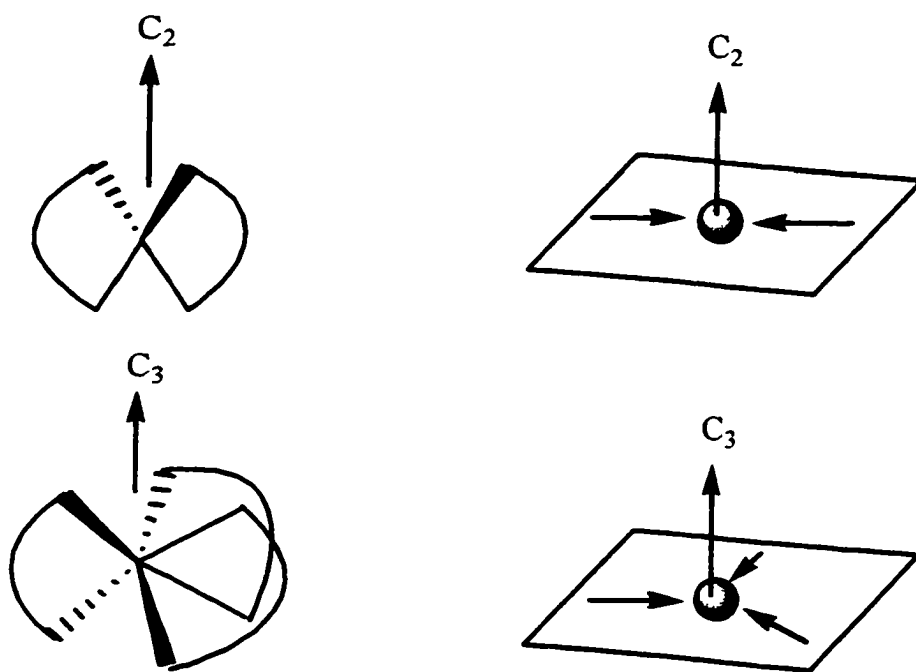
Figure 1.6 The definition of *Coordinate Plane*
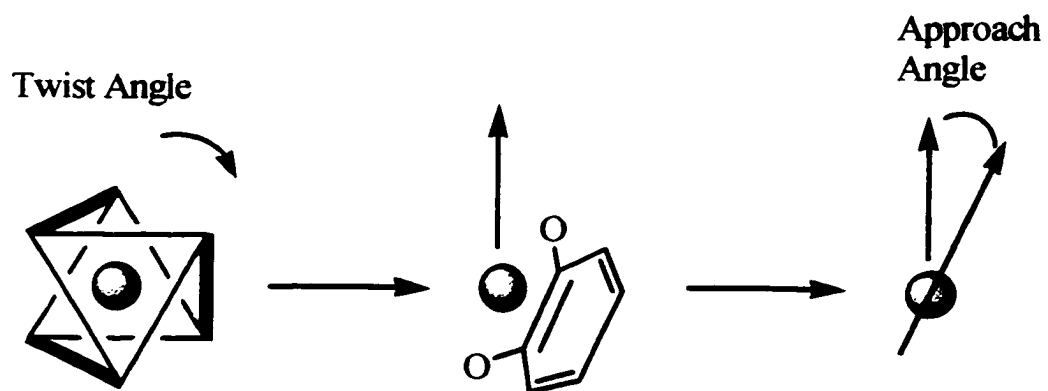
Figure 1.7 Definition of *Approach Angle*(highlighted black lines represent chelators)

10

As is well-known, *Twist Angle* is widely-used in describing the geometry of tris(bidentate) metal complexes. While a perfect octahedron has a twist angle of 60°, the twist angle for a trigonal prism is 0°. An alternative, the *Approach Angle* is the angle between the vector connecting the two coordinating atoms of a bidentate ligands projected down the (pseudo) 2-fold axis of the chelate group and the major symmetry axis of the metal center (Figure 1.7). A twist angle of 60° corresponds to an approach angle of 35.3°, while a twist angle of 0° corresponds to an approach angle of 0°. This angle has an advantage in providing a measure with respect to a cluster's angles.

(a) Design of Triple Helicate/Mesocate: There are two types of bimetallic triple-stranded coordination: Triple helicate and mesocate. Two metal ions being linked by three identical C_2-symmetry ligand strands, have either D_3 or C_{3h} symmetry. If both

Triple Helicate (D_3)   Triple Mesocate (C_{3h})
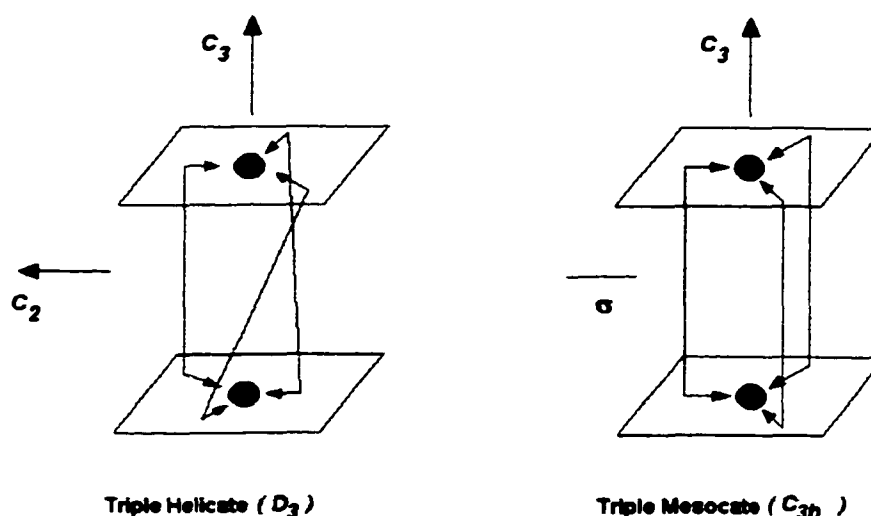
Figure 1.8 The orientations of coordinate vectors and planes in the triple helicate of D_3 symmetry and mesocate of C_{3h} symmetry.

11

metal ions have the same chirality, such a cluster is called a triple helicate (chiral, $\Delta\Delta$, or $\Lambda\Lambda$, that is D_3 symmetry), otherwise it is called a triple mesocate (achiral, $\Delta\Lambda$, that is C_{3h} symmetry). In a triple helicate, the C_3 axis is the main symmetry axis of the complex, to which the three C_2 axes are perpendicular. In a triple mesocate, there is also a mirror plane which bisects the M_2L_3 cluster, making the two metal complex halves enantiomeric (Figure 1.8).

To design a ligand which can form a triple helicate and/or mesocate, the following factors should be taken into consideration: (a) the ligand must be *bis*(bidentate), and has C_2-symmetry; (b) the coordinate vectors of the ligand must be parallel to one another and point in the same direction; (c) the coordinating metal ion must be octahedral, providing C_3-symmetry, and kinetically labile; (d) the C_2-axis and C_3-axis must be perpendicular to one another to ensure the formation of a tripe helicate and/or mesocate; (e) the ligand must be rigid enough to prevent the binding sites at two ends from coordinating the same metal ion.

To date, there has been no reliable way to predict whether a helicate or mesocate will form from a specific designed ligand, although there are some empirical approaches.[25-30]

(b) **Design of Tetrahedral Coordination Clusters:** There are two types of tetrahedral coordination clusters: M_4L_6 and M_4L_4. The M_4L_6 tetrahedral cluster has the same stoichiometry as the M_2L_3 triple helical cluster. Within a M_4L_6 tetrahedral cluster, four metal ions constitute the vertices and six ligands act as the edges, while within a M_4L_4 tetrahedral cluster, four metal ions again constitute the vertices and four ligands

12

make up the faces. Depending on the chiralities at the metal centers, the resulting cluster can have either idealized C_3 ($\Delta\Lambda\Lambda\Lambda/\Lambda\Delta\Delta\Delta$) , S_4 ($\Delta\Delta\Lambda\Lambda$) or T ($\Lambda\Lambda\Lambda\Lambda/\Delta\Delta\Delta\Delta$) symmetry. To our knowledge, there has been no report yet of a tetrahedral coordination cluster with idealized C_3 ($\Delta\Lambda\Lambda\Lambda/\Lambda\Delta\Delta\Delta$) symmetry.

Design of a M_4L_6 tetrahedral cluster

We can design two different types of ligands with C_2-symmetry: (a) one with its C_2-axis lying in the same plane as the ligand itself (Figure 1.9); (b) or one with its C_2-axis perpendicular to the ligand plane (Figure 1.10).

To design the first type of ligand, let's first take a look at the coordinate vectors, planes which may be involved in the formation of an idealized tetrahedral cluster (Figure 1.9). In order that the designed ligand satisfy the requirements of forming a tetrahedral coordination cluster with an octahedral metal ion: (a) the ligand must be bis(bidentate), and have a C_2-axis; (b) the two coordinate vectors at its two binding ends must be oriented 70.6° from each other; (c) the ligand must be rigid enough to prevent the binding sites at its two ends from coordinating the same metal ion.

To design the second type of ligand, the factors to be taken into consideration are again the coordinate vectors, planes, and approach angle which may be involved in the formation of an idealized tetrahedral cluster (Figure 1.10).

This type of ligand must satisfy the following requirements: (a) the ligand must be bis(bidentate), and have a C_2-axis which is perpendicular to the ligand plane; (b) the two coordinate vectors at two binding ends must be parallel to one another, and point in

13
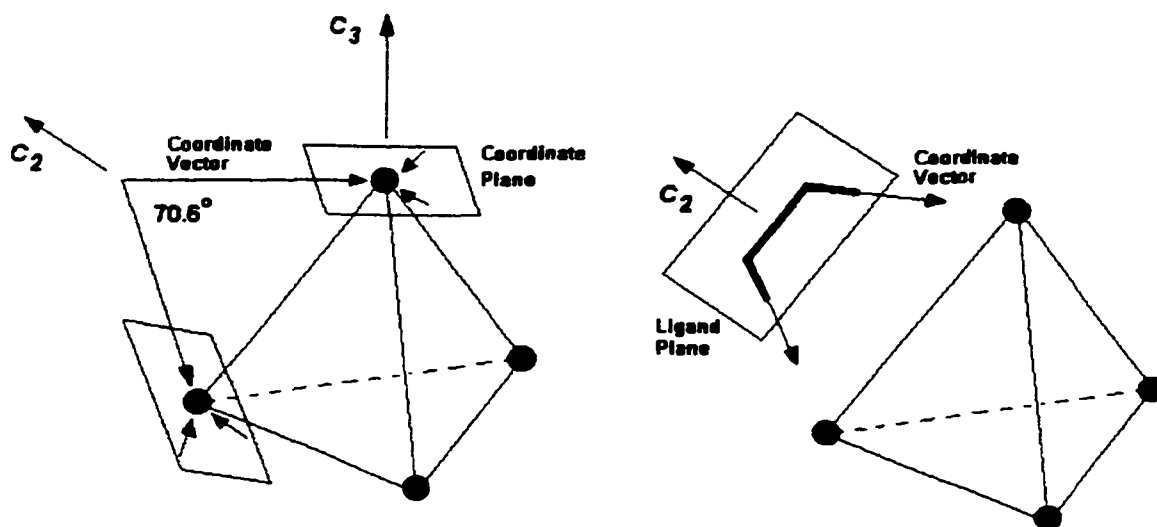
Figure 1.9 The *Coordinate Vectors* and *Planes* involved in the design of the first type of ligand (the C_3-axis lies in the same plane as the ligand itself). The highlighted black curve represents the ligand.
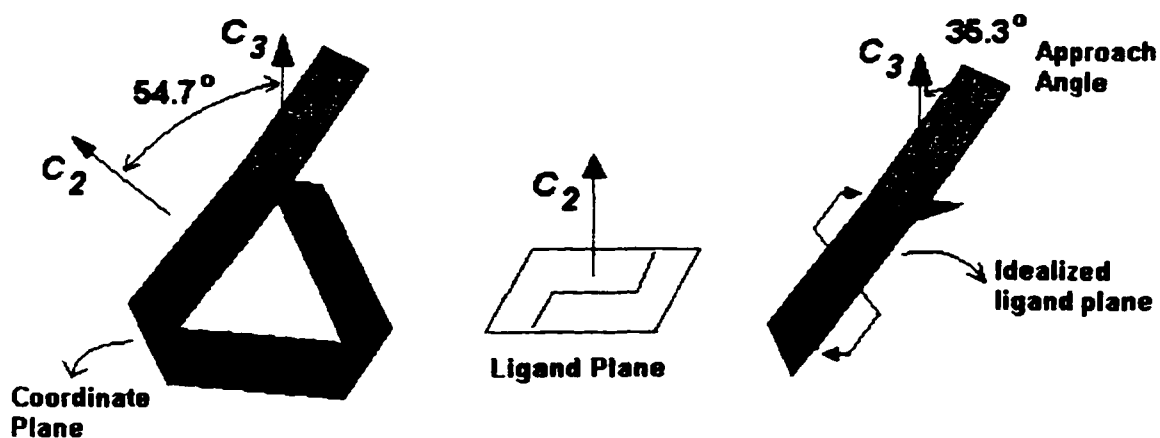
Figure 1.10. The Coordinate Vectors, Planes, and Approach angle involved in the design of the second type of ligand. The M_4L_6 cluster is drawn as a truncated tetrahedron, the C_3-axis of ligand is perpendicular to the ligand plane (blue part in the truncated tetrahedron). This design is ideally suitable for a metal center with an octahedral coordination (i. e. twist angle = 60°, approach angle = 35.3°).

14

opposite directions; (c) the ligand must be sufficiently rigid to ensure the direction of its C_2-axis and prevent the binding sites at its two ends from coordinating the same metal ion. In this type of tetrahedral clusters, the metal center should have an octahedral coordination because the ligand design makes the approach angle close to 35.3°, which corresponds to the twist angle of 60°.

Design of a M₄L₄ tetrahedral cluster

In a M₄L₄ tetrahedral cluster the metal ions occupy the four vertices and the ligands occupy each of the four faces of a tetrahedron. This implies that both the ligand and the metal ion must have 3-fold symmetry. The coordinate vectors, planes, and approach angle which may be involved in the formation of such an idealized tetrahedral
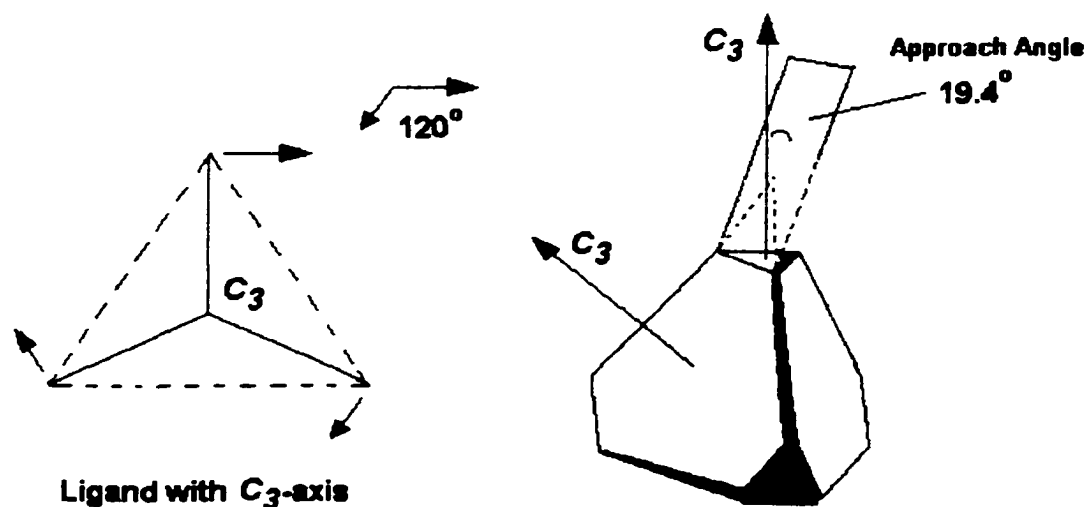
Figure 1.11 The coordinate vectors, planes, and approach angle involved in the ligand design. The M₄L₄ cluster is drawn as a truncated tetrahedron. The approach angle is 19.4°, which is close to the approach angle of 23° (corresponding twist angle: 40°) observed for *tris*(catecholate) metal complexes.

15

cluster are shown in Figure 1.11.

So the ligand must satisfy the following requirements to form a M_4L_4 tetrahedral coordination cluster with octahedral metal ions: (a) the ligand must be tris(bidentate), and have a C_3-axis which is perpendicular to the ligand plane; (b) the three-coordinate vectors at the three binding ends must be oriented 120° from one another; (c) the ligand must be sufficiently rigid to ensure the direction of its C_3-axis and prevent the binding sites at any two of its ends from coordinating the same metal ion.

In the similar way, a ligand can be designed for any cluster with higher symmetry. However, the problems involved in the actual synthetic process may impose many limitations on the cluster formation. For a cluster with any symmetry, thermodynamic factors must also be taken into consideration in the ligand design and synthetic processes. A small cluster is favored by entropy,[31] therefore, in order to favor a large cluster the geometry of the ligand must be correct and inflexible.[32] Solvent selection is also very critical for cluster formation. The physical properties of solvent, such as its polarity, cannot be neglected in any case because it may push or reverse a cluster formation. Usually, as the cluster gets larger, the solvent problem becomes more serious. Templating effect of cations or anions is a 'hot' topic in supramolecular chemistry.[33] Sometimes, choosing the right template can be the key to successful formation of a unique cluster.

3. Experimental Formation of Clusters with D_3 (or C_{3h}) symmetry, and T (or S_4) symmetry

The concepts of the *Incommensurate Symmetry-driven Cluster Formation* can be used not only as a synthetic methodology for new coordination clusters, it can also account for

16

the formation of clusters formed unintentionally, or by systematic variations of metal and ligand components. In order to understand the feasibility of the *Incommensurate Symmetry-driven Cluster Formation* in the field of supramolecular coordination chemistry, a review of the reported formation of coordination clusters with D_3 (or C_{3h}), and T (or S_4) symmetry is given prior to the systematic design of new coordination clusters in this introduction.

(a) Clusters with D_3 (or C_{3h}) Symmetry

The only known naturally-occurring triple helicate is the iron(III) complex of the dihydroxamate siderophore rhodotorulic acid, which is produced by the yeast *Rhodotorula mucilaginosa*.[34, 35] At neutral pH, Rhodotorulic acid enantioselectively forms a Δ, Δ- complex of Fe_2L_3 stoichiometry with idealized D_3 symmetry (Figure 1.12).
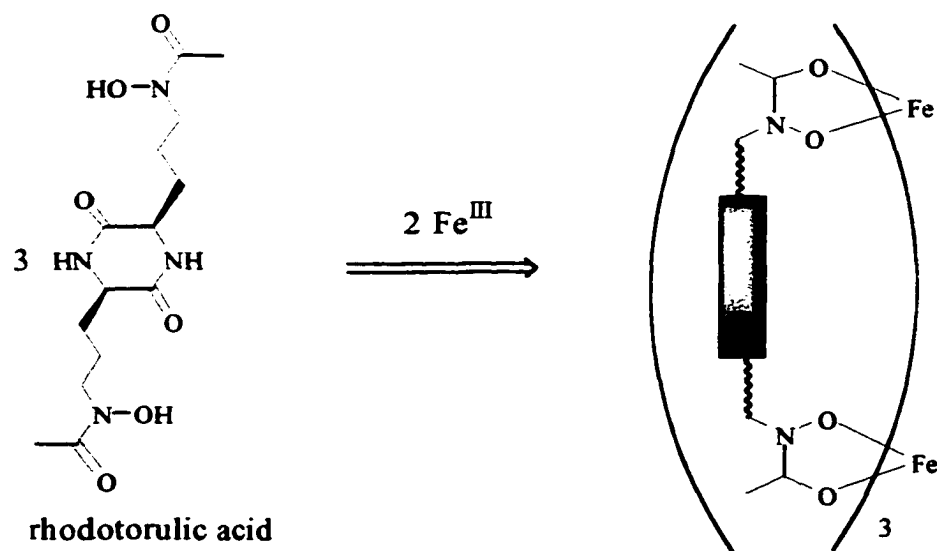
Figure 1.12 The only currently known naturally-occurring triple helicate: At neutral pH, dihydroxamate siderophore rhodotorulic acid forms an enantiomerically pure Δ,Δ-triple helicate with Fe(III).

bis(hydroxypyridinone) ligand
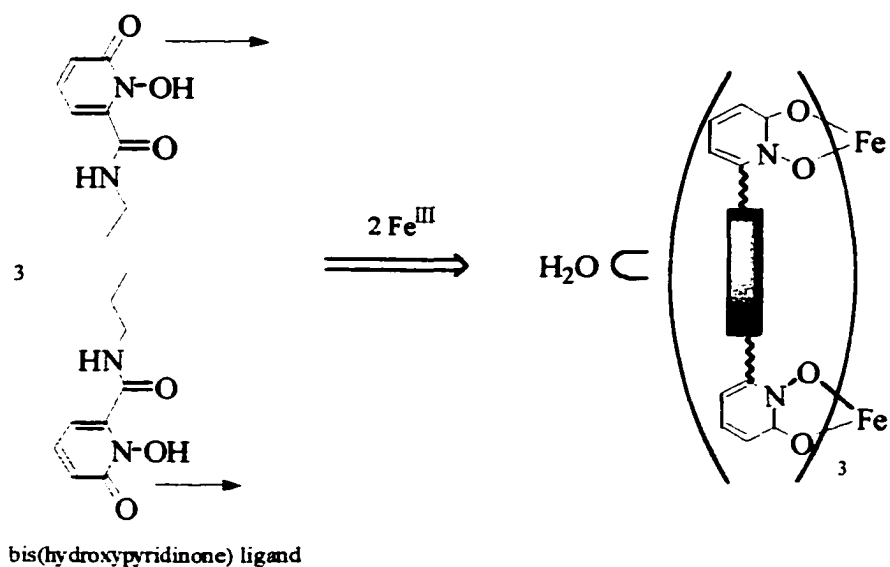
Figure 1.13 The *bis*(hydroxypyridinone) ligand was synthesized as a rhodotorulic acid analogue and forms a *rac*-($\Delta\Delta$, $\Lambda\Lambda$) mixture of triple helicates of Fe$_2$L$_3$ stoichiometry encapsulating a molecule of H$_2$O

(R$_1$ = H, CH$_3$;
R$_2$ = H, tC$_4$H$_9$; n = 1-6)

(R = H, nC$_4$H$_9$, nC$_{10}$H$_{21}$)
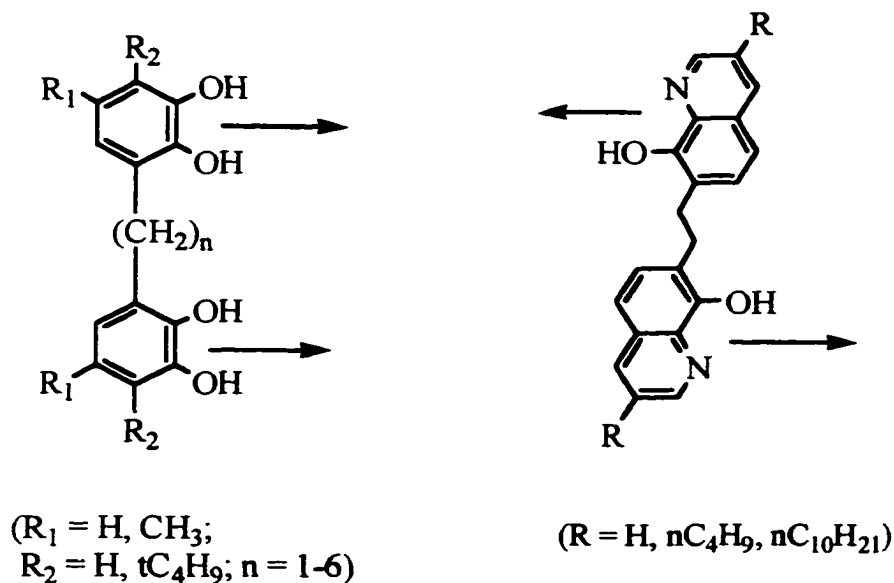
Figure 1.14 The general formula of *bis*(catecholate) ligands (left) and di(8-hydroxyquinoline) ligands (right) used by Albrecht and coworkers to form triple helicates with D_3 symmetry and triple mesocates with C_{3h} symmetry.

18

In 1985, Raymond and coworkers synthesized a hydroxypyridinone analogue of rhodotorulic acid and its Fe(III) complex. The cluster of Fe_2L_3 stoichiometry was structurally characterized, the X-ray analysis showed that a rac-$(\Delta\Delta,\Lambda\Lambda)$- mixture of triple helicates was formed, and each enantiomer encapsulates a molecule of water (Figure 1.13).[36] Both of the clusters of Fe_2L_3 stoichiometry have D_3 symmetry.

Albrecht and coworkers have done lot of work on their so-called anionic binuclear helicate- and "meso-helicate"-type coordination compounds. The ligands they used can be classified into two categories: alkyl-bridged biscatechol ligands and di(8-hydroxy-quinoline) ligands (Figure 1.14). By self-assembly processes, these ligands can form triple helicates (D_3 symmetry) and triple mesocates (C_{3h} symmetry) of M_2L_3 stoichiometry with octahedral metal ions, such as $Ti(IV)$[25, 26, 37-39] and $Ga(III)$[27], while they can also form tetrahedral clusters due to a rotation of the bridged ethylene group. [27] The researchers also demonstrated that the relative stereochemistry of the two metal complex units depends on the nature of the alkyl spacer [38]. Ligands with an even number of methylene units form chiral helicates ($\Delta\Delta/\Lambda\Lambda,D_3$ symmetry)[27, 28, 38]; ligands with an odd number apparently lead to the achiral mesocates ($\Delta\Lambda,C_{3h}$ symmetry).[29, 37, 40] Interestingly, their most recent results [39] showed a remarkable self-recognition of alkyl-bridged bis(catechol) ligands in the formation of triple helicate/mesocate (Figure 1.15). Reaction of a mixture of methylene-bridged bis(catechol) ligand and ethylene-bridged bis(catechol) ligand (1.5 equiv of each) with two equivalents $Ti(OMe)_4$ or $(acac)_2TiO$ in the presence of sodium or lithium carbonate (2 equiv) as base only yielded a mixture of the homoleptic mesocate A1 (number of methylene in the alkyl spacer: n = 1, odd) as well as the helicate A2 (number of methylenes in the alkyl spacer: n = 2, even).

19
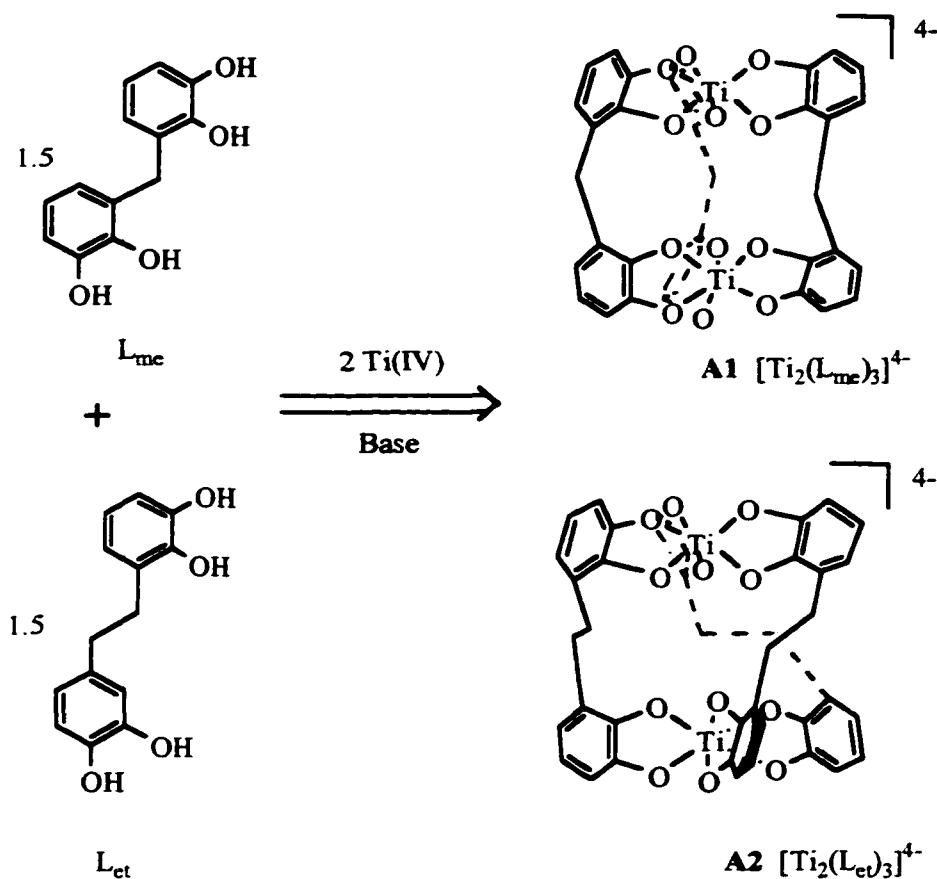
Figure 1. 15 Only homoleptic bimetallic complexes (A1, A2) formed from a 1:1 mixture of the ligands L_{me} (1.5 equiv) and L_{et} (1.5 equiv) by reaction with Ti(IV) (2 equiv) in the presence of Na_2CO_3 or Li_2CO_3 as base.

Recently, Stack and coworkers have also reported many important results on stereospecificity and self-selectivity in the formation of dinuclear triple helicate/ mesocate by using *bis*(catecholamide) ligands [41-43] (Figure 1.16) which can be regarded as analogues of *bis*(catecholamide) siderophores in biological systems.[44] The *bis*(catecholamide) siderophores, while diverse in their organic framework, may utilize similar energetic interactions to assemble a common structural form for metal

$$R = H, CH_3; n = 0, 1$$
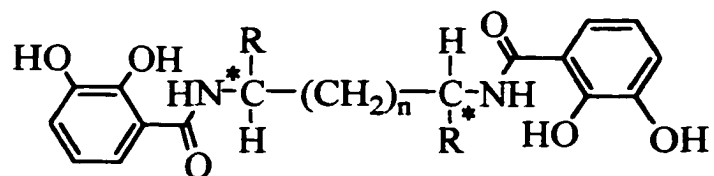
Figure 1.16 Schematic structure of the *bis*(catecholamide) ligands used by Stack and coworkers

fac - M L₃

mer - M L₃

+ 2 M
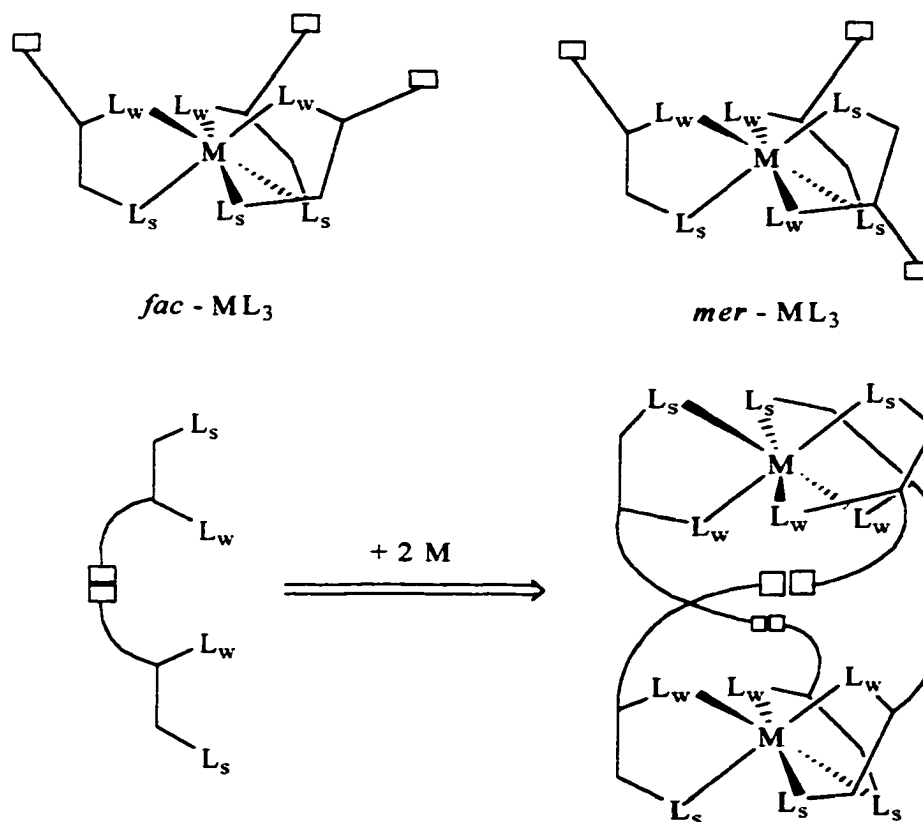
Figure 1.17 Top: *fac*-and *mer*- isomers of a monometal ML₃ complex. Lw = weak donor ligand, Ls = strong donor ligand.

Bottom: Formation of a bimetallic triple helicate.

21

complexation. In order to better define the assembly process of such siderophores, they designed these *bis*(catecholamide) ligands as simple analogues of siderophores.

The *bis*(catecholamide) ligands have similar structures to the alkyl-bridged *bis*(catechol) ligands, differing only in the spacers between the two catechol groups. Thus they can also form triple helicates (D_3 symmetry) and triple mesocates (C_{3h} symmetry) of M_2L_3 stoichiometry with octahedral metal ions, like Fe(III)[41, 45] and Ga(III).[41, 42] In these studies, Stack proposed that the phenomenon known as *trans*-influence [46] can potentially provide additional enthalpic drive towards discrete, bimetallic triple helicate/ mesocates. For a monomeric *tris*-chelate complex of three electronically nonsymmetrical bidentate ligands, two configurations, *fac-* and *mer-*, are possible (Figure 1.17, top). In the *fac*-configuration, each of the stronger donors is *trans* to a weaker one. The *fac-* isomer is thus enthalpically favored, and generates inherent structural directionality.

Incorporation of two electronically nonsymmetrical, bidentate units in a two-fold symmetric, dinucleating tetradentate ligand yields a system that should be enthalpically and entropically favored towards assembly of a helicate/mesocate with M_2L_3 stoichiometry. Based on these ideas, Stack and coworkers have synthesized many triple helicates and mesocates, some of which are shown in Figure 1.18.

There are two chiral centers in the structure of these designed ligands (Figure 1.16) which can be used as probes to study the stereochemistry and self-recognition of the self-assembly process. Their results also support that the self-assembly process of triple helix from *bis*(catecholamide) ligands and octahedral metal ions is both stereospecific and self-selective. Remarkably, the *bis*(catecholamide) ligand L_{et} [Me, Me] (when n = 0; R = CH_3) does not form a triple helix with octahedral ion Ga(III), but a

22
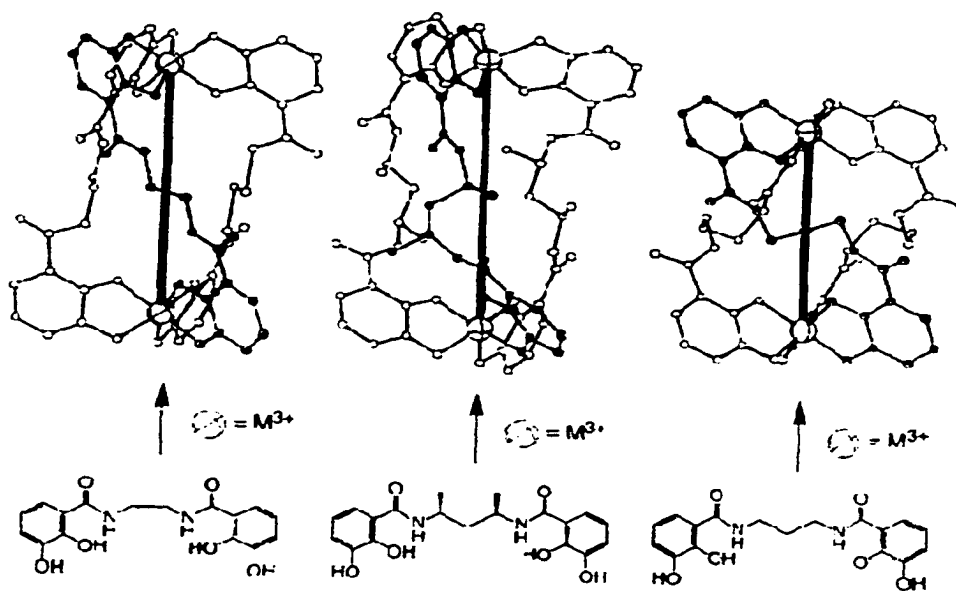
Figure 1.18 ORTEP representations of the structures of the helical 2:3 metal complexes (top) formed by the respective three bottom ligands [M = Fe(III), Ga(III)]
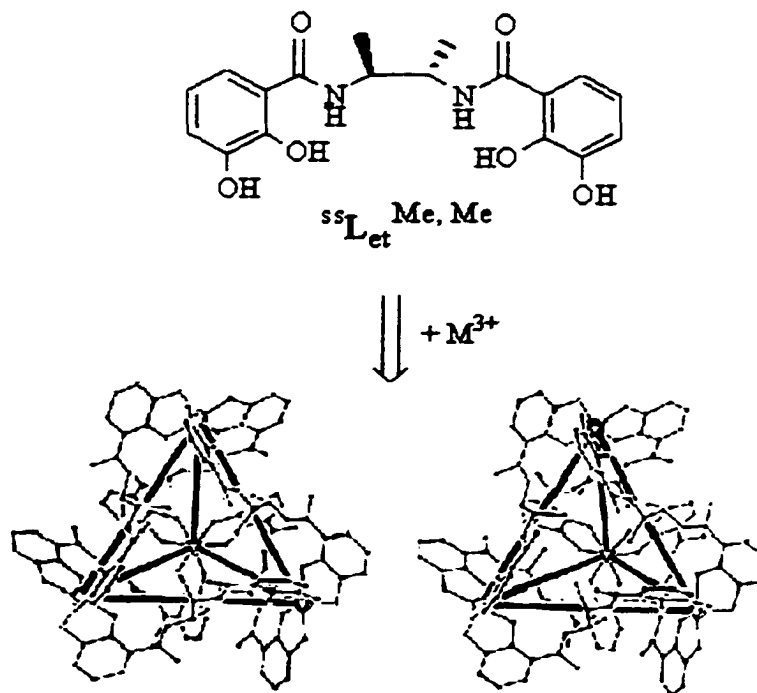
Figure 1.19 ORTEP representation of the structure of a 4:6 tetrahedral cluster $[Ga_4(^{SS}L_{et}^{Me, Me})_6]^{12-}$ formed by $^{SS}L_{et}^{Me, Me}$ (shown as a stereoview).

23

tetrahedral cluster instead, with the self-assembly process being both stereospecific and self-selective (Figure 1.19). [43]

When the ligand L_{et} $^{Me, Me}$ is enantiopure, $^{RR}L_{et}$ $^{Me, Me}$ (where both C* centers have R-chirality) or $^{SS}L_{et}$ $^{Me, Me}$ (where both C* centers have S-chirality), it forms stereoselectively a tetrahedral cluster with T symmetry (Equation 1 and 2) which has been characterized both in the solid-state and in solution. When the ligand is racemic rather than enantiopure, an enantiomeric pair of homochiral tetrahedral clusters is exclusively formed (Equation 3)

$$4Ga^{3+} + 6\ ^{RR}L_{et}\ ^{Me, Me} \longrightarrow \Delta\Delta\Delta\Delta\text{-}[Ga_4(^{RR}L_{et}\ ^{Me, Me})_6]^{12-} \qquad \text{(Equation 1)}$$

$$4Ga^{3+} + 6\ ^{SS}L_{et}\ ^{Me, Me} \longrightarrow \Lambda\Lambda\Lambda\Lambda\text{-}[Ga_4(^{SS}L_{et}\ ^{Me, Me})_6]^{12-} \qquad \text{(Equation 2)}$$

$$4(m+n)\ Ga^{3+} + 6m\ ^{RR}L_{et}\ ^{Me, Me} + 6n\ ^{SS}L_{et}\ ^{Me, Me} \longrightarrow$$

$$6m\ \Delta\Delta\Delta\Delta\text{-}[Ga_4(^{RR}L_{et}\ ^{Me, Me})_6]^{12-} + 6n\ \Lambda\Lambda\Lambda\Lambda\text{-}[Ga_4(^{SS}L_{et}\ ^{Me, Me})_6]^{12-} \qquad \text{(Equation 3)}$$
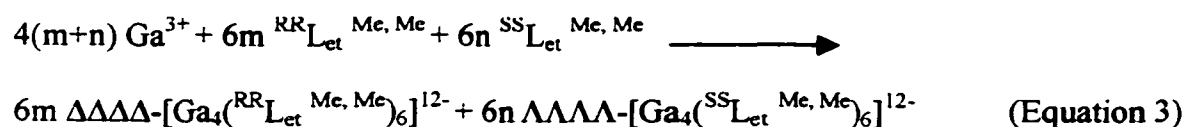
Through conformational analysis, Stack and coworkers demonstrated two important factors: a favorable torsional conformation, and efficient packing of the hydrophobic methyl groups result in the formation of a $[M_4L_6]$ complex rather than the $[M_2L_3]$ type of complex in the self-assembly of ligand ($^{RR}L_{et}$ $^{Me, Me}$ or $^{SS}L_{et}$ $^{Me, Me}$) with octahedral Ga(III). [43] Because two methyl groups on the two vicinal carbons (SS, RR) increased the ligand rigidity, making two coordinate vectors parallel to one another but in opposite positions, this is ideal for the formation of a tetrahedral cluster (Figure 1.10, 1.27b).

24
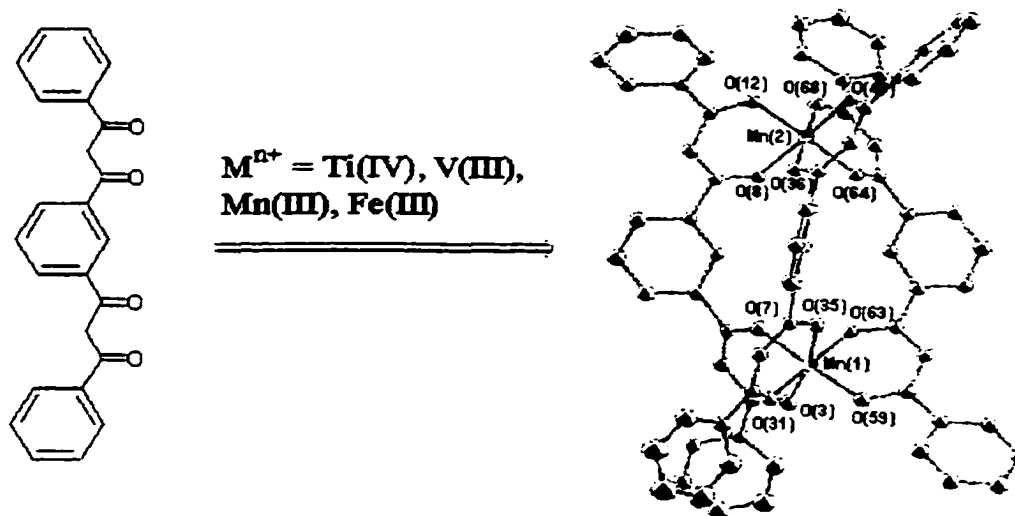
Figure 1. 20 Addition of the *bis*(β-diketone) ligand [L= 1,3-bis(3-phenyl-3-oxopropanoyl)benzene] to a suitable source of M(III) ions (M= Ti, V, Mn, Fe) in a L:M = 3:2 ratio gives the bimetallic triple helicates [M_2L_3].
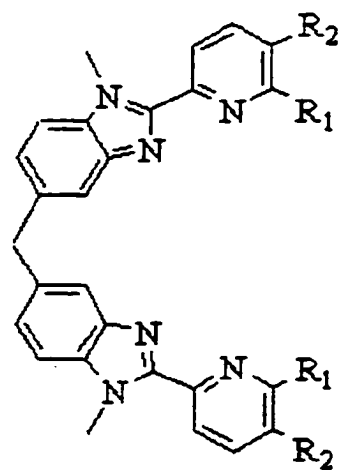
L_1: R_1= CH_3; R_2 = H
L_2: R_1 = H; R_2 = CH_3

+ Co(II)

M:L = 2:3
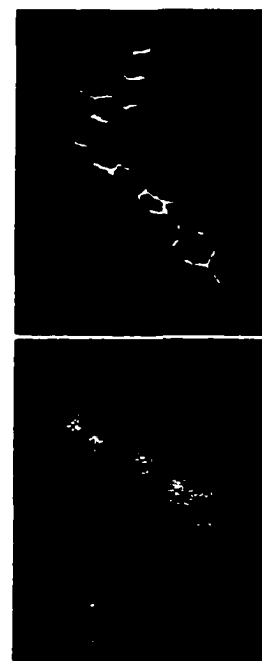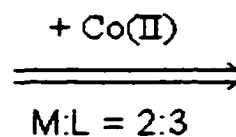
Figure 1.21 Selected helical clusters formed by *bis*(bidentate) polypyridyls.

Top: Crystal structure of [$Co_2(L_2)_3$]$^{4+}$ [47]; bottom: Crystal structure of [$Co_2(L_1)_3$]$^{4+}$ [48]

25

In addition to the ligands above, other types of oligobidentate ligands can be also used for the synthesis of bimetallic triple helicates/mesocates, including $bis(\beta$-diketone) ligands (Figure 1.20), [49] bidentate polypyridyls (Figure 1.21), [47-51] etc.

As described above, all these bimetallic coordination clusters were either synthesized as analogues of known ligands (Albrecht and Stack's work), or formed by systematic variation of metal ligand components (bis(bidentate) polypyridyls).

All of the above systems have the following characteristics in common:

1. All ligands are bis(bidentate), providing a C_2-symmetry element.

2. All coordinating metals are octahedral, providing a C_3-symmetry element.

3. The C_2-axis is perpendicular to the C_3-axis.

4. All metal ions are kinetically labile.

5. They all have sufficiently rigid framework to avoid two binding sites at any individual ligand coordinating to the same metal ion.

Clearly, these successful ligands match the criteria for *Incommensurate Symmetry-driven Cluster Formation*.

(b) Clusters with T (or S_4) Symmetry

As described above, there are two types of tetrahedral coordination clusters: M_4L_6 and M_4L_4. Depending on the chiralities at the metal centers, the cluster can have either idealized C_3 ($\Delta\Lambda\Lambda\Lambda/\Lambda\Delta\Delta\Delta$) , S_4 ($\Delta\Delta\Lambda\Lambda$) or T ($\Lambda\Lambda\Lambda\Lambda/\Delta\Delta\Delta\Delta$) symmetry. To date, there has been no report on a M_4L_6 or M_4L_4 tetrahedral cluster with C_3 symmetry.

26
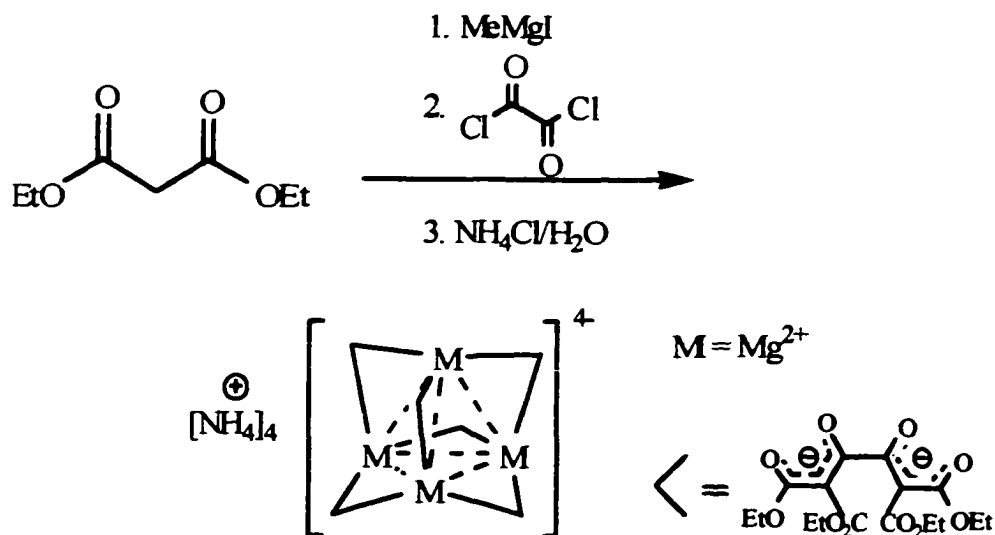
Figure 1.22 The first tetrametallic cluster with T symmetry was synthesized serendipitously in the metalation reaction of a malonic ester
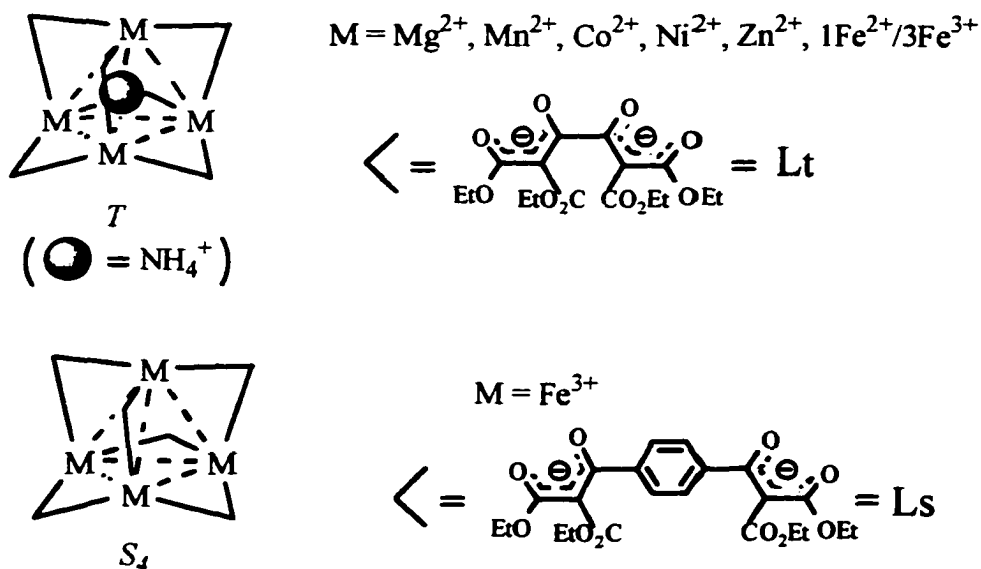
Figure 1.23 Top: the ligand without spacer (Lt) can form tetrametallic clusters with Mg^{2+}, Mn^{2+}, Co^{2+}, Ni^{2+}, Zn^{2+}, and $1Fe^{2+}/3Fe^{3+}$. All of them have idealized T symmetry. Bottom: the ligand with 1,4-phenylene as a spacer (Ls) forms a tetrahedral cluster with Fe^{3+} with idealized S_4 symmetry.

27

M₄L₆ tetrahedral clusters

The first example of a M₄L₆ tetrahedral cluster was synthesized serendipitously by Saalfrank and coworkers in the metalation reaction of a malonic ester (Figure 1.22),[52] and characterized as an adamantoid-type cluster with T symmetry (racemic ΛΛΛΛ/ΔΔΔΔ) (Figure 1.24, Left).

The *bis*(bidentate) ligand without spacer (Lt) can form tetrahedral clusters with Mg^{2+}, Mn^{2+}, Co^{2+}, Ni^{2+}, Zn^{2+}, [53, 54] and Fe^{2+}/Fe^{3+} (Figure 1.23, top).[55] All the structures of these M₄Lt₆ clusters have idealized T symmetry (Figure 24, left). Interestingly, this ligand formed the first neutral adamantanoid cluster with 1 vertex of Fe(II) and 3 vertices of Fe(III), which remarkably also has idealized T symmetry, indicating a strong coupling of four Fe atoms in the cluster.[55] Whereas the ligand with 1,4-phenylene as spacer (Ls) forms a tetrametallic Fe(III) cluster which has idealized S_4 symmetry (Figure 1.24, right,
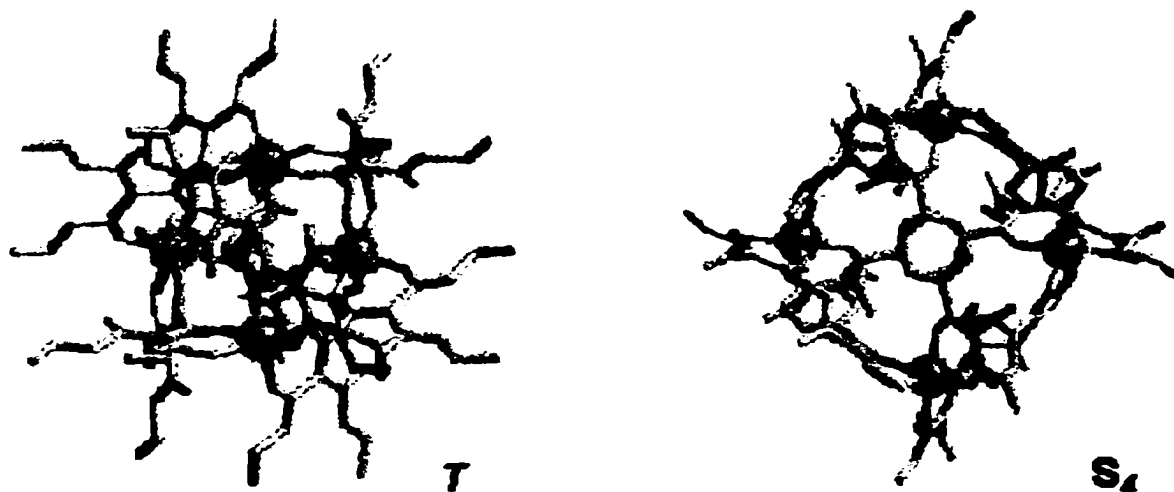
Figure 1.24 Left: Crystal structure of the first tetrametallic cluster [H₄N ⊂ Fe₄Lt₆] of T symmetry (a molecule of NH_4^+ is encapsulated as seen in yellow); Right: Crystal structure of Fe₄Ls₆ of S_4 symmetry

28

and Figure 23).[55] All of these clusters can be categorized into the first type of tetrahedron, that is, the C_2-axes of each tetrahedron lie in the ligand planes.

Recently, McCleverty and coworkers reported another ligand which forms a tetrahedral cluster with Co(III). Solution and solid-state data (Figure 1.25) indicate that the tetrametallic cluster has idealized T symmetry, and a molecule of BF_4^- anion is encapsulated in the cluster cavity. This is the second type of tetrahedron because its C_2-axes are perpendicular to the ligand planes. [56]
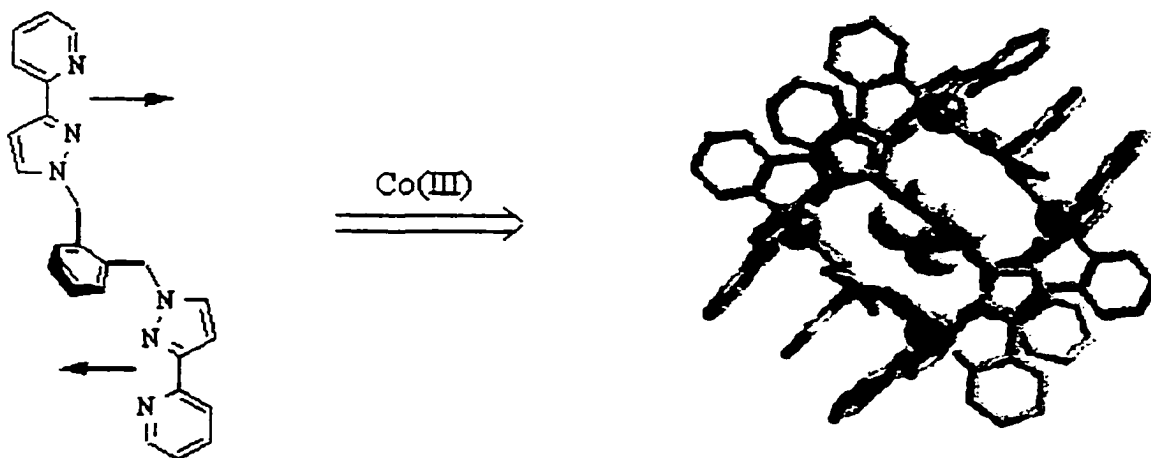
Co(III)

Figure 1.25 The ligand used by McCleverty and coworkers forms a tetrahedral cluster with Co(III) (T symmetry). The crystal structure of this cluster indicates that a molecule of BF_4^- anion is encapsulated in the cavity of cluster (yellow).

M₄L₄ tetrahedral clusters

McCleverty and coworkers also reported a manganese(II) cluster which is a M_4L_4 tetrahedron. Unlike all the ligands described above, the ligand they used is a 3-fold symmetric *tris*(bidentate) ligand (Figure 1.26). In the M_4L_4 tetrahedral cluster, the four

29

Mn(II) ions occupy the four vertices and the ligands occupy each of the faces. This

cluster is *rac-* homochiral, that is, it has idealized T ($\Lambda\Lambda\Lambda\Lambda/\Delta\Delta\Delta\Delta$) symmetry.[57]
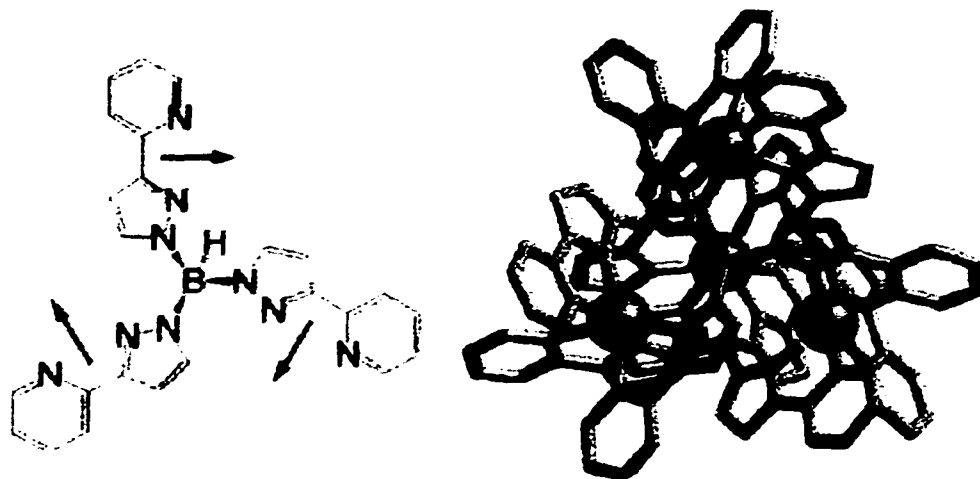
Figure 1.26 The ligand (left) and the crystal structure of the M_4L_4 tetrahedron [Mn$_4$L$_4$]$^{4+}$ reported by McCleverty and coworkers. The cluster is homochiral, has idealized T ($\Lambda\Lambda\Lambda\Lambda/\Delta\Delta\Delta\Delta$) symmetry. The manganese atoms are ferromagnetically coupled.

a   b   c   d
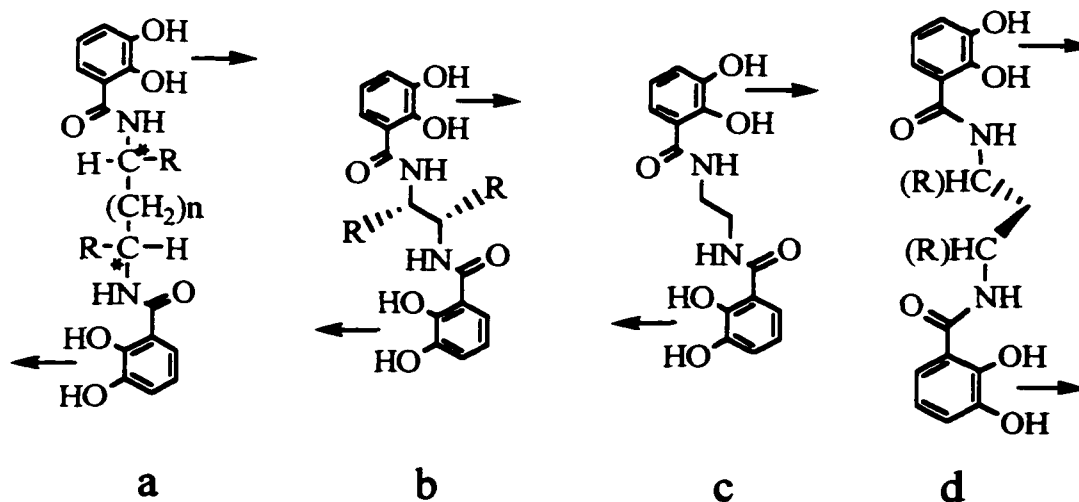
Figure 1. 27 Several possible conformations of *bis*(catecholamide)ligands (a) , the arrows represent the coordinate vectors.

30

As discussed for the triple helicate/mesocate clusters, some of *bis*(catecholamide)

ligands may also form tetrahedral clusters if they have alkyl groups at the two chiral

carbon atoms. This type of *bis*(catecholamide) ligands adopt the conformation shown

in Figure 1.27b, in which both chiral carbon atoms are in either SS- (Figure 1.27b), or

RR-configuration, and the coordinate vectors are parallel to one another, but pointing in

opposite directions. When R = H, the C-C bond of the ethylene spacer can rotate freely,

thus the coordinate vectors in this ligand can point in either the same direction or the

opposite directions (Figure 1.27c), in this case two M_2L_3 helicates or mesocates should be

favored over a M_4L_6 tetrahedral cluster by entropy. This is indeed the case when the

spacer is n-propylene, and the coordinate vectors point to the same direction (Figure

1.27d).

The orientation of the coordinate vectors in the ligands used by Saalfrank and

coworkers is different from that above. From Figure 1.28, it can be seen clearly that the

ligand framework is somewhat rigid, and the coordinate vectors are oriented 60° from

each other. Upon coordinating, this angle can become close to 70.6° by twisting each of

the chelating groups slightly out of plane, which is the ideal angle for the formation of a

tetrahedral cluster.[52-55]
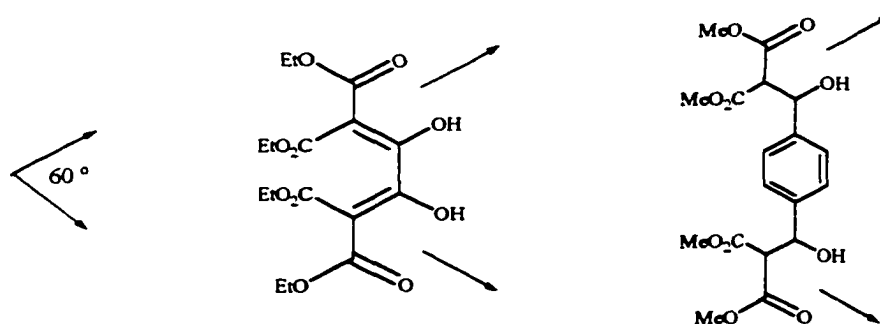
Figure 1.28 The orientation of the coordinate vectors in the two ligands used by Saalfrank and coworkers to form tetrahedral clusters with T (or S_4) symmetry.

31

In summary, these reported M_2L_3 triple helicate/mesocate and M_4L_6 tetrahedral coordination clusters unambiguously illustrate the generality of the design strategies of *Incommensurate Symmetry-driven Cluster Formation*.

4. Ligand Design for New Coordination Clusters

The *bis*(bidentate) ligands described so far can be classified into four categories: Catecholamides, hydroxamates, hydroxypyridinones, and pyrazolones (Figure 1.29).
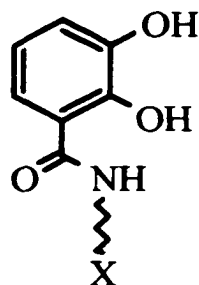
Catecholamide
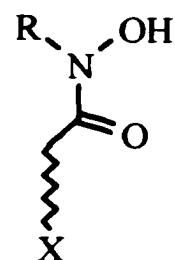
Hydroxamate
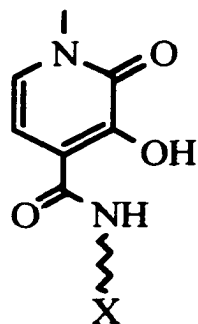
Hydroxypyridinone
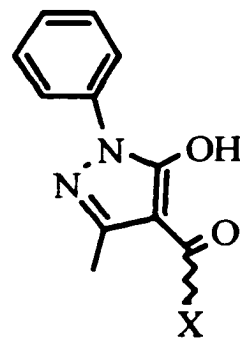
Pyrazolone

Figure 1.29 Catecholamides, hydroxamates, hydroxypyridinones and pyrazolones are useful chelating units for synthesizing supramolecular clusters because of their high stability and lability with +3 metal ions such as Al(III), Ga(III) and Fe(III)

32

Catecholamide and hydroxamate ligands are excellent choices for binding units in supramolecular complexes because of the high stability and lability of these chelates with +3 metal ions of octahedral coordination environments.[58] Hydroxy-pyridinones and pyrazolones have also proven useful in synthesizing supramolecular clusters.[59]

(a) Ligands Designed for Triple-stranded Clusters

Some of the ligands designed and synthesized by Raymond and coworkers for the formation of triple-stranded clusters are shown in Figure 1.30.[60-62] All of them are derivatives of ideally planar *bis*(bidentate) catecholamide ligands. The rigid aromatic

$H_4 4$	$R^1 = R^2 = H$
$H_4 5$	$R^1 = R^2 = Pr^i$
$H_4 6$	$R^1 = Pr^i, R^2 = Me$
$H_4 7$	$R^1 = R^2 = (S)\text{-CHMePh}$
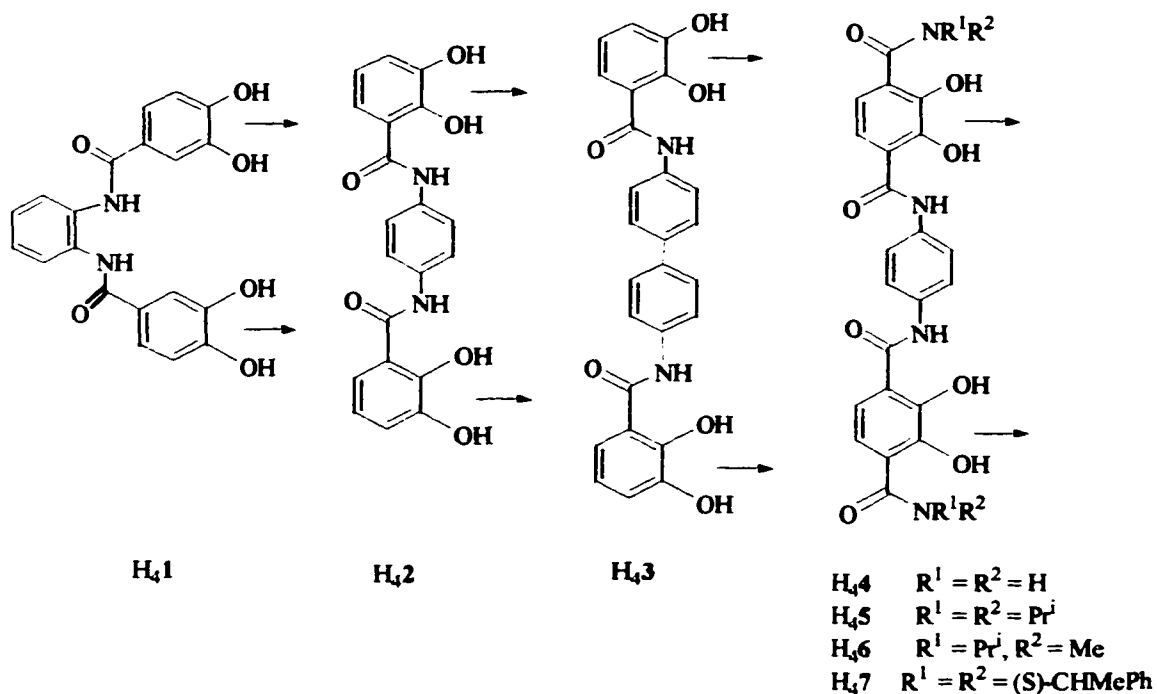
Figure 1.30 Ligands $H_4 1$-$H_4 7$ were designed to make $M_2 L_3$ triple helicates with +3 metal ions like Ga(III), Al(III) and Fe(III). The arrows represent the coordinate vectors, which should be parallel (or become parallel upon complexation), pointing in the same direction if a triple helicate is to form.

33

linkers serve to maintain preorganization of the ligand, since other topologies are possible where flexible linkers are used. The chelate vectors, indicated as arrows, are parallel (or become parallel upon complexation) and point in the same direction within each ligand. Molecular mechanics calculations indicated that for each of these ligands the chiral helicate was lower in energy than the meso-M_2L_3 cluster.[63] The M_2L_3 stoichiometry was confirmed by both fast atom bombardment (FAB$^+$) and electrospray mass spectrometry. The crystal structure of the Ga(III) complex of $H_4$4 is shown in Figure 1.31b and confirms that the rigid ligand forms a racemic mixture of homochiral triple helicates with Ga(III).

a   b
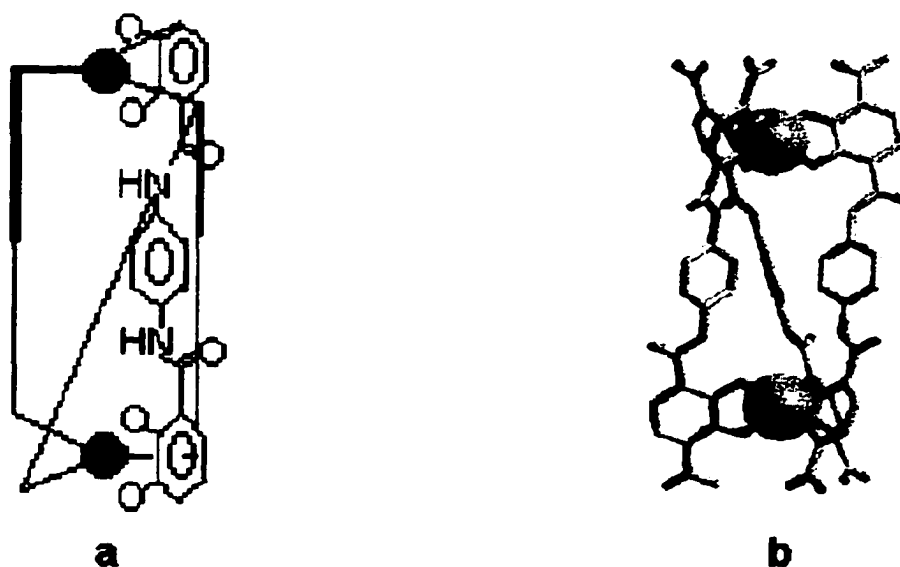
Figure 1.31 (a) In a D_3 symmetric triple helicate, the two metal chelate planes are parallel. The green spheres represent the pseudo-octahedral metal ions, the rods represent the ligands. (b) The crystal structure of the triple helicate $[Ga_24_3]^{6-}$.

A meso-complex has a Δ-configuration at one and a Λ-configuration at the other metal center. This type of clusters has idealized C_{3h} symmetry: there is an orthogonal,

34

bisecting mirror plane that relates the Δ- to the Λ-configurated metal center, rather than having three C_2 axes perpendicular to the C_3 axis. What factors control the formation of a mesocate versus a helicate? Although it has been proposed that the length of an alkyl spacer between two chelating moieties may direct helicate versus mesocate formation [37, 40] or that a chiral ligand may be able to induce a helical twist in an M_2L_3 complex, these explanations are not convincing.[39]

Most recently, Raymond and coworkers have presented the first example of a ligand that makes both a helicate and a mesocate. The X-ray analysis showed that in the solid state the Al_2L_3 complex is a chiral helicate (racemic), while the Ga_2L_3 complex is an achiral mesocate (Figure 1.32).[30]

H₂O ⊂ (ΔΔ, ΛΛ)-Al₂L₃   L   (Δ,Λ)-Ga₂L₃
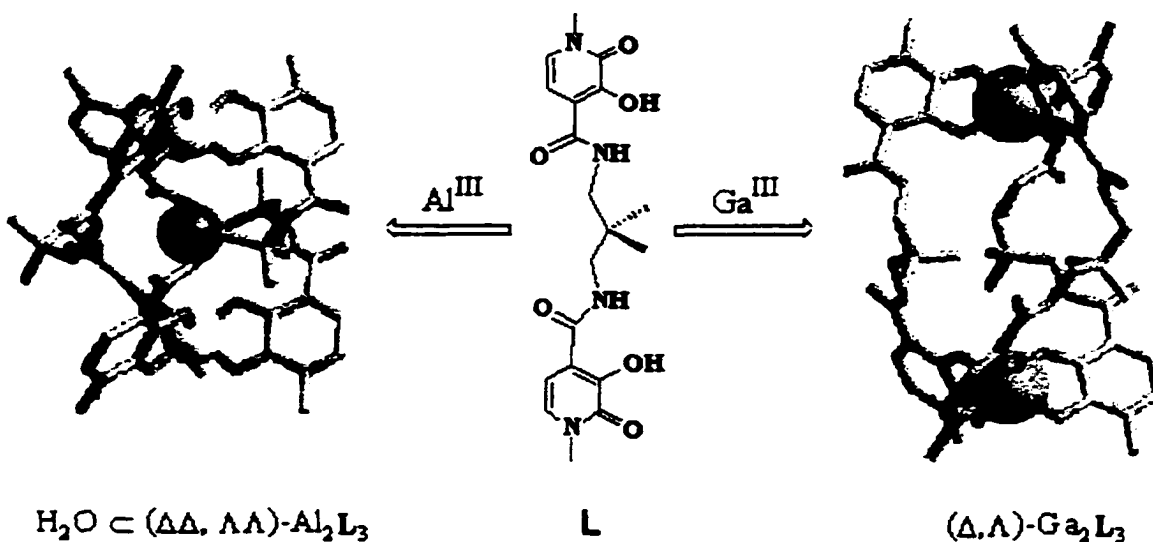
Figure 1.32 A ligand (L) forms both a chiral helicate (left) and an achiral mesocate (right). The Al₂L₃ helicate has a molecule of water in the cluster cavity. Al atoms are represented by yellow spheres, Ga atoms by green spheres, and water molecule by orange-red sphere.

35

(b) Ligands Designed for M₄L₆ Tetrahedral Clusters

Raymond and coworkers have demonstrated the utility of the incommensurate symmetry interaction model in two approaches to the rational design of such clusters. Both approaches employ an ideally planar C_2-symmetric bis(bidentate) ligand with a rigid backbone, but the orientation of the C_2 axis of the cluster with respect to the ligand plane differs.

The C_2 axes of the cluster lies in the ligand planes

Two designed ligands H₂8 and H₄9, the crystal structure of Ga₄8₆ , and the energy-minimized structure [63, 64] of the T symmetry isomer of the proposed $[Ga_49_6]^{12-}$ tetrahedron are shown in Figure 1.33. The coordinate vectors in the free ligands H₂8 and H₄9 are oriented 60° from each other. Upon coordinating, the angle between the coordinate vectors can become close to 70.6° by twisting each of the chelating groups slightly out of plane. So ligand H₂8 can form a tetrahedral clusters with Fe(III), or Ga(III). Both complexes show intense peaks for the M₄L₆ molecular ions in the FAB⁺ mass spectrum. In addition, the crystal structure of Ga₄8₆ revealed that the tetrahedral cluster has S_4 symmetry (two Δ and two Λ metal centers) in the solid state.[13] The ligand backbone is coplanar with the S_4 axis, and there is a substantial cavity which is partially open to the outside in the cluster. Four crystallographically identical DMF molecules partially fill the cavity. Ligand H₄9 also appears to form a tetrahedral cluster with Ga(III).[64] The ¹H NMR spectrum (D₂O) of the microcrystalline product shows only one set of ligand peaks, indicating a high-symmetry solution structure on the NMR timescale. In addition, preparation of the complex in the presence of excess ligand does not disrupt

36
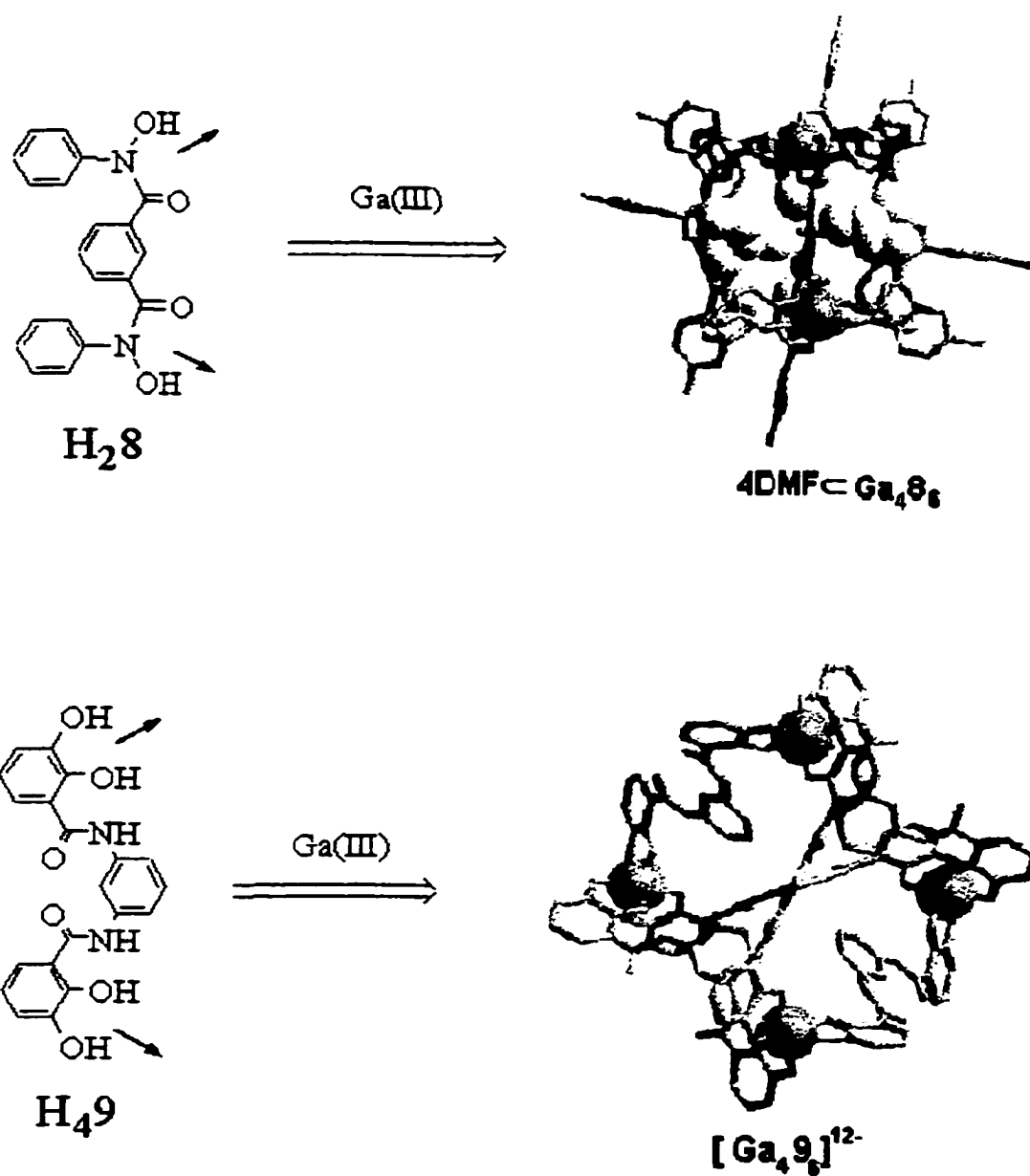
Figure 1.33 Designed and synthesized ligands and M_4L_6 clusters. The above is the structure of $Ga_4 8_6$ viewed down the crystallographic S_4 axis. Below is the minimized structure of the T symmetry isomer of the proposed $[Ga_4 9_6]^{12-}$ tetrahedron.

the formation of the desired cluster: the ^1H NMR spectrum of this mixture shows two sets

of peaks, one for the free and one for the coordinated ligand. The major ions observed in

the electrospray mass spectrum (low resolution) match those expected for $[K_{14}Ga_4 9_6]^{2+}$, $[K_{15}Ga_4 9_6]^{3+}$, $[K_{16}Ga_4 9_6]^{4+}$. However, X-ray-quality single-crystals have not been obtained due to the high charge (-12) of the cluster.

The C_2 axes of the cluster is perpendicular to the ligand planes

The ligand should be designed planar, and have parallel coordinate vectors that point in opposite directions (Figure 1.10).

The first ligand $H_4 10$ of this type was designed to form M_4L_6 tetrahedral cluster by Raymond and coworkers in 1998 (Figure 1.34, top left). [32] Molecular modeling of the metal complexes [M = Ga(III), Fe(III)] of $H_4 10$ indicated that the cluster would have a substantial cavity $(250-350\text{Å})$.[65] Solution and solid-state data show that one of the Et_4N^+ counterions is encapsulated within the cavity of $[M_4 10_6]^{12-}$ [M = Ga(III), Fe(III)] cluster with T symmetry (Figure 1.34, top right). In an attempt to make a similar cluster with a large cavity, more recently they designed ligand $H_4 11$ (Figure 34, bottom left). [33] This ligand also forms an M_4L_6 tetrahedral cluster, but only in the presence of a tetra-alkylammonium guest. The crystal structure of $(Me_4N)_8[Ti_4 11_6]$ shows one molecule of Me_4N^+ encapsulated in the cavity of the T symmetry cluster. The distance between the titanium atoms averages 16.1Å (Figure 1.34, bottom right). Interesting, in the absence of a tetra-alkylammonium guest molecule, $H_4 11$ forms instead an M_2L_3 triple helicate with Ti(IV) of D_3 symmetry (Figure 1.35).[33]

From the crystal structure of $[Ti_2 11_3]^{4-}$, the *bis*(catecholate) binding sites are clearly twisted out of the ligand plane to make the orientation of the coordinate vectors

38
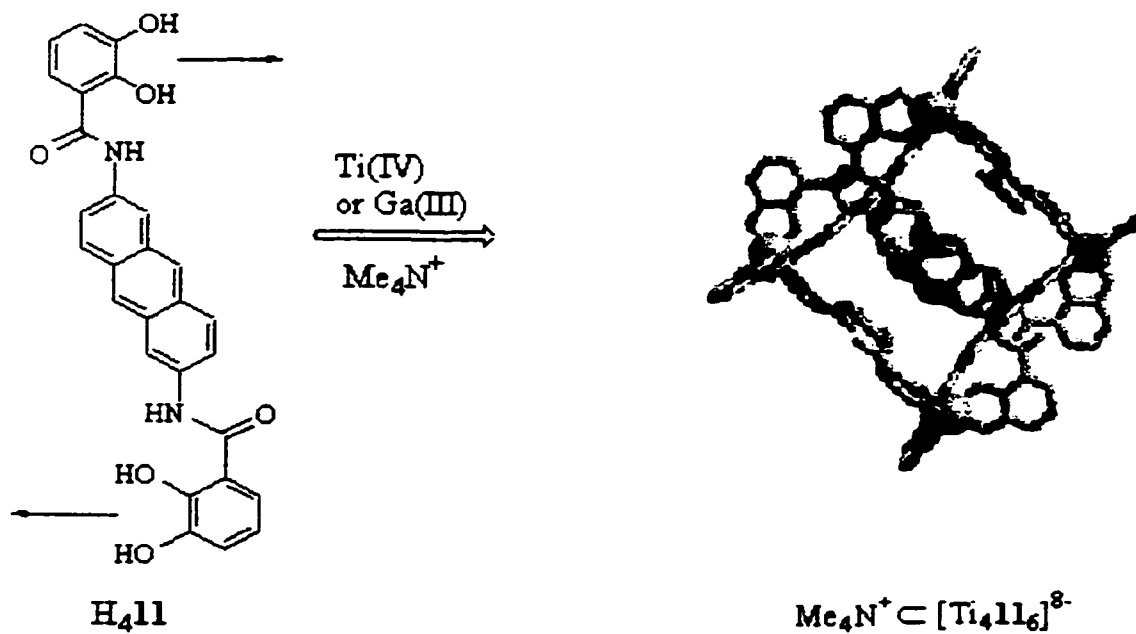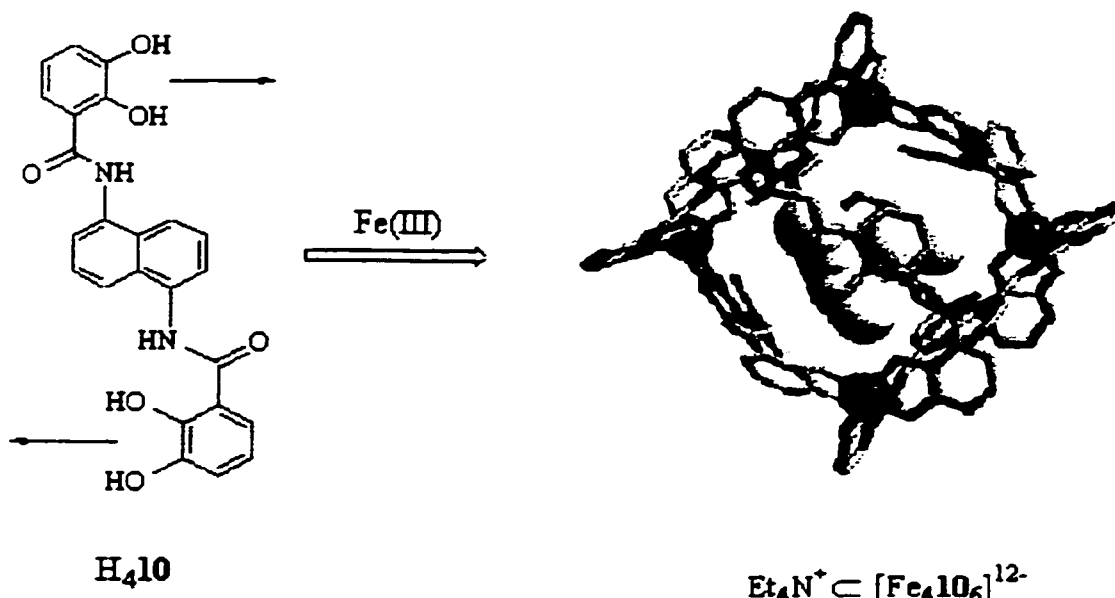
Figure 1.34 Ligands H_410 and H_411 (left) were designed to make M_4L_6 tetrahedral clusters. The crystal structure of $[Fe_410_6]^{12-}$ (top right) shows the cluster has T symmetry, encapsulating a molecule of Et_4N^+. The crystal structure of $[Ti_411_6]^{8-}$ (bottom right) also has T symmetry, and encapsulates a molecule of Me_4N^+.

39
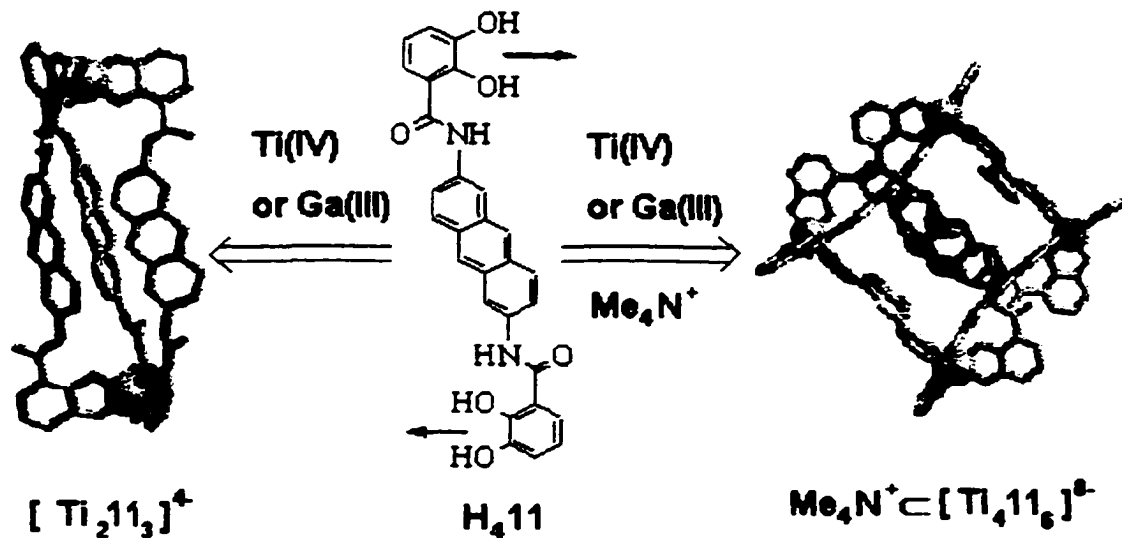
Figure 1.35 Ligand $H_4 11$ forms a M_2L_3 helicate in the absence of a Me_4N^+ guest, but a M_4L_6 tetrahedron in the presence of Me_4N^+. The crystal structures of $[Ti_2 11_3]^{4-}$ (left) and $Me_4N^+ [Ti_4 11_6]^{8-}$ (right) are shown.

suitable for the formation of triple helicate with D_3 symmetry. So if the framework of a designed ligand is not absolutely rigid, it is possible to form clusters with other symmetry besides the desired one.

(c) Ligands Designed for M_4L_4 Tetrahedral Clusters

Ligand $H_6 12$ was designed to form M_4L_4 Tetrahedral Clusters by Raymond and workers. Its coordinate vectors and ligand plane are shown in Figure 1.36.

Upon coordinating, its approach angle for a M_4L_4 tetrahedral cluster is $19.4°$. This ideal angle is less than four degrees from the approach angle of $23°$ (corresponding twist angle = $40°$) observed for the *tris*-(catecholate) complexes of Ti(IV), Ga(III) and

40
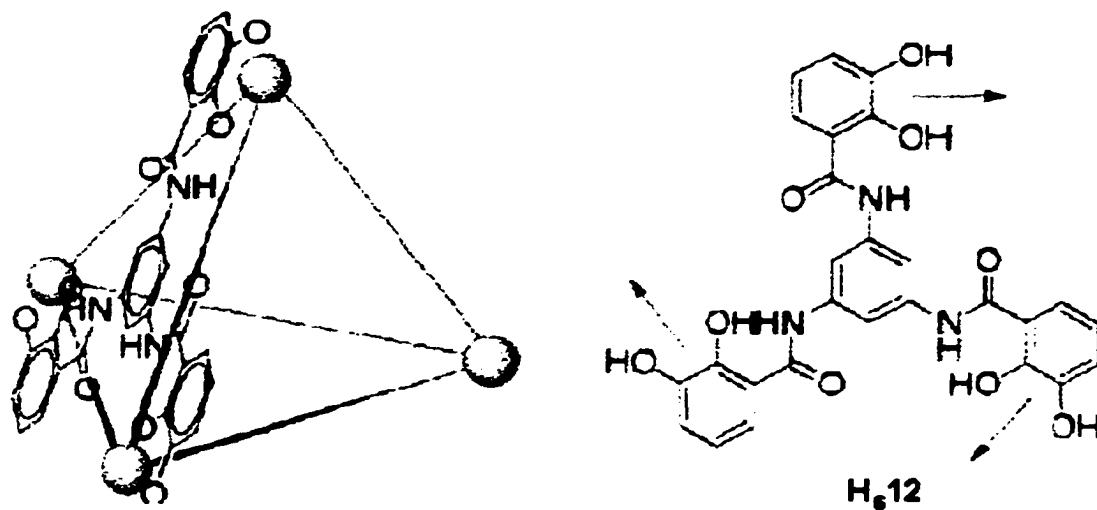
$H_6 12$

Figure 1.36 A M_4L_4 tetrahedral cluster with the metals on the vertices and ligands on the faces of the tetrahedron can be synthesized using ligand $H_6 12$.

Ti(IV)
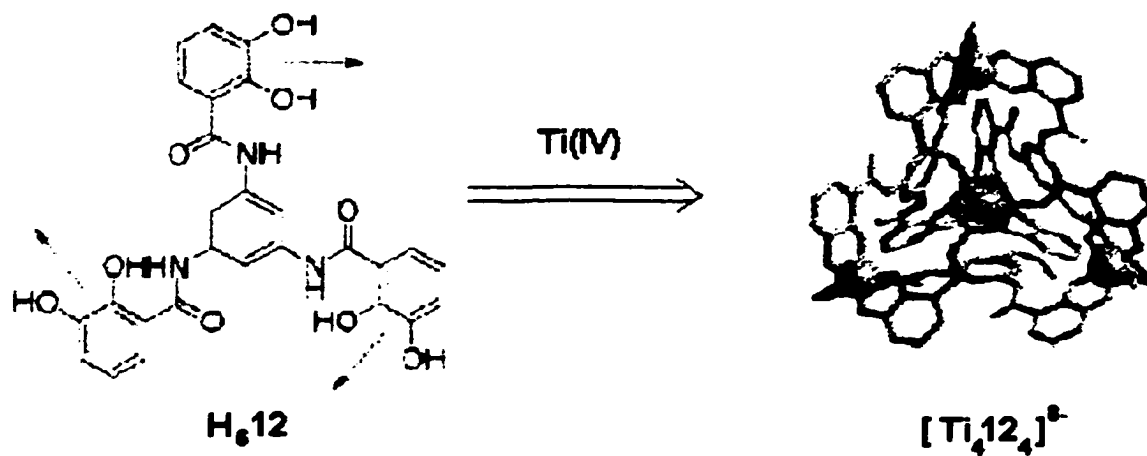
$H_6 12$

$[Ti_4 12_4]^{8-}$

Figure 1.37 Ligand $H_6 12$ and the crystal structure of $[Ti_4 12_4]^{8-}$ (right).

41

Fe(III).[66-68] The design of ligand $H_6$12 seems optimized for metal ions with significant distortions toward trigonal prismatic geometry. Thus, ligand $H_6$12 reacted with Al(III), Fe(III) and Ga(III) under basic conditions to give precipitates whose ^1H NMR and mass spectra indicated the expected M_4L_4 species. However, the high charge (12-) of these clusters precluded the isolation of X-ray quality single-crystals. So, Ti(IV) was used to lower the overall charge of the cluster to 8-, an M_4L_4 tetrahedral cluster of Ti(IV) was formed and crystallized. The crystal structure of the $(Et_3NH)_8[Ti_412_4]$ complex shows the cluster is indeed a racemic mixture of homochiral tetrahedron, that is, it has T symmetry (Figure 1.37).[69]

A correctly-designed ligand is just one of the prerequisites for the formation of the desired cluster. Most recently, Raymond and coworkers reported a designed pyrazolone-based ligand $H_3$13, which is rigid, three-fold symmetric, and tri-bidentate. It was designed for the formation of a M_4L_4 tetrahedral cluster. Because the high charge of any cluster anion renders the crystal-growth difficult, this pyrazolone-based ligand is also designed to overcome the problem. Surprisingly, it forms a M_6L_6 "cylinder" cluster with Ga(III), having idealized D_3 symmetry (Figure 1.38).[70]

This cylindrical geometry is confirmed unequivocally by single-crystal X-ray diffraction, ^1H and ^{13}C NMR spectra, as well as FAB^+-MS. The crystal structure shows that the Ga_613_6 has idealized D_3 symmetry. The gallium atoms define a distorted trigonal antiprism in which six ligands make up the equatorial faces of the cylinder with a hole on the top and the bottom (Figure 1.39a, b, c).

42
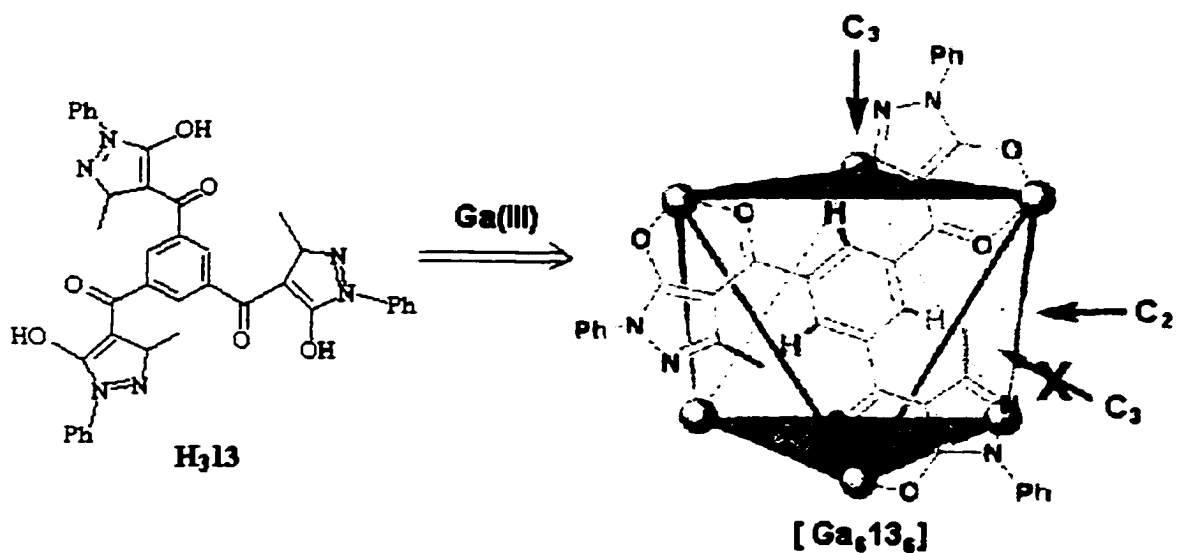
Figure 1.38 The designed ligand H₃13, which was designed to form a M₄L₄ tetrahedral cluster, forms an M₆L₆ cylinder (right) with Ga(III) instead.
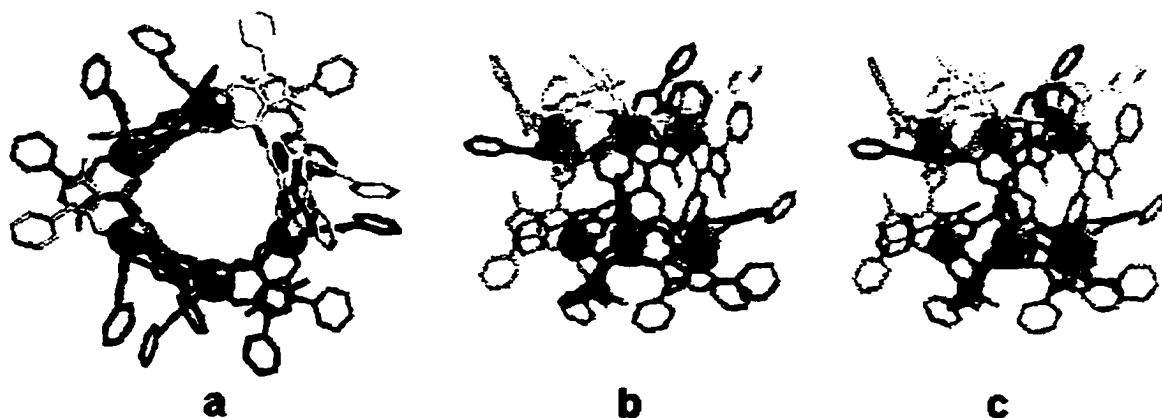
Figure 1.39 Wire frame and sphere representation of the crystal structure of [Ga₆13₆]. (a) as viewed down the pseudo three-fold axis of the cluster; (b) and (c) as viewed down the pseudo two-fold axis of the cluster. (Ga ions represented by tan spheres)

43

In summary, a ligand can be designed for any cluster with any symmetry by the design strategies of *Incommensurate Symmetry-driven Cluster Formation*. The examples of supramolecular coordination clusters reported so far convincingly illustrate the generality and feasibility of this synthetic methodology in the formation of supramolecular coordination assemblies. A well-designed ligand can provide a better chance for the formation of the desired cluster, but cannot ensure that it will happen. Numerous unforeseen problems encountered in the synthetic process may complicate the cluster formation, or even make the cluster formation impossible.

Notwithstanding these difficulties, it is important to consider several major factors in cluster formation:

(a) Thermodynamic and kinetic factors:

All components and reactions including intermediate assemblies and reactions must be kept under thermodynamic control. Any kinetic product, if inert, may destroy the stoichiometry needed for the formation of product. At the same stoichiometry, the formation of the smaller cluster is always entropically favored. Therefore, in order to selectively form the larger cluster, the geometry of the designed ligand must be correct and inflexible.

(b) Solvent factors:

The solvent selection is also very critical for cluster formation. In order to maintain the stoichiometry required for the cluster formation, a homogeneous solution

44

(single or mixed-solvents) will be preferred. When it is impossible to keep every component homogeneous, a multi-phasic solvent system may be considered as long as each component in stoichiometric ratio can be supplied from its own phase. In this case, any intermediate species must be kinetically labile. Physical properties of solvent, such as polarity, may also play important roles. Failed cluster formation in non-polar solvents may become possible upon switching to a polar solvent, and *vice versa*. Usually, as the cluster gets larger and more highly charged, the solvent problem becomes more serious.

(c) Template ions:

The templating effect of cations or anions is currently a hot topic in the supramolecular chemistry. As seen in several described examples above [30, 33, 65], a different templating ion may direct formation of a different cluster. Sometimes, choosing a right template is the key to successful cluster formation. The encapsulated ion in the cavity of a cluster can be regarded as the template which directed the formation of its own cluster host. Some counterions may appear innocent, but in some transient stage of the cluster formation, they may act as templates. Thus the choice of a proper counterion must also be considered.

45

5. Towards Mixed-Metal Clusters

(a) Background and Design of 4-Phosphino-Catechols

From the discussion above, we have seen many examples of supramolecular assemblies based on metal-ligand interactions. All the ligands designed by Raymond and coworkers as well as by others have one characteristic in common: they are all symmetric, and provide elements of symmetry, such as C_2 or C_3, which are essential for cluster formation. All the clusters synthesized also have another characteristic in common: they are all homometallic complexes. The metal ions used in all cases described in this introduction form octahedral complexes, providing C_3 symmetry sites.

Let us take a look again at the model which is employed to account for the formation of apoferritin (Figure 1.1-2). The protein subunit itself is asymmetric, the symmetry elements needed for the assembly are provided by the non-covalent interactions occurring at two distinct ends of the individual subunits.

The design of an asymmetric hybrid ligand targeted for mixed-metal cluster formation is relatively rare. Recently, Lam and coworkers reported the assembly of a mixed-metal helicate of $Ru_2 14_6 Cu_3$ ($H14$ = 3-(pyridin-2-yl)pyrazole) where a substitution-inert $[Ru(II)(14H)_3]^{2+}$ complex was used as the three-fold interaction site to coordinate labile $Cu(I)$ as the two-fold site to form a triple helicate of D_3 symmetry (Figure 1.40). [71] However, the ligand H14, 3-(pyridin-2-yl)pyrazole, only has N atoms as donor sites, therefore it will not have much discriminating coordination preference for two distinct metals.

46
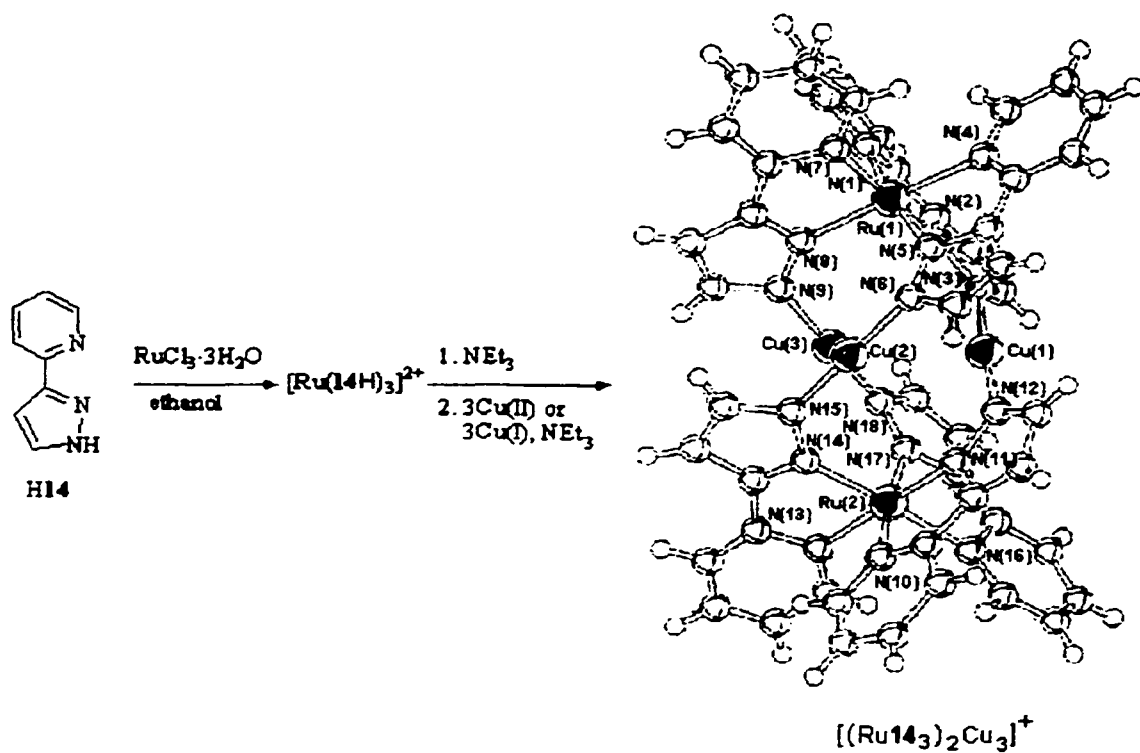
Figure 1.40 The ligand **14** used by Lam and coworkers forms a triple helicate of D_3 symmetry with Ru(II) and Cu(I) via two-steps.
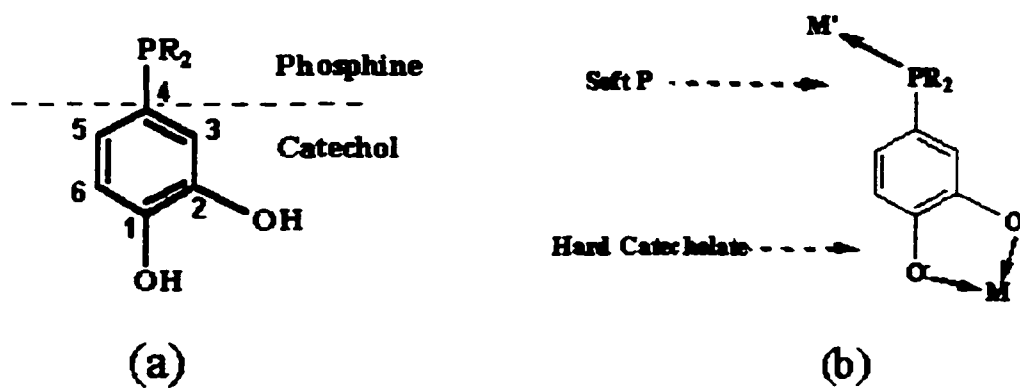
Figure 1.41 4-Phosphino-Catechols (a) and their ambidentate donor sites (b)

47

We designed 4-Phosphino-Catechol ligands for the formation of supramolecular coordination clusters by bridging two very different metal ions (Figure 1.41).

As seen in Figure 1.41, the 4-Phosphino-Catechols are asymmetric ligands which incorporate both phosphine and catecholate donor sites. In order to ensure that the hybrid ligands will bridge two metals rather than chelate one with a mixed P/O⁻ donor set, the ligands were designed with the phosphino- group on the 4-position of the catechol ring. This phosphine positioning makes these ligands ambidentate (Figure 1.41b), permitting selective binding and bridging of two very different metal centers.

Additionally at the phosphino- group, modifications on the two substituent R groups will provide a wide variety of new ligands with tunable stereoelectronic properties and coordination abilities. For example, increasingly bulky R groups can be used to adjust the metal coordination number from 4 to 2, thus generating four, three, and two-fold symmetry elements, respectively; a fluorinated R group can be used to enhance the π-acceptor ability of the ligand. Furthermore, different R groups can be introduced to enhance hydrophilicity or lipophilicity, add positive or negative charges, etc.

(b) Related Hybrid Phosphine-Oxygen Ligands and Their Complexes

There were no known phosphino-catechol ligands before our work. However, several related hybrid phosphine-oxygen ligands have been investigated. Herein is given a brief review on the complexes of the ligands shown in Figure 1.42 , and their redox chemistry.

48
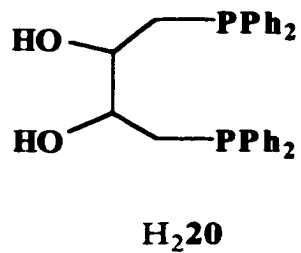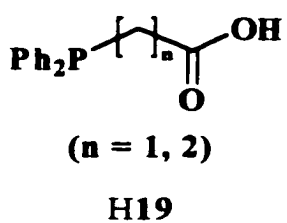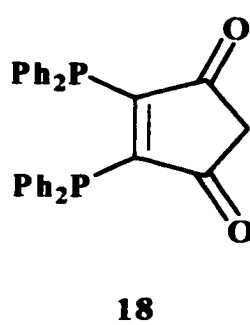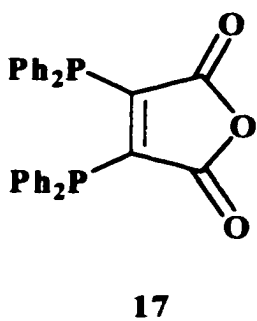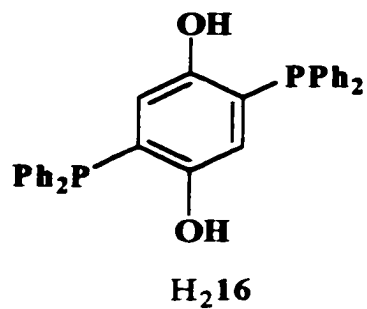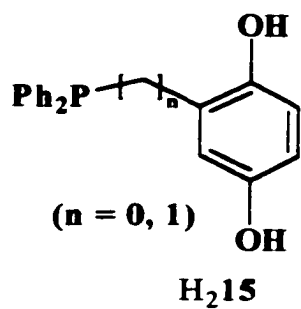
Figure 1.43 Several related hybrid phosphine-oxygen ligands

Colbran and coworkers have studied the complexes of $H_2 15$ (1,4-dihydroxy-2-diphenylphosphino-benzene) since 1990.[72-75] Because of the mutual incompatibility of parabenzoquinones and phosphines, $Me_2 15$ was used as the 'protected' precursor ligand. The complexes $[MCl_2(Me_2 15)_2]$ (Pd(II), Pt(II), Ni(II)) were prepared and the methoxy groups were cleaved using BBr_3 to give, after workup, the chelated hydroquinonyl complexes $[M(H15)_2]$ which featured chelating P/O donor sets.[72]

In 1989, Kaim and coworker reported a complex, $\{[Ru(bpy)_2]_2(\mu\text{-}16)\}^{3+}$, of $H_2 16$ with the electron transfer active metal fragment $[Ru(bpy)_2]^{2+}$. In this complex, ligand 16 acted as a bridge between the Ru(II) moieties.[76] Again, this complex featured chelating P/O donor sets.

p-Quinones along with their redox products, p-semiquinones and p-hydroquinones (all dioxolenes) are important intermediates in chemical and biochemical reactions.[77] They may play crucial roles in biological redox chains, as in the structurally-characterized reaction center of bacterial photosynthesis.[78] Electron transfer reactions between transition metal centers and p-quinone cofactors are vital for all life. $H_2 15$ and $H_2 16$ are p-hydroquinone ligands integrated with phosphine substituents at the 2-position, 2- and 5-positions, respectively. The ligands themselves are of great interest in redox chemistry. Further, multi-valent transition metals provide another redox center for their complexes. The data from Colbran's group demonstrated multiple electron/proton transfer steps,[75] while Kaim's group observed that their complexes have a general feature of highly delocalized multi-metal complexes of strongly-interacting redox-active ligands.[76]

The complexes of 17 with Group VI [79] and X [80,81] metals, as well as Mn, Fe [82] and Co [83] have been synthesized since $[Co(CO)_2 L17]$ (L = CO, PPh_3) were reported by

50

Rieger and coworkers in 1991.[84] Complex $Ru_3(CO)_7(\mu_2\text{-}H)(\mu_3\text{-}\eta^2\text{-}C\equiv C^tBu)$(18) was reported by Richmond and coworkers in 1995.[85] The metals in all these complexes are chelated by the two diphenylphosphine groups.

Both 17 and 18 are also redox active. By Extended Hückel calculations, Richmond's group demonstrated that ligand 17 possesses a low-lying π^* orbital that is delocalized over the maleic anhydride ring. Its complexes with this type of LUMO is expected to serve as an efficient electron reservoir by stabilizing electron counts in excess of 18-electrons.[79] The studies on the ruthenium complex of 18 revealed the presence of a reversible one-electron reduction process (ligand 18-based) and an irreversible oxidation (metal based).[85]

Like our 4-Phosphino-Catechols, phosphino-carboxylic acids, H19,[86, 87] have incorporated two very different donor groups: phosphine and carboxylate. Upon deprotonation, bidentate ligand behavior is observed , either in a chelating or bridging mode, whereas the neutral ligands can also bind unidentally through the phosphorus atom. However, the alkylene spacer is not rigid and it cannot prevent the two ends from binding the same metal atom in a chelating P/O mode. Thus this type of ligands cannot be employed in the formation of a desired cluster. In 1998, Heller and coworkers reported the rhodium(I) complex of $H_2$20 featuring a tridentate P, P/O mode which was used as a hydrogenation catalyst.[88]

Taken together, complexes featuring a chelating P/O donor set have a rich redox chemistry. Besides chelated transition metals, the ligands themselves are often redox-active, and some can be considered as typical redox-switchable hemilabile ligands (RHLs, Scheme 1.1) because of their hybrid phosphine-oxygen nature.[89]

51
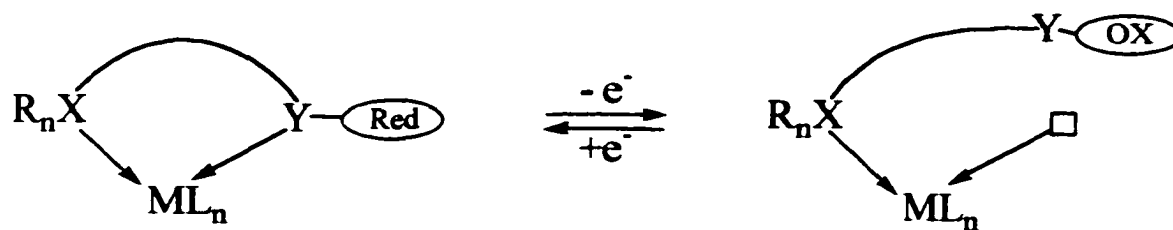
Scheme 1.1 Redox-switchable hemilabile ligands (RHLs, represented by arch). (X = strongly binding donor site, Y = weakly binding donor site, R = substituent of tunable electronic nature, □ = unidentate ligand or solvent, L = unidentate ligand.)
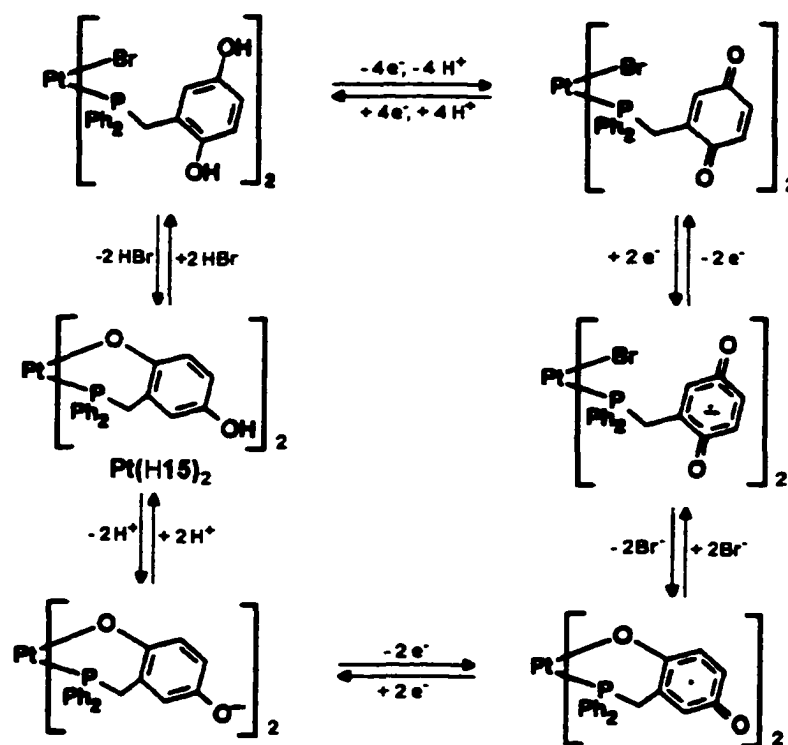
Scheme 1.2 Pt(H15)₂ exhibits proton and electrochemically-modulated oxygen binding to Pt(II). (H₂15 is a quinone-based redox-switchable ligand.)

The use of redox switchable hemilabile ligands (RHLs) is a strategy recently developed by Mirkin and coworkers for controlling transition metal center reactivity. [90, 91] The RHLs have a substitutionally inert group and a substitutionally-labile one. When bound to a late transition metal center (soft metal), the bonding affinity of the substitutionally-labile end of the RHL can be controlled by adjusting the oxidation state of a redox group that is covalently attached to it (Scheme 1.1). This effect can be further tailored by changing the RHL phosphine (inert group) substituents, varying the weakly donating group, or controlling the distance between the redox-active group and the transition metal center. [92, 93]

The complexes of several known hybrid phosphine-oxygen ligands have exhibited this redox switchable hemilability. For example, $Pt(H15)_2$ (and $Pd(H15)_2$) exhibits both pH and electrochemically-induced changes in its coordination sphere (Scheme 1.2). [93, 94] Upon treatment of this complex with HBr, the bond between the Pt center and anionic oxygen atom (labile donor) is broken, and the latter is replace by a Br⁻. This reaction is reversible, $Pt(H15)_2$ reforms when treated with sodium carbonate in methanol. The reversible oxygen coordination with Pt(II) observed by its cyclic voltammograms from electrochemical investigations can also be triggered by electron loss or gain (Scheme 1.2). [94]

In summary, hybrid phosphine-oxygen ligands have been found to exhibit extensive redox chemistry, and their chemistry of hemilability has been studied and applied in homogeneous catalysis since replacement of a labile donor by a substrate can

53

often be a critical mechanistic step. It can be inferred that our hybrid ligands and their complexes (and clusters) may exhibit similar redox and catalytic chemistry.

With regard to metal-chelating modes, although all these ligands have hybrid phosphine-oxygen donor sites, they cannot bridge two metals at two discrete binding sites, but instead chelate one metal with a mixed P/O⁻ donor set or coordinate one metal with only one donor group. As seen in Figure 1.43, the phosphino groups in all these ligands are adjacent or are linked by a flexible spacer to the oxygen donor sites, thus stable five- or six-member chelating rings can be easily formed in a chelating P/O mode. To avoid this complication, we designed the 4-Phosphino-Catechols in which the phosphine group is on the 4-position of the catechol ring (rigid). With two isolated and discrete binding sites, our ligands can therefore be used in selective binding and bridging of two different metal centers, while retaining the inherent redox activity of known hybrid phosphine-oxygen ligands.

(c) Potential Chemistry of 4-Phosphino-Catechols

Catechol forms extremely stable and kinetically labile complexes with many transition metals (e.g. the $Fe(Catecholate)_3^{3-}$ complex has a formation constant $K_f = 10^{44}$) and is nature's choice in iron-sequestering ligands called siderophores.[45, 95] It has also been found that metal complexes of 1,2 - dioxolene ligands have structural and electrochemical relevance to metal-quinone chemistry in biological systems.[96] Some of

54

its derivatives and complexes have been used in pharmaceuticals.[97, 98] Vanadium catecholates are even reported to have nitrogenase activity.[99, 100]
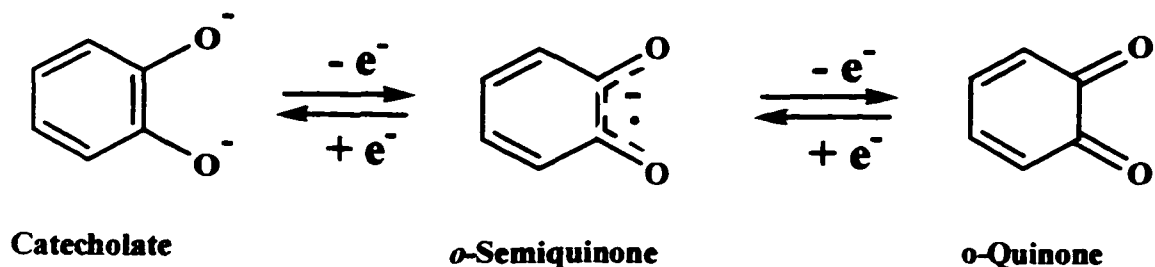
Figure 1.44 Redox chemistry of 1,2-Dioxolenes
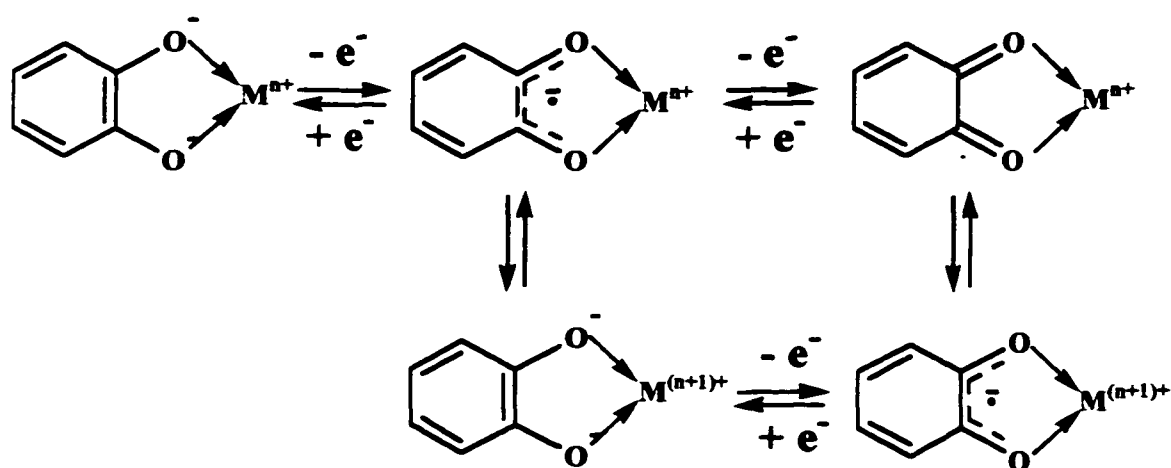
Figure 1.45 Inter- and intra-molecular redox chemistry of catecholate complexes

Catechol (o-hydroquinone) as its dianion, catecholate, is one of the three possible dioxolenes (o-semiquinone and o-quinone are the others) with different oxidation states(Figure 1.44)[100, 101]

Thus its coordination complexes are of great interest in redox chemistry since both the ligand and the coordinated metal can be potential redox sites (Figure 1.45).[102, 103]

It can therefore be expected that bimetallic complexes featuring a 4-Phosphino-Catechol bridging ligand can have three redox-active sites and extensive electron-transfer (Figure 1.46).
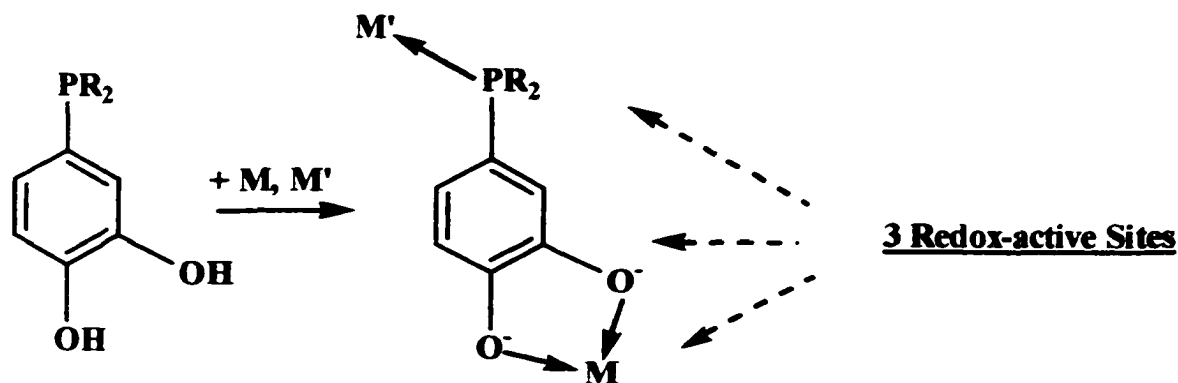
Figure 1.46 Potential redox active centers of bimetallic complexes of 4-Phosphino-Catechols

Furthermore, coordination complexes featuring two " different" metal centers (these can be different metals or even the same metal at different oxidation states) have been the target of considerable research.[93, 104] This is because they have potential intramolecular mixed-valent, charge-transfer, photo, and redox chemistry between the two bridged metals,[105-110] possible cooperative reactivity (multi-electron, " push-pull", sequential)[105a, 106, 110] and catalytic activity due to presence of two different metal centers. [106, 110-112] Thus it is expected that our target of this project, mixed-metal clusters, may have similar properties and applications.

56

(d) The Concept of Hard-Soft Metals

Pearson first formalized the soft-soft and hard-hard preferences for acid(metal ions)-base(ligands) interaction in the 1960's. This concept has major relevance and applications in all areas of acid-base chemistry and metal-ligand bonding in particular.[113a]

The term "hard" refers to species that are small and less easily polarized, whereas "soft" species are large and fairly polarizable. For our 4-Phosphino-Catechol ligands, metals having coordination preference to the soft phosphine ligand are defined as "soft", while metals having coordination preference to the hard catecholate ligand are defined as "hard". This classification of common metal ions are listed in **Table 1** .[113 b]

Table 1.1 Hard-soft acid-base classification of metal ions and ligands

	Hard	borderline	Soft
Metals	H^+, Li^+, Na^+, K^+, Cs^+, Be^{2+}, Mg^{2+}, Ca^{2+}, Sr^{2+}, Al^{3+}, Ga^{3+}, Cr^{3+}, Sc^{3+}, La^{3+}, Ce^{3+}, Ti^{4+}, Sn^{4+}, Zr^{4+}, Hf^{4+}, Th^{4+}, Pu^{4+}	Fe^{2+}, Co^{2+}, Ni^{2+}, Cu^{2+}, Zn^{2+}, Ru^{2+}, Rh^{2+}, Sn^{2+}, Sb^{3+}, Rh^{3+}, Ir^{3+}, Pb^{2+}	GaX_3 ($X= Cl^-, Br^-, I^-$) Cu^+, $Co(CN)_5^{3-}$, Ag^+, Cd^{2+}, Pt^{2+}, Pt^{4+}, Au^+, Hg_2^{2+}, Hg^{2+}, Tl^+, M^0

(e) Mixed-metal clusters from 4-Phosphino-Catechols

The 4-Phosphino-Catechol ligands are therefore designed to target the different coordination preferences of two very different metals (hard/soft metal ions). This design permits binding of soft metals, such as Pt(II), and Pd(II) at the PR_2 site to give 4-fold or

2-fold symmetry centers (M'), [114, 115] as well as hard metal cations, such as Ti(IV), Sn(IV), Fe(III), Al(III), and Ga(III) at anionic catecholate sites to give 3-fold symmetry centers (M).[66, 116, 117] The incommensurate symmetry required by these two different metal centers at the two discrete binding sites of 4-Phosphino-Catechol ligands makes this hybrid ligand system suitable for the formation of clusters based on the concepts of *Incommensurate Symmetry-driven Cluster Formation.*

Some possible mixed-metal clusters that can be formed by 4-Phosphino-Catechols are shown in Scheme 1.3.

PR$_2$

+ M, M'
base

OH
OH

2-fold (M') + 3-fold (M) symmetry
in 3:2 stoichiometry (M'/M)

M$_2$L$_6$M'$_3$ (C_{3h} or D_3 symmetry)
M$_4$L$_{12}$M'$_6$ (T or S_4 symmetry)

4-fold (M') + 3-fold (M) symmetry
in 3:4 stoichiometry (M'/M)

M$_8$L$_{24}$M'$_6$ (O or other symmetry)
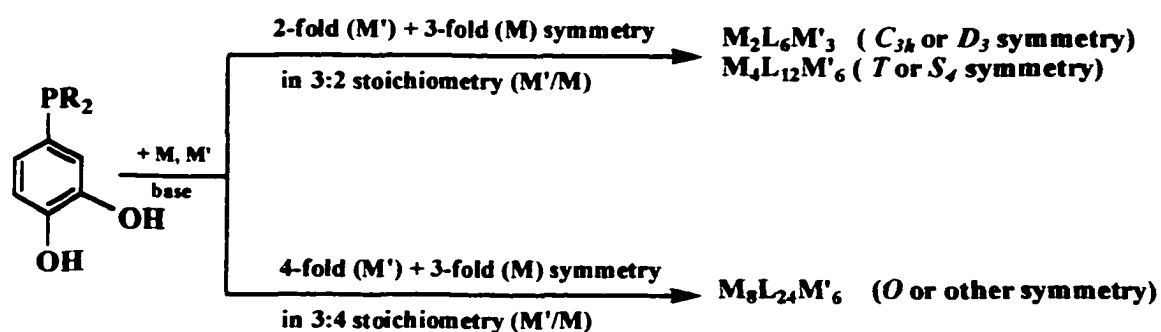
Scheme 1.3 Possible clusters formed by 4-Phosphino-Catechols (M' represents a soft metal while M represents a hard metal center)

How C_2 and C_3 symmetry may be generated:

If the substituents at phosphine ligands are bulky, or the number of available coordination sites of a soft square-planar metal is only two, a two-fold symmetry can be generated at the phosphine-coordinated metal center. The combination of this two-fold symmetry element and the three-fold symmetry center generated at a catecholate-coordinated hard metal requires a 3n/2n (soft metal/hard metal) stoichiometry to form three-stranded, tetrahedral, or even larger clusters (Scheme 1.3). Based on the concepts of

58

Incommensurate Symmetry-driven Cluster Formation, the formation of a specific cluster requires specific orientation of the ligand coordinate vectors and approach angle. Let us take a look at the possible geometries which may be involved in the formation of the simplest three-stranded or tetrahedral cluster.
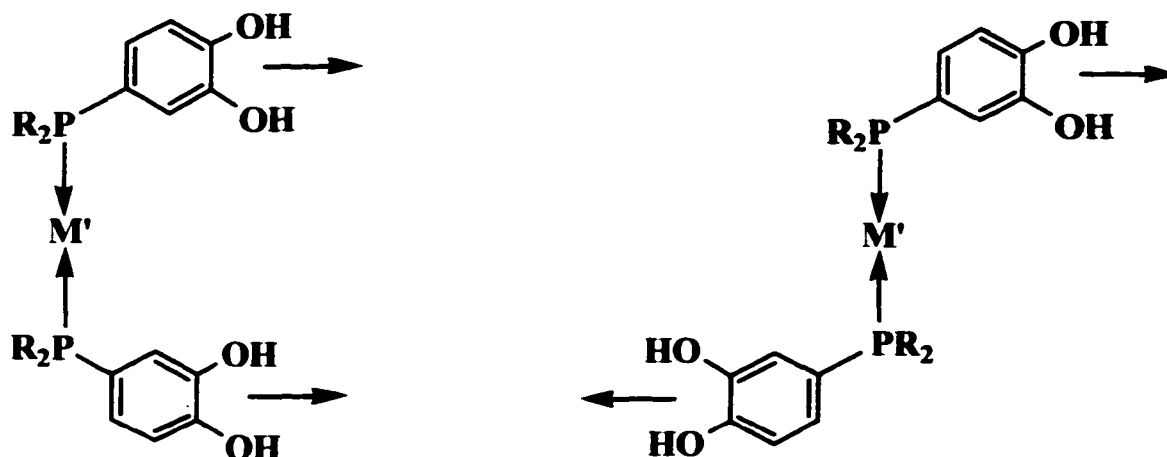
Figure 1.47 The orientation of coordinate vectors of 4-Phosphino-Catechols when its phosphine site coordinates a soft metal , generating two-fold symmetry.

To prevent two catechol ligands from binding to the same hard metal ion, they must be coordinated to the soft metal center in a *trans*-fashion. The orientation of the two coordinate vectors of the *trans*-phosphino-metal complex   is shown in Figure 1.47. Because the P-M bond can rotate, the coordinate vectors can point to any direction, while remaining parallel to one another.

Formation of M₂L₆M'₃ three-stranded clusters

If the P-M-P angle is linear, the coordinate planes will be parallel to one another in a three-stranded cluster (helicate or mesocate). So the 4-Phosphino-Catechol ligands

can be used for the formation of three-stranded clusters with either D_3 or C_{3h} symmetry (Figure 1.48).

Helicate (D_3) Mesocate (C_{3h})
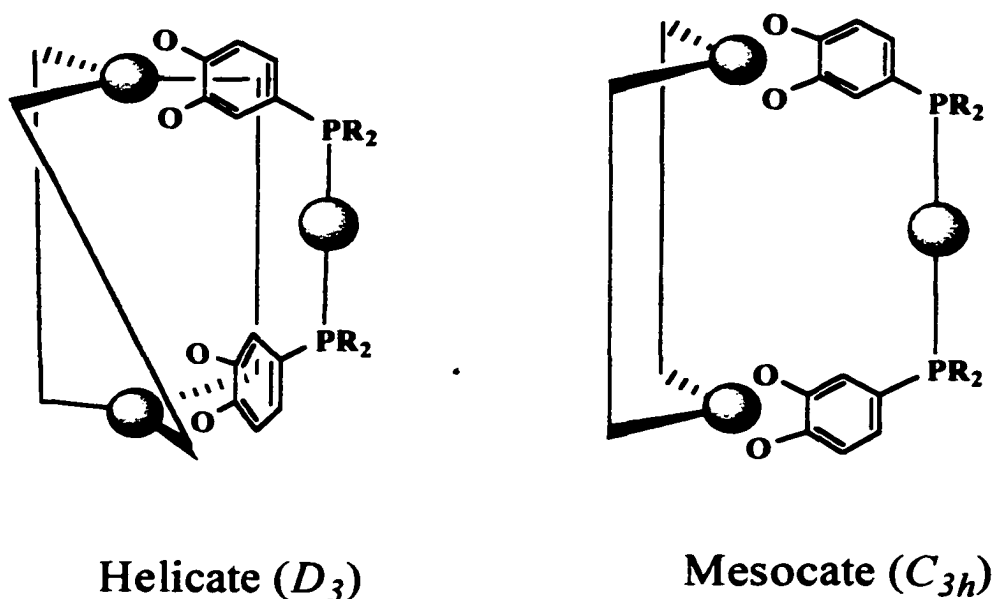
Figure 1.48 Possible three-stranded clusters from 4-Phosphino-Catechols (a red sphere represents a soft metal, while a blue sphere represents a hard metal ion).

Formation of a $M_4L_{12}M'_6$ tetrahedral cluster

If the coordinate vectors point at opposite directions while maintaining the coordinate plane parallel to one another (Figure 1.46, right), the 4-Phosphino-Catechol ligands may form a $M_4L_{12}M'_6$ tetrahedral cluster with T or S_4 symmetry, in which the C_2-axes of the tetrahedral cluster are perpendicular to the ligand planes (Figure 1.49, left).

If the P-M-P linkage twists slightly out of plane, it is possible to make the orientations of the ligand coordinate planes 70.6° from each other. In this case, it may have a chance to form a $M_4L_{12}M'_6$ tetrahedral cluster with T or S_4 symmetry, in which the C_2-axes of the tetrahedral cluster lie in the ligand planes (Figure 1.48, right).

60
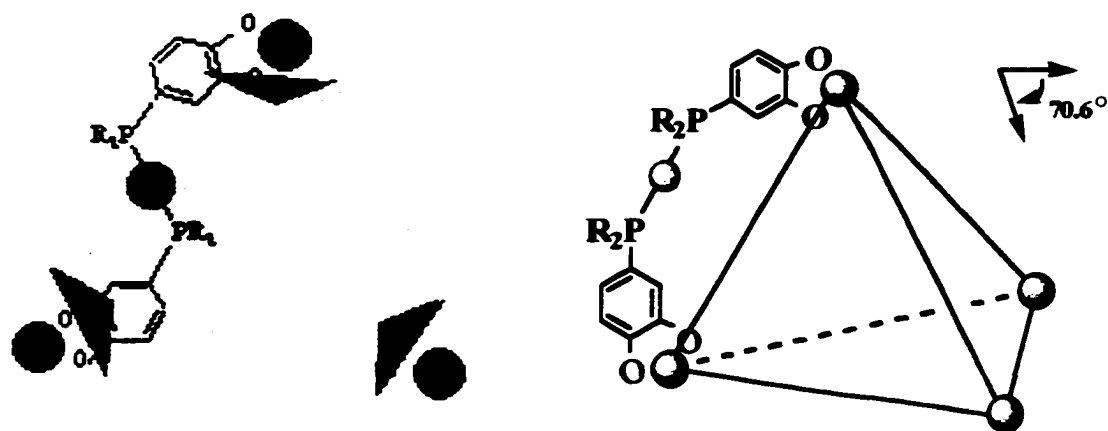
Figure 1.49 Two types of $M_4L_{12}M'_6$ tetrahedral clusters may be formed by 4-Phosphino-Catechols. The C_2 axis of the left tetrahedral cluster is perpendicular to the ligand plane, while the C_2 axis of the right one lies in the ligand plane.
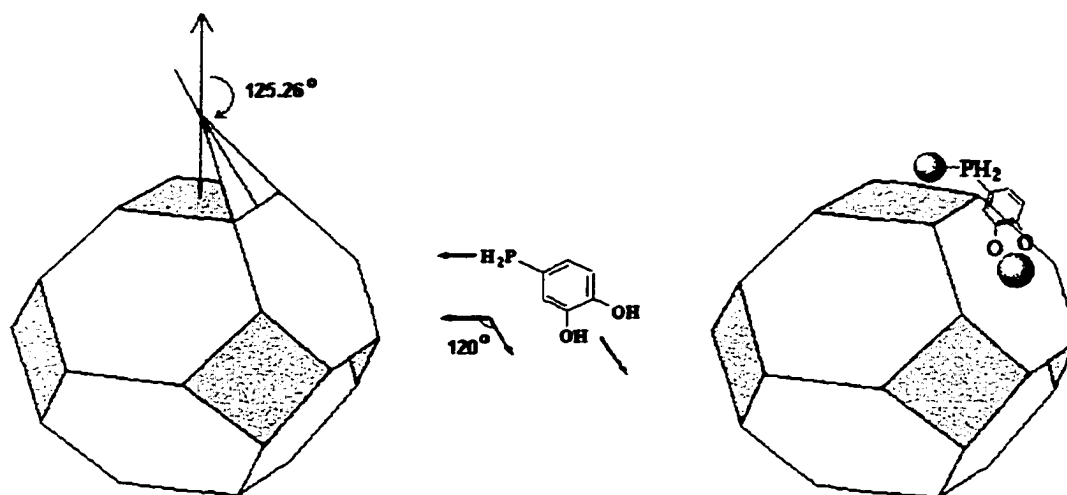
Figure 1.50 The $M_8L_{24}M'_6$ octahedral cluster is represented by a truncated octahedron. In order to form the cluster, the coordinate planes of phosphine and catechol of the ligand must be positioned 125.26° to each other. The angle can be approached by twisting the M'-P-C. The red sphere represents the soft metal, giving C_4 symmetry, while the blue sphere represents the hard metal, giving C_3 symmetry (The red sphere represents a soft metal ion, while the blue sphere represents a hard metal ion).

How C_4 and C_3 symmetry may be generated

A square-planar soft metal (M') with 4 available coordinate sites may provide a C_4 symmetry element when coordinated to phosphine ligands. This will require a stoichiometry of 3n:4n (molar ratio of soft metal M'/hard metal M) to form a cluster by the combination of this C_4 symmetry and the C_3 symmetry provided by an octahedral metal ion (M) coordinated to catecholate ligands. In this case, a $M_8L_{24}M'_6$ octahedral cluster with O symmetry may be formed. (Figure 1.50). The ligand, PH_2-Catechol, will be a good candidate for the octahedral cluster because, being sterically unencumbered, it can coordinate giving C_4 symmetry at the soft metal center, while simultaneously binding hard metals, providing C_3 symmetry. Since this phosphine ligand has no bulky substituents, the M'-P-C angle should be easier to adjust to the ideal donor/donor angle of 125.26° for octahedral cluster formation.

If this cluster is formed, there should be a large cavity inside which will make this octahedral cluster a potential host for guest molecules.

(f) Potential Applications of Supramolecular Mixed-Metal Clusters

In the context of supramolecular science, these desired mixed-metal clusters are supramolecules based on metal-ligand interactions. Therefore it can be expected that they may have potential applications similar to other supramolecular assemblies in common areas, such as molecular recognition (ion and molecule sensing), transformation, and translocation, etc.[118, 119] These functions are executed by the assembled supramolecular species, but not by their individual components. Specific applications reported currently

62

include light conversion,[120] energy transfer,[121] electron transfer,[122] non-linear optical usages,[123] heterogeneous catalysis,[124] electro-photoswitching,[125] etc.

As discussed above, our desired mixed-metal complexes are expected to have extensive redox chemistry, and may therefore have potential applications related to their redox active properties, like light conversion, multi-electron transfer, and heterogeneous catalysis.

Raymond and coworkers have shown that their tetrahedral $M_4 1O_6$[32] and $M_4 1l_6$[33] clusters can encapsulate one molecule of countercations selectively in their cavities. The former cluster host preferentially encapsulates Et_4N^+ over Pr_4N^+, Pr_4N^+ over Me_4N^+,[65, 32] while the encapsulation of Me_4N^+ is essential for the formation of the latter cluster.[33] These observations demonstrate that artificial supramolecular coordination clusters do exhibit the properties of molecular recognition. Thus it is reasonable to expect that our desired mixed-metal clusters based on 4-Phosphino-catechols should also have the interesting molecular recognition ability. Because our clusters are in anionic forms (4-Phosphino-catechols must be deprotonated before coordinted to hard metals), they can only be used for detection of cations or neutral molecules. However, attachment of cationic groups at the PR_2-sites may allow reversal of these overall charges.

In collaboration with Dr. Raymond's group at the University of California at Berkeley, this project was initiated for the exploration of the possible use of hybrid ligands with disparate metal coordination preferences in the formation of supramolecular coordination clusters. There are three subsequent chapters in this Ph. D. dissertation. Chapter II will describe the syntheses and characterization of ligands. The key precursor used for the syntheses of ligands is 4-Dichlorophosphino-Veratrole. Three 4-Phosphino-Catechol ligands have been synthesized and fully characterized.

In Chapter III, the syntheses and characterization of mono-metallic complexes of the 4-Phosphino-Catechol and 4-Phosphino-Veratrole ligands will be presented. Studies into the stereochemistry of these mono-metallic complexes will also be described. Chapter IV will center on the syntheses and characterization of the main goal of this project, mixed-metal clusters. Both stepwise *aufbau* and self-assembly processes were explored for the formation of these clusters. Numerous three-stranded mixed-metal clusters have been synthesized from the ligand 4-Diphenylphosphino-Catechol bridging hard metal ions (e.g Ti(IV), Sn(IV), Ga(III)) and soft metals (Pd(II), Cr(0), Ag(I)). In addition, several clusters have been crystallographically characterized to be three-stranded mesocates with C_{3h} symmetry.

The successful formation of these mixed-metal clusters further extend the generality and feasibility of the synthetic methodology of *Incommensurate Symmetry-driven Cluster Formation.*

64

Chapter II

Syntheses and Characterization of

4-Phosphino-Catechol Hybrid Ligands:

The starting material used in the syntheses is veratrole, or 1,2-dimethoxybenzene. From it, all our desired ligands can be synthesized (Scheme 2.1).

```
                    ┌──────────────────────┐
                    │   Veratrole + PCl₃    │
                    └──────────────────────┘
                              │
                              │ SnCl₄
                              ▼
                    ┌──────────────────────┐
                    │   4-PCl₂—Veratrole    │
                    └──────────────────────┘
                              │
         PhMgBr/Ether         │         LiAlH₄/Ether
       ┌──────────────────────┴──────────────────────┐
       ▼                                              ▼
┌─────────────────────┐                    ┌─────────────────────┐
│  4-PPh₂—Veratrole   │                    │   4-PH₂—Veratrole   │
└─────────────────────┘                    └─────────────────────┘
       │                                              │
       │ 48% aq. HBr                                  │ BBr₃/CH₂Cl₂
       ▼                                              ▼
┌─────────────────────────┐              ┌──────────────────────────┐
│ 4-PPh₂—Catechol·HBr     │              │  4-PH₂—Catechol·HBr      │
└─────────────────────────┘              └──────────────────────────┘
                                                      │
                                                      │ 37 % aq. CH₂O
                                                      │ ethanol
                                                      ▼
                                         ┌──────────────────────────────┐
                                         │ 4-P(CH₂OH)₂-Catechol·HBr     │
                                         └──────────────────────────────┘
```
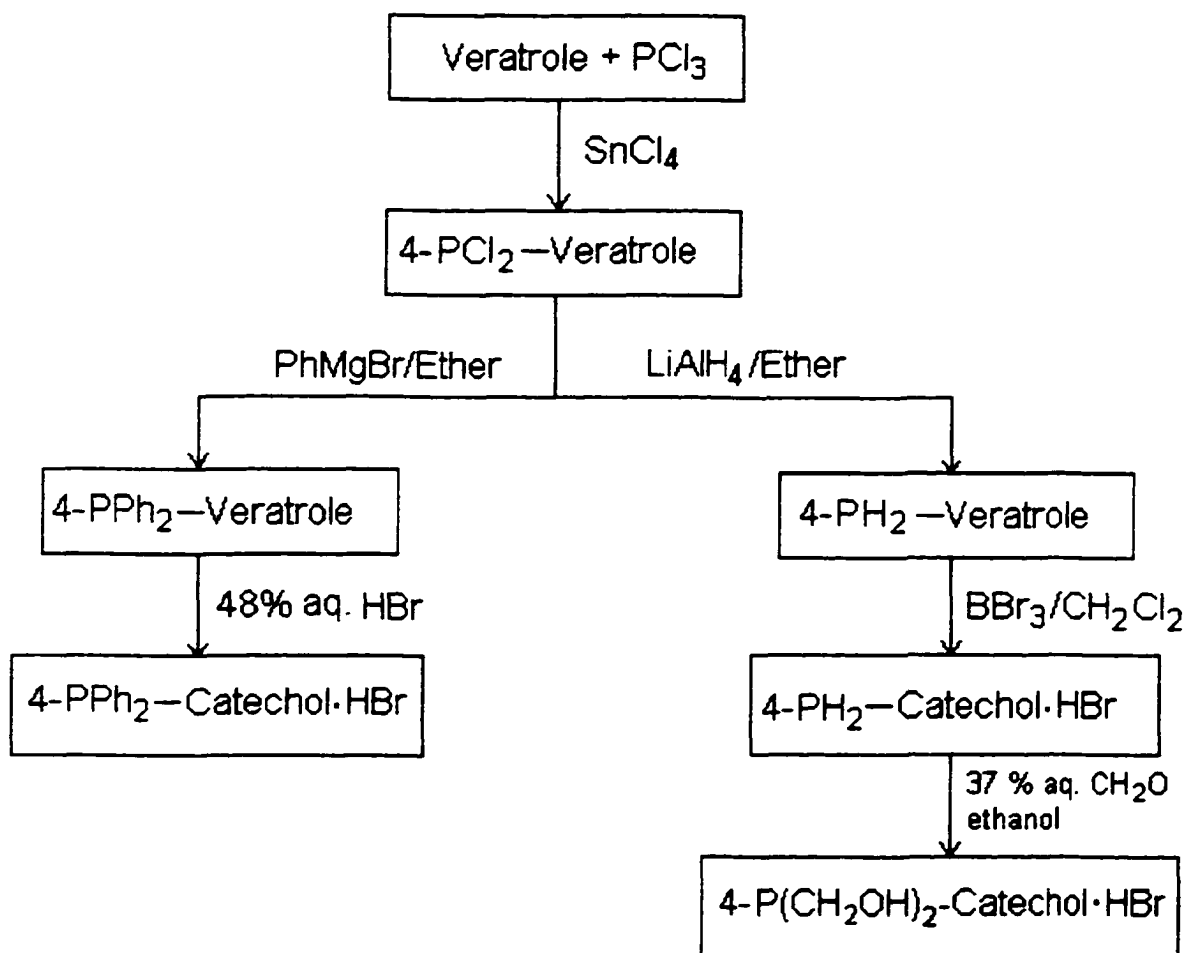
Scheme 2.1 Flowchart of Syntheses of 4-Phosphino-Catechol Hybrid Ligands

65

Results and Discussion

1. Preparation of 4-Dichlorophosphino-Veratrole

4-Dichlorophosphino-Veratrole was synthesized by phosphinylation of 1,2-dimethoxybenzene (Veratrole) using PCl_3 in the presence of $SnCl_4$ catalyst (Rxn. 2.1). [126] At 0.4 mmHg pressure, vacuum distillation afforded 4-Dichlorophosphino-Veratrole (4-PCl_2-Veratrole) at the temperature range of 120 to 135 °C in about 30% yield. The purity of this 4-PCl_2-Veratrole can be increased to nearly 100% after a second distillation, as shown by ^{31}P NMR spectroscopy.

(Rxn. 2.1)
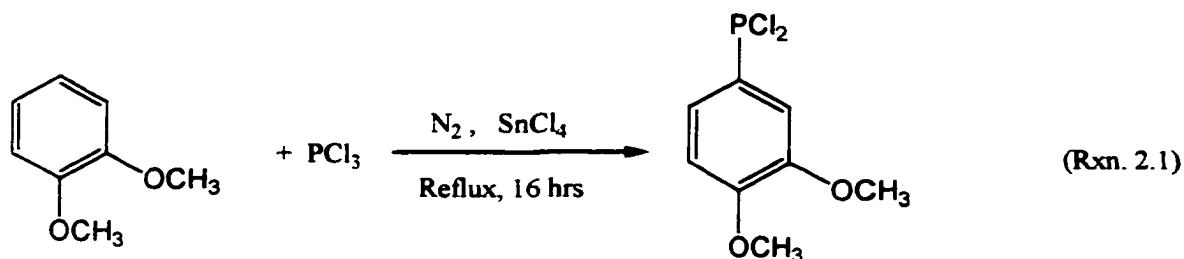
2. Preparation and Characterization of 4-Diphenylphosphino-Veratrole

4-Diphenylphosphino-Veratrole (4-PPh_2-Veratrole) was synthesized by the reaction of PCl_2-Veratrole and excess PhMgBr (Rxn. 2.2).

(Rxn. 2.2)

66
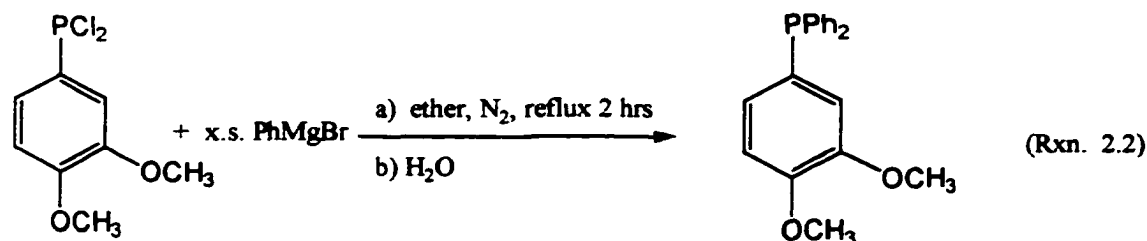
Workup and rotary evaporation gave a yellowish-white solid. Recrystallization of this solid from 95% ethanol afforded pure white product in a yield of 88%. 4-PPh$_2$-Veratrole has been characterized by IR, ^{1}H, ^{13}C{^{1}H} and ^{31}P{^{1}H} NMR spectroscopy, as well as CHN elemental analysis (see experimental section).

3. Preparation and Characterization of 4-Diphenylphosphino-Catechol

Deprotection of the hydroxyl groups of 4-PPh$_2$-Veratrole by 48% aq. HBr afforded the pure white product of 4-PPh$_2$-Catechol as its hydrobromide salt in a yield of 70% (Rxn. 2.3). [127]
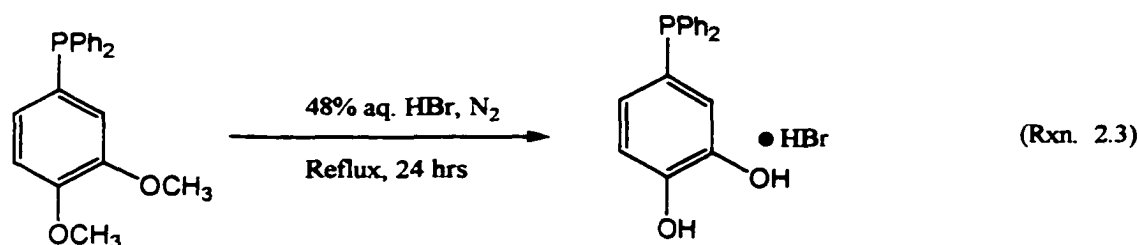
(Rxn. 2.3)

It has been characterized by IR, ^{1}H, ^{13}C{^{1}H} and ^{31}P{^{1}H} NMR spectroscopy, as well as CHN elemental analysis. The three proton signals of catechol are well-resolved in
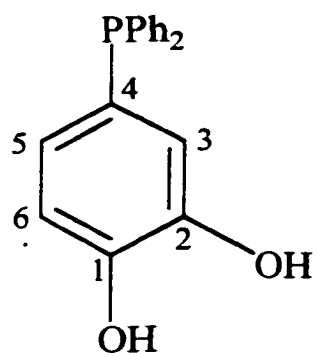
Figure 2.1 4-Diphenyl-phosphino-Catechol

its ^{1}H NMR spectrum (Figure 2.2, in DMF-d$_7$); two doublets of doublets and a higher-field triplet of doublets. In its ^{13}C{^{1}H} NMR spectrum (Figure 2.3), the ^{13}C catechol resonances are also well-ressolved with the six unique ring carbons ranging from δ 147.7 to 116.6. All carbon signals except the carbons at positions *para* to the phosphine are doublets due to the

67
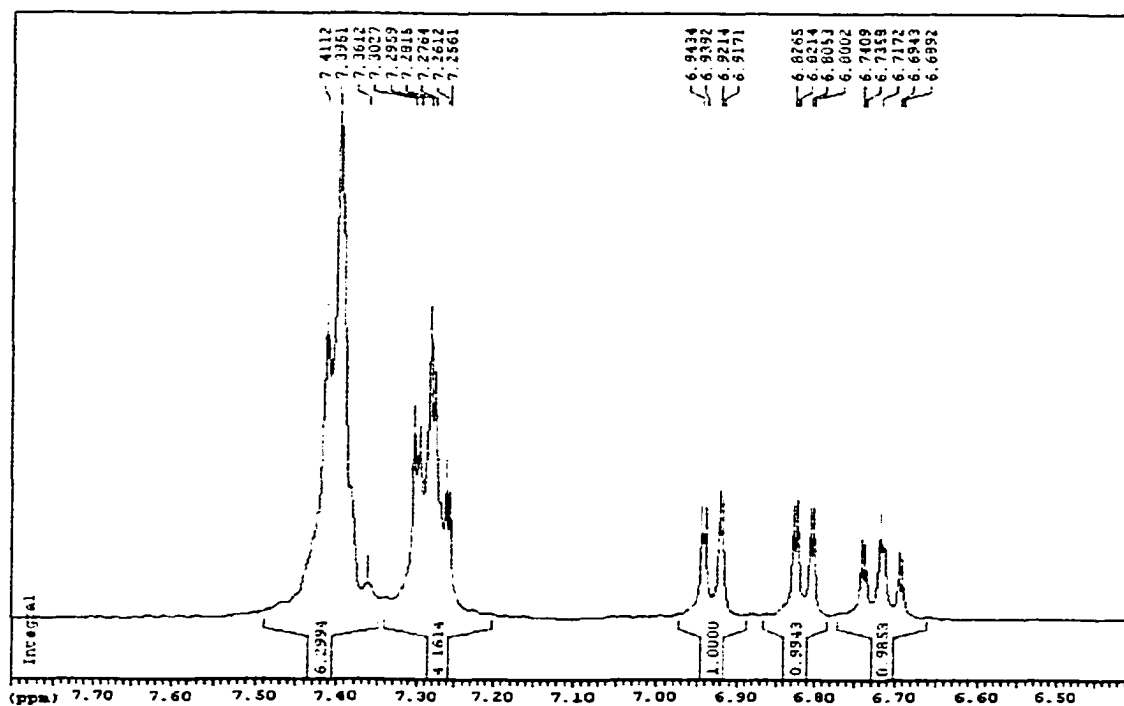
Figure 2.2 ^{1}H NMR spectrum of 4-PPh$_2$-Catechol•HBr in DMF-d$_7$
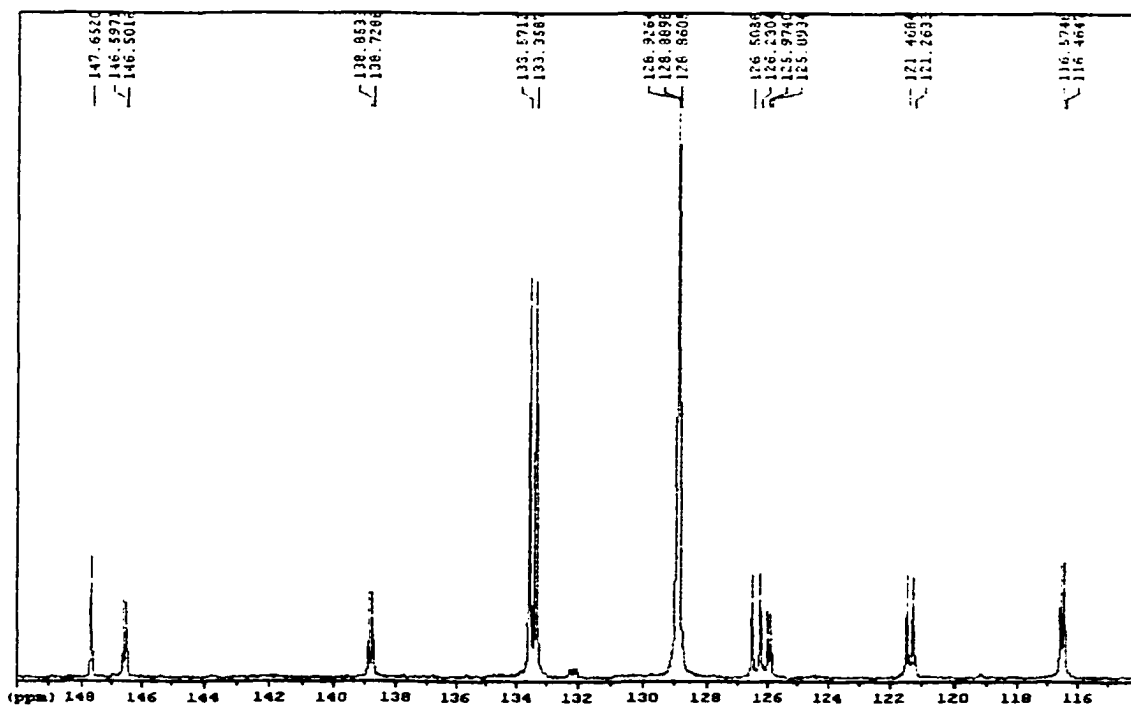
Figure 2.3 ^{13}C{^{1}H} NMR spectrum of 4-PPh$_2$-Catechol•HBr in DMF-d$_7$

68
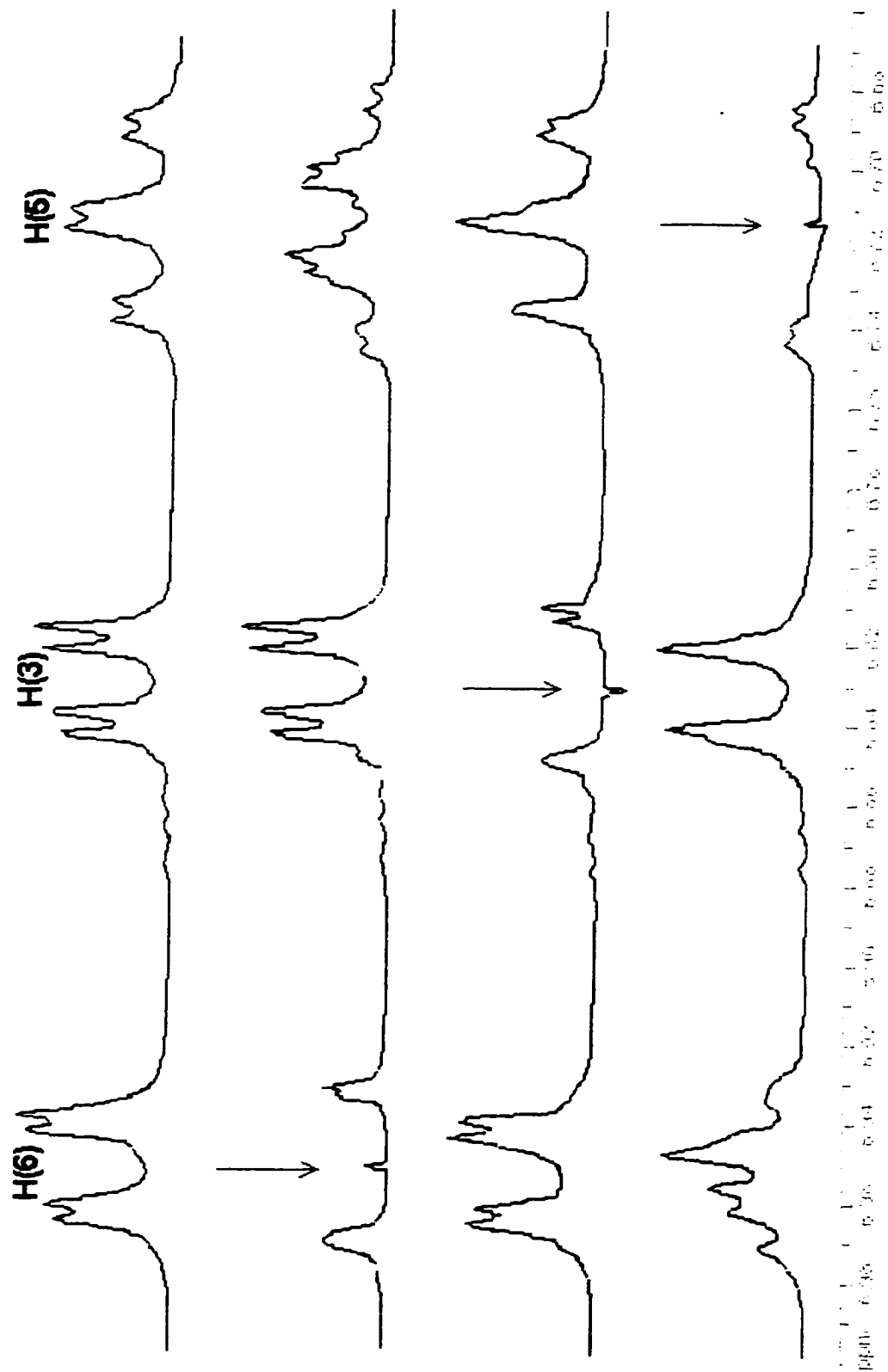
Figure 2.4 Comparative ^1H NMR spectra of selective irradiation experiments of 4-PPh$_2$-Catechol·HBr in DMF-d$_7$

69
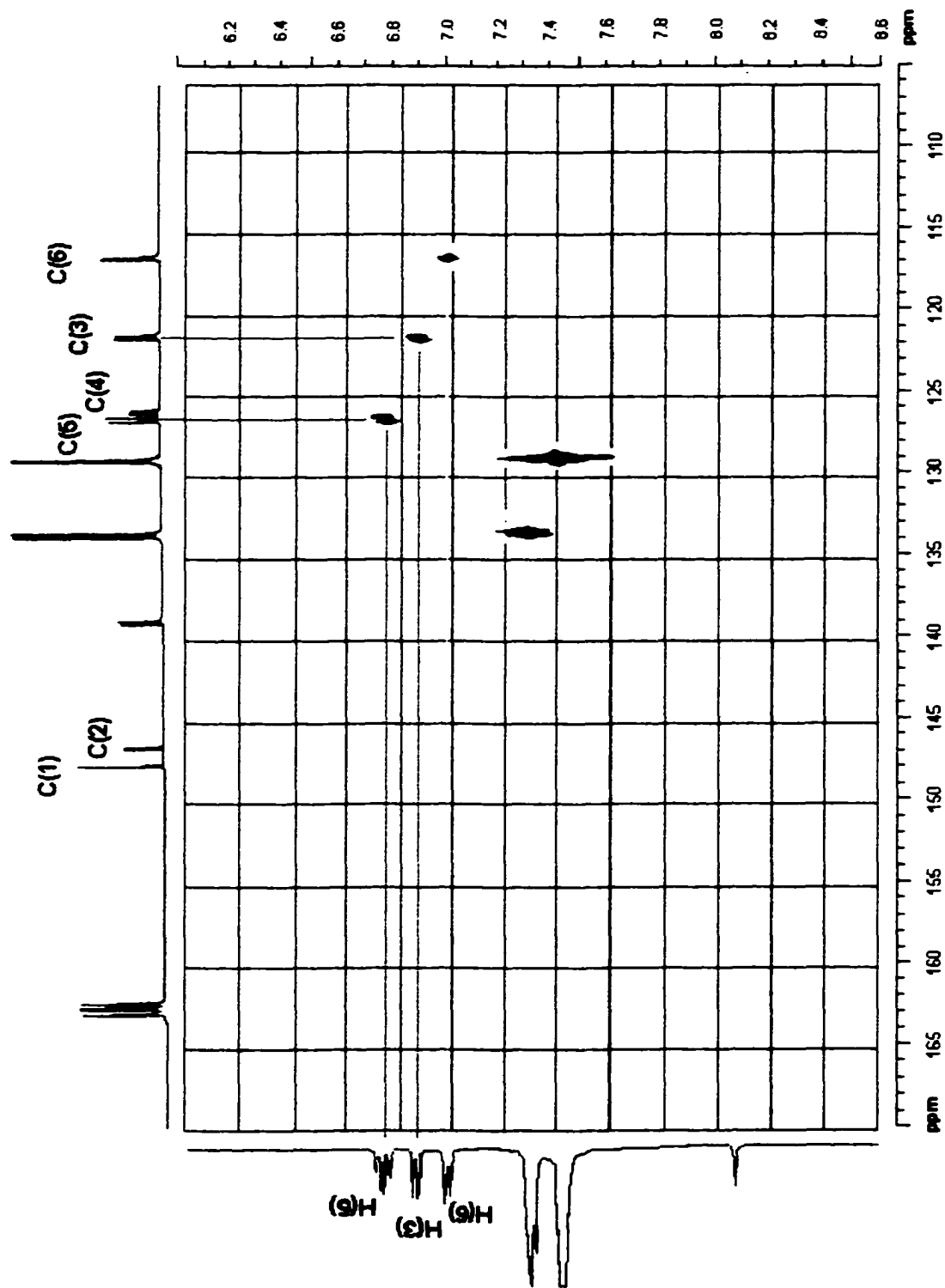
Figure 2.5 ^{1}H-^{13}C HETCOR NMR Spectrum of Ligand PPh$_2$-Cat·HBr in DMF-d$_7$

70

couplings to ^{31}P (I = 1/2, 100%).

Assignments of the catechol protons have been made by selective irradiation NMR experiments (Figure 2.1, 2.4). With the proton assignments, the catechol carbon signals have also been unambiguously assigned from the ^1H-^{13}C HETCOR NMR spectrum (Figure 2.5).

4. Preparation and characterization of 4-Dihydrophosphino-Veratrole

Reduction of 4-Dichlorophosphino-Veratrole by LiAlH₄ in ether gave a clear oil, 4-Dihydrophosphino-Veratrole (4-PH₂-Veratrole) in a yield of 71% (Rxn. 2.4).

(Rxn. 2.4)
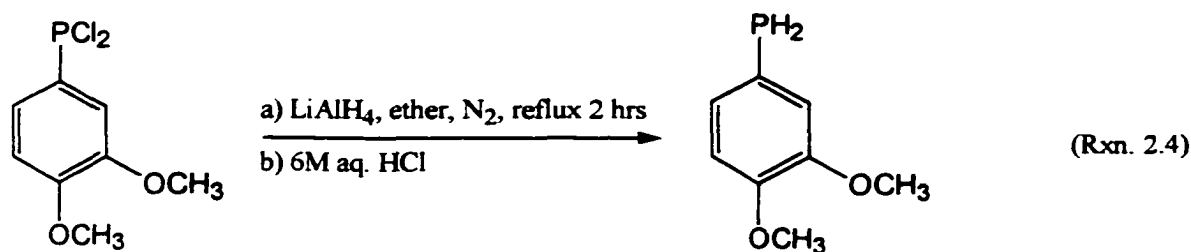
4-PH₂-veratrole has been characterized by IR, ^1H, ^{31}P and $^{13}C\{^1H\}$NMR spectroscopy, as well as by EI mass spectrometry.[128] Its proton-coupled ^{31}P NMR spectrum (CDCl₃) (Figure 2.6) shows a triplet of triplets because of $^1J_{P-H}$ and $^3J_{P-H}$ couplings to two pairs of equivalent protons respectively. Its EI mass spectrum clearly shows the molecular peak at 170 m/z (♦), and several major fragments [(♦-CH₃): 155 m/z; (♦-PH): 138 m/z; (♦-PH-CH₃): 123 m/z; (♦-PH-2CH₃): 109 m/z; (♦-PH-2O-2CH₃): 77 m/z] (Figure 2.7). Its IR spectrum shows characteristic medium stretching bands of a PH₂- group at 2368, 2302 cm⁻¹.

71
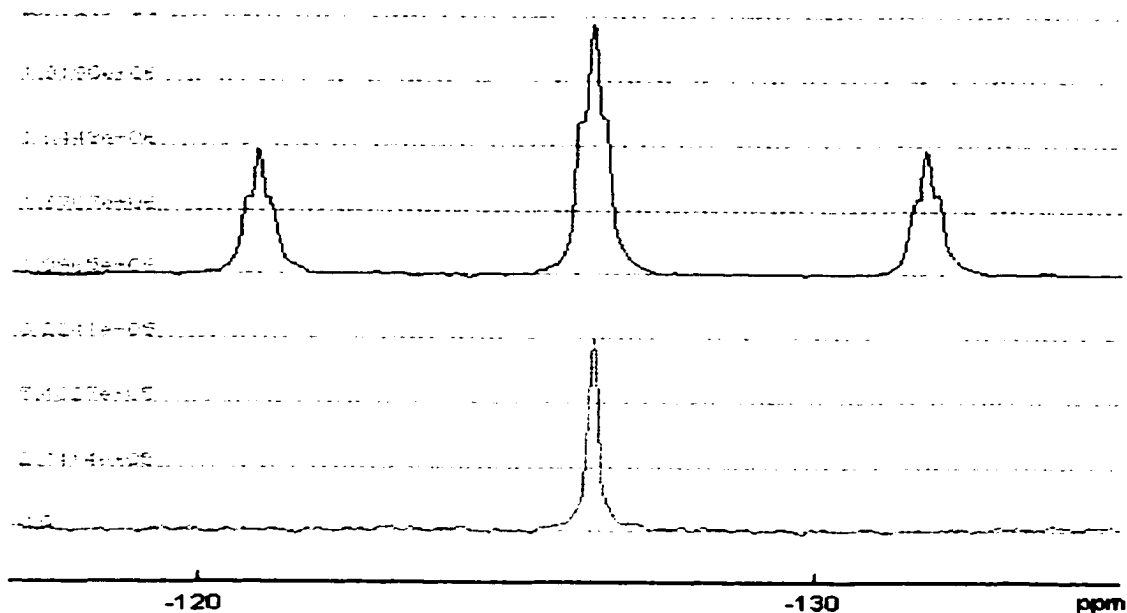
Figure 2.6 Comparative ^{31}P NMR spectra of 4-PH$_2$-Veratrole in CDCl$_3$. The bottom one is proton-decoupled, while the upper one is proton-coupled ($^1J_{P-H}$ = 201.4 Hz, $^3J_{PH}$ = 6.1 Hz).
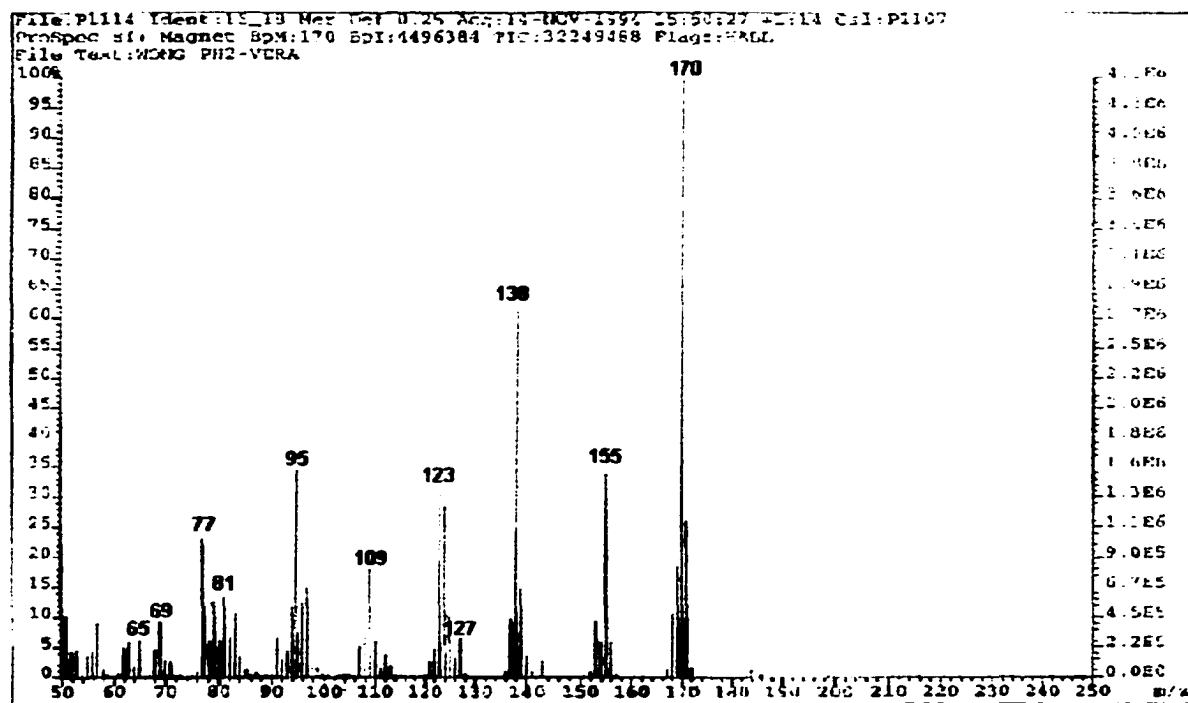
Figure 2.7 Low-resolution EI mass spectrum of 4-PH$_2$-Veratrole

72

5. Preparation and characterization of 4- Dihydrophosphino-Catechol

Deprotection of 4-PH$_2$-veratrole was achieved by reaction with BBr$_3$ in methylene chloride to give the hydrobromide salt of 4-Dihydrophosphino-Catechol (PH$_2$-Catechol•HBr) in a yield of 57% (Rxn. 2.5).

a) BBr$_3$/CH$_2$Cl$_2$,
N$_2$,-78℃

b) Methanol

(Rxn. 2.5)
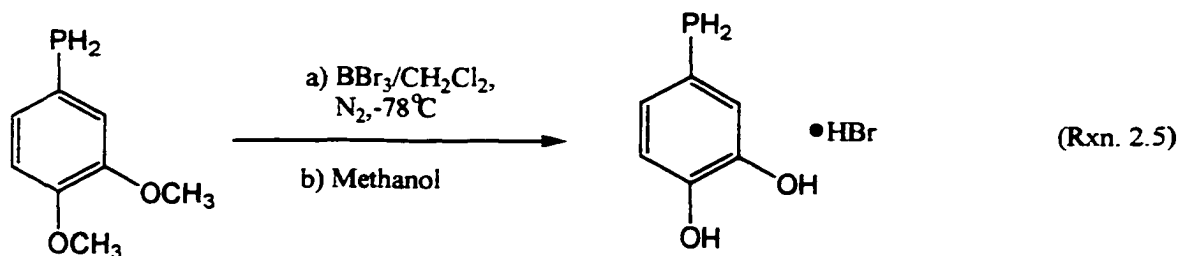
This hydrobromide salt has been characterized by IR, ^{1}H, ^{13}C{^{1}H}, ^{31}P NMR spectroscopy, and CHN elemental analysis, as well as by EI mass spectrometry.

The three proton signals of catechol are again well-resolved in its ^{1}H NMR spectrum (Figure 2.8, in CD$_3$OD); a doublet of doublets at δ 6.91, a doublet of doublets of doublets at δ 6.82, and a doublet of doublets at δ 6.69. In its ^{13}C{^{1}H} NMR spectrum (Figure 2.9), the ^{13}C catechol resonances are also well-resolved with the six unique ring carbon shifts ranging from δ 147.2 to 116.7. The couplings of ^{13}C-^{31}P are observable in all carbon resonances except the *ipso*-C(1). Its IR spectrum shows characteristic medium stretching bands typical of PH$_2$- groups at 2346 and 2290 cm^{-1}.

Its EI mass spectrum shows the molecular peak at 142 mz (♦), and a major fragment [(♦-PH), 100%] at 110 m/z (Figure 2.10).

Potentiometric titration of the ligand salt against standard base showed three pK$_a$'s. The first was calculated to be at 1.8, the second 8.8, and the third at around 13.[129]

73
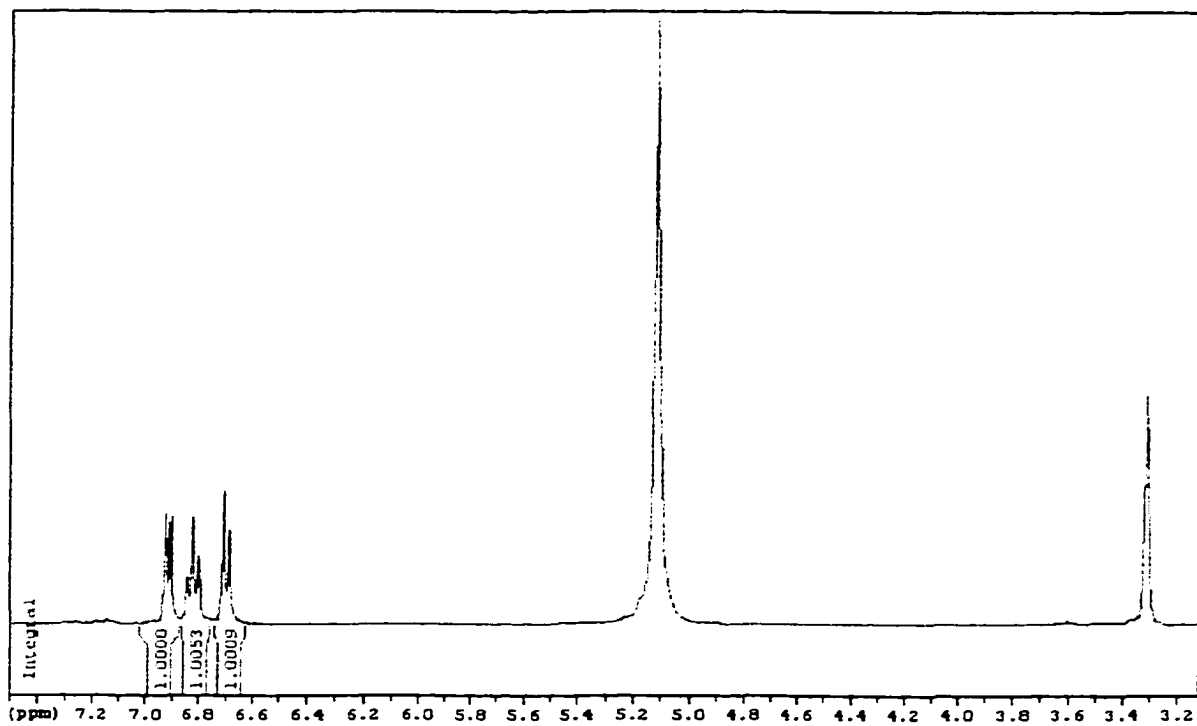
Figure 2.8 ^{1}H NMR spectrum of 4-PH$_2$-Catechol•HBr in CD$_3$OD
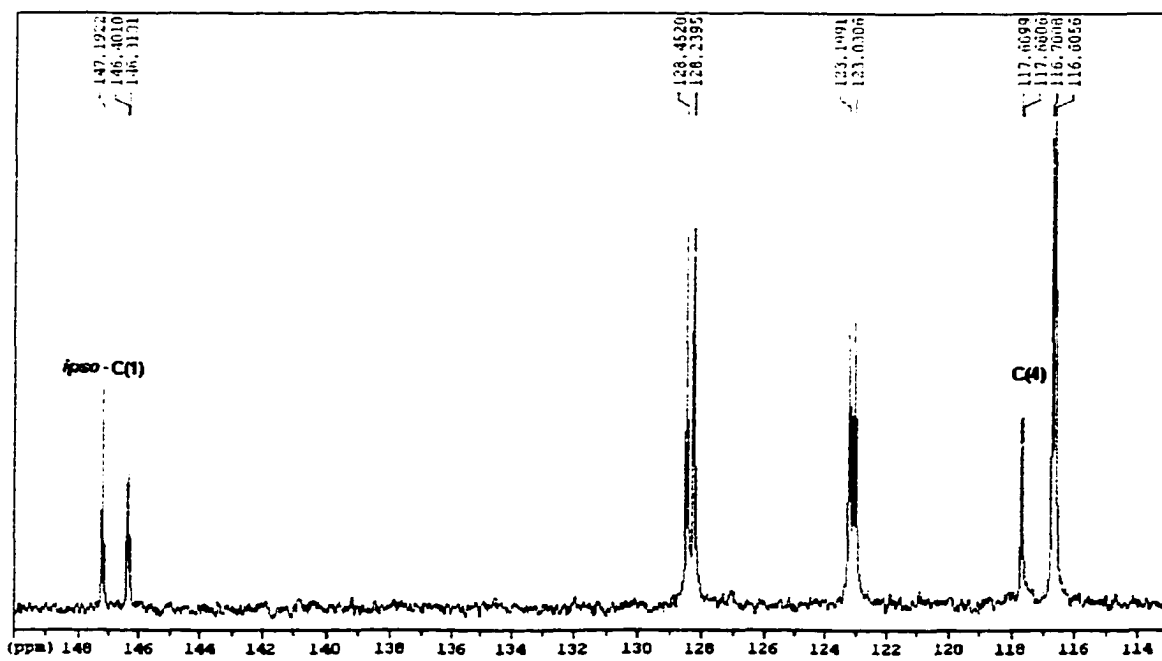
Figure 2.9 ^{13}C{^{1}H} NMR spectrum of 4-PH$_2$-Catechol•HBr in CD$_3$OD

74
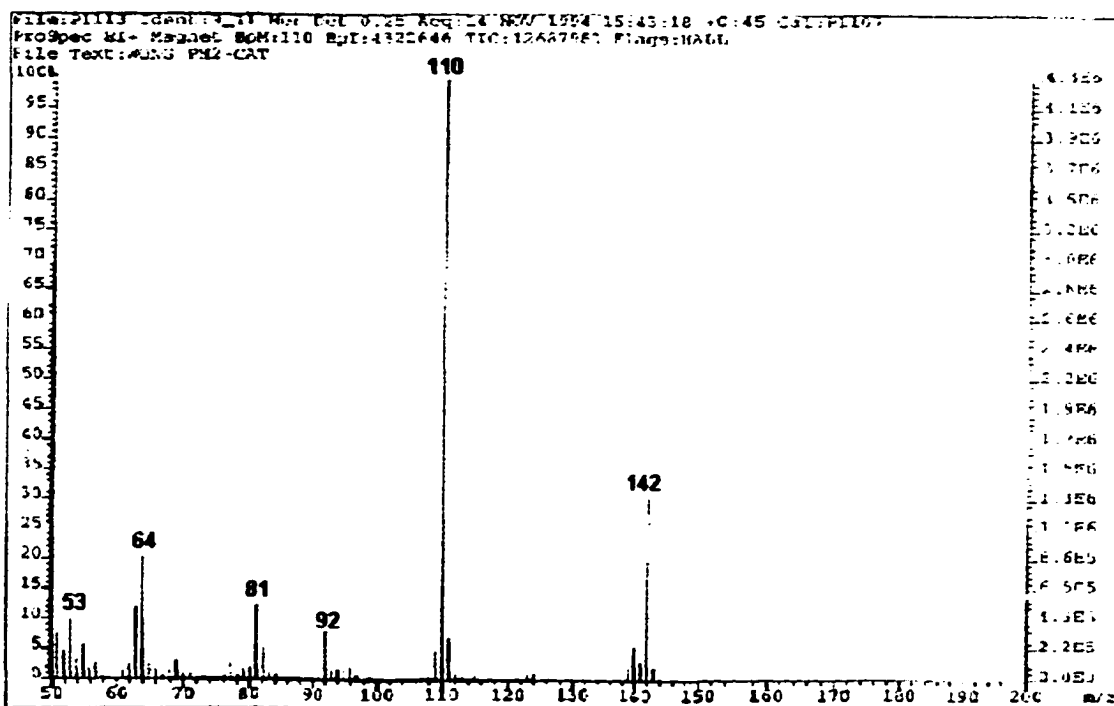
Figure 2.10 Low-resolution EI mass spectrum of 4-PH$_2$-Catechol

6. Preparation and characterization of 4-Dihydroxymethylphosphino-Catechol

The hydrobromide salt of 4-P(CH$_2$OH)$_2$-Catechol was synthesized by the reaction of 4-PH$_2$-Catechol•HBr and formaldehyde in absolute ethanol in yields of around 90 % (Rxn. 2.6).[130]
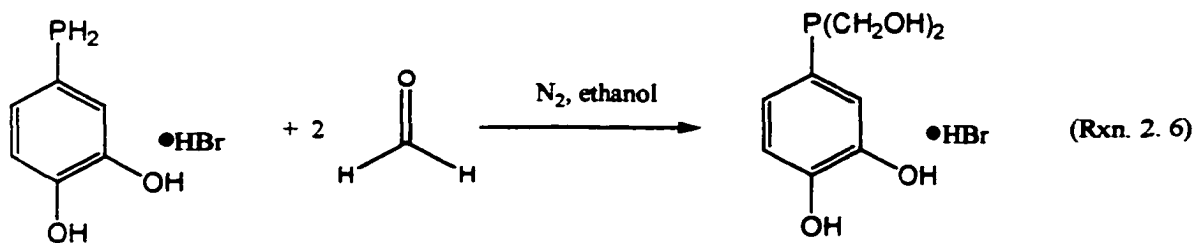
(Rxn. 2. 6)

75

This hydrobromide salt has been characterized by IR, ^{1}H, ^{13}C{^{1}H } and ^{31}P{^{1}H}

NMR spectroscopy, as well as CHN elemental analysis.

In its ^{1}H NMR spectrum (Figure 2.11), two catechol proton resonances are

overlapped at δ 7.28, the third one is a doublet of doublets at δ 6.91.
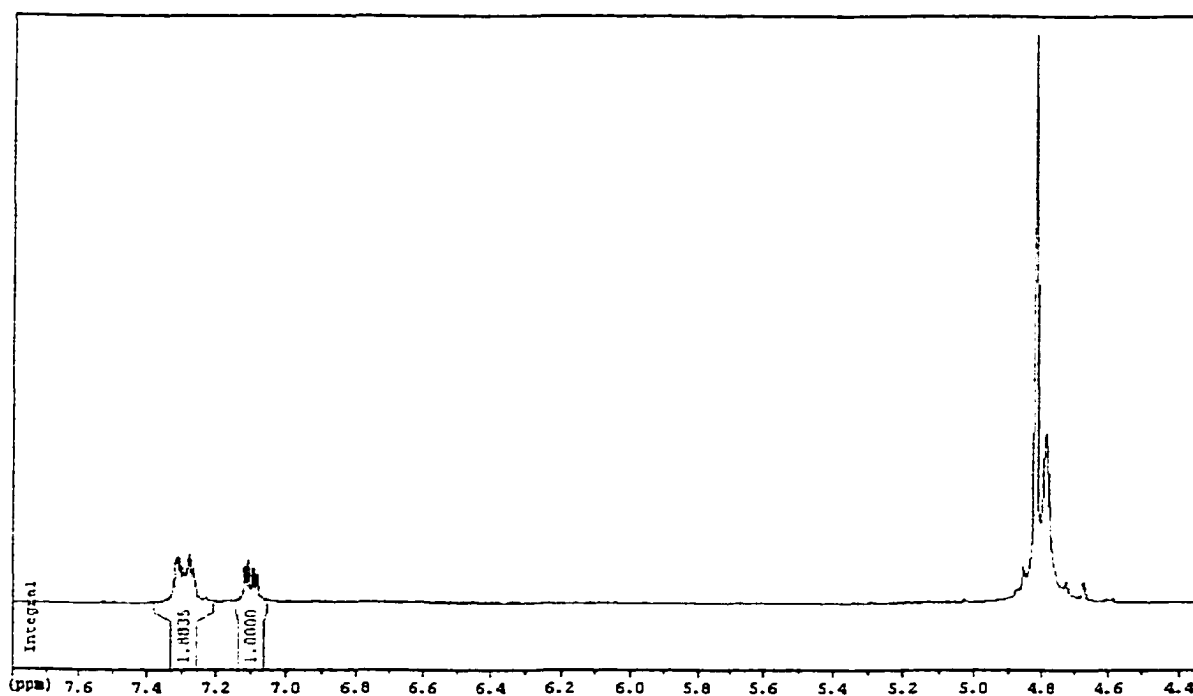
Figure 2.11 ^{1}H NMR spectrum of 4-P(CH$_2$OH)$_2$-Catechol•HBr in D$_2$O

As shown in Figure 2.12, the ^{13}C catechol resonances are well-ressolved with the

six unique ring carbon shifts ranging from δ 154.0 to 104.5. The ^{13}C-^{31}P couplings are

observable in all carbon resonances including the ipso-C(1). Compared to those in 4-PH$_2$-

Catechol•HBr (2.7 Hz)   and 4-PPh$_2$-Catechol•HBr (11.3 Hz), the coupling constant

between ^{31}P and C(4) in this ligand (78.6 Hz) is significantly larger. This is because the

basicity of the phosphine group in this compound has been significantly increased by its

two hydroxymethyl substituents, such that the P atom of 4-P(CH$_2$OH)$_2$-Catechol•HBr

76
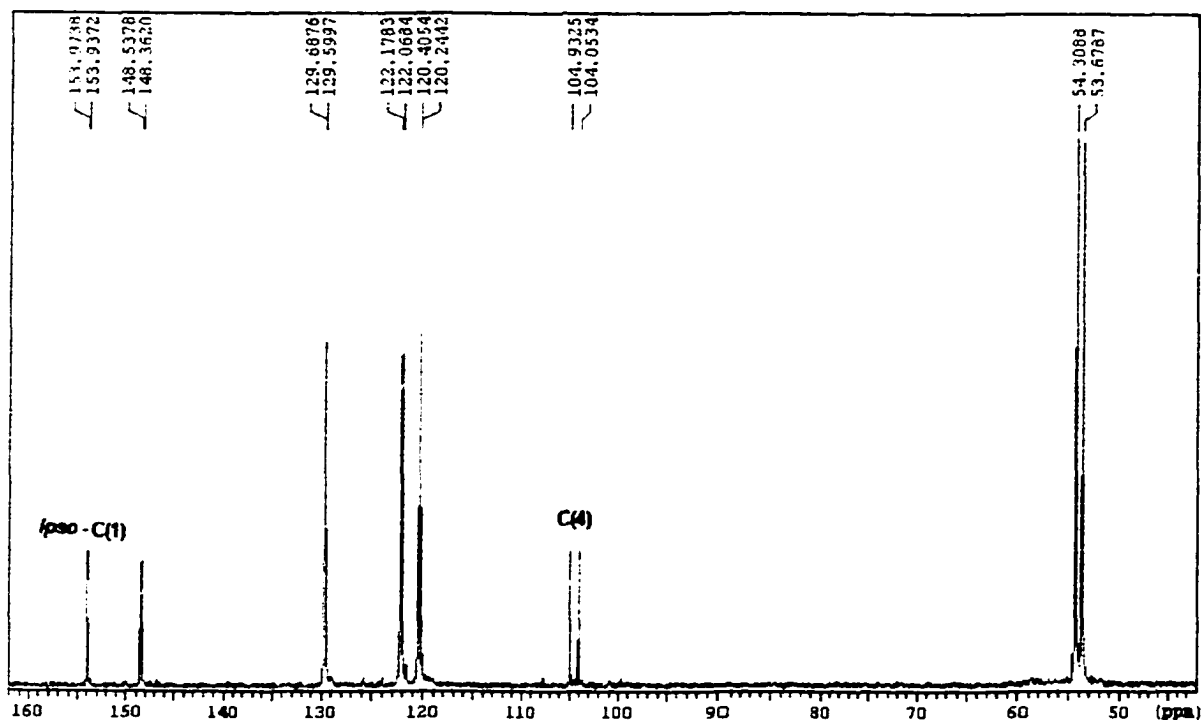
Figure 2.12 $^{13}C\{^1H\}$ NMR spectrum of 4-P(CH$_2$OH)$_2$-Catechol•HBr in D$_2$O

remains protonated even in D$_2$O solution. This explanation was further supported by the ^{31}P chemical shift of +19.86 ppm in its ^{31}P$\{^1H\}$ NMR spectrum (δ -6.73 for 4-PPh$_2$-Catechol•HBr; -127.2 for 4-PH$_2$-Catechol•HBr which indicate unprotonated phosphine groups).

In summary, 4-Dichlorophosphino-Veratrole (4-PCl$_2$-Veratrole) is an excellent precursor for the syntheses of 4-Phosphino-Catechols. From it, three new ligands, 4-Diphenylphosphino-Catechol (4-PPh$_2$-Catechol), 4-Dihydrophosphino-Catechol (4-PH$_2$-Catechol), and 4-Dihydroxymethylphosphino-Catechol [4-P(CH$_2$OH)$_2$-Catechol], have been synthesized and characterized, as well as their veratrole precursors in which the catechol group is protected in the form of veratrole. The three ligands are all isolated in the form of hydrobromide salts in the solid-state. While 4-PPh$_2$-Catechol•HBr and 4-PH$_2$-Catechol•HBr are deprotonated upon dissolving into solutions of donor solvents, 4-P(CH$_2$OH)$_2$-Catechol•HBr remains protonated in water.

78

Chapter III

Syntheses and Characterization of Monometallic Complexes

In order to explore the coordination chemistry of our designed hybrid ligands, two types of monometallic complexes, phosphine-coordinated and catecholate-coordinated metal complexes, have been synthesized and characterized.

1. Phosphine-Coordinated Metal Complexes

The phosphine binding sites of 4-Phosphino-Catechols are typical soft donors. When they coordinate to soft metal ions, two-fold, three-fold or four-fold symmetry at the metal centers may be generated. Because their catechol groups also coordinate, albeit weakly, to soft metal ions, 4-Phosphino-Catechols cannot be used to synthesize the exclusively phosphine-coordinated complexes of soft metal ions directly. Instead, 4-Phosphino-Veratroles were used. The hydroxyl groups are protected in the form of methoxy groups which can then be deprotected by reaction with BBr_3 in methylene chloride after initial phosphine complexation with soft metal ions.

Results and Discussion

(a) Preparation and Characterization of Phosphine-Coordinated Metal Complexes of Two-fold Symmetry

In order to ensure the formation of phosphine-coordinated metal complexes of two-fold symmetry with *trans*-configuration, (1) the soft-metal precursors must have only

two available coordination sites, (2) the two substituent R groups of 4-Phosphino-Veratroles (4-PR$_2$-Veratroles) must be bulky enough to favor the *trans*-configuration at the metal center, which is essential for the formation of mixed-metal clusters.

Based on these considerations, PdBr$_2$•2PhCN, K$_2$PtCl$_4$, RuCl$_3$•3H$_2$O and Cr(CO)$_4$ (Piperidine)$_2$ were used as soft-metal precursors, 4-PPh$_2$-Veratrole was used as the ligand.

Syntheses and Characterization of *trans*-PdX$_2$(4-PPh$_2$-Veratrole)$_2$ (X = Cl, Br, I):

Trans-PdX$_2$(4-PPh$_2$-Veratrole)$_2$ (X = Cl, Br, I) were synthesized in good yields according to Scheme 3.1. Detailed spectral and analytical data of these products are presented in their respective experimental sections.
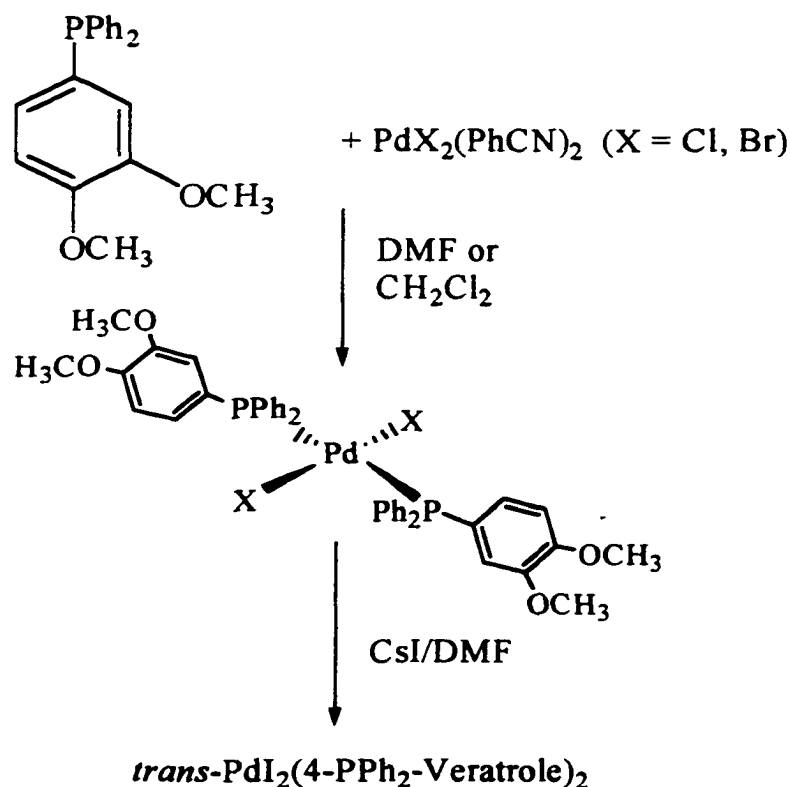
Scheme 3.1 Syntheses of PdX$_2$(4-PPh$_2$-Veratrole)$_2$ (X = Cl, Br, I)

80

These *trans*-complexes have been characterized by IR, $^{31}P\{^1H\}$, ^1H, $^{13}C\{^1H\}$ NMR spectra as well as CHN elemental analyses. The singlet $^{31}P\{^1H\}$ NMR PPh$_2$ signal is downfield shifted from the initial δ -5.35 for the free ligand to δ 22.4 for the bromo complex, δ 23.4 for the chloro complex, and δ13.7 for the iodo complex, which indicates that the PPh$_2$- group have been coordinated to Pd(II), and that either the *cis*- or the *trans*- isomers of PdX$_2$(4-PPh$_2$-Veratrole)$_2$ has been formed. This result is also supported by its ^1H and $^{13}C\{^1H\}$ NMR spectra, both of which show one set of veratrole and phenyl signals. Characteristically, their $^{13}C\{^1H\}$ NMR spectra exhibited both veratrole and phenyl ring carbon resonances virtual triplets (Figure 3.1, see inset) which were doublets in the spectrum of the free ligand. This strongly suggests a *trans*-phosphine coordination mode at the Pd(II) center. [131]
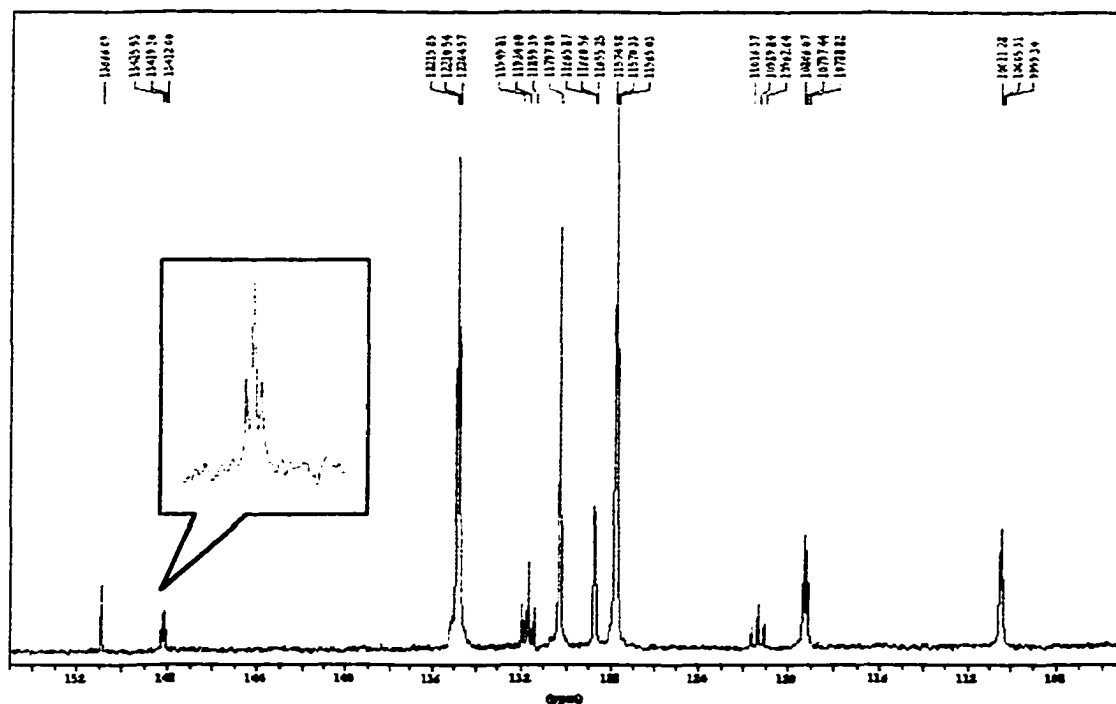
Figure 3.1 $^{13}C\{^1H\}$ NMR spectrum of *trans*-PdBr$_2$(4-PPh$_2$-Veratrole)$_2$ in CDCl$_3$

81

Why do $^{13}C\{^{1}H\}$ virtual triplets indicate a *trans*-confirguration of a *bis*-phosphine metal complex? From the studies which were carried out by Redfield and coworkers on *bis*-phosphine metal complexes,[132] it has suggested that a virtual triplet will be observed in the ^{13}C spectrum of the AXX' system (A = ^{13}C, X, X' = ^{31}P) when: $|J_{AX}\text{-}J_{AX'}|^2 < (8\ J_{XX'} \times \Delta v_{1/2})$. In *bis*-phosphine metal complexes, the $^1J_{PC}$ values will be only 25-35 Hz, while $\Delta v_{1/2}$ is usually greater than 1 Hz.[133] Thus a $J_{XX'}$ of greater than 153 Hz will be required to give a virtual triplet.

As seen in Figure 3.2, the simulation results of AXX' systems show that a virtual triplet *ipso*-carbon resonance results if $J_{XX'}$ is around 500 Hz.

In *trans*- *bis*-phosphine PdX_2 and PtX_2 (X = Cl, Br, I) complexes, $J_{XX'}$ values are typical larger than 440 Hz while they are usually less than 20 Hz in *cis*-complexes.[134] Thus the observation of virtual triplets in the $^{13}C\{^{1}H\}$ NMR spectrum of a *bis*-phosphine metal complex is a strong evidence that the complex is in a *trans*-configuration.
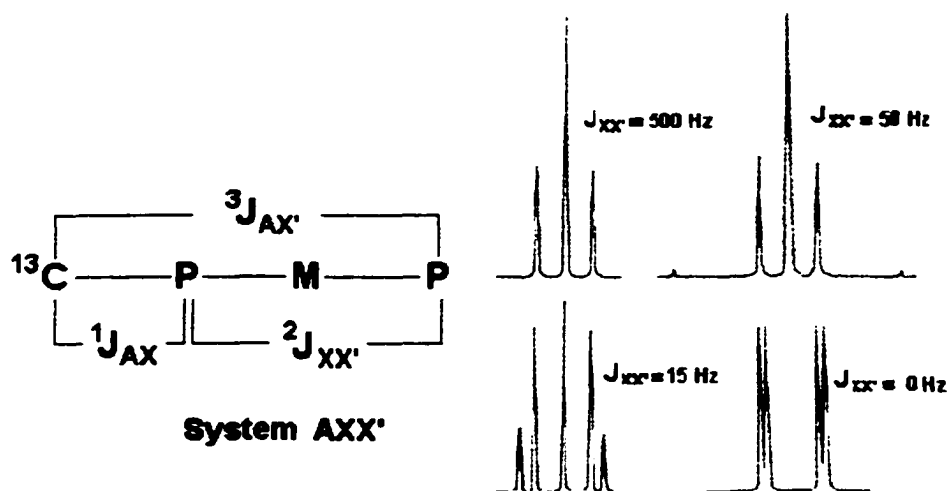
Figure 3.2 Computer simulations for the system AXX' where $^1J_{AX}$ = 25 Hz, $^3J_{AX'}$ = 3 Hz and $^2J_{XX'}$ is varied. When $^2J_{XX'}$ is around 500 Hz, the $^{13}C\{^{1}H\}$ resonance becomes a virtual triplet.

82

Syntheses and Characterization of *trans*-Cr(CO)$_4$(4-PPh$_2$-Veratrole)$_2$:

Trans-Cr(CO)$_4$(4-PPh$_2$-Veratrole)$_2$ was synthesized in a good yield by the reaction of one equivalent of Cr(CO)$_4$(Piperidine)$_2$ with two equivalents of 4-PPh$_2$-Veratrole in methylene chloride (Rxn. 3.1).

$$Cr(CO)_4(Piperidine)_2 + 2 \ 4\text{-PPh}_2\text{-Veratrole}$$

$$\xrightarrow{\text{CH}_2\text{Cl}_2} trans\text{-} Cr(CO)_4(4\text{-PPh}_2\text{-Veratrole})_2$$

(Rxn. 3.1)
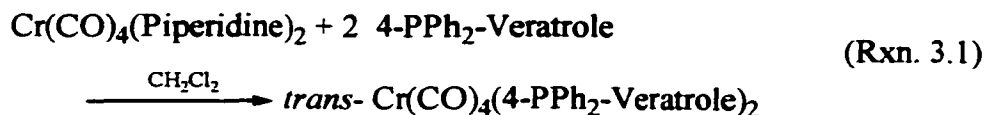
Addition of diethyl ether into the light yellow solution gave a fluffy, needle-like product as a precipitate in yields of around 86%. This complex has been characterized by IR, ^{31}P{^{1}H}, ^{1}H, ^{13}C{^{1}H} NMR and CHN elemental analyses. Besides the already discussed virtual triplets in its ^{13}C{^{1}H} NMR spectrum, a single triplet at 221.1 ppm ($^2J_{CO-Cr-P}$ = 12.9 Hz) directly indicates (Figure 3.3) that the complex is in the *trans*-
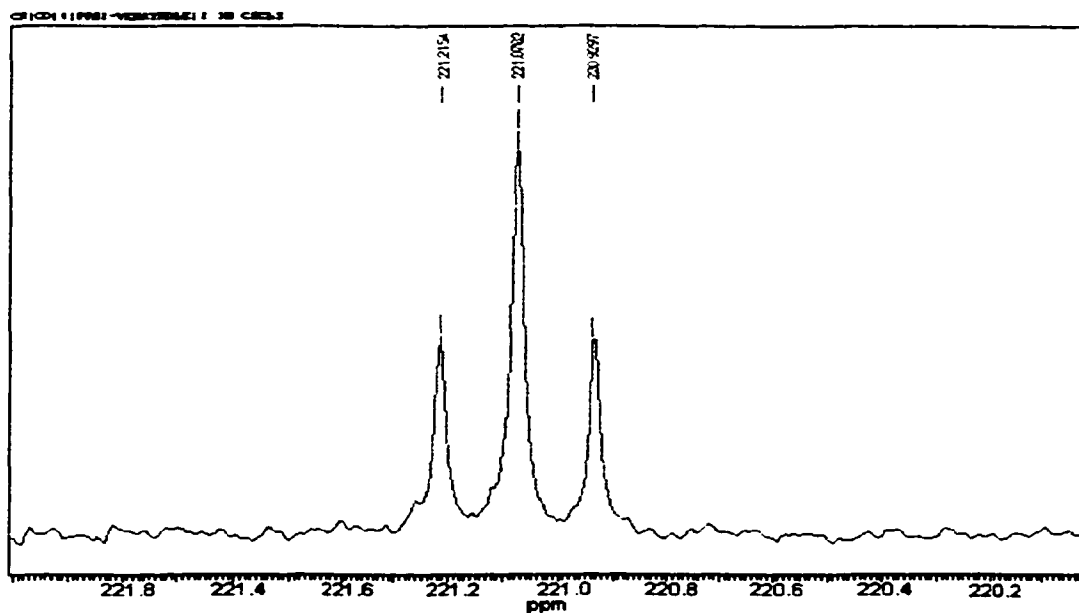
Figure 3.3 The triplet ^{13}C{^{1}H} resonance due to the four carbonyl groups of Cr(CO)$_4$(4-PPh$_2$-Veratrole)$_2$ in CDCl$_3$

83

configuration since a cis-geometry will result in two different types of CO's and hence two triplet resonances. This assignment is also supported by a strong single stretching band at 1856 cm⁻¹ in its IR spectrum (KBr pellet) since four bands are expected for a cis-confirguration.

Syntheses and Characterization of PtCl₂(4-PPh₂-Veratrole)₂:

PtCl₂(4-PPh₂-Veratrole)₂ was synthesized by the biphasic reaction of one equivalent of K₂PtCl₄ in water with two equivalents of 4-PPh₂-veratrole in methylene chloride (Rxn. 3.2). The biphasic mixture was stirred until the yellow color of the

$$K_2PtCl_4 + 2\ 4\text{-}PPh_2\text{-Veratrole} \xrightarrow{\ CH_2Cl_2/H_2O\ }$$

(Rxn. 3.2)

$$PtCl_2(4\text{-}PPh_2\text{-Veratrole})_2\ \text{(in CH}_2\text{Cl}_2\text{)} + 2KCl\ \text{(in H}_2\text{O)}$$
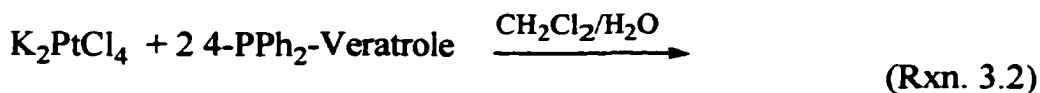
aqueous phase was gone. This product PtCl₂(PPh₂-Veratrole)₂ can then be isolated from the CH₂Cl₂ phase in a yield of 94%. This complex has been characterized by IR,

peak	ppm	freq	amp
1	65.154	2363.28	768085.00
2	14.404	522.46	3299887.25
3	-36.346	-1318.36	756121.88
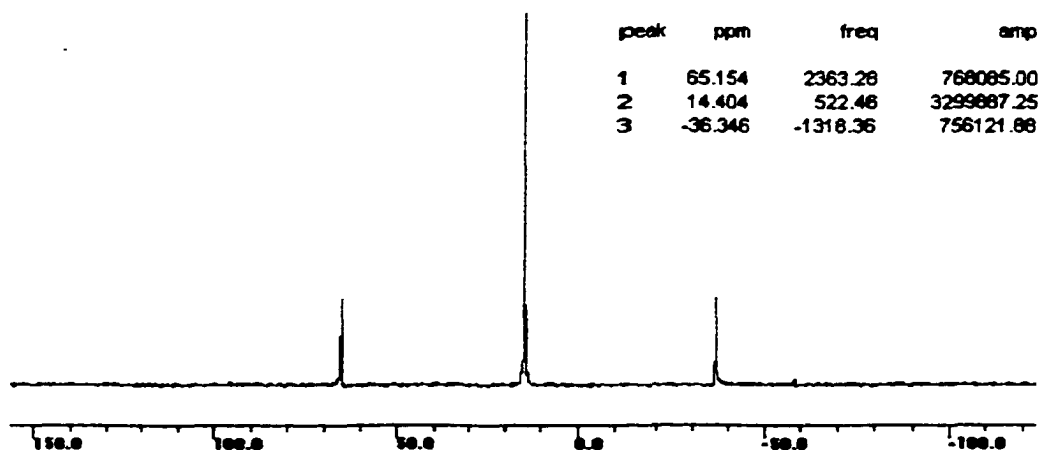
Figure 3.4 ³¹P{¹H} NMR spectrum of PtCl₂(4-PPh₂-Veratrole)₂. The satellites (¹J₁₉₅Pt-P = 3682 Hz) are caused by ¹⁹⁵Pt (I = 1/2, 33.8 %).

84

$^{31}P\{^1H\}$, ^1H, $^{13}C\{^1H\}$ NMR and CHN elemental analysis. Its $^{31}P\{^1H\}$NMR spectrum (Figure 3.4) showed two satellites with $^1J_{195Pt-P}$ (3682 Hz) indicative of a *cis*-conformation of the complex since the $^1J_{195Pt-P}$ value in a *trans*-complex should be only around 2500 Hz.[135]

.

(b) Preparation and Characterization of Phosphine-Coordinated Metal Complexes with Three-fold Symmetry

RuCl₂(4-PPh₂-Veratrole)₃ is the only phosphine-coordinated metal complex we successfully synthesized which has three-fold symmetry. It was prepared by the reaction of RuCl₃•3H₂O and excess 4-PPh₂-Veratrole in refluxing ethanol under the protection of a N₂ atmosphere (Scheme 3.2). The reaction was complete when the mixture turned to a

$$2\ RuCl_3\bullet3H_2O + 6\ 4\text{-PPh}_2\text{-Veratrole} + CH_3CH_2OH$$

$$\downarrow N_2, \text{reflux}$$
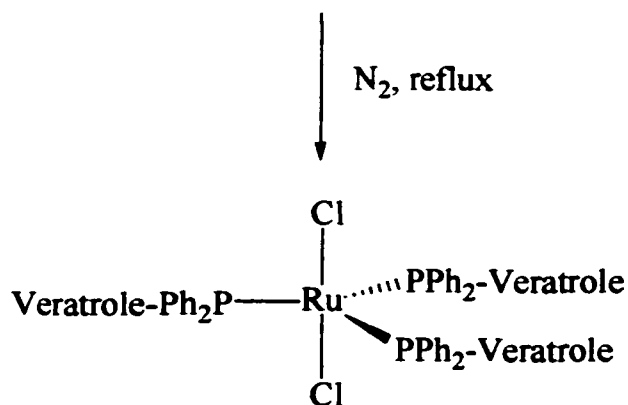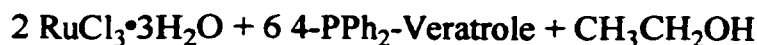
Scheme 3.2 Synthesis of RuCl₂(4-PPh₂-Veratrole)₃

clear dark-brown solution in 5 hours. Upon chilling, the product came out of the solution as a dark-brown solid in a yield of 85%. The oxidation state of ruthenium had changed from (III) to (II) because of ethanol reduction. Due to the bulky phosphine environment, the coordination number of ruthenium(II) is only five and the geometry trigonal

85

bypyramidal. This complex has been characterized by IR, $^{31}P\{^1H\}$, ^1H, $^{13}C\{^1H\}$ NMR, as well as CHN elemental analysis. A sharp singlet in its $^{31}P\{^1H\}$ NMR spectrum indicates that this complex indeed has three-fold symmetry. This result is supported by its ^1H and $^{13}C\{^1H\}$ NMR spectra, both of them showing one set of veratrole signals.

(c) Attempted Demethylation of Catechol Groups of Phosphine-Coordinated Veratrole Complexes of 2-fold or 3-fold symmetry

The conversion of veratrole to catechol of the phosphine-coordinated metal complexes of 2-fold or 3-fold symmetry described above was carried out by their reactions with BBr_3 in methylene chloride solution.

Surprisingly, all the products have very poor solubility in acetone, DMSO, ether, methylene chloride, chloroform, acetonitrile, and protic solvents. They are only slightly soluble in DMF. The absence of the veratrole methoxy resonances at δ 3.7 ppm in their ^1H NMR spectra demonstrated that the deprotection reactions were complete. However, the ^1H, $^{13}C\{^1H\}$, and $^{31}P\{^1H\}$ NMR spectra were far too complicated to interpret.

In the cases of the halido complexes, the substitution reaction of M-halides with generated catechol groups may have caused oligomer formation. As for the other complexes with 2-fold or 3-fold symmetry, since the coordination numbers at these soft metal centers are only 4 or 5, these low coordination numbers render the soft metal centers susceptible to nucleophilic attack. Thus, the intermolecular substitution of catechol groups liberated by the deprotection with other metal centers could have also led to the formation of an oligomeric or polymeric product which contains indiscriminate P- and catecholate coordination to each soft metal ion.

(d) Preparation and Characterization of Phosphine-Coordinated Metal Complexes of Four-fold Symmetry

Preparation and Characterization of RuCl₂ (4-PH₂-Veratrole)₄:

RuCl₂(4-PH₂-veatrole)₄ was synthesized by the reaction of RuCl₃•3H₂O and excessive 4-PH₂-Veratrole in refluxing ethanol under a N₂ atmosphere (Scheme 3.3). The reaction was complete in 4 hrs, as shown by a color change from dark-brown to

$$RuCl_3 + x.s. \ 4\text{-}PH_2\text{-Veratrole}$$

$$\downarrow \ N_2, \text{ reflux}$$
$$\text{ethanol}$$

Veratrole-H₂P⟋⟍   Cl   ⟍PH₂-Veratrole
                Ru
Veratrole-H₂P⟋ | ⟍PH₂-Veratrole
                Cl
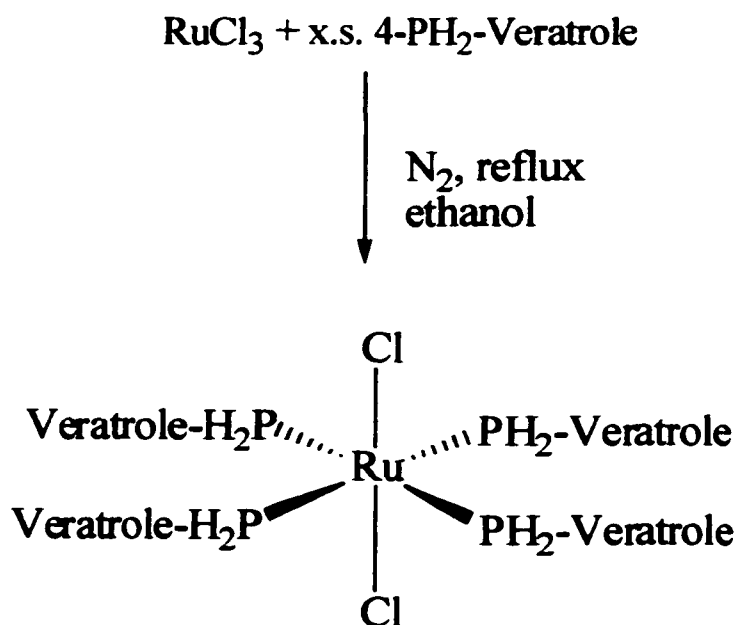
Scheme 3.3 Synthesis of RuCl₂(4-PH₂-Veratrole)₄

yellow. Upon cooling, the product came out of solution as a yellow solid in a yield of

87

76%. This complex has been characterized by IR, $^{31}P\{^1H\}$, ^1H, $^{13}C\{^1H\}$ NMR and CHN elemental analysis.

Conversion of RuCl₂ (4-PH₂-Veratrole)₄ to RuBr₂ (4-PH₂-Catechol)₄:

The deprotection of $RuCl_2(4\text{-}PH_2\text{-}Veratrole)_4$ was achieved by reaction with BBr_3 in CH_2Cl_2 (Rxn. 3.3). Workup and vacuum evaporation afforded a yellow solid, $RuBr_2(PH_2\text{-}Catechol)_4$, in a yield of 86%.

trans-Dichloro-Ru(4-PH₂-Veratrole)₄
a) BBr₃/CH₂Cl₂
N₂, -78° to R.T.
——————————→
b) Methanol

(Rxn. 3.3)

trans-Dibromo-Ru(4-PH₂-Catechol)₄
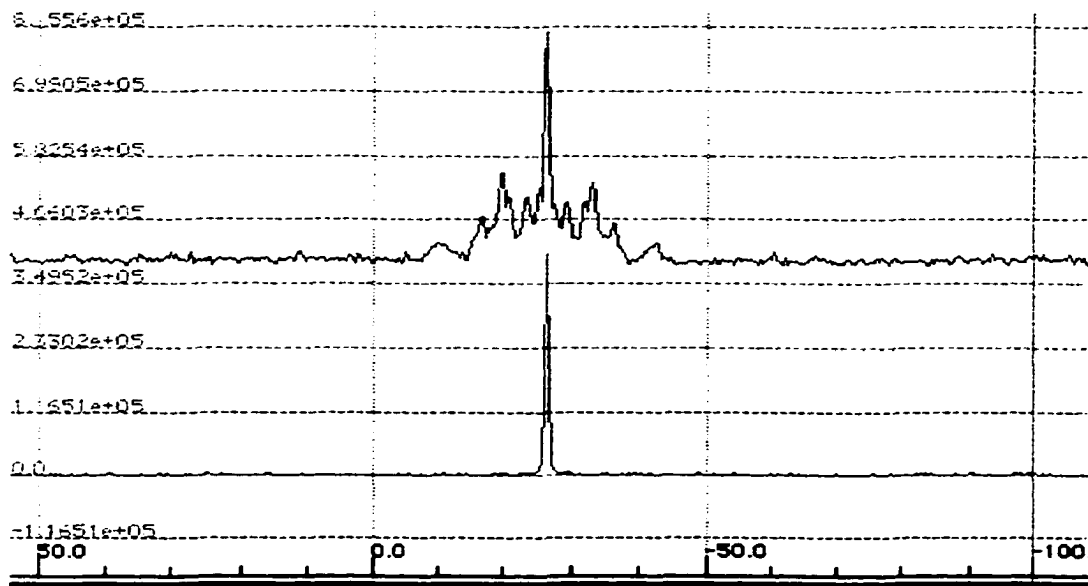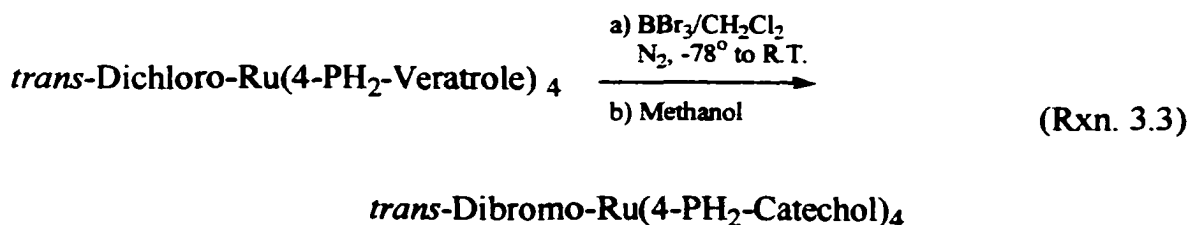
Figure 3.5 ^{31}P NMR spectra of trans-dibromo-Ru(4-PH₂-Catechol)₄. The top is ^1H-coupled, while the bottom one is ^1H-decoupled.

The sharp singlet in its $^{31}P\{^1H\}$ NMR spectrum (Figure 3.4, bottom) confirms that the complex has 4-fold symmetry. The pattern of the proton-coupled ^{31}P NMR spectrum (Figure 3.5, top) is also characteristic of a C_4 symmetry at the metal center, as is the second-order pattern of the -PH$_2$ resonance centered at δ 5.44 in its ^1H spectrum (Figure 2.6). If its two bromide atoms are in the trans-configuration, the complex can be regarded as a twelve-half-spin-system of AA'A"A'''X$_2$X$_2$'X$_2$"X$_2$''' (Figure 3.7). ^1H and ^{31}P NMR spectral simulations were carried out by using the gNMR program,[136] the coupling constants used in the simulation are shown in Figure 3.7.
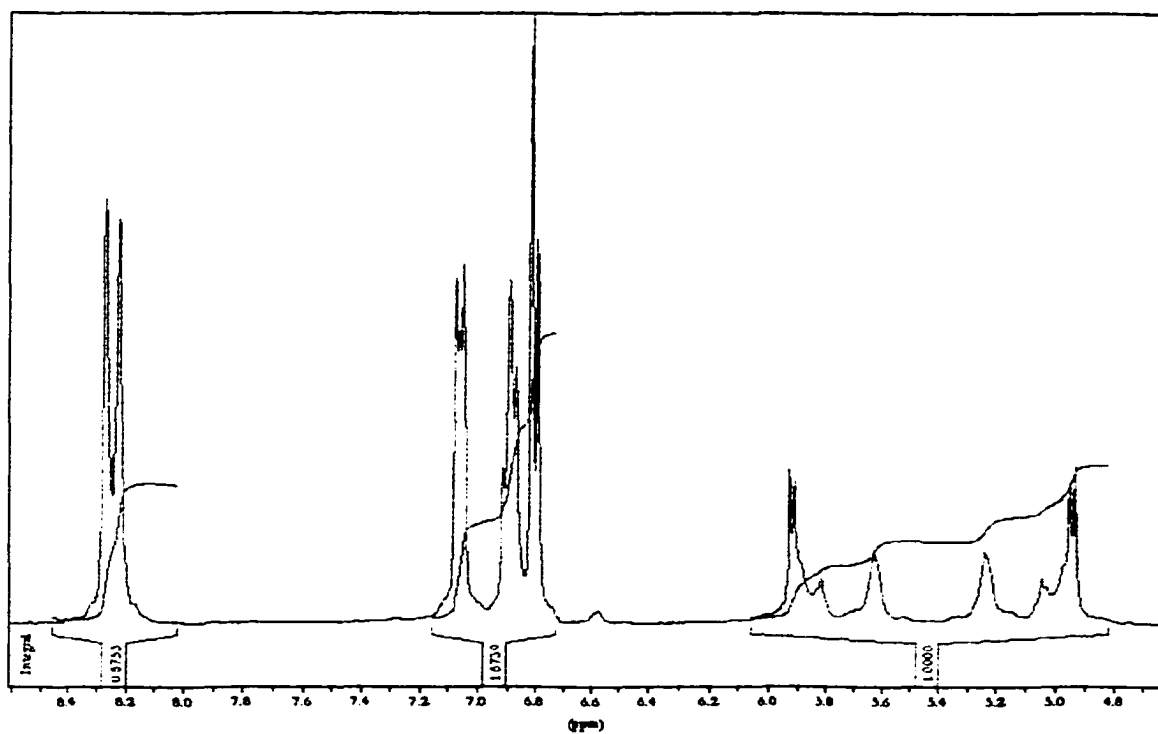
Figure 3.6 ^1H NMR spectra of trans-dibromo-Ru(4-PH$_2$-Catechol)$_4$ in acetone-d$_6$

89
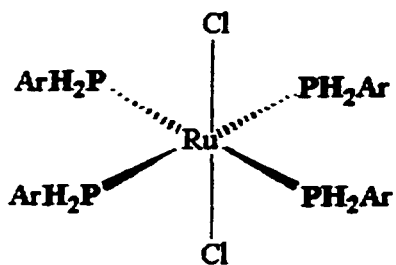
$^2J_{PH} = 360\,Hz$

$^2J_{trans\text{-}PRuP} = 400\,Hz$ $^2J_{cis\text{-}PRuP} = -30\,Hz$

$^3J_{trans\text{-}PH} = -3\,Hz$ $^3J_{cis\text{-}PH} = 6\,Hz$

Twelve 1/2 Spin AA'A"A'"X₂X'₂X"₂X'"₂

Figure 3.7 The twelve-half-spin system of *trans*-dibromo-Ru(4-PH₂-Cat)₄ and coupling constants used for the simulation of ^1H and ^{31}P NMR spectra.
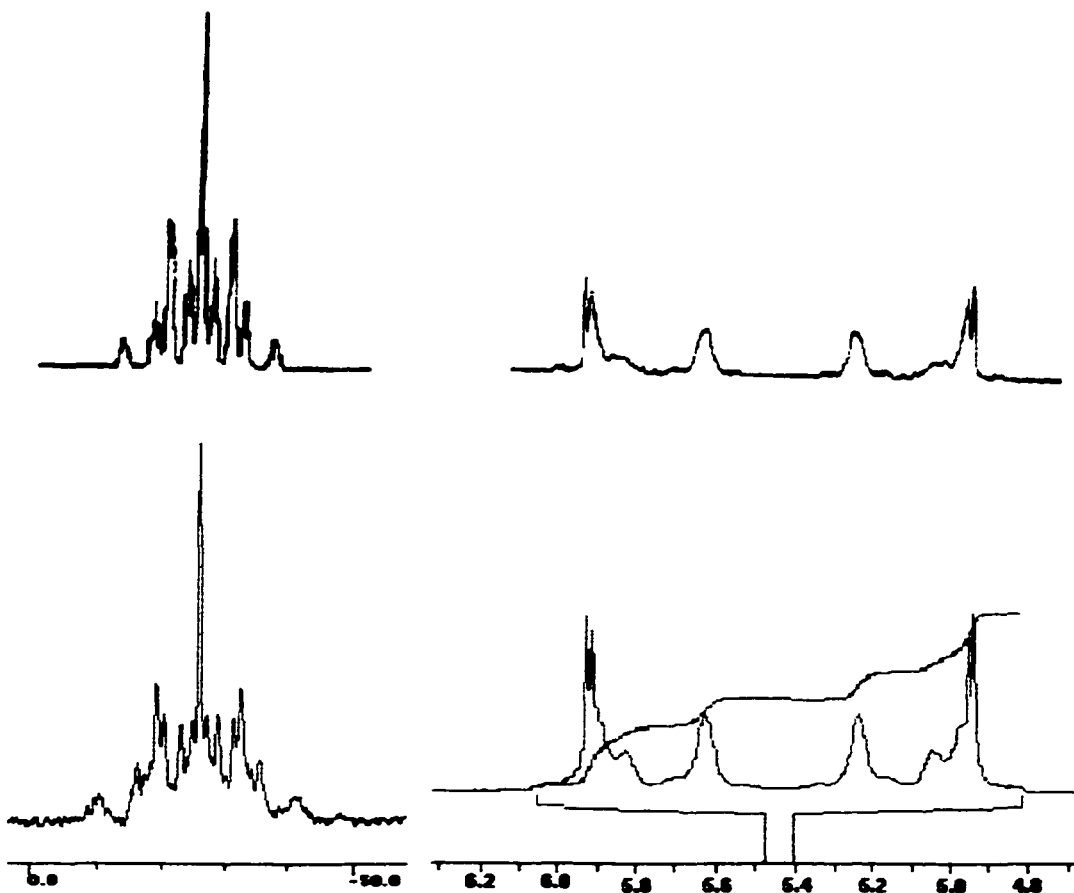
Figure 3.8 Comparative simulated ^{31}P and ^1H NMR (-PH₂) spectra (top left and right, respectively) and experimental ^{31}P and ^1H NMR (-PH₂) spectra (bottom right and left, respectively)

90

The results of these ^{1}H and ^{31}P NMR spectral simulations are shown in Figure 3.8. Comparing the simulated spectra to the experimental spectra, we can see that they are quite similar, which indicates that the two bromide anions in the $RuBr_2(4\text{-}PH_2\text{-}Catechol)_4$ complex are indeed in a *trans*-configuration, and thus the complex has a 4-fold overall symmetry.

91

2. Catecholate Complexes

The 4-Phosphino-Catechol ligands reacted smoothly with hard tri- and tetra-valent metals like Ga(III), Fe(III), Ti(IV), and Sn(IV) under basic conditions in a 3/1 stoichiometry to give *tris*-catecholate complexes without interference from the P-donor groups. Three new ligands, 4-PPh$_2$-Catechol•HBr, 4-PH$_2$-Catechol•HBr and 4-P(CH$_2$OH)$_2$-Catechol•HBr, have been used for the formation of pseudo-octahedral catecholate complexes which should provide C_3 symmetry metal centers.

Results and Discussion

(a) Syntheses and Characterization of [(4-PPh$_2$-Catecholato)$_3$M]$^{n-}$ Complexes

The *tris*(4-PPh$_2$-Catecholate) metal complexes [(4-PPh$_2$-Catecholato)$_3$M]$^{3-}$ (M = Fe^{III}, Ga^{III}) and [(4-PPh$_2$-Catecholato)$_3$M]$^{2-}$ (M = Ti^{IV}, Sn^{IV}) were synthesized in good yields according to Scheme 2.4. Bases used in the syntheses were chosen according to consideration of their basic strengths, the solubility of complexes, and countercations. The successful countercations of these *tris*(4-PPh$_2$-Catecholato) metal complexes include alkali metal ions, triethylammonium (HNEt$_3^+$), tetramethylammonium (TMA$^+$), tetra-phenylphosphonium (Ph$_4$P$^+$), and *bis*(triphenylphosphoranylidene)ammonium (PPN$^+$).

The trianionic products are considerably more air-sensitive than the dianionic complexes, with partial air oxidation of their PPh$_2$-groups evident after overnight exposure, probably because these trianions are more highly charged. Detailed spectral and analytical data of these products are presented in the respective experimental

92

sections. IR spectra of all complexes contained strong bands at around 1246 cm^{-1} assignable to coordinated catecholate C-O groups. [137]
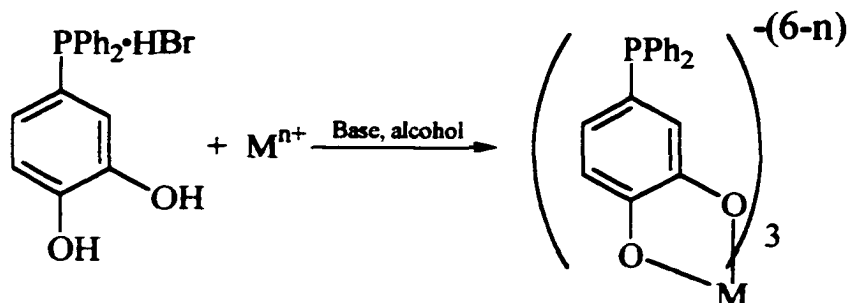
Scheme 3.4 Synthesis of *tris*(4-PPh₂-Catecholato) metal complexes

[(4-PPh₂-Catecholato)₃Fe]³⁻ Complexes (Countercations = Li⁺, K⁺, Cs⁺): The Fe(III) complexes are dark red in color, and have been characterized by IR, UV-vis, EPR, and elemental analysis. The electronic spectrum of the Cs₃Fe(4-PPh₂-Catecholate)₃ complex in methanol solution exhibited a LMCT band with a λ_{max} at 490 nm (ε = 6,050 L cm^{-1} mol^{-1}).[138, 139] EPR spectra of the complex in the solid state or in methanol solution at room temperature both exhibit a major g = 4.25 signal typical of high-spin ferric catecholate complexes.[139]

Diamagnetic [(4-PPh₂-Catecholato)₃M]ⁿ⁻ Complexes: While the Ti(IV) complex is red-orange in color, the Ga(III) and Sn(IV) complexes are both white solids. Compared to the chemical shift (δ -6.73 ppm in DMF-d₇) of the free ligand, 4-PPh₂-Catechol, the $^{31}P\{^{1}H\}$ singlet chemical shifts (δ-2.0 to -6.0) of the diamagnetic Ga(III), Ti(IV), and Sn(IV) [(4-PPh₂-Catecholate)₃M]ⁿ⁻ complexes are only slightly downfield shifted. This observation indicates that the PPh₂-groups indeed remain uncoordinated as anticipated.[140] Further,

C_3

C_1
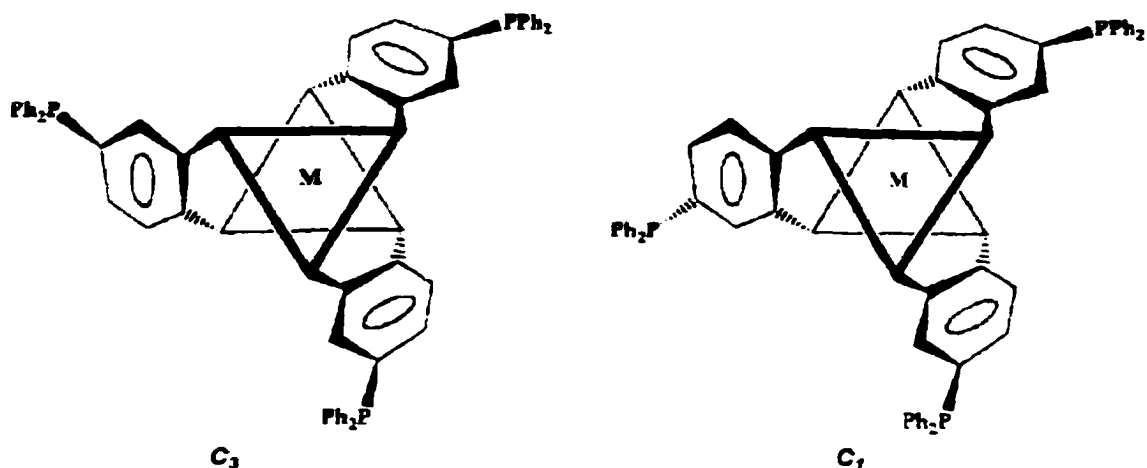
Figure 3. 9 Configuration of $[(4\text{-}PPh_2\text{-}Catecholato)_3M]^{n-}$ complexes. *Fac*-isomer of C_3 symmetry is shown at the left, and *mer*-isomer of C_1 symmetry at the right. (Only Λ enantiomers are shown)
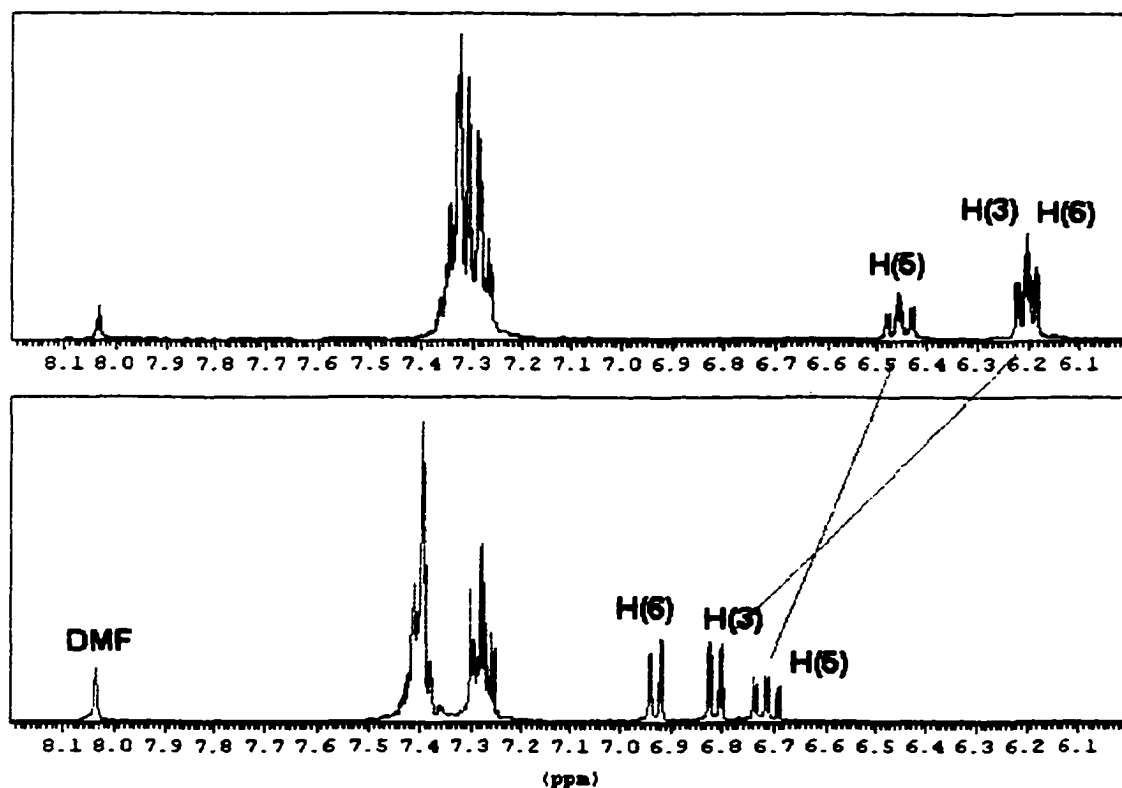
Figure 3.10 Comparative ${}^1H$ NMR spectra of Ligand, 4-PPh₂-Catechol•HBr (bottom), and Complex, Cs₂(4-PPh₂-Catecholato)₃Ti (upper) in DMF-d₇

94

room temperature solution ^{1}H and ^{13}C{1H} NMR spectra of these complexes all exhibit a single set of ligand catecholate and phenyl resonances indicative of C_3 symmetry. This is consistent with either exclusive formation of the *fac*-isomer or rapid isomerization involving the *mer*-isomer of only C_1 symmetry (Figure 3.9 *fac/mer*).

All three catecholate proton resonances shift upfield upon metal complexation by 0.26 up to 0.73 ppm (Figure 3.10), as previously observed for Ga(III) and Rh(III) *tris*-catecholate complexes.[141] These shifts have been attributed to reduced ring currents as a result of cation coordination. Significant ^{13}C coordination shifts are found for the catechol ring carbons only. Both C(1) and C(2) signals are shifted sizeably downfield by about 15 ppm upon the coordination of the catecholate with metal ion. Upfield shifts of over 5 ppm were observed for C(3), C(4), and C(6) signals (Figure 3.11). Of the phenyl carbons, only the *ipso*-C shifted slightly downfield by 1.8 ppm, again confirming the uncoordinated status of the PPh$_2$- moiety.
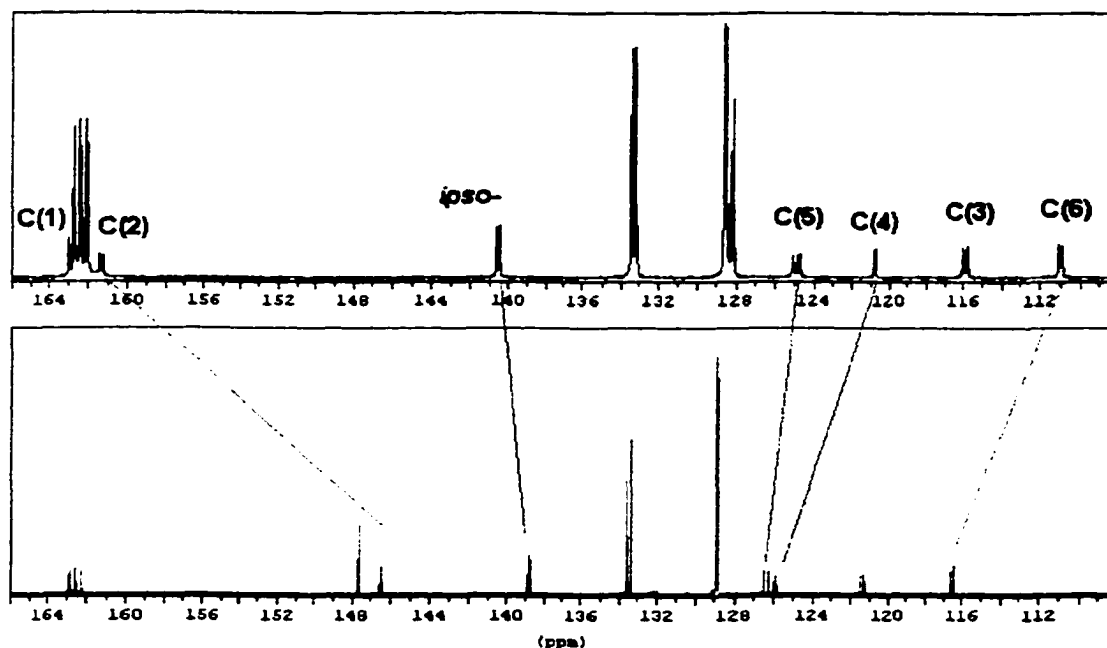
Figure 3.11 Comparative ^{13}C{^{1}H} NMR spectra of Ligand, 4-PPh$_2$-Catechol·HBr (bottom), and Complex, Cs$_2$(4-PPh$_2$-Catecholato)$_3$Ti (top) in DMF-d$_7$

95

X-ray Structure of the Cs₂(4-PPh₂-Catecholato)₃Ti Complex

The complex crystallizes in the triclinic space group P $\bar{1}$ with two formula units in the unit cell. It has no crystallographic symmetry and thus one entire molecule makes up the asymmetric unit. The structural study of Cs₂(4-PPh₂-Catecholato)₃Ti •2DMF•0.5H₂O revealed a *mer*-configuration in the solid-state (Figure 3.12). While P(1) and P(2) are in an *anti* configuration, the third phosphorus is disordered equally over two sites, P(3) and P(4). Despite this disorder, the *mer*-isomer is clearly the only one present, with the disorder merely generating the two possible *mer*-isomers (two "up" and one "down" versus two"down" and one "up") as seen in Figure 3.12 (left). Due to the close proximity of the four phenyl rings on these two disordered PPh₂- fragments, these rings were refined as rigid groups.
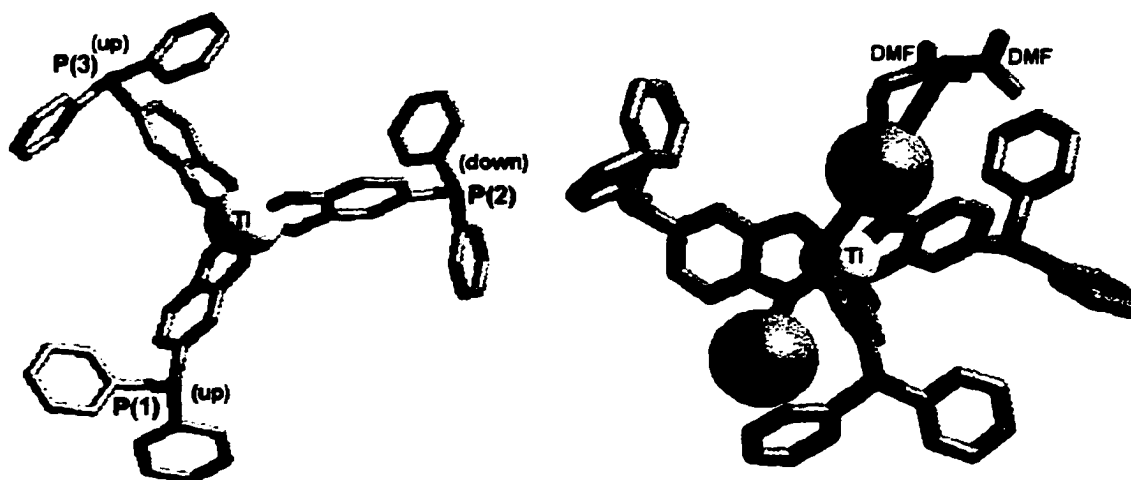
Figure 3.12 X-ray structure of Cs₂(4-PPh₂-Catecholato)₃Ti (wireframe and sphere model). At left is the top-view of the complex excluding cesium atoms, while at right is the side-view of one formula unit of the complex.
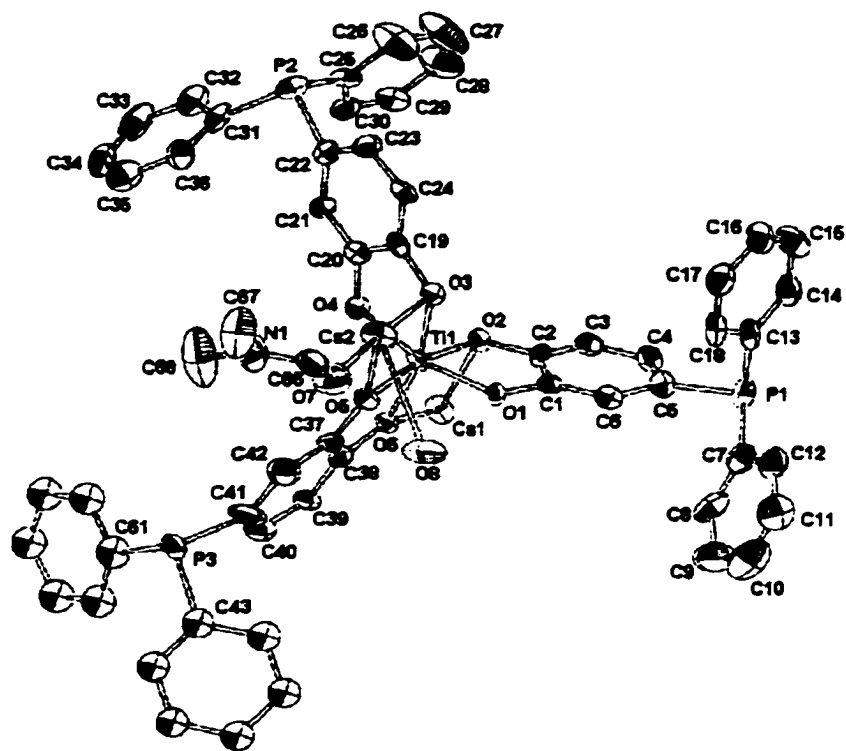
Figure 3.13 ORTEP of X-ray structure of $Cs_2(4\text{-PPh}_2\text{-Catecholato})_3Ti$ (topview), P(4) is not shown.
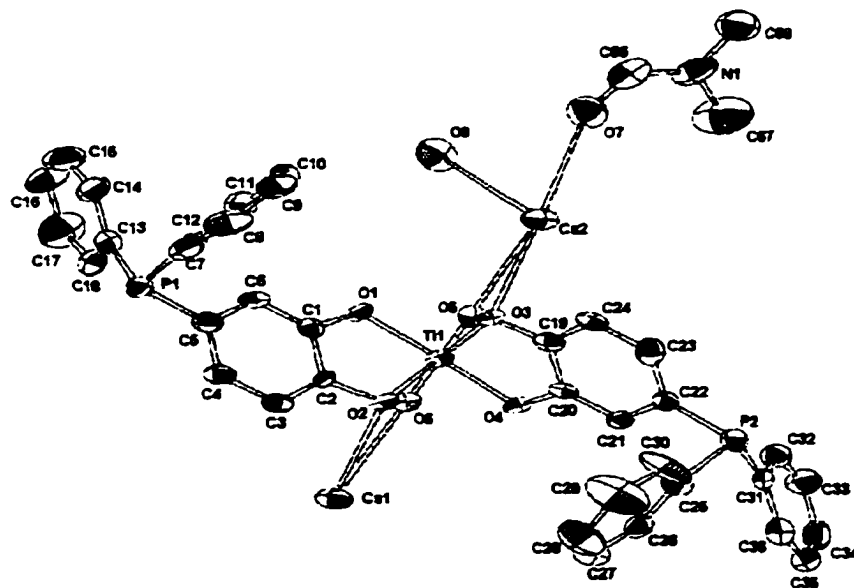
Figure 3.14 ORTEP of X-ray structure of $Cs_2(4\text{-PPh}_2\text{-Catecholato})_3Ti$ (side-view), P(3) is not shown.

97

The complex crystallizes as a racemic mixture of Δ and Λ configuration at the titanium centers. The twist angle around Ti is 42.3°, indicative of an intermediate O_h/TP (0° for a trigonal prism, 60° for an octahedron) coordination geometry. The six Ti-O bond lengths average to 1.96Å with only Ti-O(1) and Ti-O(2) significantly different from the mean at 1.936(7)Å and 1.996(9)Å respectively. Of the six catecholate oxygens only O(1) is not coordinated to a Cs cation, which may account for its shorter bond-length to the Ti cation. No clear trend for the existence of any *trans*-influence on the bond lengths of Ti-O or C-O can be seen for the phenolic oxygens *meta* to or *para* to the PPh$_2$- groups.

The compound crystallizes with two cesium countercations per complex. Each Cs atom is coordinated by two catecholate oxygens and one catecholate oxygen on an adjacent complex. Furthermore, Cs(2) is coordinated by one DMF molecule and one disordered DMF/water molecule, whereas Cs(1) is coordinated by these same solvent molecules of an adjacent complex (Figure 3.13-14). Each of these disordered solvents was refined to 1/2 occupancy (i.e. either a water molecule or DMF molecule is coordinated to these Cs atoms, each solvent having 1/2 occupancy). Interestingly, both Cs atoms are also within 3.7Å of a phenyl ring on an adjacent molecule, thereby blocking these countercations from further solvation. The Cs-O bond distances range from 3.034(9)Å for Cs(2)-O(5) to 3.305(7)Å for Cs(1)-O(2'). The intracomplex Cs(1) and Cs(2) separation is 5.176(2)Å. Other relevant bond distances and angles are listed in Table 3.1

Table 3.1 Selected bond distances(Å) and bond angles(°) for $Cs_2(4\text{-PPh}_2\text{-Catecholato})_3Ti$

Cs(1)-O(2)	3.097(8)	O(1)-C(1)	1.35(2)
Cs(1)-O(2')	3.305(7)	O(2)-C(2)	1.34(1)
Cs(1)-O(6)	3.051(8)	O(3)-C(19)	1.36(1)
Cs(1)-O(7)	3.21(1)	O(4)-C(20)	1.35(2)
Cs(1)-O(8)	3.11(1)	O(5)-C(37)	1.34(2)
Cs(2)-O(3)	3.164 (8)	O(6)-C(38)	1.37(2)
Cs(2)-O(3')	3.272(9)	O(7)-C(66)	1.26(2)
Cs(2)-O(5)	3.034(9)	O(8)-C(69)	1.10(4)
Cs(2)-O(7)	3.30(1)	P(1)-C(5)	1.83(1)
Cs(2)-O(8)	3.089(9)	P(1)-C(7)	1.84(1)
Ti(1)-O(1)	1.936(7)	P(1)-C(13)	1.87(1)
Ti(1)-O(2)	1.996(9)	P(2)-C(22)	1.81(1)
Ti(1)-O(3)	1.963(9)	P(2)-C(25)	1.82(1)
Ti(1)-O(4)	1.964(7)	P(2)-C(31)	1.82(1)
Ti(1)-O(5)	1.957(9)	P(3)-C(41)	1.84(2)
Ti(1)-O(6)	1.962(9)	P(3)-C(43)	1.86(2)
		P(3)-C(61)	1.87(2)
		P(4)-C(40)	1.92(3)
		P(4)-C(49)	1.90(2)
		P(4)-C(55)	1.92(3)

99

O(1)-Ti(1)-O(2)	79.8(3)	O(1)-Ti(1)-O(3)	88.5(3)
O(1)-Ti(1)-O(4)	162.8(4)	O(1)-Ti(1)-O(5)	92.8(3)
O(1)-Ti(1)-O(6)	103.1(3)	O(2)-Ti(1)-O(3)	98.6(4)
O(1)-Ti(1)-O(4)	89.3(3)	O(2)-Ti(1)-O(5)	166.8(3)
O(2)-Ti(1)-O(6)	90.0(4)	O(3)-Ti(1)-O(4)	80.0(3)
O(3)-Ti(1)-O(5)	92.0(4)	O(3)-Ti(1)-O(6)	166.7(4)
O(4)-Ti(1)-O(5)	100.2(3)	O(4)-Ti(1)-O(6)	90.1(3)
O(5)-Ti(1)-O(6)	81.1(4)		

Stereochemistry of [(4-PPh$_2$-Catecholato)$_3$M]$^{n-}$ Complexes.

The [(4-PPh$_2$-Catecholato)$_3$M]$^{n-}$ complexes have two potential isomers: *fac*-isomer of C_3 symmetry and *mer*-isomer of C_1 symmetry, each of which has a pair of enantiomers (Δ/Λ) (Figure 3.9). In the absence of steric, electronic, ion-pairing, or solvation effects, the C_1 *mer*-isomers of [(4-PPh$_2$-Catecholato)$_3$M]$^{3-}$ (M = Fe, Ga) and [(4-PPh$_2$-Catecholate)$_3$M]$^{2-}$ (M = Ti, Sn) are statistically favored over the C_3 *fac*-isomers by a 3:1 ratio. Of these two isomers, only the *fac* configuration has all three phosphino-donor groups disposed *syn* to each other which is essential for successful formation of any endohedral metal clusters. It is expected that each C_1 *mer*-isomer should exhibit up to three sets of ligand phosphino, catecholate and phenyl resonances in their ^{31}P{^{1}H}, ^{1}H and ^{13}C{^{1}H} NMR spectra of these complexes, while the C_3 *fac*-isomers only give a single set. At room temperature, a single set of ligand phosphino, catecholate and phenyl

resonances found in their ^{31}P, ^{1}H and $^{13}C\{^{1}H\}$ NMR spectra are fully consistent with either exclusive presence of the high-symmetry species in all cases or extremely facile *fac/mer* equilibration. In either case, the *tris*(4-PPh₂-Catecholato) metal complexes [(4-PPh₂-Catecholato)₃M]³⁻ (M = Fe, Ga) and [(4-PPh₂-Catecholato)₃M]²⁻ (M = Ti, Sn) can be used for mixed-metal cluster formation by providing C_3 symmetry sites.

In order to investigate the factors that may cause a strong preference for a *fac*-over the *mer*-isomer in solution, we examined three possible factors that may favor the *fac*-isomer at least in solution. (1) <u>Sterics</u>: The remoteness of the three diphenylphosphino-substituents from the metal center and from each other renders no significant differences in *fac* versus *mer* steric factors. Molecular mechanics indeed showed very similar strain energies. Therefore, we consider that the steric factor does not play a significant role in this preference. (2) <u>Electronic Effect</u>: Electronically the PPh₂-group is known to be moderately electron-withdrawing, [142] thus the existence of an intrinsic electronic effect favoring the *fac*-isomer is feasible.[143] However, DFT(Density Functional Theory) molecular orbital calculations on [(4-PH₂-Catecholato)₃Ti]²⁻ actually favored the *mer*-isomer over the *fac*-isomer as the ground state configuration by 2.785 Kcal/mol (Table 3.2).[144] Further, no convincing X-ray data consistent with differing

Table 3.2 Density Functional Theory Molecular Calculation Results for [(4-PH₂-Catecholate)₃Ti]²⁻

	Ground state energy (Kcal/mol)	Dipole (debye)
Fac-[(4-PH₂-Catecholate)₃Ti]²⁻	-1895517.118	1.11615
Mer-[(4-PH₂-Catecholate)₃Ti]²⁻	-1895519.903	0.540239

metal-oxygen bond distances due to such a substituent effect have been found in either the *fac*-(HNEt$_3$)$_2$(4-NO$_2$-Catecholato)$_3$Sn [145] or the *mer*-Cs$_2$(4-PPh$_2$-Catecholato)$_3$Ti structure described above. (3) <u>Solvation Effect</u>: Since the *fac*-isomer can be expected to have a substantially larger dipole moment than the *mer*-isomer (Table 3.2),[146] the resulting higher solvation energy in a polar solvent may be the origin of its predominance. If so, a significant solvent polarity-dependence of the speciation can be anticipated. Our NMR spectral data do show some solvent-dependence. For example, in data summarized in Table 3.3, TMA$^+$, Li$^+$, and Cs$^+$ salts of [(4-PPh$_2$-Catecholato)$_3$Ti]$^{2-}$ showed broadened room-temperature ^{31}P signals in CD$_2$Cl$_2$ compared to spectra in the

Table 3.3 The line-widths (Hz) at half-height ($\Delta v_{1/2}$) of ^{31}P {^{1}H} NMR resonances of [Monocation]$_2$Ti(4-PPh$_2$-Catecholato)$_3$ (Monocation = PPN$^+$, TMA$^+$, Li$^+$, Cs$^+$)

	PPN$^+$	TMA$^+$	Li$^+$	Cs$^+$
CD$_2$Cl$_2$	6.1	18.3	12.4	8.5
CD$_3$OD	6.3	7.4	7.3	6.1

more polar solvent CD$_3$OD. This line broadening can be attributed to either the emergence of a *mer*-isomer in a low polarity solvent or differing extents of ion-pairing. Therefore we seeked to remove the latter influence by studying the PPN$^+$ salt of [(4-PPh$_2$-Catecholato)$_3$Ti]$^{2-}$ since this bulky cation is not expected to participate in tight ion pairing. Both the ^{31}P{^{1}H} NMR spectra of PPN$_2$ (4-PPh$_2$-Catecholato)$_3$Ti in CD$_2$Cl$_2$ and CD$_3$OD gave sharp singlet signals indicative of a single *C$_3$* solution species. Thus tight

102

ion pairing is most likely the origin of the solvent-dependent NMR spectra of these TMA$^+$, Li$^+$, and Cs$^+$ salts.

(b) Variable-Temperature NMR studies of Catecholate Metal Complexes

As described above, the $^{31}P\{^1H\}$, ^1H and $^{13}C\{1H\}$ NMR spectra of the *tris*(4-PPh$_2$-Catecholato) metal complexes [(4-PPh$_2$-Catecholato)$_3$M]$^{3-}$ (M = Ga) and [(4-PPh$_2$-Catecholato)$_3$M]$^{2-}$ (M = Ti, Sn) are fully consistent with either exclusive presence of the C_3-symmetry species in all cases or extremely facile *fac/mer* equilibration at room-temperature. In order to investigate possible facile *fac/mer* equilibration, variable-temperature ^1H, $^{31}P\{^1H\}$, and $^{119}Sn\{^1H\}$ NMR spectral studies were carried out on TMA$_2$(4-PPh$_2$-Catecholato)$_3$Ti and PPN$_2$(4-PPh$_2$-Catecholato)$_3$Sn.

TMA$_2$Ti(4-PPh$_2$-Catecholato)$_3$: Its room-temperature ^1H NMR spectrum in CD$_3$OD displayed well-resolved resonances for a single set of three distinct catecholate proton multiplets and a sharp singlet for the ammonium methyl groups. By contrast, its room-temperature ^1H NMR spectrum in the low-polarity solvent CD$_2$Cl$_2$ clearly exhibited broadened proton resonances of both the catecholate and methyl (where a distinct upfield shoulder appeared, Figure 3.15) signals. Thus, variable-temperature experiments were conducted in CD$_2$Cl$_2$. Compared to the spectrum at room temperature, both these catecholate and methyl resonances sharpened up when the temperature was increased to 308 K. As the temperature was lowered, the small upfield shoulder merged into a broad signal with the methyl resonance at around 278 K. Upon further cooling the catecholate

103
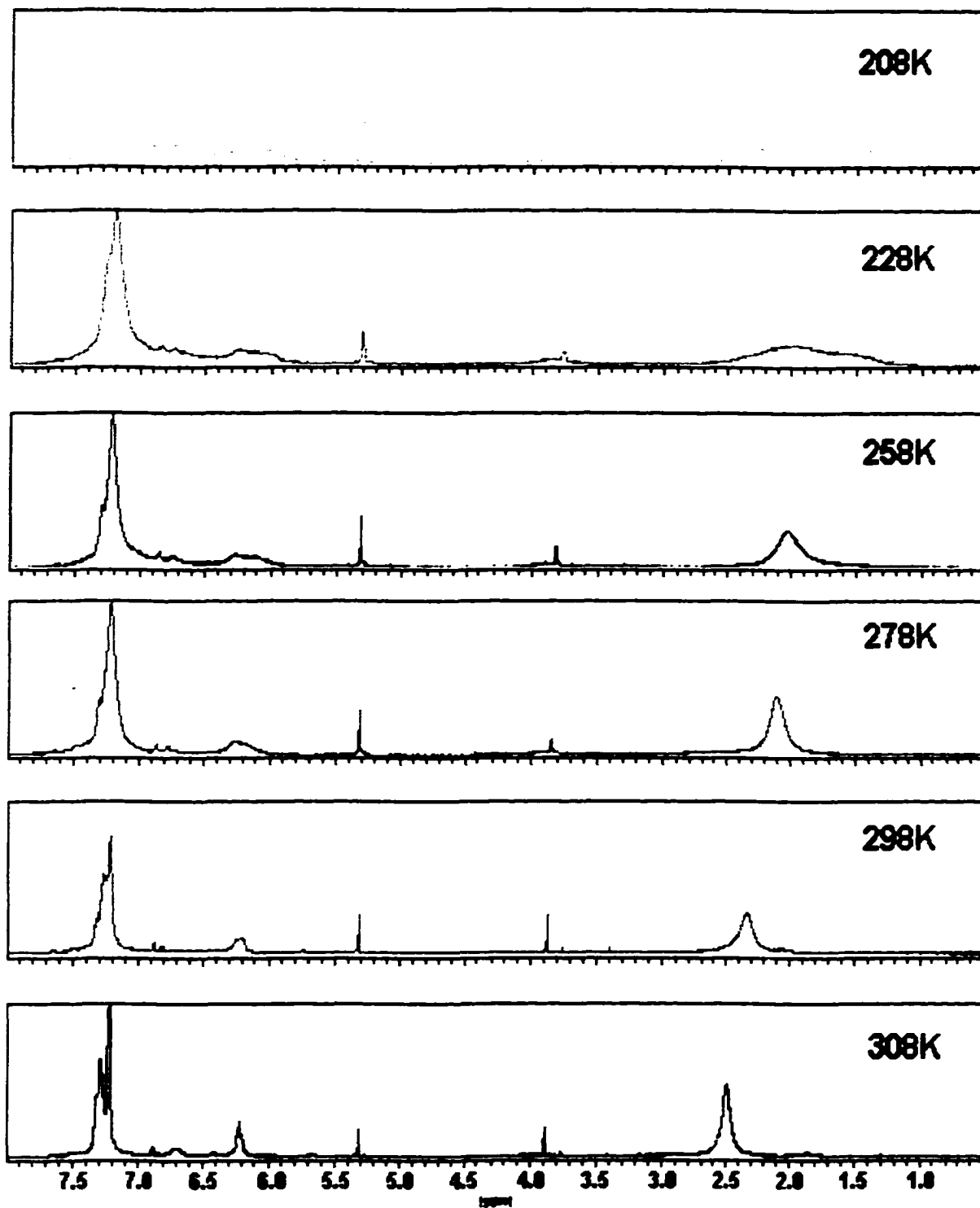
Figure 3.15 Comparative VT-^{1}H NMR spectra of TMA$_2$(4-PPh$_2$-Catecholato)$_3$Ti in CD$_2$Cl$_2$
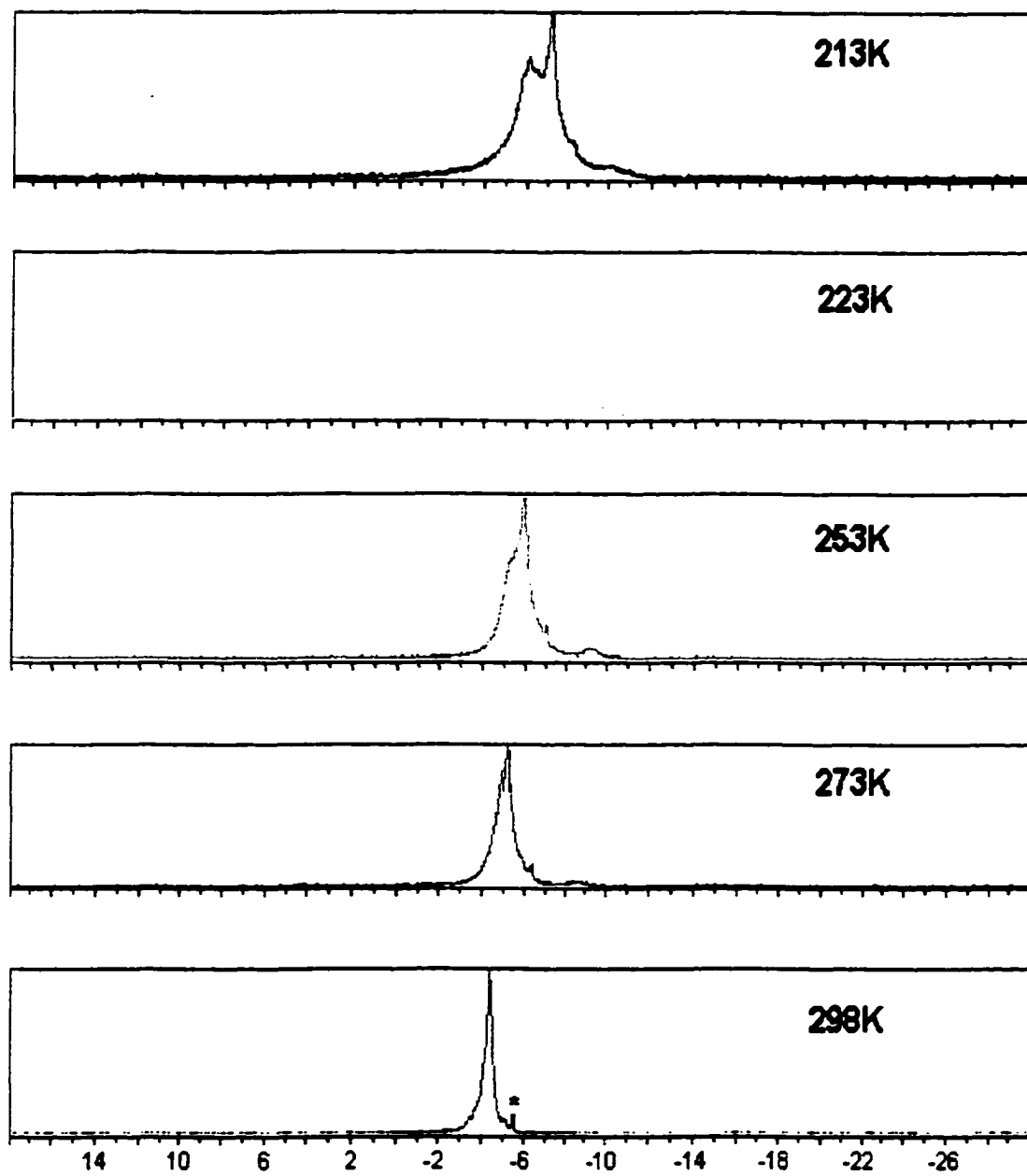
Figure 3.16 Comparative VT-^{31}P{^{1}H} NMR spectra of TMA$_2$(4-PPh$_2$-Catecholato)$_3$Ti in CD$_2$Cl$_2$ (* denotes free ligand impurity)

resonances broadened into featureless lumps at 208 K, while the methyl protons were broadened into at least 3 overlapping signals over a 1 ppm region (Figure 3.15). In parallel, the broad singlet $^{31}P\{^{1}H\}$ NMR PPh$_2$- signal at δ -4.3 ppm in CD$_2$Cl$_2$ at room temperature broadened further into at least 3 peaks over a 3 ppm range at around 210 K (Figure 3.16).

As discussed above, either the emergence of a *mer*-isomer in a low polarity solvent or the differing ion-pairing effects can account for these results. PPN$_2$(4-PPh$_2$-Catecholato)$_3$Sn was therefore synthesized to eliminate any tight ion-pairing possibility. In addition, $^{119}Sn\{^{1}H\}$ NMR at the possible inter-conversion center may provide us with an alternative probe for any possible facile *fac/mer* isomerization.

PPN$_2$(4-PPh$_2$-Catecholato)$_3$Sn : As seen in Figure 3.17, the sharp singlet $^{31}P\{^{1}H\}$ NMR PPh$_2$- signal at δ -2.9 ppm in CD$_2$Cl$_2$ at room temperature broadened a little when its temperature was lowered to 203 K, but no additional peaks appeared. Importantly, the PPN$^+$ singlet served as a usefu internal reference. The comparable broading of these two singlets can only be consistent with either exclusive existence of *fac*-isomer or a facile *fac/mer* isomerization in solution even at 203 K, since any ion-pairing can be ruled out. This conclusion is further supported by the variable-temperature ^{1}H (Figure 3.18) and $^{119}Sn\{^{1}H\}$ NMR (Figure 3.19) studies, neither of which showed any evidence for additional signals. Thus the emergence of extra spectral signals in the low-temperature TMA$_2$(4-PPh$_2$-Catecholato)$_3$Ti spectra is most likely due to ion-pairing and not a slowdown in *fac/mer* isomerization.
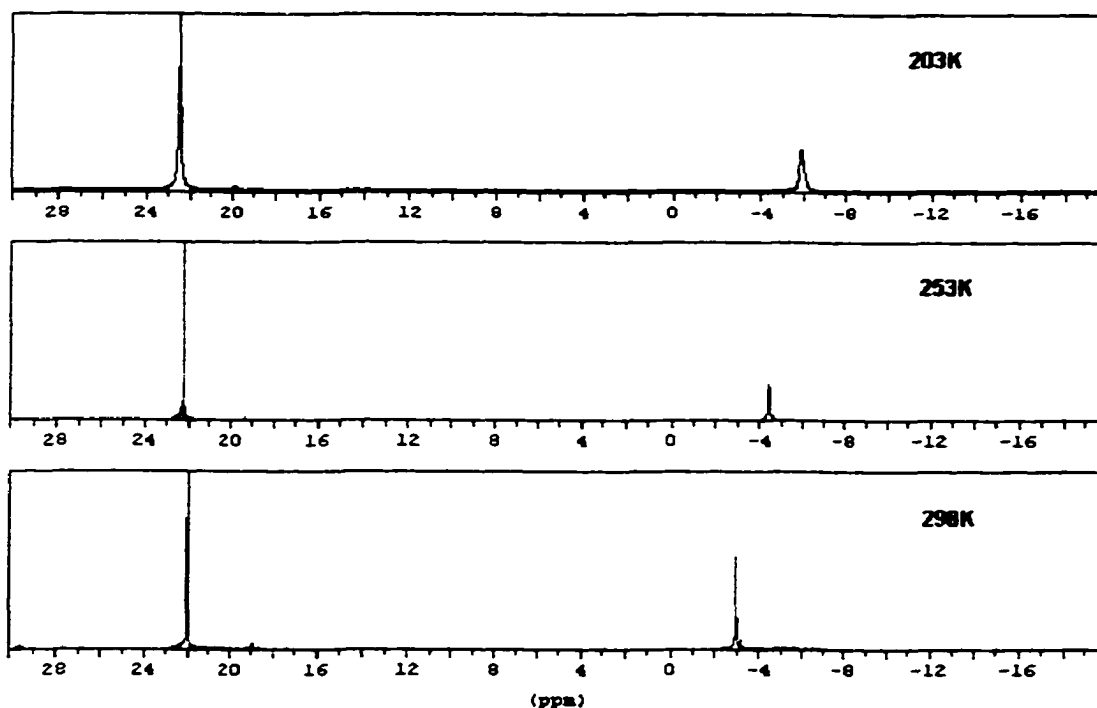
Figure 3.17 Comparative VT-^{31}P{^{1}H} NMR spectra of PPN$_2$(4-PPh$_2$-Catecholato)$_3$Sn in CD$_2$Cl$_2$
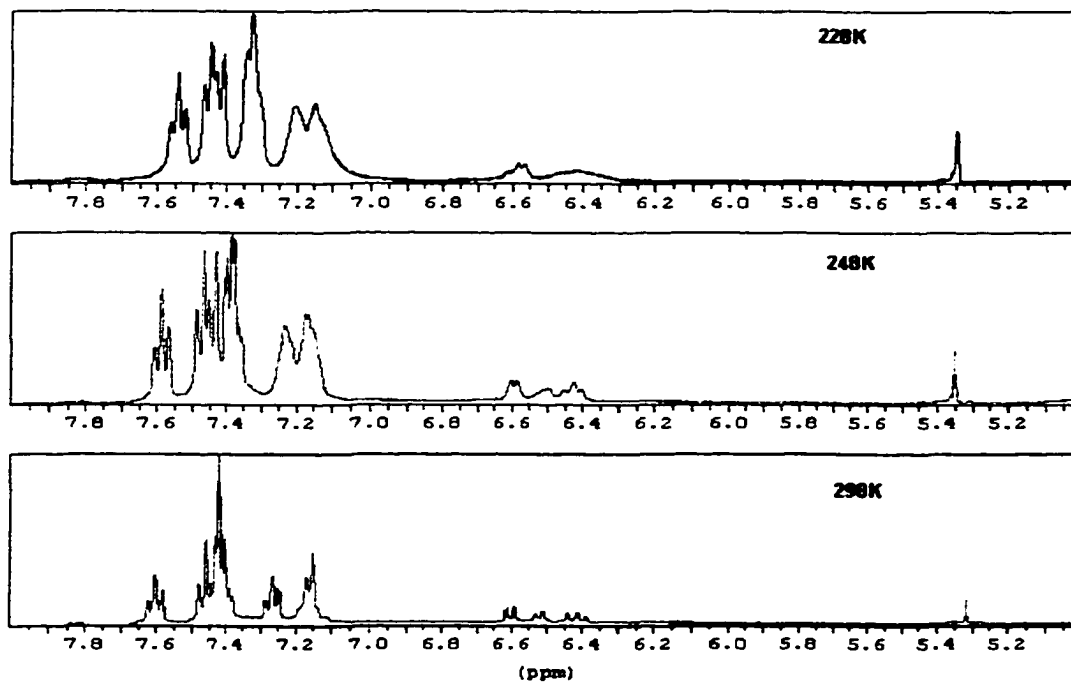
Figure 3.18 Comparative VT-^{1}H NMR spectra of PPN$_2$(4-PPh$_2$-Catecholato)$_3$Sn in CD$_2$Cl$_2$

107
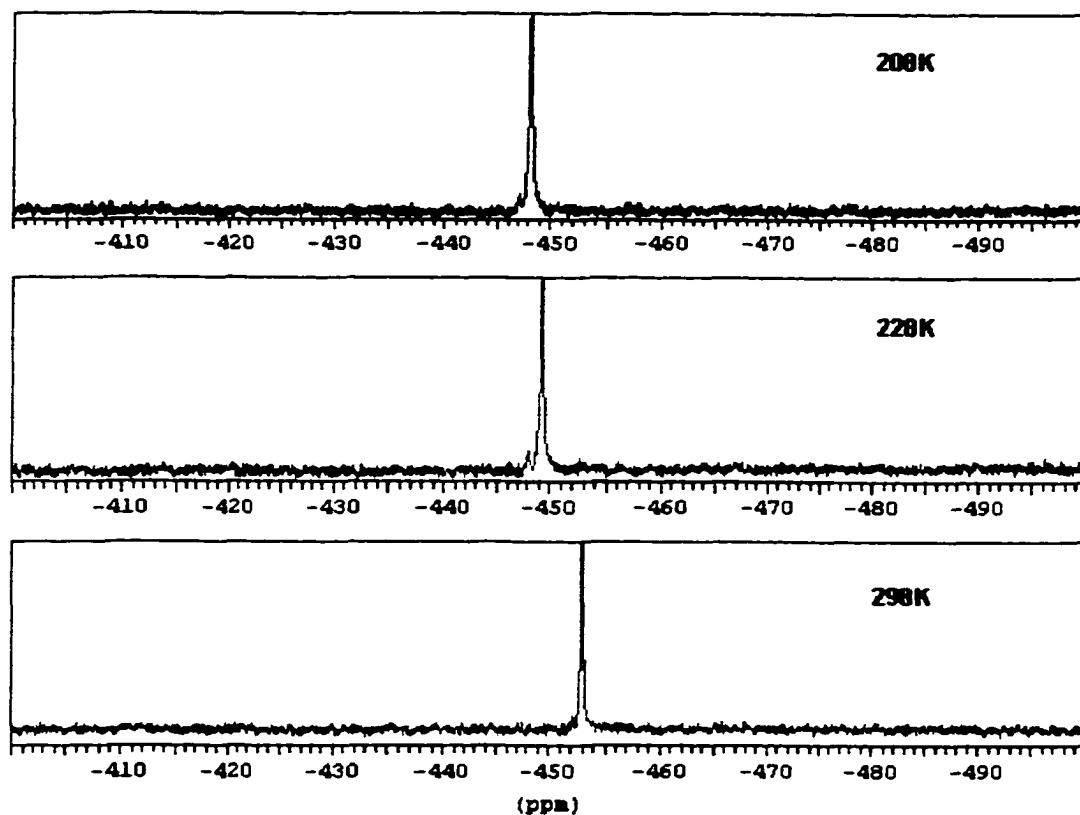
Figure 3.19 Comparative VT-^{119}Sn$\{^1$H$\}$ NMR spectra of PPN$_2$ (4-PPh$_2$-Catecholato)$_3$Sn in CD$_2$Cl$_2$

In summary, none of the three proposed factors: sterics, electronic effect or solvation effect, can be convincingly shown to support the exclusive formation of only the *fac*-isomer in solution. The alternative explanation for the observed high solution symmetry of *tris*(4-PPh$_2$-Catecholato) metal complexes must then be facile solution *fac/mer* isomerization processes that result in averaged spectra of C_3 symmetry. Variable-temperature ^{1}H, ^{31}P$\{^1$H$\}$ and ^{119}Sn NMR studies of *tris*(4-PPh$_2$-Catecholato) metal complexes so far have failed to yield any unequivocal evidence for the slowing down of a

108

fac/mer equilibration. Literature data on fluxional behavior for Ti(IV) and Sn(IV) complexes with six-oxygen donors are relatively rare. Fay and Lindmark reported in 1983 that both Ti(IV) *tris*(β-diketonate) and *bis*(β-diketonate)(OR)$_2$ complexes of unsymmetrical ligands are fluxional down to 173K in CD$_2$Cl$_2$ solution.[10] A 1994 review on Sn(IV) complexes of unsymmetrically-substituted catechols (e.g. 4-cyano, 4-methyl, 4-nitro, 4-chloro, etc) initially claimed that they exist as *fac/mer* mixtures in solution according to ^{1}H and ^{119}Sn{^{1}H} NMR data.[147] This claim, however, appears to be unfounded.[148] Instead, only a single set of resonances was obtained in all the cases studied. The implication is that the dynamical behavior of Ti(IV) and Sn(IV) complexes with six-oxygen donors may indeed be quite facile even at low-temperature.

On the other hand, silicon(IV) complexes of unsymmetrical catechols have been shown by ^{1}H and ^{13}C NMR to exist in both *mer* and *fac* forms.[12] An aluminum(III) complex of Tiron was also shown to exist as a statistical mixture of both isomers.[149] Gallium(III) (ionic radius: 76 pm) complexes of unsymmetrically-substituted catecholamides have been reported to show both species with a preference for the *fac*-isomer.[150] Since Ti(IV) (ionic radius: 74.5 pm) and Sn(IV) (83 pm) are substantially larger ions than Si(IV) (54 nm), Ge(IV) (67 pm) and Al(III) (67.5 pm), the nonrigidity of their catecholate complexes may indeed be significantly higher.

(c) Possible Mechanism for *Fac/Mer* Equilibration

Because no exchange between the [(4-PPh$_2$-Catecholato)$_3$M]$^{n-}$ with free ligand has been observed even at ambient temperature and above, it is not reasonable that any *fac/mer* isomerization occurs through a dissociation mechanism. Therefore the *fac/mer*
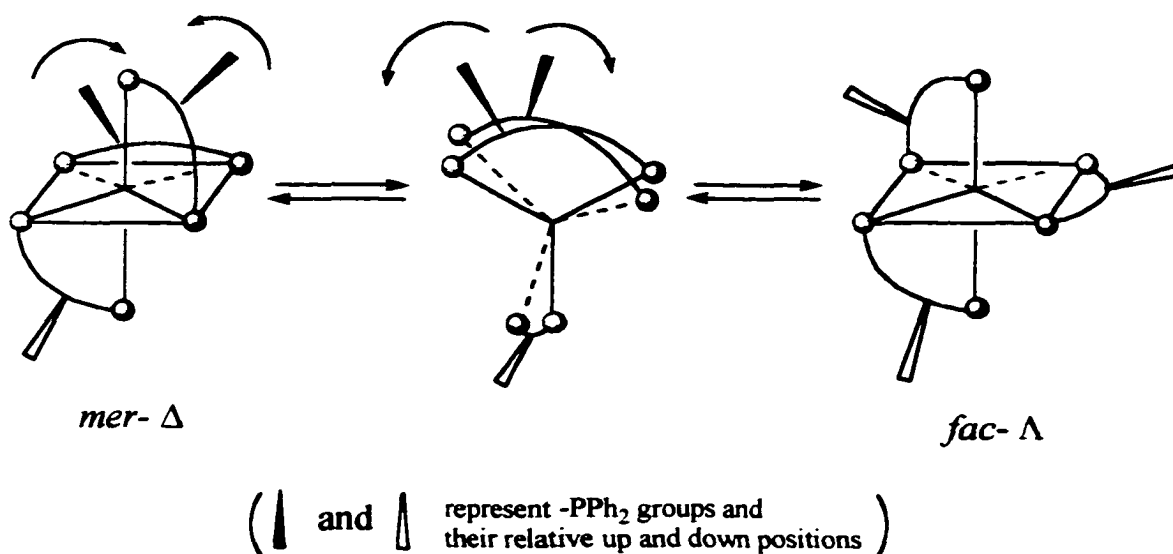
Figure 3.20 Ray-Dutt twist mechanism for intramolecular isomerization and racemization of $[(4\text{-}PPh_2\text{-}Catecholato)_3M]^{n-}$ complexes. Both gray and red spheres represent catecholate oxygen atoms.

equilibrium most likely utilizes a so-called Ray-Dutt (rhomboid twist) mechanism which has been suggested to be operative for intramolecular geometrical isomerization and racemization of octahedral coordination compunds [151](Figure 3.20).

For our purposes, the successful formation of endohedral mixed-metal clusters to be described in the next chapter mandates that the *fac*-isomer of our *tris*(4-PPh₂-Catecholato) metal complexes must be accessible in solution whether due to its exclusive formation or through a facile *fac/mer* exchange.

110

(d) Derivatives of [(4-PPh₂-Catecholato)₃M]²⁻ [M = Ti(IV), Sn(IV)]

As discussed above, the PPh₂- groups remain uncoordinated in these *tris*(4-PPh₂-catecholate) metal complexes. They can therefore be easily functionalized.

Since the tetravalent titanium and tin complexes are substantially less air-sensitive than their trivalent analogues, we have concentrated on their derivative chemistry which includes oxidation, sulfuration, and alkylation reactions.

Cs₂[4-P(O)Ph₂-Catecholato)₃]Sn:

The oxidation of Cs₂(4-PPh₂-Catecholato)₃Sn by aqueous H₂O₂ in refluxing acetone afforded a light yellow product (Rxn. 3.4). The reaction was complete in an overnight, as monitored by ^{31}P{^{1}H} NMR spectroscopy.

$$Cs_2(4\text{-}PPh_2\text{-}Catecholato)_3Sn \xrightarrow[\text{reflux, 24 hrs}]{\text{H}_2\text{O}_2/\text{acetone,}}$$ (Rxn. 3.4)

$$Cs_2[4\text{-}P(O)Ph_2\text{-}Catecholato]_3Sn$$
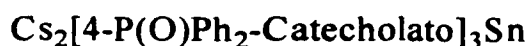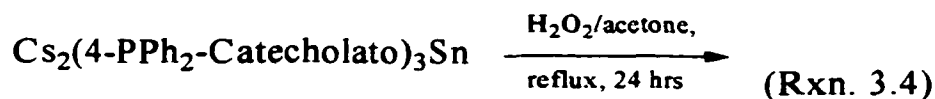
Cs₂[4-P(O)Ph₂-Catecholato)₃]Sn has been characterized by IR, ^{1}H, ^{13}C{^{1}H}, ^{31}P{^{1}H} NMR, as well as CHN elemental analysis. These data are fully consistent with conversion of all three PPh₂- groups to phosphoryls. Its IR spectrum contains a strong P=O stretching band at 1480 cm^{-1} and its ^{31}P{^{1}H} NMR spectrum revealed a singlet at δ +30.76 ppm which is also diagnostic of the three equivalent P(O)PPh₂- groups. [140, 152]

111

Cs$_2$[4-P(S)Ph$_2$-Catecholato)$_3$]Ti:

The sulfuration of Cs$_2$(4-PPh$_2$-Catecholato)$_3$Ti by elemental sulfur powder in refluxing acetonitrile under protection of a N$_2$ atmosphere afforded a red-orange product (Rxn. 3.5). The reaction was complete in 7 days, as monitored by ^{31}P{^{1}H} NMR spectroscopy.

$$Cs_2(4\text{-}PPh_2\text{-}Catecholato)_3Ti \xrightarrow[\text{N}_2, \text{ reflux, 24 hrs}]{\text{Sulfur powder/CH}_3\text{CN,}}$$ (Rxn. 3.5)

$$Cs_2[4\text{-}P(S)Ph_2\text{-}Catecholato]_3Ti$$
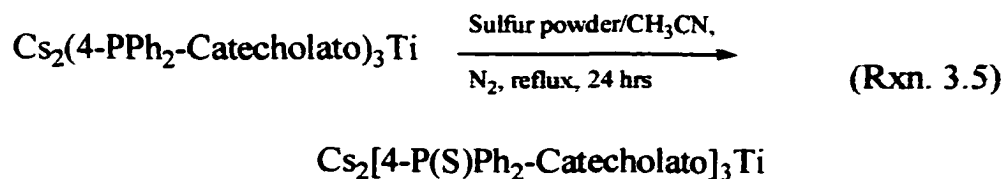
Cs$_2$[4-P(S)Ph$_2$-Catecholato)$_3$]Ti has been spectrally characterized. These data are fully consistent with conversion of all three PPh$_2$- groups to (S)PPh$_2$. The product's IR spectrum contains a P=S stretching band at 712 cm^{-1} and its ^{31}P{^{1}H} NMR spectrum shows a single resonance at δ +42.88 ppm, again confirming sulfuration. [140, 152]

{[4-P(CH$_3$)Ph$_2$-Catecholato]$_3$Ti}I:

The complex was synthesized by the peralkylation of Cs$_2$(4-PPh$_2$-Catecholato)$_3$Ti with excess methyl iodide in acetonitrile under N$_2$ (Rxn.3.6). This reaction was complete in 20 hrs at room-temperature, as shown by ^{31}P{^{1}H} NMR spectroscopy.

$$Cs_2(4\text{-}PPh_2\text{-}Catecholato)_3Ti \xrightarrow[\text{N}_2, \text{ R.T., 20 hrs}]{\text{x.s CH}_3\text{I /CH}_3\text{CN,}}$$ (Rxn. 3.6)

$$\{[4\text{-}(CH_3)PPh_2\text{-}Catecholato]_3Ti\}I + 2\ CsI$$

112
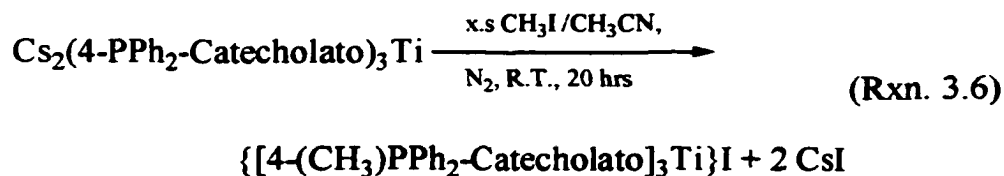
The product is yellow in color, and has been characterized by IR, ^{1}H, ^{13}C$\{^1$H$\}$, ^{31}P$\{^1$H$\}$ NMR, and CHN elemental analysis. These data are consistent with conversion of all three PPh$_2$- to Me-PPh$_2$- groups. Its IR spectrum contains methyl C-H stretching bands at 2963, 2891cm^{-1} and its ^{31}P$\{^1$H$\}$ NMR spectrum shows a singlet at δ +20.09 ppm which directly supports the fully methylation of its three PPh$_2$- groups.

These three derivatives: $Cs_2[4\text{-}P(O)Ph_2\text{-}Catecholato)_3]Sn$, $Cs_2[4\text{-}P(S)Ph_2\text{-}Catecholato)_3]Ti$ and $\{[4\text{-}P(CH_3)Ph_2\text{-}Catecholato]_3Ti\}I$, all exhibit a single set of PPh$_2$-, catecholate and phenyl resonances in their ^{31}P$\{^1$H$\}$, ^{1}H and ^{13}C$\{^1$H$\}$ NMR spectra, which confirms that they have retained the same C_3 symmetry of their parent complexes, at least in solution.

113

(e) Syntheses and Characterization of Ti(IV) Complexes of 4-PH₂-Catechol•HBr and 4-P(CH₂OH)₂-Catechol•HBr

$\text{Cs}_2(4\text{-PH}_2\text{-Catecholato})_3\text{Ti}$: Under protection of a N_2 atmosphere, the reaction of stoichiometric amounts (in a molar ratio of 6:2:5) of 4-PH₂-Catechol•HBr, Ti(OMe)₄ and Cs₂CO₃ in degassed methanol at room temperature was complete in two days, affording a dark-red product in a yield of 84% (Rxn. 3.7).

$$6 \ \textit{4}\text{-PH}_2\text{-Catechol•HBr} + 2 \ \text{Ti(OMe)}_4 + 5 \ \text{Cs}_2\text{CO}_3 \xrightarrow[\text{R. T., 2 days}]{\text{methanol, } N_2}$$

$$2 \ \text{Cs}_2(4\text{-PH}_2\text{-Catecholato})_3\text{Ti} + 6 \ \text{CsBr} + 5 \ \text{H}_2\text{CO}_3 + 8 \ \text{MeOH}$$

(Rxn. 3.7)
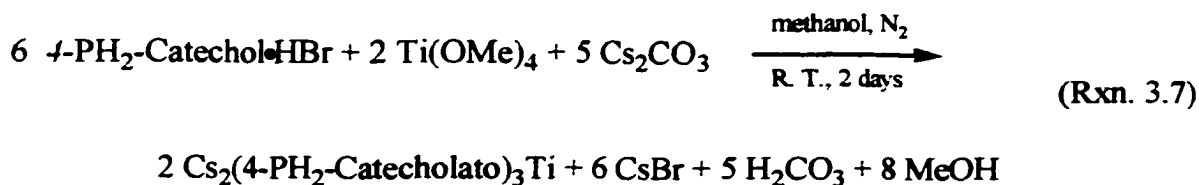
Again, only one set of ligand phosphino, catecholato resonances was observed in its ^{31}P, ^1H, and $^{13}C\{^1H\}$ NMR spectra, indicating either the exclusive formation of *fac*-isomer or a facile *fac/mer* exchange. Its IR spectrum contains a characteristic medium - PH₂ stretching band at 2285 cm⁻¹, and a strong band at 1246 cm⁻¹ indicative of coordinated catecholate C-O groups. As with the PPh₂ groups in Cs₂Ti(4-PPh₂-Catecholato)₃, the PH₂- groups were also uncoordinated in accord with their observed $^{31}P\{^1H\}$ singlet chemical shift (δ -123.8 ppm). As shown in Figure 3.21, the protons of these PH₂- groups can exchange with D₂O, with the conversion of PH₂- to PD₂- essentially complete after an overnight standing. All three catecholate proton resonances shifted upfield upon Ti(IV) complexation by 0.15 up to 0.37 ppm, as previously observed for the Cs₂(4-PPh₂-Catecholato)₃Ti complex. These upfield shifts have been attributed to the reduced ring current as a result of Ti(IV) coordination. As seen in Figure 3.22, both

114

C(1) and C(2) signals are shifted downfield by about 13.2 ppm upon C-O metal coordination, whereas other carbon resonances are observed to have small upfield shifts of 0.7 to 3.6 ppm.
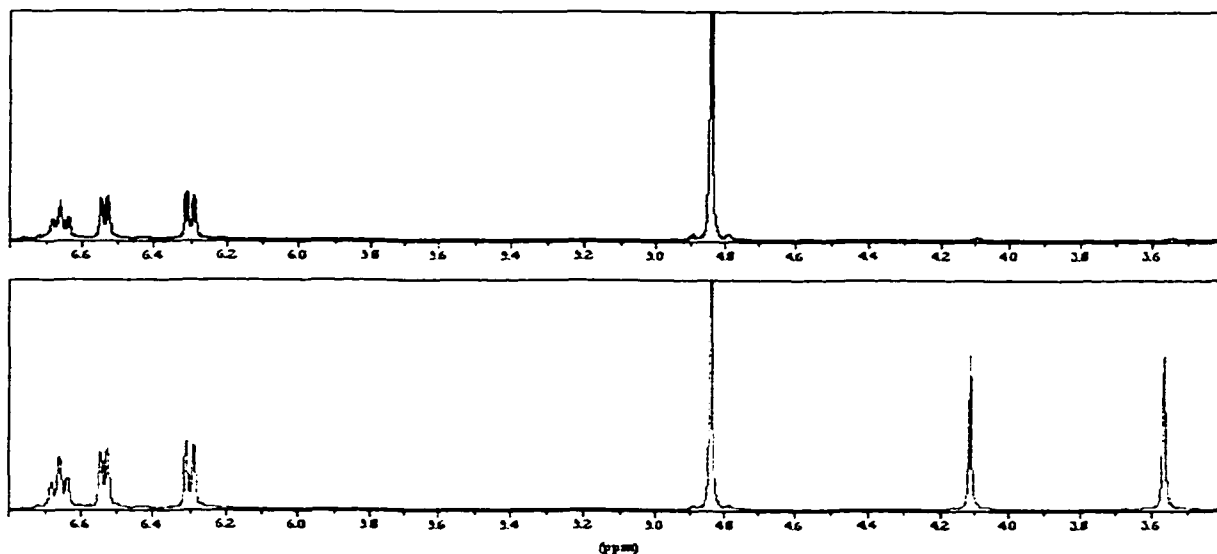
Figure 3.21 The ^{1}H NMR spectra of Cs$_2$(4-PH$_2$-Catecholato)$_3$Ti in D$_2$O. The bottom one was taken immediately after dissolution, the upper one was taken after overnight.
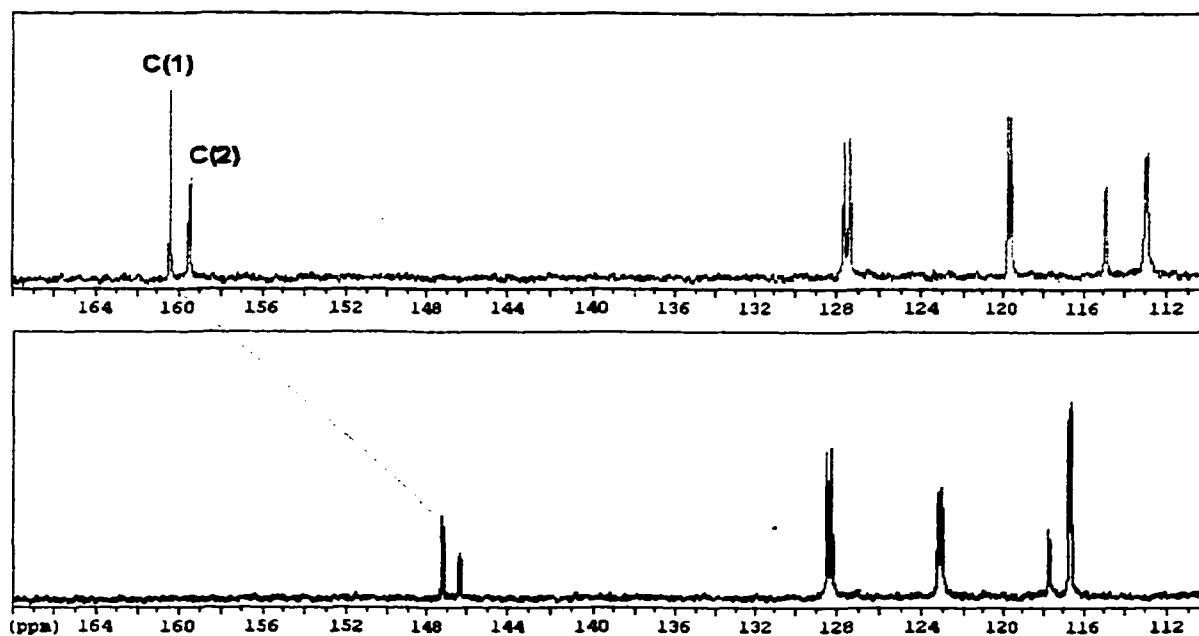
Figure 3.22 The ^{13}C{^{1}H} NMR spectra of 4-PH$_2$-Catechol•HBr (bottom) and Cs$_2$(4-PH$_2$-Catecholato)$_3$Ti (top) in D$_2$O

115

Cs$_2$[4-P(CH$_2$OH)$_2$-Catecholato]$_3$Ti: This complex can be synthesized via two synthetic routes, both in good yields (Scheme 3.5): (1) In degassed methanol, direct reaction of 4-P(CH$_2$OH)$_2$-Catechol•HBr, Ti(OMe)$_4$ and Cs$_2$CO$_3$ in a molar ratio of 6:2:5, and (2) Formylation of Cs$_2$(4-PH$_2$-Catecholato)$_3$Ti by 37 % aqueous formaldehyde in ethanol.

6 4-PH$_2$-Catechol•HBr + 2 Ti(OMe)$_4$ + 5 Cs$_2$CO$_3$

methanol, N$_2$
R. T., 2 days

2 Cs$_2$(4-PH$_2$-Catecholato)$_3$Ti

ethanol, N$_2$
37 wt% CH$_2$O

2 Cs$_2$[4-P(CH$_2$OH)$_2$-Catecholato] $_3$Ti

methanol, N$_2$
R. T., 2 days

6 4-P(CH$_2$OH)$_2$-Catechol•HBr + 2 Ti(OMe)$_4$ + 5 Cs$_2$CO$_3$
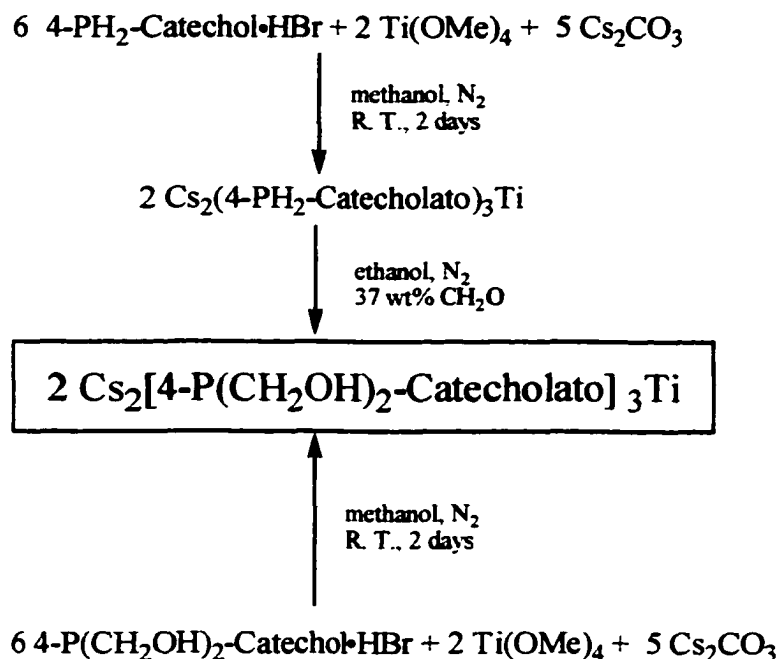
Scheme 3.5 Two synthetic routes to Cs$_2$[4-P(CH$_2$OH)$_2$-Catecholato]$_3$Ti

The absence of any -PH$_2$ stretching bands around 2285 cm^{-1} in its IR spectrum indicates fully formylation of Cs$_2$ (4-PH$_2$-Catecholato)$_3$Ti. The product is a water-soluble orange-red solid. As observed for other catecholate metal complexes, it also exhibited only one set of ligand phosphino, catecholato and methylene resonances in its ^{31}P{^{1}H}, ^{1}H, and ^{13}C{^{1}H} NMR spectra in solution, again indicating either only the *fac*-isomer or a facile *fac/mer* exchange. Its IR spectrum contains a strong band at 1250 cm^{-1} indicative of coordinated catecholate C-O groups.

116
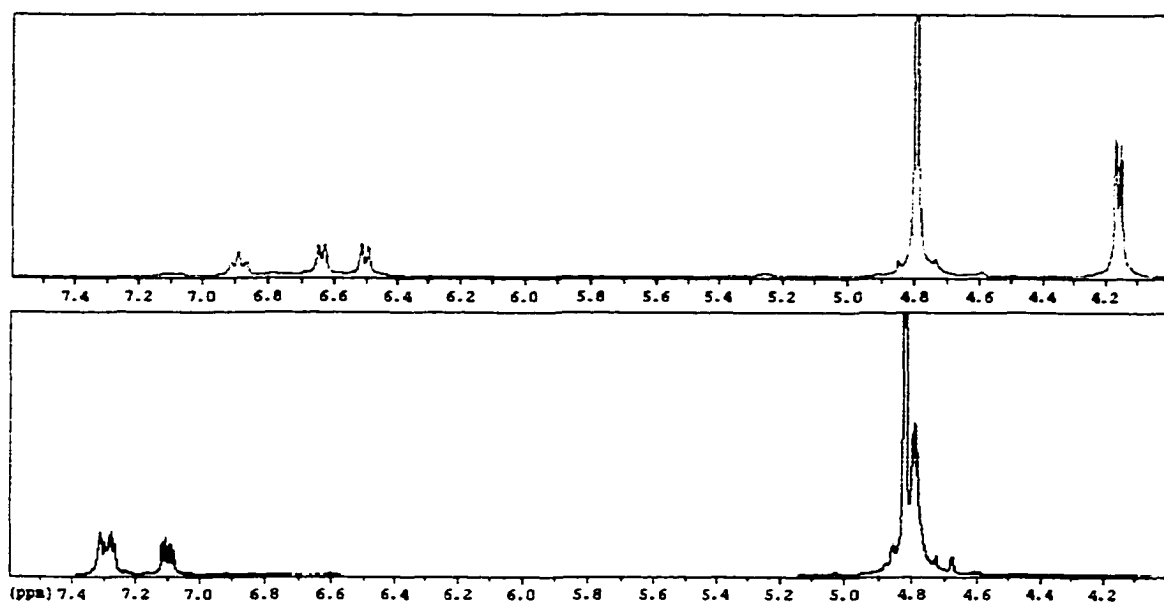
Figure 3.23 Comparative ^{1}H NMR spectra of 4-P(CH$_2$OH)$_2$-Catechol•HBr (bottom) and Cs$_2$[4-P(CH$_2$OH)$_2$-Catecholato]$_3$Ti (top) in D$_2$O
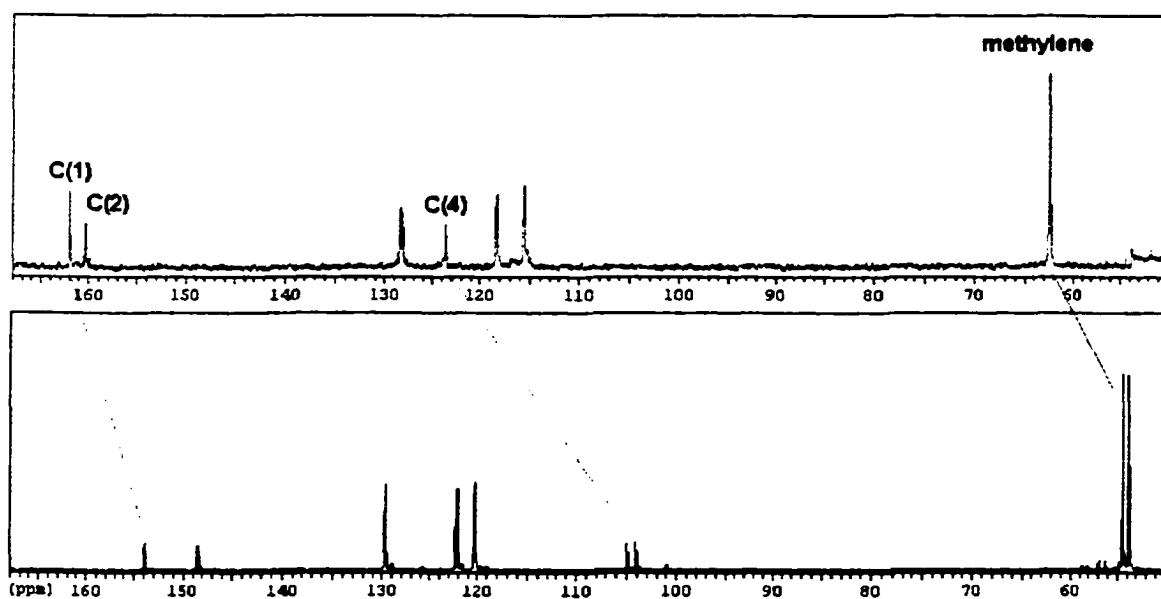
Figure 3.24 Comparative ^{13}C NMR spectra of 4-P(CH$_2$OH)$_2$-Catechol•HBr (bottom) and Cs$_2$[4-P(CH$_2$OH)$_2$-Catecholato]$_3$Ti (top) in D$_2$O.

117

As can be seen in Figure 3.23, all three catecholate proton resonances again shift upfield upon Ti(IV) complexation by 0.36 up to 0.61 ppm, as previously observed for other catecholato metal complex. The broad methylene signal shifted upfield from 4.78 to 4.15, becoming a resolved doublet ($^2J_{PCH}$ = 5.49 Hz). As seen in Figure 3.24, C(1) and C(2) resonances are shifted downfield by 7.8 ppm and 11.7 ppm, respectively upon C-O metal coordination. Interestingly, while other carbons had normal upfield shifts by 1.4 to 4.8 ppm, the C(4) significantly shifted downfield from 104.5 to 123.6 ppm, and the associated $^1J_{P\text{-}ipso\text{-}C}$ decreased from 78.6 to 5.3 Hz. The methylene C also shifted downfield from 54.0 to 62.2 ppm, and the associated $^1J_{P\text{-}CH2}$ decreased from 57.1 to 4.6 Hz. These observations indicate that the phosphino- groups of the ligand 4-P(CH$_2$OH)$_2$-Catechol•HBr remains protonated in water, which is consistent with its ^{31}P{^{1}H} resonance at δ +19.86. Upon C-O metal coordination, this ^{31}P{^{1}H} resonance shifted upfield from δ +19.86 to -21.7, which strongly suggests a deprotonation of the HP(CH$_2$OH)$_2$- groups after complexation, decreasing the $^1J_{P\text{-}C}$ coupling constant. The sizeable downfield shifts of both the C(4) and methylene carbon signals may be similarly explained.

As discussed for the diamagnetic *tris*(4-PPh$_2$-catecholate) metal complexes, these two titanium complexes of 4-PH$_2$-Catechol and 4-P(CH$_2$OH)$_2$-Catechol are either exclusively the *fac*-isomers or in facile *fac/mer* exchange in solution at room temperature. The accessibility of these *fac*-isomers of C_3 symmetry makes the two complexes also potential precursors for the formation of endohedral mixed-metal clusters.

118

Chapter IV

Syntheses and Characterization of Mixed-Metal Clusters

As described in Chapter I, our 4-Phosphino-Catechol hybrid ligands combined hard catecholate and soft phosphine donor sites which are isolated due to the 4-positioning of the phosphine group on the catechol ring. This unique design contains all necessary structural information *input* into the hybrid ligand for assembling mixed-metal clusters, whereby a hybrid ligand serves as a bridge connecting pairs of hard and soft metals. Along with the required stoichiometry, the respective incommensurate symmetry generated at the soft metal center (4- or 2-fold symmetry) and hard metal center (3-fold symmetry) provides the driving force for cluster formation.

There are two ways of synthesizing mixed-metal clusters from 4-Phosphino-Catechols: (1) An *aufbau* (stepwise) process, and (2) Self-assembly.

By *aufbau*, in principle, we can prepare either phosphino complexes of 2- or 4-fold symmetry or catecholato complexes of 3-fold symmetry as intermediates, and then synthesize mixed-metal clusters by reacting these intermediates with appropriate hard- or soft-metal precursors. As discussed in Chapter III, the only soft-metal phosphino complex of 4-Phosphino-Catechols we have successfully synthesized is $RuBr_2(4-PH_2-Catechol)_4$ of 4-fold symmetry. Thus for the combination of 2-fold (soft-metal) and 3-fold (hard-metal) centers, we decided to start with catecholato complexes of 3-fold symmetry in the first step. As for the combination of 4-fold (soft-metal) and 3-fold (hard-metal) centers, we can take either approach.

119

Self-assembly is the preferred way adopted by nature in making high-symmetry molecular clusters. A biomolecular cluster is usually composed of only *one* kind of protein subunits. In other words, a specific natural cluster only requires a single component. By contrast, the formation of metal-ligand coordination clusters involves at least two components: metal and ligand. For our hybrid ligand, a mixed-metal cluster formation must have at least three components: soft-metal, hard-metal and hybrid ligand. Of the two discrete binding sites of 4-Phosphino-Catechols, the phosphine group has a strong preference to soft-metals, while the catecholate can coordinate both hard and soft metals with a preference for hard metals. Therefore, the successful self-assembly of a mixed-metal cluster will depend on whether any transient catecholato soft-metal products are kinetically labile.

By employing both *aufbau* and self-assembly approaches, we have successfully synthesized many mixed-metal clusters of C_3 symmetry from the hybrid ligand 4-PPh$_2$-Catechol (H$_2$L). Several of these have been crystallographically characterized as triple mesocates of C_{3h} symmetry.

Results and Discussion

As discussed in Chapter II, the *tris*(4-PPh$_2$-Catecholato) metal complexes [M-(L)$_3$]$^{2-}$ [M = Ti(IV), Sn(IV)] and [M-(L)$_3$]$^{3-}$ [Ga(III)] of C_3 symmetry (or averaged C_3 symmetry) have three divergent diphenylphosphino groups, which are *syn* (or averaged *syn*) to each other in solution. These uncoordinated PPh$_2$- groups can coordinate to three separate soft-metal centers (M'). If these soft-metal centers have C_2 symmetry,

supramolecular mixed-metal clusters of the type $M_2L_6M'_3$ can be assembled (Scheme 4.1). To date, three soft-metals [Pd(II), Ag(I), Cr(0)] have successfully played this role in the formation of mixed-metal clusters.
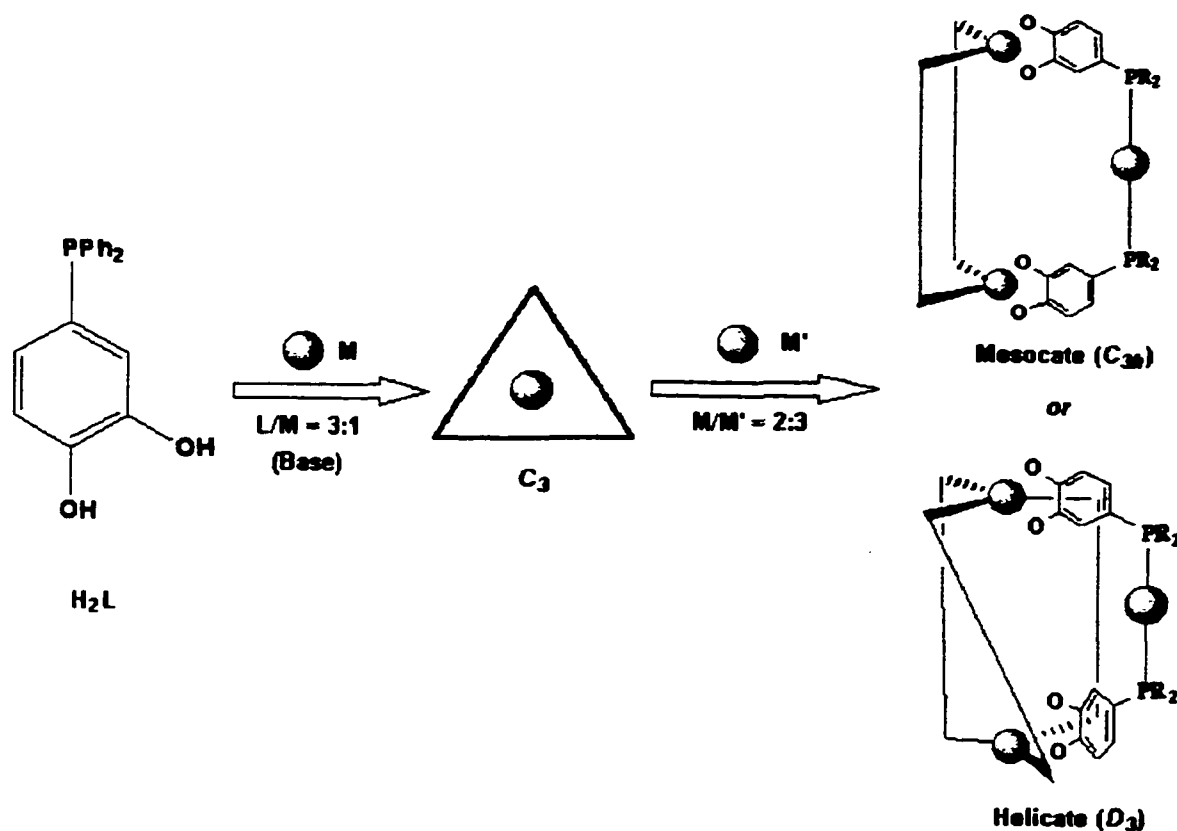
Scheme 4.1 *Aufbau* route to synthesize $[M_2L_6M'_3]^{4-}$ mixed-metal clusters

1. **Syntheses and Characterization of $[M_2L_6Pd_3X_6]^{4-}$ Clusters [M = Ti(IV), Sn(IV); L = 4-Diphenylphosphino-Catecholato, X = Cl⁻, Br⁻, I⁻]**

(a) *Aufbau Synthesis and Characterization of the $[Ti_2L_6Pd_3Br_6]^{4-}$ Cluster*

Aufbau of the $Cs_4Ti_2L_6Pd_3Br_6$ Cluster: This cluster was synthesized by a stepwise process, in two reactions (Rxn. 4.1 and 4.2). In the second reaction, three equivalents of

121

PdBr$_2\bullet$2PhCN was reacted with two equivalents of Cs$_2$TiL$_3$ in a DMF solution, giving a single product in 2 hours, as shown by ^{31}P{^{1}H} NMR spectroscopy. No exchange between this cluster with free Cs$_2$TiL$_3$ was observed on the NMR timescale at ambient temperature. Workup and isolation of the orange-red product gave a yield of 95%.

$$6 \ H_2L\cdot HBr + 2 \ Ti(OMe)_4 + 5 \ Cs_2CO_3 \xrightarrow[\text{42 hrs}]{\text{MeOH, N}_2}$$

(Rxn. 4.1)

$$2 \ Cs_2TiL_3 + 6 \ CsBr + 8 \ MeOH + 5 \ H_2CO_3$$

$$2 \ Cs_2TiL_3 + 3 \ PdBr_2(PhCN)_2 \xrightarrow[\text{2 hrs}]{\text{DMF, N}_2}$$

(Rxn. 4.2)

$$Cs_4Ti_2L_6Pd_3Br_6 + 6 \ PhCN$$
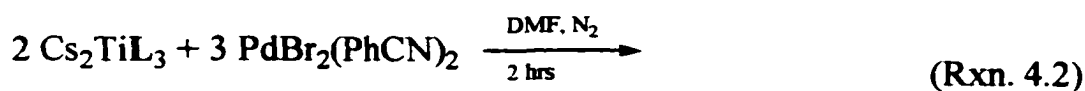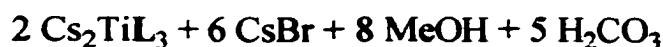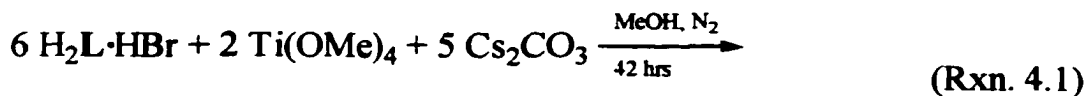
This product has been characterized by IR, ^{31}P{^{1}H}, ^{1}H, ^{13}C{^{1}H} NMR spectroscopy, and CHN elemental analyses as well as positive ion FAB mass spectrometry. Specifically, a singlet ^{31}P{^{1}H}NMR resonance, and a single set of proton, carbon signals in its ^{1}H, ^{13}C{^{1}H} NMR spectra (Figure 4.2-3) confirmed the formation of this mixed-metal cluster of C_3 symmetry (or averaged C_3 symmetry) in DMF solution. As shown in Figure 4.2, the three proton signals of the complex, catecholate are well-resolved, though all proton resonances are relatively broad due perhaps to the large molecular size of the new mixed-metal cluster or to dynamic

Figure 4.1 L-bridged Pd^{II} and Ti^{IV} in the [Ti$_2$L$_6$Pd$_3$Br$_6$]$^{4-}$ cluster

behavior. The assignment of catecholate protons can be made by selective-irradiation NMR experiments (Figure 4.1, 4.4).

In its $^{13}C\{^1H\}$ NMR spectrum, the most significant observation is the appearance of virtual triplets which were doublets in the precursor Cs_2TiL_3 spectrum (see insets) in resonances for both catecholate and phenyl ring carbons which strongly suggests a *trans*-phosphine coordination mode at the Pd(II) centers.[131, 132] Assignments of the catecholate carbon signals can be unambiguously made from the ^1H-^{13}C HETCOR NMR spectrum (Figure 4.1, 4.3, 4.5).
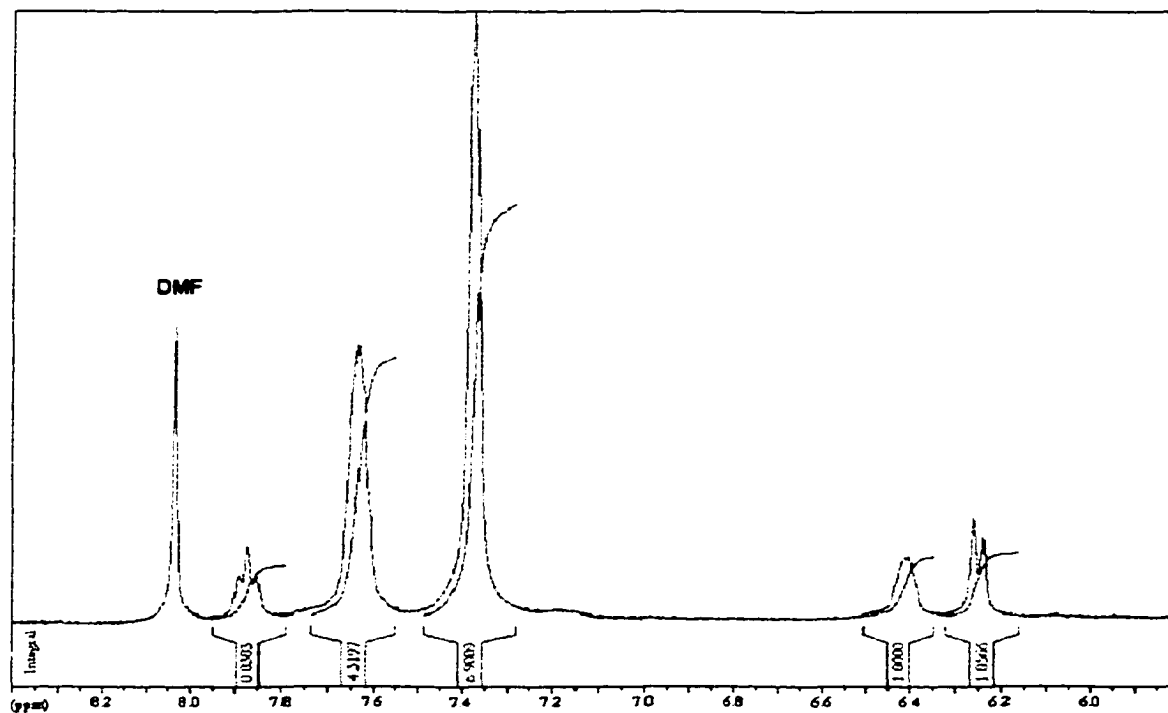
Figure 4.1 ^1H NMR spectrum of $Cs_4Ti_2L_6Pd_3Br_6$ cluster in DMF-d_7

123
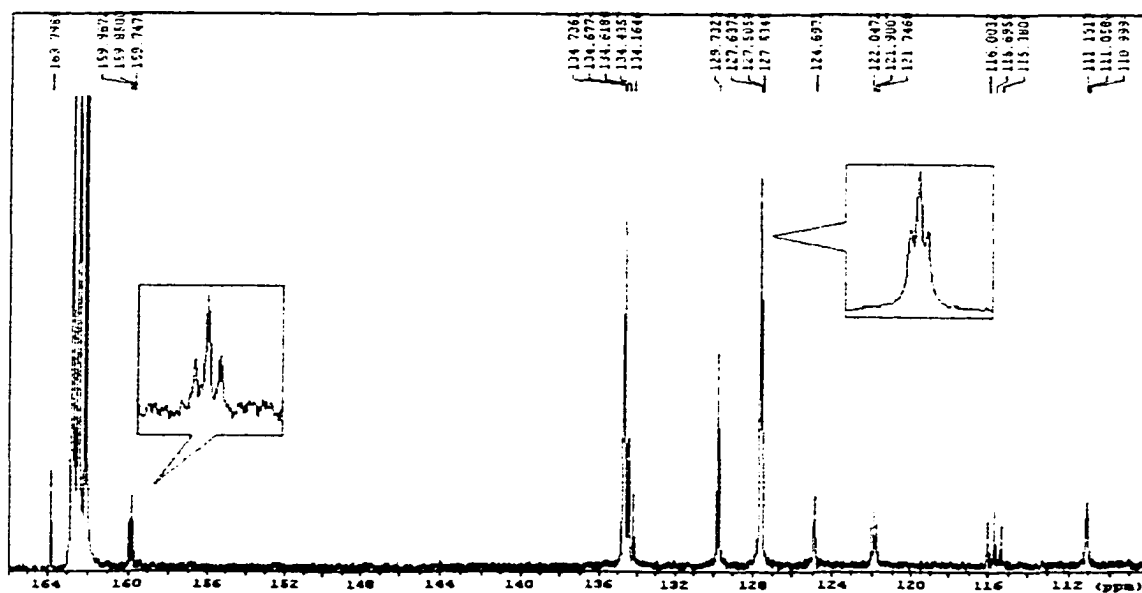
Figure 4.3 $^{13}C\{^1H\}$ NMR spectrum of $Cs_4Ti_2L_6Pd_3Br_6$ cluster in DMF-d_7. All doublets in the $^{13}C\{^1H\}$ NMR spectrum of Cs_2TiL_3 have become *virtual triplets* indicative of the $PdBr_2$ moiety *trans*-coordinated by two PPh_2- groups.
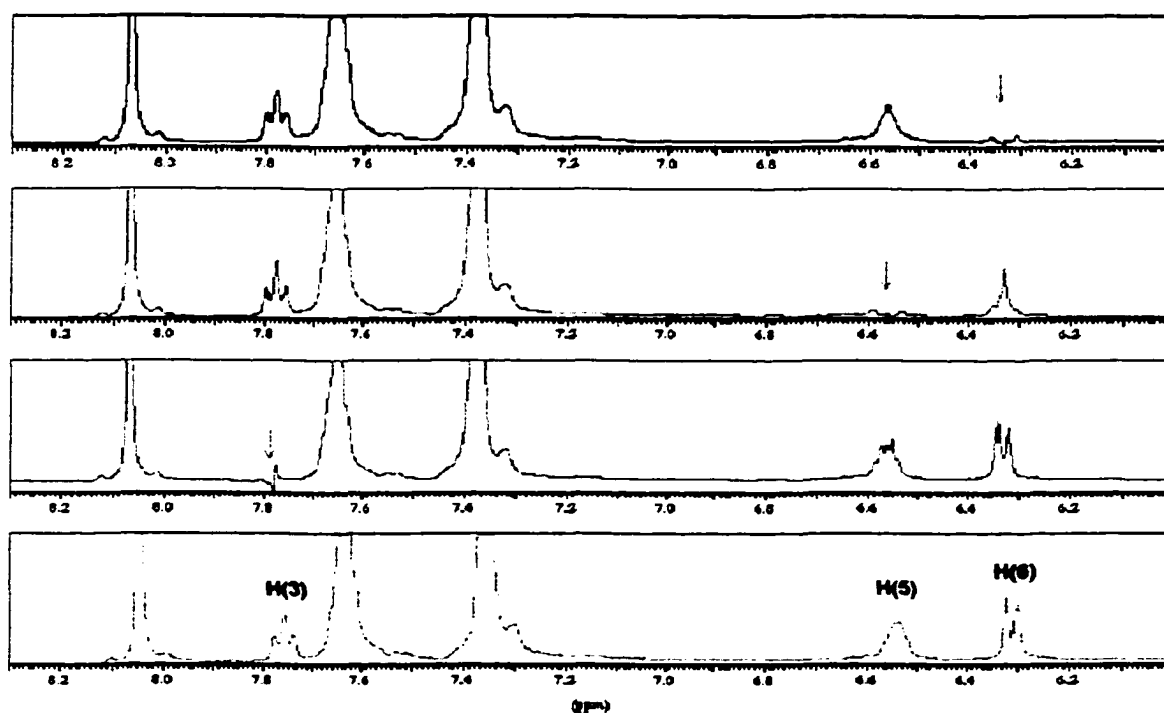
Figure 4.4 Comparative ^1H-NMR spectra of selective irradiation of $[Ti_2L_6Pd_3Br_6]^{4-}$ cluster in DMF-d_7 (the bottom one is the ^1H-NMR spectrum without irradiation)

124
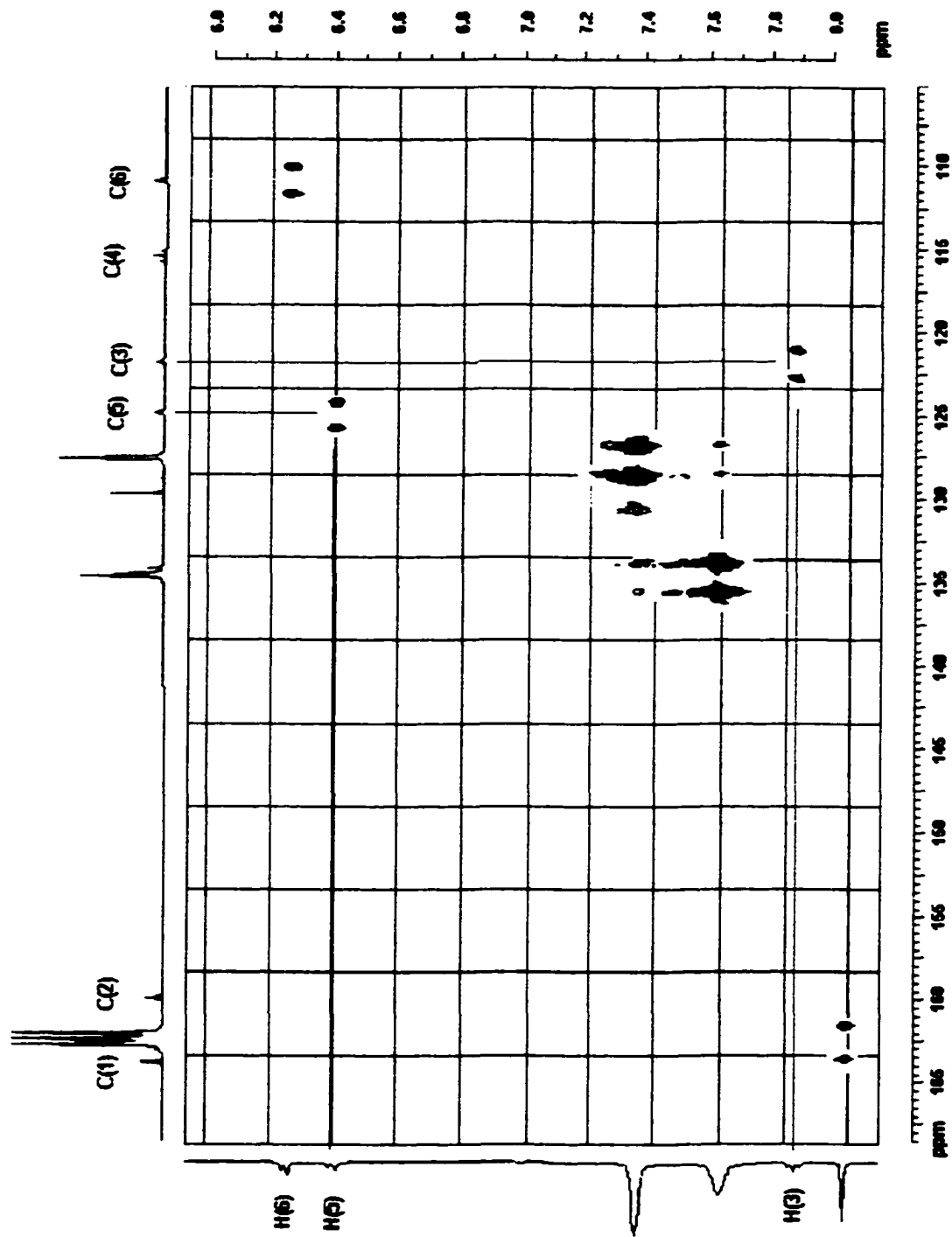
Figure 4.5 ^{1}H-^{13}C HETCOR NMR spectrum of $Cs_4Ti_2L_6Pd_3Br_6$ in DMF-d$_7$

125

In the comparative ^{1}H NMR spectra of $H_2L\bullet HBr$, Cs_2TiL_3, and the $Cs_4Ti_2L_6Pd_3Br_6$ cluster in DMF-d_7, all three catecholate proton resonances of $H_2L\bullet HBr$ are shifted upfield by 0.26 up to 0.73 ppm upon titanium(IV) complexation to form Cs_2TiL_3, as discussed in Chapter III. After the formation of the $Cs_4Ti_2L_6Pd_3Br_6$ cluster, the H(3) catecholate proton multiplet shifted dramatically downfield from δ 6.21 to 7.87 and broadened into a virtual triplet, while H(5) and H(6) are just slightly shifted. This large shift may be caused by: (1) magnetic anisotropy, and(or) (2) steric compression because of the cluster formation. In the latter case, the H(3) attached carbon C(3) resonances should shift upfield, which is contrary to the actual observed downfield shift of C(3) (Figure 4.7). Thus a significant change in magnetic anisotropy upon cluster formation is the more likely explanation.

The enhanced electron-withdrawing effect on phosphine groups upon Pd(II) coordination resulted in deshielding of the *ortho*-protons of the phenyl groups, and their downfield shift from δ 7.28 to 7.63 (Figure 4.2 and 4.6).

A change of ^{13}C-^{31}P coupling constants ($^1J_{PC}$) of P-bonded carbons of both phenyl and catecholate groups is also noteworthy. As noted in Figure 4.6, upon titanium(IV) complexation, the coupling constants ($^1J_{PC}$) of both these phenyl carbons and catecholate C(4) only changed slightly (from 11.3 Hz to 12.5 Hz, and 7.3 Hz to 3.8 Hz, respectively), indicating that the diphenylphosphino (PPh$_2$-) groups of H_2L and Cs_2TiL_3 both remain uncoordinated and unprotonated in solution. Once the $Cs_4Ti_2L_6Pd_3Br_6$ cluster is formed, these coupling constants changed significantly to 20.2 Hz (phenyl) and 28.2 Hz [C(4)] suggesting Pd(II)-coordination of these phosphine groups.

126
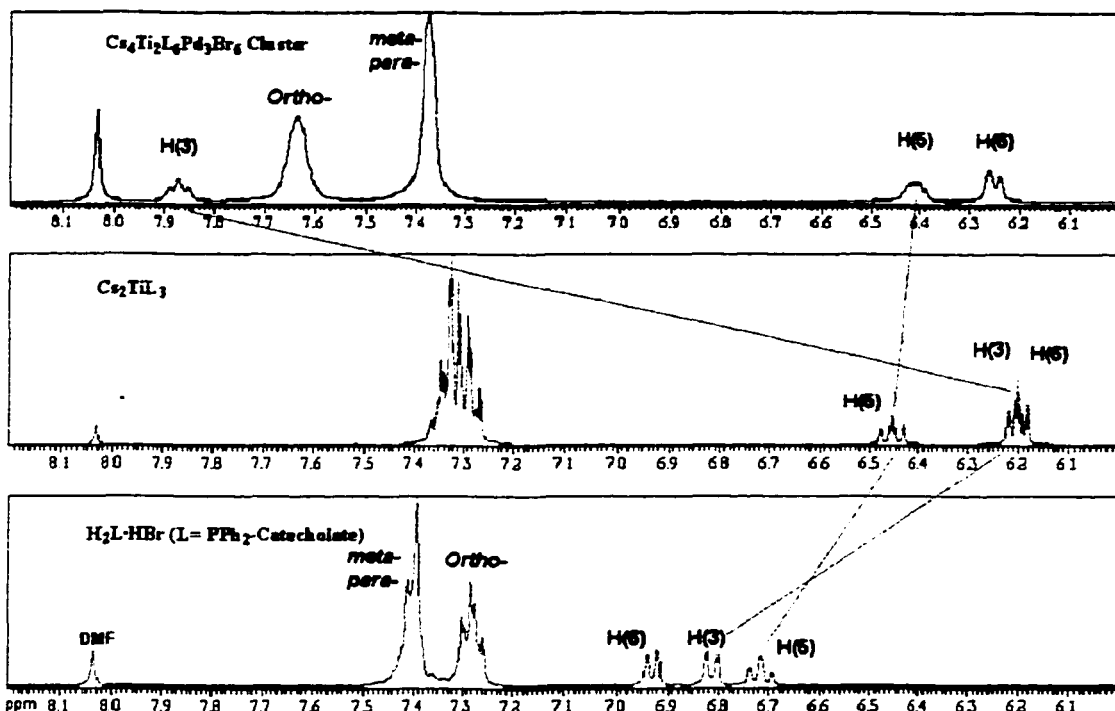
Figure 4.6 Comparative ¹H NMR spectra of H₂L, Cs₂TiL₃, and Cs₄Ti₂L₆Pd₃Br₆ in DMF-d₇
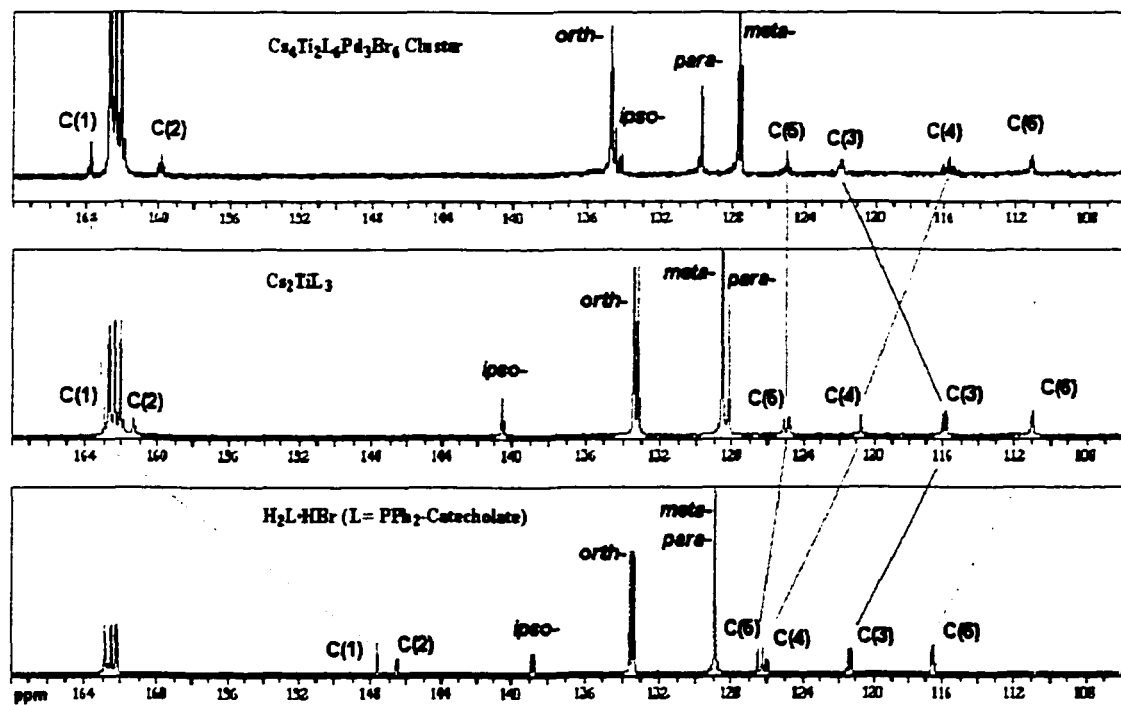
Figure 4.7 Comparative ¹³C{¹H} NMR spectra of H₂L, Cs₂TiL₃, and Cs₄Ti₂L₆Pd₃Br₆ in DMF-d₇

127

The positive ion Fast Atom Bombardment (FAB$^+$) mass spectrum of Cs$_4$Ti$_2$L$_6$Pd$_3$Br$_6$ cluster is shown in Figure 4.8. The molecular formula of the mixed-metal cluster is confirmed to be Cs$_4$Ti$_2$L$_6$Pd$_3$Br$_6$ (Cs$_4$Ti$_2$C$_{108}$H$_{78}$O$_{12}$P$_6$Pd$_3$Br$_6$, MW = 3179.70), which is also supported by its CHN elemental analyses. Calculated and experimental FAB$^+$ mass peaks are listed in Table 4.1.

128
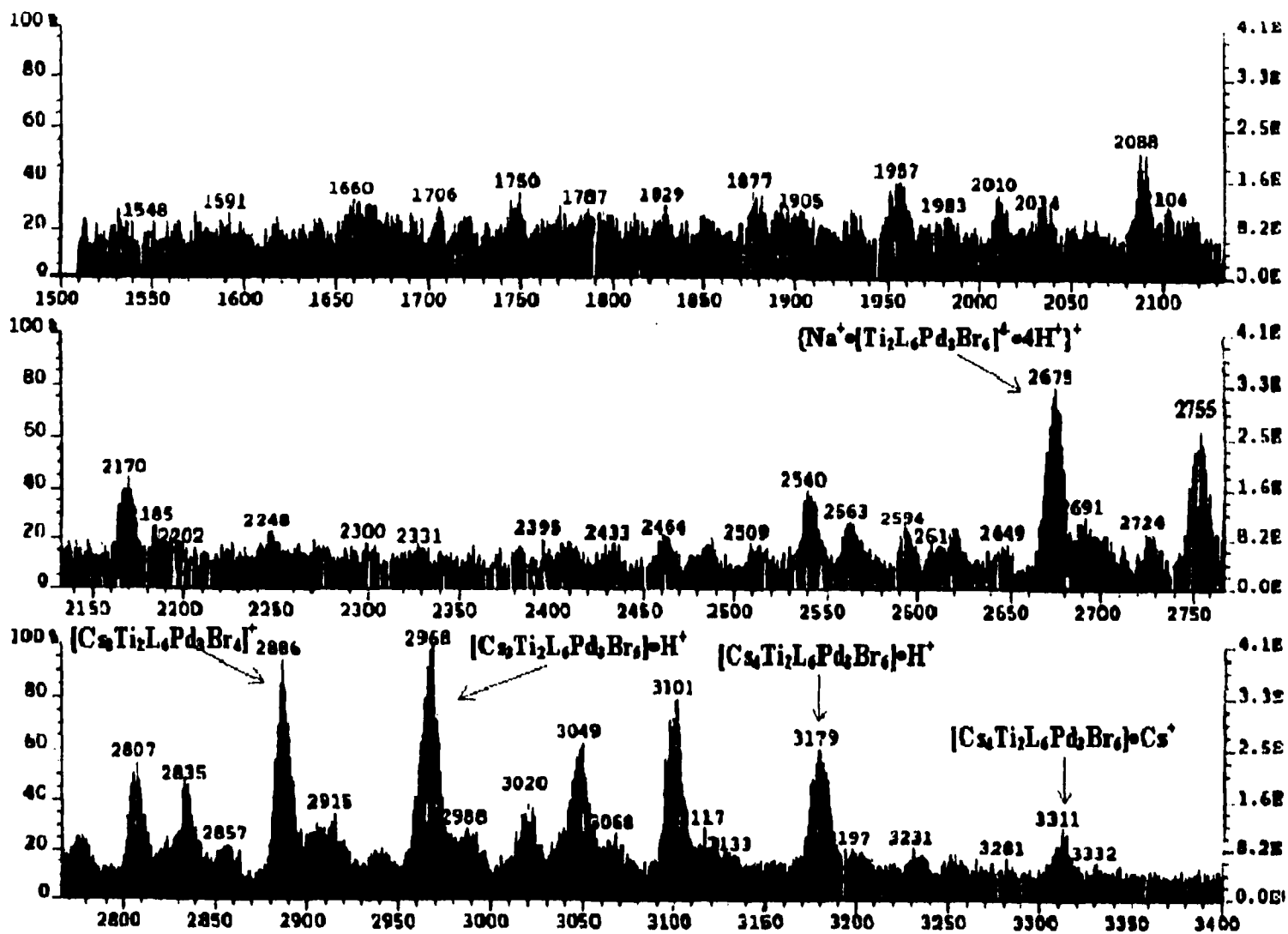
Figure 4.8 FAB$^+$ mass spectrum of $Cs_4Ti_2L_6Pd_3Br_6$ cluster in DMF (nitrobenzyl alcohol matrix)

Table 4.1 FAB^+ mass peaks (m/z) and calculated peaks of the $Cs_4Ti_2L_6Pd_3Br_6$ cluster

Fragments	Calc'd Peaks (m/z)	FAB^+ Mass Peaks (m/z)
$[Cs_4Ti_2L_6Pd_3Br_6] \bullet Cs^+$	3312.61	3311
$[Cs_4Ti_2L_6Pd_3Br_6] \bullet H^+$	3180.71	3179
$[Cs_4Ti_2L_6Pd_3Br_5]^+$	3099.79	3101
$\{[Cs_3Ti_2L_6Pd_3Br_6]^- \bullet 2H^+\}^+$	3048.81	3049
$[Cs_3Ti_2L_6Pd_3Br_5] \bullet H^+$	2967.89	2968
$[Cs_3Ti_2L_6Pd_3Br_4]^+$	2886.97	2886
$\{[Cs_2Ti_2L_6Pd_3Br_5]^- \bullet 2H^+\}^+$	2835.99	2835
$\{Na^+ \bullet [CsTi_2L_6Pd_3Br_6]^{3-} \bullet 3H^+\}^+$	2806.99	2807
$[Cs_2Ti_2L_6Pd_3Br_4] \bullet H^+$	2755.08	2755
$\{Na^+ \bullet [Ti_2L_6Pd_3Br_6]^{4-} \bullet 4H^+\}^+$	2675.10	2675

X-ray Structure of $[Cs_4Ti_2L_6Pd_3Br_6] \bullet 9THF \bullet H_2O \bullet 1.5Et_2O \bullet 1.5DMF$. A single-crystal X-ray diffraction study confirmed the successful assembly of the desired heterometallic cluster which crystallizes in the hexagonal space group P6₃/m (#176) with two formula units in the unit cell. The cluster anion has crystallographic 3/m symmetry (Figure 4.9) (three-fold symmetry along the Ti • • • Ti axis with a perpendicular mirror plane: C_{3h} point group), namely, it is a triple mesocate featuring one Ti center having Δ and the other a Λ configuration. This tetraanion can be described as a pentametallic

130

Figure 4.9 Space-filling model of X-ray structure of the $Cs_4Ti_2L_6Pd_3Br_6$ cluster. On the left is a topview of the cluster down the crystallographic three-fold axis, the disordered Cs atom is omitted for clarity. The right is a sideview of the cluster, the Cs atom is disordered 50/50 at both capping sites, as shown here only on the top. (Cs atoms are in green, Ti atoms in light brown, Pd atoms in ocean-blue, Br atom in dark-blue, O atoms in red, P atoms in yellow, C and H atoms in gray)
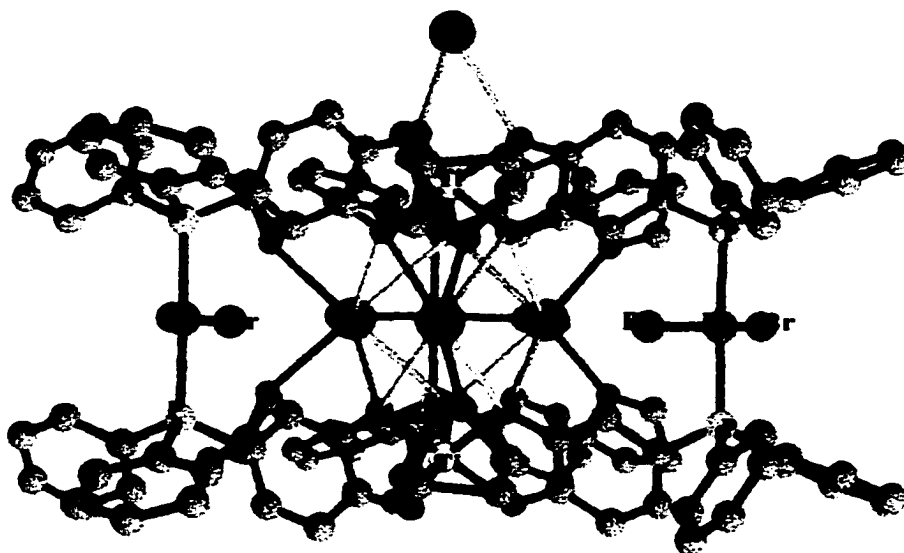
Figure 4.10. Stereographic representation (sideview) of the $Cs_4Ti_2L_6Pd_3Br_6$ cluster. Each of the two titanium(IV) ions is coordinated by three bidentate catechol ligands, with the three palladium(II) ions acting as bridges between the two *tris*(catecholato)titanium caps. A three-fold symmetry axis goes through the Ti • • • Ti axis with the metal centers separated by 6.76 Å. Three Cs atoms are deeply embedded in the clefts along with their coordinating THF molecules.

131
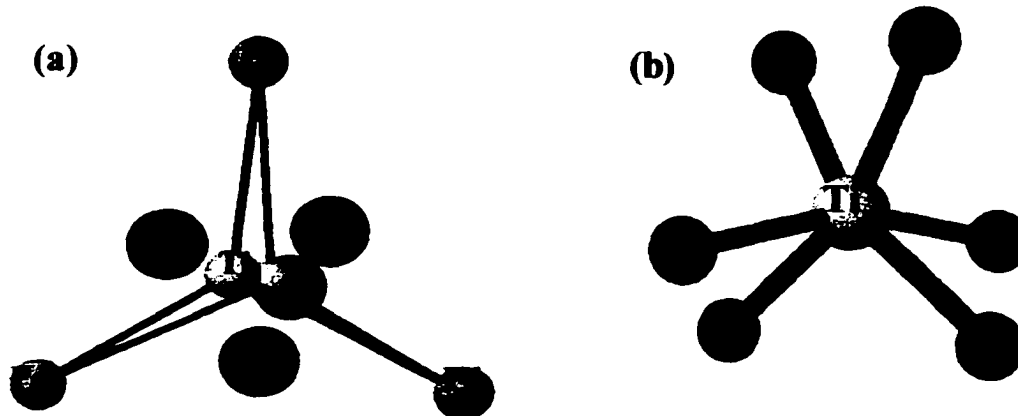
Figure 4.11 (a) The metal core of the $Cs_4Ti_2L_6Pd_3Br_6$ cluster. A three-fold symmetry axis goes through the Ti • • • Ti axis, three palladium atoms acting as bridges between the two *tris*(catecholato)titanium caps. Three Cs atoms are deeply embedded in the clefts, while the fourth Cs atom is disordered 50/50 at both capping sites. (b) The coordination geometry of titanium(IV) is distorted towards trigonal prismatic, with a twist angle of $36.9°$ ($0°$ for a trigonal prism, $60°$ for an octahedron).
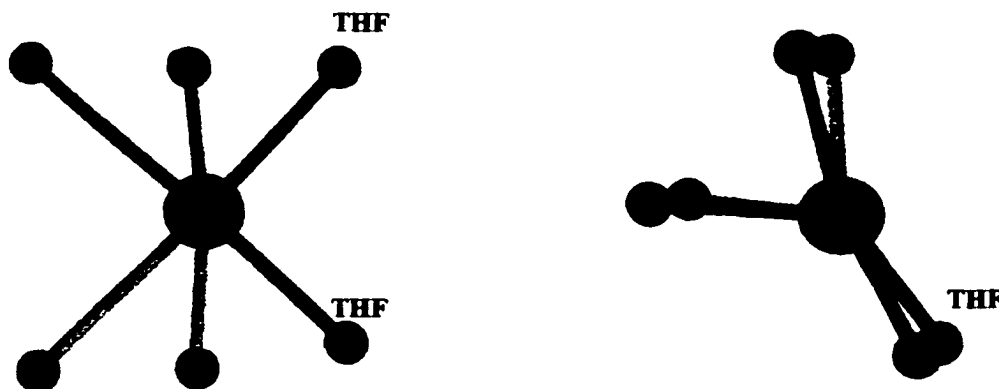
Figure 4.12 The coordination sphere and geometry of the cleft-embedded cesium cation Cs(2). From the interior of the cluster, Cs(2) is coordinated by four *endo*-catecholato oxygens in a rectangular array (represented by light-red bonds, left) and two *exo*-THF solvent molecules (represented by dark-red bonds, right). The coordination geometry is a pseudo-trigonal prism (right).

132

coordination cluster: each of the two titanium(IV) ions is coordinated by three bidentate catecholate ligands, with the three palladium(II) ions acting as bridges between the two *tris*(catecholato)titanium caps (Figure 4.10-11a). A three-fold symmetry axis goes through the Ti • • • Ti axis with the metal centers separated by 6.76 Å (Figure 4.10-11a). The coordination geometry of the titanium is distorted towards trigonal prismatic, with a twist angle of 36.9° (0° for a trigonal prism, 60° for an octahedron) (Figure 4.11b). While the average Ti-catecholato oxygen distance of 1.97 Å is normal, the Ti-O(1) distance of 1.949(5) Å is significantly shorter than the Ti-O(2) distance of 1.984(5) Å (Figure 4.13). This may be a result of the strain imposed by formation of the cluster whereby *endo* Ti-O(2) bonds are stretched while *exo* Ti-O(1) bonds are compressed to accommodate the supramolecular structure. In accord with this, *exo* cluster O(1)-Ti-O(1') angles are 88.3(2)° while *endo* O(2)-Ti-O(2') are 89.2(2)°. Both O(1) and O(2) are also coordinated to Cs$^+$ cations.

Of particular interest is the location of the four cesium counterions. The three symmetry-equivalent Cs(2) atoms (related by a crystallographic 3-fold axis) are deeply embedded in the three clefts of the cluster. From the interior of the cluster, Cs(2) is coordinated by four *endo*-catecholato oxygens in a rectangular array and two *exo*-THF solvent molecules (Figure 4.12). The clefts of the cluster are so deep that the coordinating THF molecules can also be described as being buried. The shortest distance between cesium and bromine atoms [Cs(2)-Br(1)] is 4.85 Å, well out of range for the 3.6-4.0 Å distances observed in the Cambridge Structural Database, which reveals that the bromine atoms are not in van der Waals contact with the cesium cations. However, the peripheral

133

bromine atoms from the three $PdBr_2$ moieties effectively block other donors from coordinating $Cs(2)$, which can account for the usually low coordination number (CN 6) of these cesiums. As a result, relatively short Cs-O distances are observed. Specifically, $Cs(2)$ to catecholate $O(2)$ has a distance of 3.160(5) Å while the $Cs(2)$ to the THF $O(3)$ distance of 2.918(9) Å is one of the shortest reported (Figure 4.12). The distance between the embedded cesium cations is 4.45 Å. The fourth cesium cation $Cs(1)$ is located on the exterior of the anionic cluster and is coordinated by three oxygens of the *tris*(catecholato)titanium cap. The $Cs(1)$-$O(1)$ distance of 3.080(5) Å is again one of the shortest Cs-O distances observed in the Cambridge Structural Database. The remaining coordinating sphere of this cesium most likely is filled by solvent, of which disordered diethyl ether and DMF molecules are in the near vicinity of the uncoordinated side of this cesium atom. To maintain the crystallographically imposed symmetry requirements, $Cs(1)$ is disordered 50/50 at both capping sites (Figure 4.10 and 11a).

As suggested by the $^{13}C\{^1H\}$ NMR data, each of the three Pd(II) ions is effectively square-planar and coordinated by two *trans*-phosphines, with the remaining coordination sphere being filled by two bromine atoms. The Pd-P distance of 2.326(2) Å and P-Pd-P angle of 178.20(1)° are typical of such square-planar complexes. The $Pd(1)$-$Br(1)$ distance of 2.431 Å is unexceptional, whereas the second bromine is disordered over three sites, $Br(2)$, $Br(3)$, and $Br(4)$ with 72%, 16%, and 12% occupancies respectively. While the $Br(1)$-Pd-$Br(3)$ bond angle of 179.0(9)° is near linearity, $Br(2)$ is deflected into the interior of the cluster with a $Br(1)$-Pd-$Br(2)$ angle of 161.9(2)° while $Br(4)$ is deflected away from the cluster interior with a $Br(1)$-Pd-$Br(4)$ angle of 166.7(9)°. The respective Pd-Br bond distances range from a short Pd-$Br(2)$ of 2.405(2) Å, normal

134

.

Pd-Br(3) of 2.468(9) Å , to a long Pd-Br(4) of 2.50(1) Å (Figure 4.13). Considering the extent of disorder, the actual significance of these individual values is probably suspect. Other relevant bond distances and angles are listed in Table 4.2

In summary, the structure of the $Cs_4Ti_2L_6Pd_3Br_6$ cluster in the solid-state is a triple mesocate of C_{3h} symmetry with both Δ and Λ configurations of Ti centers mirrored in the same cluster.
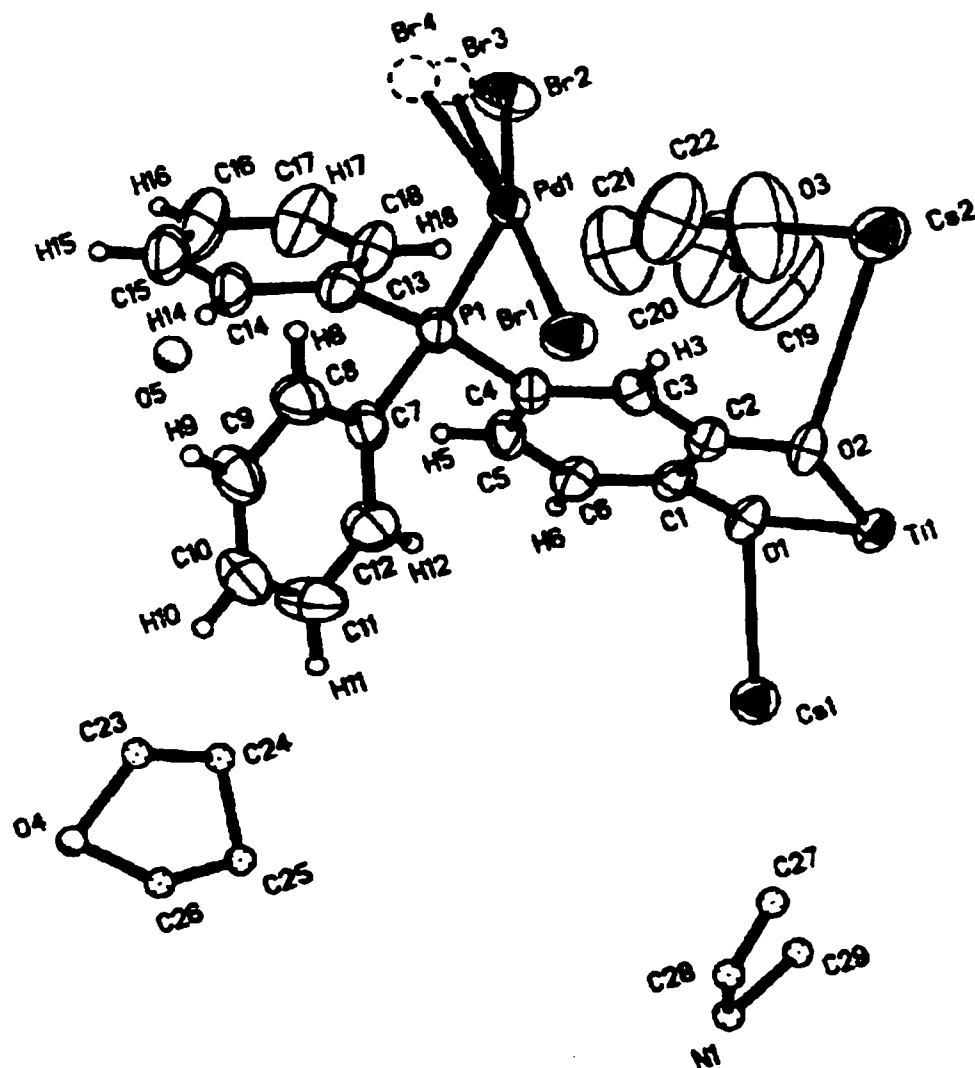
Figure 4.13 ORTEP of the asymmetric unit of the $Cs_4Ti_2L_6Pd_3Br_6$ cluster.

135

Table 4.2 Selected bond distances (Å) and bond angles (°) for the $Cs_4Ti_2L_6Pd_3Br_6$ cluster

Cs(1)-O(1)	3.080(5)	O(1)-C(1)	1.340(8)
Cs(2)-O(3)	2.918(10)	O(2)-C(2)	1.344(8)
Cs(2)-O(2)	3.138(5)	O(3)-C(22)	1.28(2)
Cs(2)-O(2')	3.080(5)	O(3)-C(19)	1.47(2)
Pd(1)-P(1)	2.326(2)	O(4)-C(26)	1.36(3)
Pd(1)-Br(2)	2.405(2)	O(4)-C(23)	1.58(2)
Pd(1)-Br(1)	2.4309(13)		
Pd(1)-Br(3)	2.468(9)		
Pd(1)-Br(3)	2.501(14)		
Ti(1)-O(1)	1.949(5)		
Ti(1)-O(2)	1.984(5)		

O(1)-Cs(1)-O(1')	52.3(2)	O(3)-Cs(2)-O(3')	83.9(6)
O(3)-Cs(2)-O(2)	91.4(3)	O(3)-Cs(2)-O(2')	141.4(2)
P(1)-Pd(1)-P(1')	178.17(10)	P(1)-Pd(1)-Br(2)	90.17(5)
P(1)-Pd(1)-Br(1)	90.12(2)	Br(2)-Pd(1)-Br(1)	161.9(2)
P(1)-Pd(1)-Br(3)	89.86(5)	Br(1)-Pd(1)-Br(3)	179.0(9)
P(1)-Pd(1)-Br(4)	89.67(5)	Br(3)-Pd(1)-Br(4)	166.7(9)
O(1)-Ti(1)-O(1')	88.67(5)	O(1')-Ti(1)-O(2)	105.7(2)
O(1)-Ti(1)-O(2)	80.0(2)	O(1')-Ti(1)-O(2)	161.3(2)

136

^{133}Cs NMR studies of the $Cs_4Ti_2L_6Pd_3Br_6$ cluster: There are two types of cesium atoms in the cluster in the solid-state structure. Three symmetry-equivalent Cs(2) atoms are deeply buried in the three clefts of the cluster, while the fourth Cs atom is disordered 50/50 at both capping sites (Figure 4.10-11a). In order to determine whether the three embedded Cs cations remain bounded to the cluster in solution, ^{133}Cs NMR spectroscopy was employed to study its solution behavior. At room-temperature, the ^{133}Cs NMR spectrum of the cluster (in DMF-d_7) showed a singlet at 11.16 ppm. This singlet shifted upfield to 7.37 ppm upon the addition of four equivalents of cesium triflate to this NMR sample (Figure 4.14), but no additional peaks appeared. This observation suggests that the cluster-bounded cesium cations are in fast-exchange with free cesium cations in solution at least at room temperature.

137
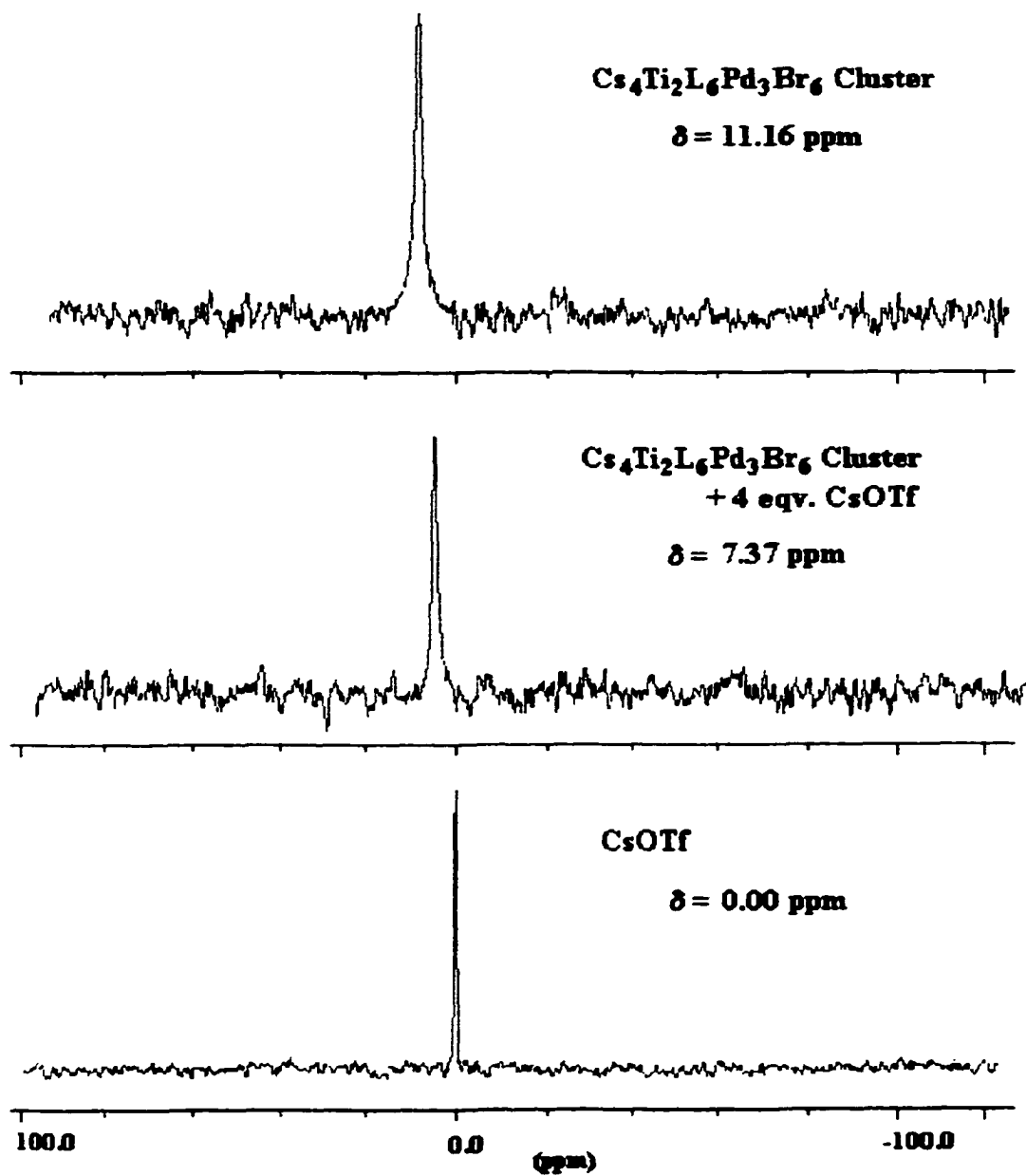
Figure 4.14 Comparative ^{133}Cs NMR spectra of the $Cs_4Ti_2L_6Pd_3Br_6$ cluster, $Cs_4Ti_2L_6Pd_3Br_6$ + 4 CsOTf, and CsOTf alone in DMF-d_7.

138

***Aufbau* of Other Alkali Metal Salts of the [Ti₂L₄Pd₃Br₆]⁺ Cluster:** Two
[Ti₂L₆Pd₃Br₆]⁴⁻ clusters, Rb₄Ti₂L₆Pd₃Br₆ and Li₄Ti₂L₆Pd₃Br₆, were synthesized by the
similar *aufbau* route as described in the synthesis of Cs₄Ti₂L₆Pd₃Br₆ cluster from the
respective Rb₂TiL₃ and Li₂TiL₃ precursors. Both of them have been characterized by IR,
³¹P{¹H}, ¹H, ¹³C{¹H} NMR spectroscopy as well as CHN elemental analyses.

Spectral Comparison of Rb₄Ti₂L₆Pd₃Br₆ and Li₄Ti₂L₆Pd₃Br₆ to Cs₄Ti₂L₆Pd₃Br₆

As shown in Figure 4.15, the ¹H NMR chemical shift of catecholate H(3) varies
significantly with the alkali metal cation (7.89 ppm for Cs⁺, 8.06 ppm for Rb⁺, 7.81 ppm
for Li⁺) but in an unpredictable way. While the H(5) and H(6) resonances move closer as
the alkali metal cation becomes smaller [Δδ (δ_{H(5)}- δ_{H(6)}): 0.15 ppm for Cs⁺, 0.11 ppm for
Rb⁺, 0.08 ppm for Li⁺], the H(3) signal is farthest downfield for the Rb⁺ salt. Another
significant change upon the Cs⁺ replacement by Rb⁺ and Li⁺ is the order-switching of
ipso- and *ortho-* phenyl carbon signals(Figure 4.16). Other carbon signals are only shifted
upfield or downfield by less than 1.1 ppm. The chemical shift of the ³¹P{¹H} NMR
singlet of PPh₂- groups only changed slightly with different alkali metal cations (22.10
ppm for Cs⁺, 22.20 ppm for Rb⁺, 21.17 ppm for Li⁺).

Because of the spectral similarities of these two clusters to the Cs₄Ti₂L₆Pd₃Br₆
cluster, both Rb₄Ti₂L₆Pd₃Br₆ and Li₄Ti₂L₆Pd₃Br₆ most likely adopt the same triple
mesocate structure of C_{3h} symmetry.

139
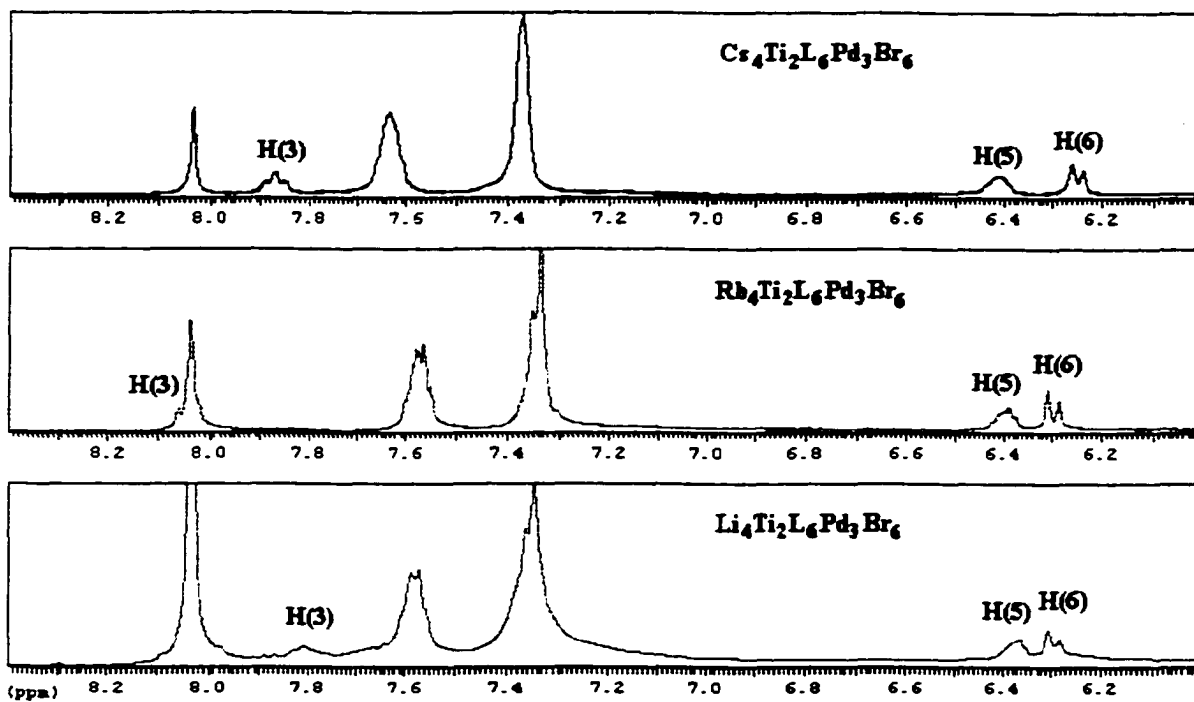
Figure 4.15 Comparative ^1H NMR spectra of alkali metal salts of the $[Ti_2L_6Pd_3Br_6]^{4-}$ cluster in DMF-d_7.
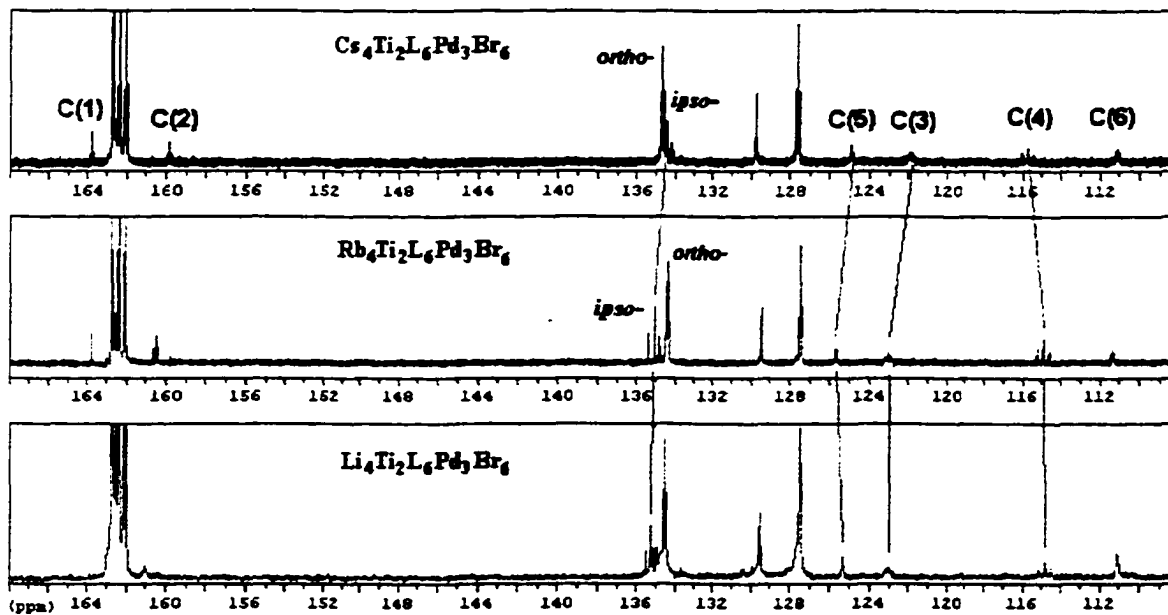
Figure 4.16 Comparative ^{13}C {^1H} NMR spectra of alkali metal salts of the $[Ti_2L_6Pd_3Br_6]^{4-}$ cluster in DMF-d_7.

140

(b) _Aufbau_ Synthesis and Characterization of [Sn₂L₆Pd₃Br₆]⁴⁺ Clusters

Aufbau **of the Cs₄Sn₂L₆Pd₃Br₆ cluster:** This cluster was synthesized from the Cs₂SnL₃ precursor by a similar stepwise route as described for the Cs₄Ti₂L₆Pd₃Br₆ cluster in yields of around 90% . Slow diethyl ether diffusion into a DMF solution of it afforded X-ray quality crystals. Similar to the Cs₄Ti₂L₆Pd₃Br₆ cluster, this cluster's C_3 symmetry in solution is confirmed by spectral data (see discussion on page 123, 127).

X-ray Structure of Cs₄Sn₂L₆Pd₃Br₆ •3.5DMF • 2H₂O •THF •x(solvent): This cluster crystallizes in the triclinic space group P1 with two formula units in the unit cell. This cluster has no crystallographically imposed symmetry, however, the molecule is a triple mesocate and has idealized C_{3h} symmetry with three-fold symmetry along the Sn • • • Sn axis and a pseudo-mirror plane running through the three palladium atoms. The Δ- and Λ-_tris_(catecholato)tin halves are linked by three PdBr₂ moieties via _trans_-coordination of the PPh₂- groups (Figure 4.17-18). The Sn(1) • • • Sn(2) distance is 6.88 Å, slightly longer than the Ti • • • Ti of 6.73 Å, presumably a result of the larger ionic radius of Sn(IV) (0.830 Å) compared to Ti(IV) (0.745 Å). The average Sn-O distance of 2.06 Å is unexceptional. The coordination geometry of the tin atoms is less distorted from octahedral than in the Ti analogue with twist angles of 44.0° and 46.1°.

Three of the four cesium countercations [Cs(1), Cs(2), and Cs(3)] are well-ordered in the crystal lattice, while the fourth Cs atom is disordered over three sites [Cs(4), Cs(5), and Cs(6)]. Cs(1) and Cs(3) are located in two of the three clefts of the cluster and are seven-coordinated. Cs(1) is coordinated by a rectangular array of _endo_-catecholate oxygens, two DMF molecules, and a bromide, Br(3), from a PdBr₂ moiety.

141
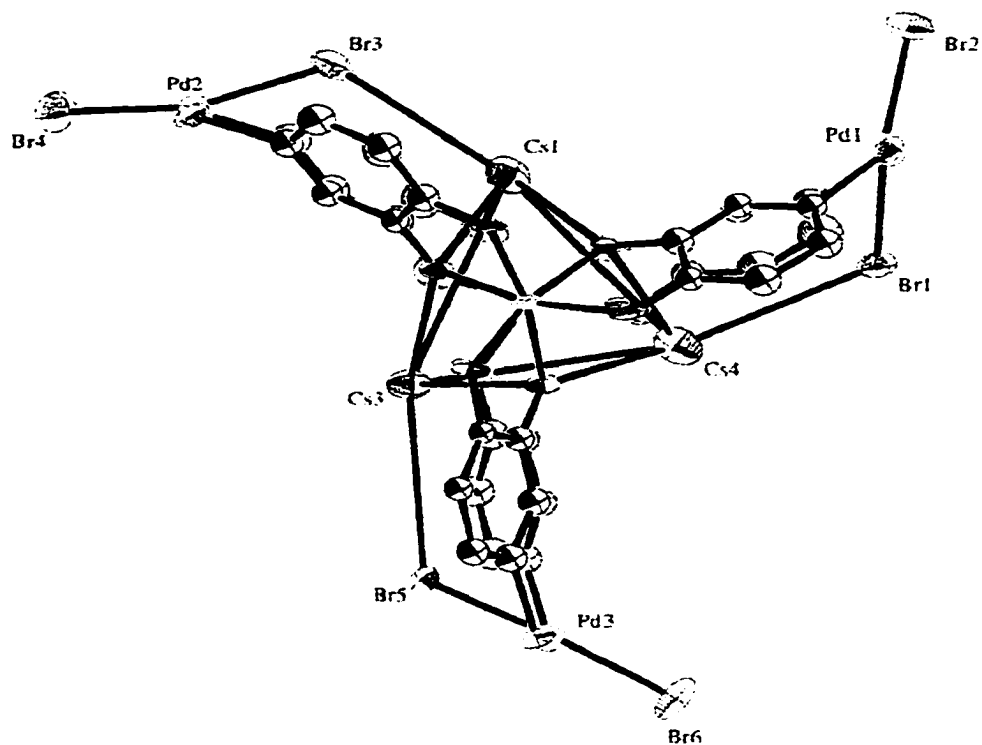
Figure 4.17 ORTEP of X-ray structure of the $Cs_4Sn_2L_6Pd_3Br_6$ cluster (topview).
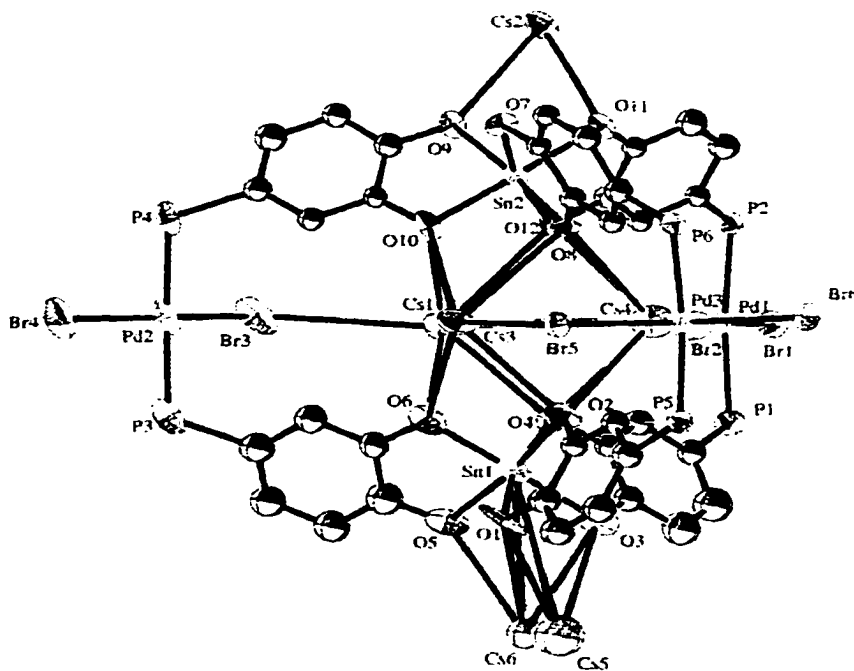
Figure 4.18 ORTEP of X-ray structure of the $Cs_4Sn_2L_6Pd_3Br_6$ cluster (sideview).

142

Cs(3) is coordinated by four *endo*-catecholate oxygens, one DMF, one water molecules as well as a bromide, Br(5). Cs(2) sits atop Sn(2), slightly off the pseudo three-fold axis and is coordinated to three *exo*-catecholate oxygens, one DMF, and one water molecule. In addition, distorted solvent molecules probably complete its coordination sphere. The disordered fourth cesium cation is located with 2/3 occupancy as Cs(4) in the third cluster cleft. The remaining 1/3 occupancy is equally divided between two capping *exo* sites above Sn(1) at Cs(5) and Cs(6) (Figure 4.17-18).

The palladium centers are in a pseudo square-planar geometry with normal Pd-P bond distances of 2.32-2.35 Å and near linear P-Pd-P angles of 172°-173°. Pd-Br bond lengths range from quite short [Pd(2)-Br(4), 2.405(4) Å; Pd(3)-Br(6), 2.412(3) Å] to more normal 2.44-2.45 Å values. Two Br-Pd-Br angles are near linearity at 172° and 174° while Br(3)-Pd(2)-Br(4) is more distorted at 162.9(2)°. An interesting feature is the deflection of one Br from each $PdBr_2$ linker towards the cluster cleft in order to coordinate the embedded Cs^+ cations. The larger intracluster Sn • • • Sn separation of 6.88 Å may facilitate this interaction. The average Cs-Br distance of 3.82 Å is well within the normal range of reported Cs-Br distances in the Cambridge Structural Database.

The cluster crystallizes with 3.5 DMF, two water, and one THF molecules. These are well-ordered in the crystal lattice. In addition, there is a significant amount of residual electron density in the different maps due to highly-disordered solvent molecules, which are denoted "x(solvent)" in the chemical formula. Other important bond distances and bond angles are listed in Table 4.3.

143

Table 4.3 Selected bond distances (Å) and bond angles (°) for the $Cs_4Sn_2L_6Pd_3Br_6$ cluster

Cs(1)-Br(3)	3.754(3)	Sn(1)-O(1)	2.05(2)
Cs(1)-O(4)	3.08(2)	Sn(1)-O(2)	2.08(2)
Cs(1)-O(6)	3.22(2)	Sn(1)-O(3)	2.06(2)
Cs(1)-O(10)	3.28(2)	Sn(1)-O(4)	2.07(2)
Cs(1)-O(12)	3.23(1)	Sn(1)-O(5)	2.06(2)
Cs(1)-O(15)	2.97(5)	Sn(1)-O(6)	2.04(2)
Cs(2)-O(9)	3.14(1)	Sn(2)-O(7)	2.06(2)
Cs(2)-O(11)	3.16(1)	Sn(2)-O(8)	2.07(2)
Cs(2)-O(11')	3.18(2)	Sn(2)-O(9)	2.03(1)
Cs(2)-O(13)	3.07(2)	Sn(2)-O(10)	2.04(1)
Cs(2)-O(20)	3.14(5)	Sn(2)-O(11)	2.07(1)
Cs(3)-Br(5)	3.960(3)	Sn(2)-O(12)	2.08(2)
Cs(3)-O(2)	3.17(2)	Pd(1)-Br(1)	2.451(4)
Cs(3)-O(6)	3.25(2)	Pd(1)-Br(2)	2.424(4)
Cs(3)-O(8)	3.19(1)	Pd(1)-P(1)	2.331(7)
Cs(3)-O(10)	3.28(2)	Pd(1)-P(2)	2.345(6)
Cs(3)-O(16)	3.08(4)	Pd(2)-Br(3)	2.442(4)
Cs(4)-Br(1)	3.741(5)	Pd(2)-Br(4)	2.4059(4)
Cs(4)-O(2)	3.27(2)	Pd(2)-P(3)	2.336(8)
Cs(4)-O(4)	3.27(1)	Pd(2)-P(4)	2.332(8)

144

Cs(4)-O(8)	3.21(2)	Pd(3)-Br(5)	2.446(2)
Cs(4)-O(12)	3.23(1)	Pd(3)-Br(6)	2.412(2)
Cs(4)-O(23)	2.90(4)	Pd(3)-P(5)	2.331(7)
Cs(5)-O(3)	2.96(2)	Pd(3)-P(6)	2.316(7)
Cs(5)-O(19)	3.31(8)		
Cs(6)-O(1)	3.10(2)		
Cs(6)-O(3)	3.05(2)		
Cs(6)-O(5)	3.23(2)		
Cs(6)-O(19)	3.30(8)		

Br(3)-Cs(1)-O(4)	138.5(2)	Br(3)-Cs(1)-O(6)	95.0(2)
Br(3)-Cs(1)-O(10)	89.9(2)	Br(3)-Cs(1)-O(12)	128.8(3)
Br(3)-Cs(1)-O(15)	103.8(7)	O(4)-Cs(1)-O(6)	55.3(4)
O(4)-Cs(1)-O(10)	115.0(4)	O(4)-Cs(1)-O(12)	92.1(3)
O(4)-Cs(1)-O(15)	89.3(8)	O(4)-Cs(1)-O(10)	89.4(5)
O(6)-Cs(1)-O(12)	115.4(4)	O(6)-Cs(1)-O(15)	140.6(8)
O(10)-Cs(1)-O(12)	52.8(4)	O(10)-Cs(1)-O(15)	124.4(7)
O(12)-Cs(1)-O(15)	78.8(7)		
O(1)-Sn(1)-O(2)	81.9(7)	O(1)-Sn(1)-O(3)	88.2(8)
O(1)-Sn(1)-O(4)	165.2(5)	O(1)-Sn(1)-O(5)	90.7(7)
O(1)-Sn(1)-O(6)	100.8(8)	O(2)-Sn(1)-O(3)	100.4(6)
O(2)-Sn(1)-O(4)	89.2(7)	O(2)-Sn(1)-O(5)	166.8(7)
O(2)-Sn(1)-O(6)	89.0(6)	O(3)-Sn(1)-O(4)	81.8(7)

145

O(3)-Sn(1)-O(5)	90.2(7)	O(3)-Sn(1)-O(6)	167.8(9)
O(4)-Sn(1)-O(5)	90.7(7)	O(4)-Sn(1)-O(6)	90.7(7)
O(5)-Sn(1)-O(6)	81.7(7)	O(7)-Sn(2)-O(8)	82.3(6)
O(7)-Sn(2)-O(9)	90.6(7)	O(7)-Sn(2)-O(10)	101.2(6)
O(7)-Sn(2)-O(11)	88.6(6)	O(7)-Sn(2)-O(12)	167.8(4)
O(8)-Sn(2)-O(9)	189.1(6)	O(8)-Sn(2)-O(10)	91.4(5)
O(8)-Sn(2)-O(11)	97.8(5)	O(8)-Sn(2)-O(12)	91.6(6)
O(9)-Sn(2)-O(10)	81.8(6)	O(9)-Sn(2)-O(11)	90.3(5)
O(9)-Sn(2)-O(12)	96.8(7)	O(10)-Sn(2)-O(11)	89.6(6)
O(10)-Sn(2)-O(12)	81.7(6)		
Br(1)-Pd(1)-Br(2)	172.4(1)	Br(1)-Pd(1)-P(1)	86.0(2)
Br(1)-Pd(1)-P(2)	87.7(2)	Br(2)-Pd(1)-P(1)	91.2(2)
Br(2)-Pd(1)-P(2)	93.6(2)	P(1)-Pd(1)-P(2)	172.7(2)
Br(3)-Pd(2)-Br(4)	162.9(2)	Br(3)-Pd(2)-P(3)	90.9(2)
Br(3)-Pd(2)-P(4)	91.7(2)	Br(4)-Pd(2)-P(3)	89.4(2)
Br(4)-Pd(2)-P(4)	89.9(2)	P(3)-Pd(2)-P(4)	173.4(3)
Br(5)-Pd(3)-Br(6)	174.4(2)	Br(5)-Pd(3)-P(5)	87.0(1)
Br(5)-Pd(3)-P(6)	87.4(1)	Br(6)-Pd(3)-P(5)	93.8(1)
Br(6)-Pd(3)-P(6)	91.2(1)	P(5)-Pd(3)-P(6)	171.5(3)
Cs(4)-Br(1)-Pd(1)	118.93(9)	Cs(1)-Br(3)-Pd(2)	123.8(1)
Cs(3)-Br(5)-Pd(3)	120.6(1)		

Aufbau **of the Rb$_4$Sn$_2$L$_6$Pd$_3$Br$_6$ clusters:** The Rb$_4$Sn$_2$L$_6$Pd$_3$Br$_6$ cluster was synthesized in a yield of 89 % from the Rb$_2$SnL$_3$ precursor by a similar stepwise route as described for the synthesis of the Cs$_4$Ti$_2$L$_6$Pd$_3$Br$_6$ cluster. It has been characterized by IR, ^{31}P{^{1}H }, ^{1}H, ^{13}C{^{1}H } NMR spectroscopy as well as CHN elemental analyses.

Spectral Comparison of Rb$_4$Sn$_2$L$_6$Pd$_3$Br$_6$ to Cs$_4$Sn$_2$L$_6$Pd$_3$Br$_6$

As the countercation is changed from Cs$^+$ to Rb$^+$, the resonance of catecholate H(3) shifted downfield from 8.15 ppm to 8.42 ppm (Figure 4.19). This is consistent with the observed downfield shift of the same proton in the [Ti$_2$L$_6$Pd$_3$Br$_6$]$^{4-}$ cluster. However the separation between H(5) and H(6) becomes larger [$\Delta\delta$ ($\delta_{H(5)}$- $\delta_{H(6)}$): 0.32 ppm for Cs$^+$, 0.39 ppm for Rb$^+$], not smaller as for the [Ti$_2$L$_6$Pd$_3$Br$_6$]$^{4-}$ cluster (see page 138).

In Figure 4.20, a significant change is that three pairs of carbon resonances have switched their orders (*ipso-* and *ortho-* phenyl carbon signals, C(5) and C(3), C(6) and C(4)) upon Cs$^+$ displacement by Rb$^+$. Other carbon signals shifted upfield or downfield by less than 0.9 ppm (Figure 4.20). The chemical shift of the ^{31}P{^{1}H} NMR singlet of PPh$_2$- groups only changed slightly with different alkali metal cations (21.61 ppm for Cs$^+$, 21.30 ppm for Rb$^+$). We believe that this Rb$_4$Sn$_2$L$_6$Pd$_3$Br$_6$ cluster is most likely also in the C_{3h} mesocate form.

147
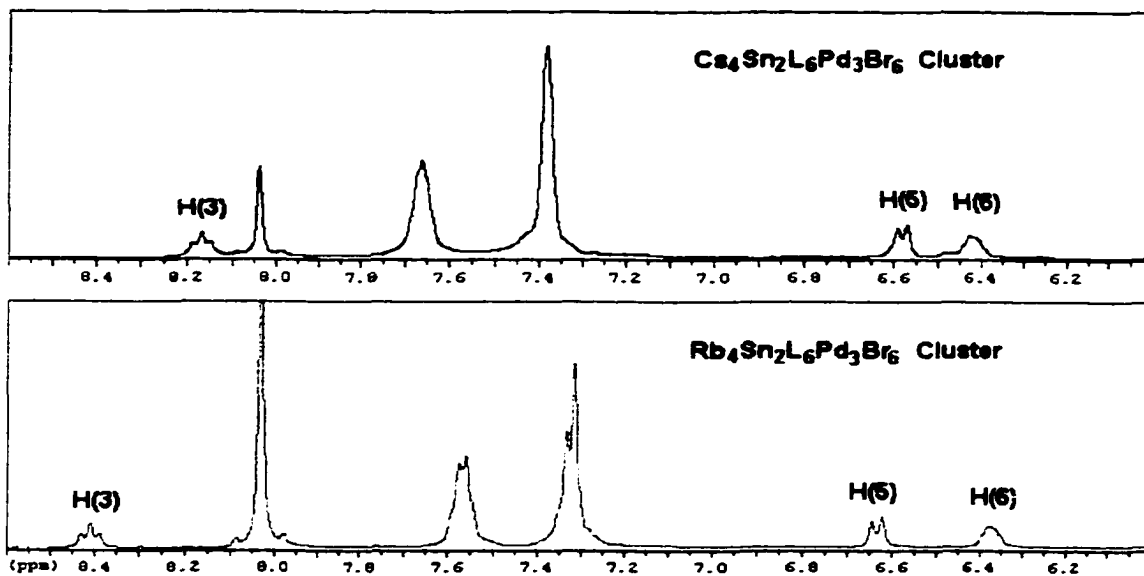
Figure 4.19 Comparative ^{1}H NMR spectra of $Cs_4Sn_2L_6Pd_3Br_6$ and $Rb_4Sn_2L_6Pd_3Br_6$ clusters in DMF-d_7.
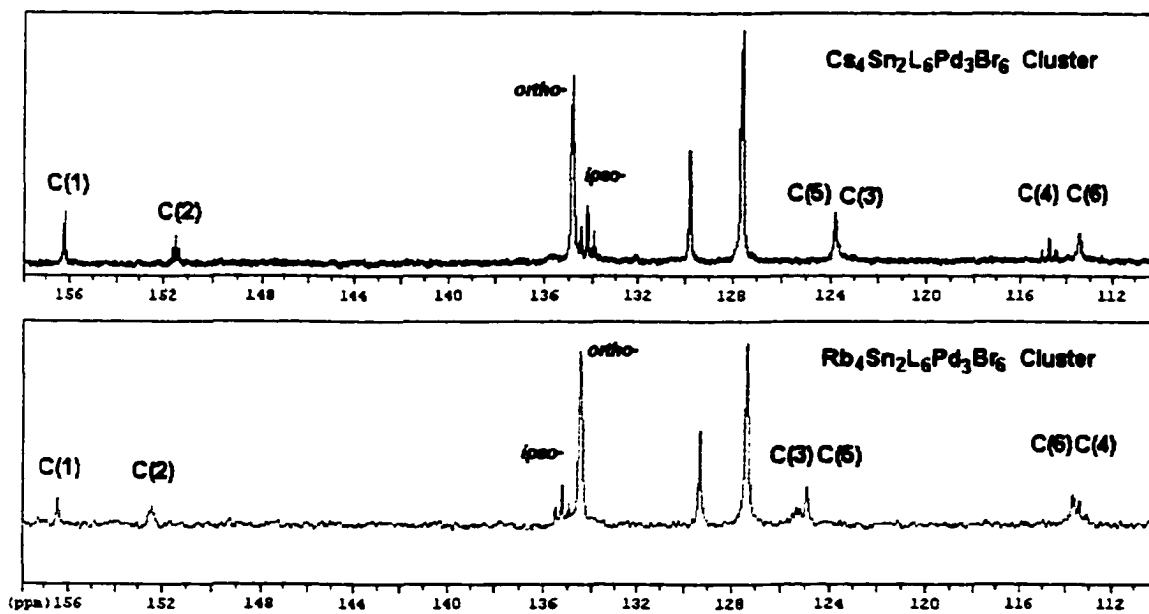
Figure 4.20 Comparative ^{13}C NMR spectra of $Cs_4Sn_2L_6Pd_3Br_6$ and $Rb_4Sn_2L_6Pd_3Br_6$ clusters in DMF-d_7.

148

The Possibility of a Triple Mesocate versus Triple helicate form of the [M₂L₆Pd₃Br₆] Clusters: Computer modeling studies of both Ti(IV) and Sn(IV) clusters have demonstrated that the triple mesocates have a larger M(IV) • • • M(IV) separation and a substantially steric lower energy. [63] For instance, the results indicate that the $Cs_4Ti_2L_6Pd_3Br_6$ mesocate has a longer Ti • • • Ti distance (6.5 Å compared to 6.1 Å for the triple helicate), along with a lower energy by 26 Kcal/mol. This large energy difference can account for the sole formation of the triple mesocates of $Cs_4M_2L_6Pd_3Br_6$ clusters as indeed observed in their X-ray structures.

In the X-ray structure of the $Cs_4Ti_2L_6Pd_3Br_6$ cluster, the two titanium atoms in the mesocate are separated by 6.76 Å which is close to the value 6.5 Å predicated by molecular modeling. In the mesocate, three cesium atoms are deeply buried in the cluster clefts, each of them is coordinated by _four_ endo-catecholate oxygens, two from each tris(catecholato)titanium cap. Whereas, in the "helicate", only three endo-catecholate oxygens can be available for Cs^+ coordination at each of the three molecular clefts (Figure 4.21). Thus the mesocate provides a better coordination environment for the large Cs^+ counter ion. Therefore, it might be speculated that smaller alkali metal cations may better fit the coordination environment provided by the "helicate", thus pulling the two tris(catecholato)titanium caps closer (to 6.1 Å). However, as discussed on page 138 and 147, use of Li^+, or Rb^+ did not resulted in any evidence for formation of helicates. Therefore, the substantially different steric energy between a helicate and a mesocate probably dictates the formation of only a mesocate.

149
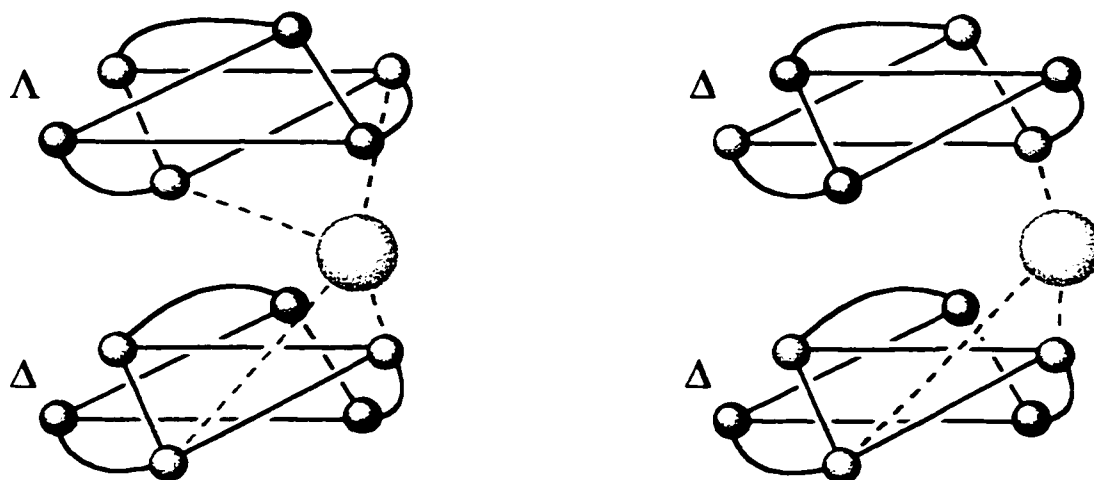
Figure 4. 21 Schematic coordination environments for cesium countercations in a triple mesocate (left) and a triple helicate (right). Gray spheres represent *exo*-catecholate oxygen atoms, red spheres *endo*-catecholate oxygen atoms, and green spheres cesium cations.

(c) Countercation effects on the formation of [M₂L₆Pd₃Br₆]⁴⁺ Clusters

In order to explore possible action templating effects on the formation of $[M_2L_6Pd_3Br_6]^{4-}$ clusters, several other countercations for $[ML_3]^{2-}$ have been used. Of these, tetramethylammonium (Me_4N^+), tetraphenylphosphonium (Ph_4P^+), and *bis*(triphenyl-phosphoranylidene)ammonium (PPN^+) salts yielded oligomeric or polymeric insoluble and intractable dark-brown solids when reacted with $PdBr_2$•$2PhCN$ in a DMF solution. Interestingly, the use of the triethylammonium (Et_3NH^+) salt in the syntheses of the $[M_2L_6Pd_3Br_6]^{4-}$ clusters led to at least two different species, as shown by $^{31}P\{^1H\}$ NMR spectroscopy (Figure 4.22). It is tempting to speculate that these two products are the mesocate and helicate forms of the desired cluster. Thus we tried several methods of separating them, including TLC and HPLC, which all failed. The ^1H, and

150
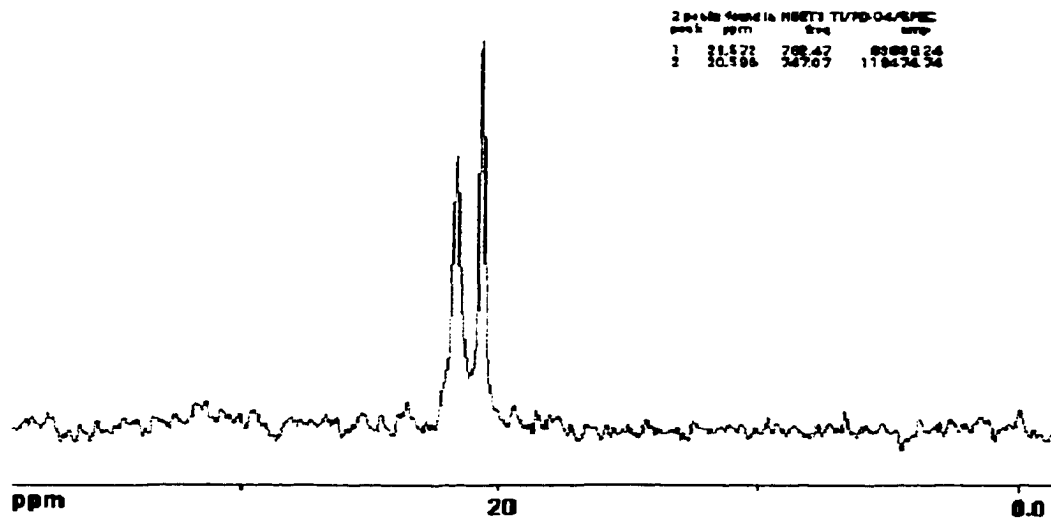
Figure 4.22 $(HNEt_3)_2Ti(Cat-PPh_2)_3$ and $PdBr_2.2PhCN$ (molar ratio 2/3) in DMF/DMF-d_7.
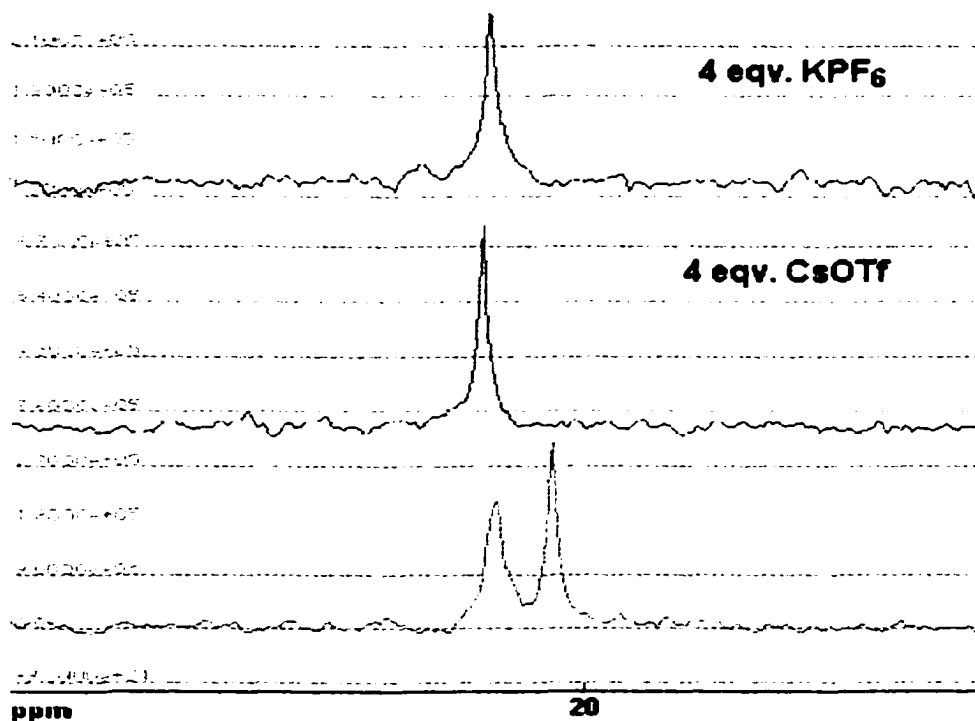
Figure 4.23 Comparative $^{31}P\{^1H\}$ NMR spectra of cation effects on the synthesis of $[Ti_2L_6Pd_3Br_6]^{4-}$ using Et_3NH^+ as a countercation in DMF/DMF-d_7 solution. Alkali metal cations, such as Cs^+, K^+, added as triflate salts, induced the cluster formation.

151

$^{13}C\{^1H\}$ NMR spectra were too broad to be meaningfully interpreted. Most importantly, the FAB^+ mass spectrum showed that no $[M_2L_6Pd_3Br_6]^{4-}$ cluster of any kind had actually formed. These observations indicate that cluster formation without proper cation templating may not be feasible. Thus the alkali metal countercations most likely play a crucial role in the cluster formations. Accordingly, upon addition of four equivalents of alkali metal salts (CsOTf or KOTf), immediate formation of a single product cluster was confirmed by $^{31}P\{^1H\}$ NMR spectroscopy (Figure 4.23).

The cations, PPh_4P^+, Me_4N^+, PPN^+, and Et_3NH^+ may have overly bulky substituents that prevent them from fitting into the cluster clefts. Thus they cannot be used as countercations in the formation of $[M_2L_6Pd_3Br_6]^{4-}$ clusters. Unlike these cations, $(DABCO-H)^+$ $(DABCO = 1,4\text{-diazabicyclo-}[2,2,2]octane)$ has all three ethylene groups at N ends tied back. Not surprisingly, it can be used successfully as a countercation in the syntheses of these $[M_2L_6Pd_3Br_6]^{4-}$ clusters.

Aufbau of **DABCO-H$^+$** salts of **[M$_2$L$_6$Pd$_3$Br$_6$]$^{4-}$** clusters [M =Ti(IV), Sn(IV)]: Both $(DABCO-H)_4[Ti_2L_6Pd_3Br_6]$ and $(DABCO-H)_4[Sn_2L_6Pd_3Br_6]$ have been synthesized by the similar method as described before from the respective $(DABCO-H)_2TiL_3$ and $(DABCO-H)_2SnL_3$ precursors. These two clusters have been characterized by IR, $^{31}P\{^1H\}$, ^1H, $^{13}C\{^1H\}$ NMR spectroscopy in addition to CHN elemental analyses. Spectral data again indicated that both of them have C_3 symmetry in solution. Slow diethyl ether diffusion into their DMF solutions yielded crystals of X-ray quality.

152

X-ray structure of (DABCO-H)$_4$[Sn$_2$L$_6$Pd$_3$Br$_6$] •3H$_2$O •x(solvent): This cluster crystallizes in the trigonal space group P6$_3$/m with two formula units in the unit cell. There is a three-fold symmetry axis along the Sn-Sn vector, and the three symmetry equivalent Pd atoms plus all Br atoms reside on a mirror plane by which the two *tris*(catecholato)tin caps are related. One Sn is in a Δ-configuration and the other in a Λ-configuration. Hence, this cluster is also a mesocate of C_{3h} symmetry (Figure 4.24), as are the two X-ray structures described above.

The two Sn atoms are coordinated in a distorted octahedral fashion by six catecholate oxygens with a twist angle of 41.9°. The average Sn-O distance of 2.05 Å is typical. Interestingly, the Sn • • • Sn separation is 7.47 Å, significantly larger than the 6.88 Å observed in the Cs$_4$Sn$_2$L$_6$Pd$_3$Br$_6$ structure. This is presumably necessary to accommodate the three bulkier DABCO-H$^+$ counterions in the clefts of the cluster (Figure 4.24).

Each of the three Pd atoms is coordinated in a *trans* square-planar geometry by two PPh$_2$- groups with a normal Pd-P bond length of 2.363(2) Å and nearly linear P-Pd-P angle of 174.5(1) ° (Figure 4.24, 25, 26). While Br(1) is well-behaved at 2.445(2) Å from the Pd center, the second Br is disordered over Br(2) and Br(3) (not shown) sites 0.63 Å apart.

This cluster crystallizes with three DABCO-H$^+$ cations within its clefts. The fourth protonated DABCO is not associated with the cluster and is treated as disordered x(solvent). The three DABCO-H$^+$ cations sit in the expanded cluster clefts. Interestingly, three water molecules are sandwiched between the two Sn atoms and each is hydrogen-bonded to two *endo*-catecholate oxygens as well as a protonated DABCO.

153
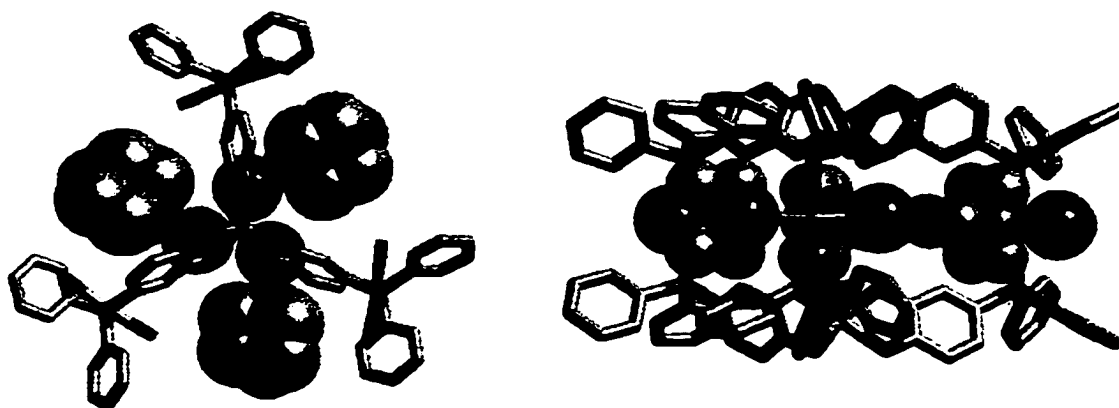
Figure 4.24 Stereographic representation of (DABCO-H)$_3$Sn$_2$L$_6$Pd$_3$Br$_6$•x(solvent). The hydrogen atoms, solvent molecules are omitted for clarity. The left is a top view of the cluster down the crystallographic three-fold axis, while the right is a side view. The water molecules are represented by red spheres, DABCOs by blue and gray spheres, Br atoms by dark-red. In the wireframe, the Sn atoms are shown in green, carbon atoms in gray, Pd atoms in orange, P atoms in purple, and oxygen atoms in red.
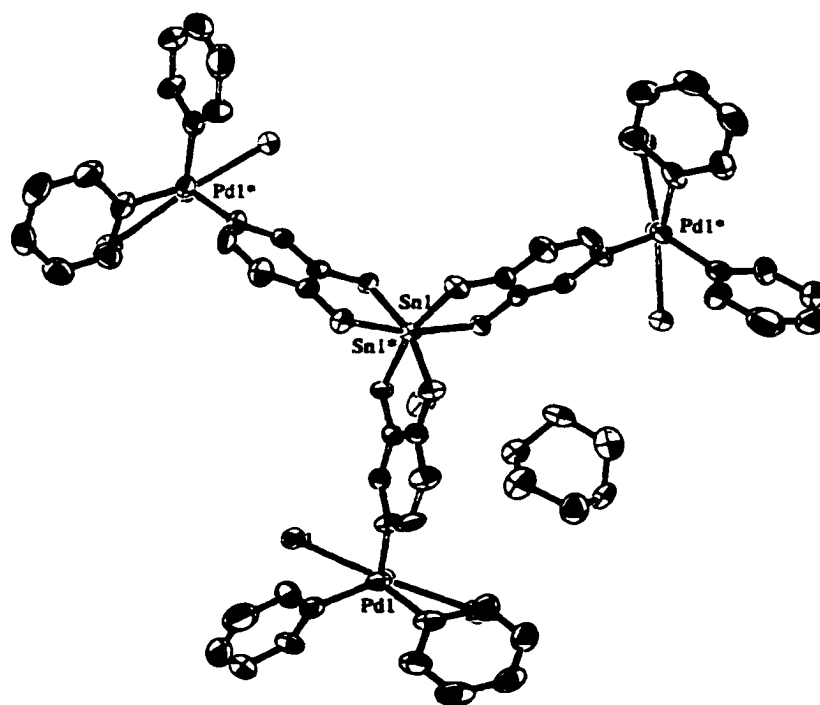
Figure 4.25 ORTEP of the X-ray structure of (DABCO-H)$_3$Sn$_2$L$_6$Pd$_3$Br$_6$ •x(solvent) (top view). The hydrogen atoms, solvent molecules are omitted for clarity. Only one sandwiched water molecule and part of its hydrogen-bonded DABCO-H$^+$ cation are shown.

154
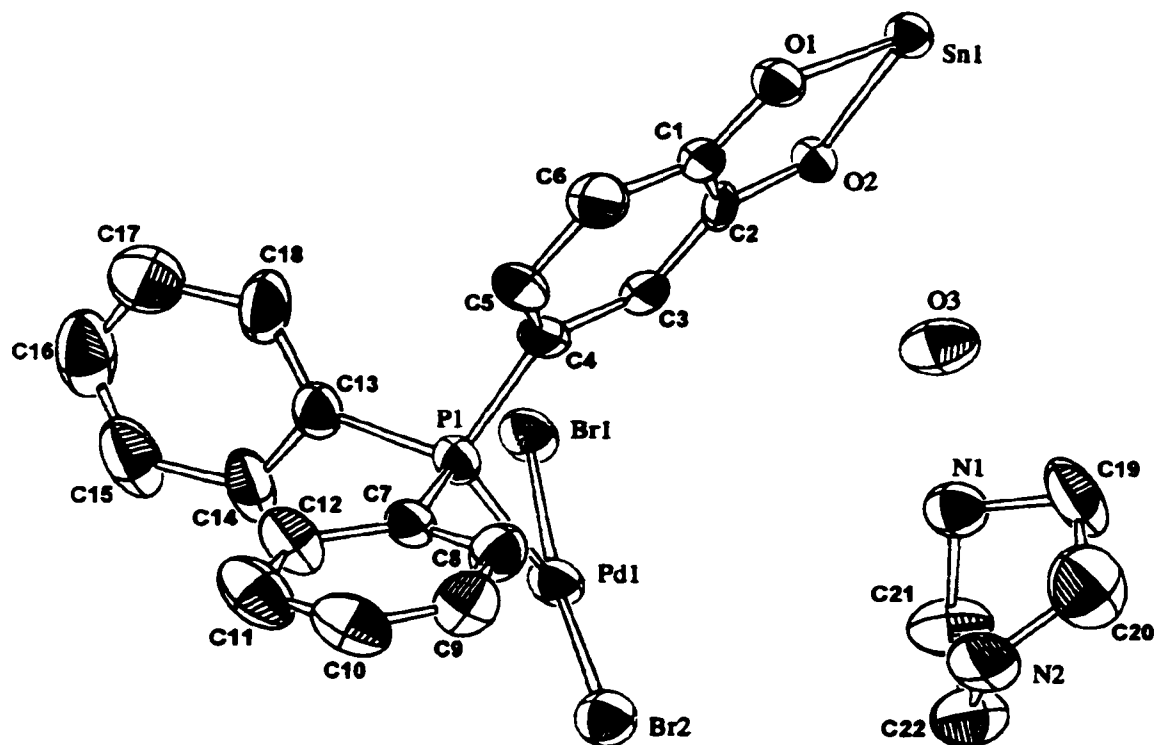
Figure 4.26 ORTEP of X-ray structure of the asymmetric unit [a sandwiched water molecule O(3) and its hydrogen-bonded DABCO-H$^+$ cation plus two metal centers: Sn(IV) and PdBr$_2$ bridged by 4-PPh$_2$-Catecholate. The hydrogen atoms are omitted for clarity.

The hydrogen-bonded, presumably protonated N(1)-ring C distances of 1.49(2) and 1.51(1) Å are marginally longer than the N(2)-ring C distances of 1.44(2) and 1.47(1) Å (Figure 4.26). Important bond distances and angles are presented in Table 4.4.

155

Table 4.4 Selected bond distances (Å) and bond angles (°) for the (DABCO-H)$_4$Sn$_2$L$_6$Pd$_3$Br$_6$ cluster

Sn(1)-O(1)	2.044(5)	N(1)-C(19)	1.513(10)
Sn(1)-O(2)	2.065(10)	N(1)-C(21)	1.49(2)
Pd(1)-Br(1)	2.445(2)	N(2)-C(20)	1.47(1)
Pd(1)-Br(2)	2.424(2)	N(2)-C(22)	1.44(2)
Pd(1)-Br(3)	2.393(8)	O(1)-C(1)	1.332(8)
Pd(1)-P(1)	2.363(2)	O(2)-C(2)	1.371(8)
Br(2)-Br(3)	0.63(2)	C(1)-C(2)	1.39(1)
P(1)-C(4)	1.799(8)	C(1)-C(6)	1.41(1)
P(1)-C(7)	1.804(9)	C(2)-C(3)	1.372(10)
P(1)-C(13)	1.813(9)	C(3)-C(4)	1.381(10)

O(1)-Sn(1)-O(1)	89.7(2)	O(1)-Sn(1)-O(2')	164.9(2)
O(1)-Sn(1)-O(2)	80.4(2)	O(1')-Sn(2)-O(2')	101.6(2)
O(2)-Sn(2)-O(2')	90.3(2)	Br(1)-Pd(1)-Br(2)	173.7(1)
Br(1)-Pd(1)-Br(3)	171.3(5)	Br(2)-Pd(1)-Br(3)	15.0(4)
Br(1)-Pd(1)-P(1)	88.88(6)	Br(3)-Pd(1)-P(1)	90.73(6)
Br(2)-Pd(1)-P(1)	91.39(6)	Pd(1)-P(1)-O(4)	115.0(3)
Pd(1)-Br(3)-Br(2)	85.4(9)	Pd(1)-P(1)-O(13)	116.5(3)
Pd(1)-P(1)-C(7)	108.8(3)	Sn(1)-O(1)-C(1)	112.2(5)
Sn(1)-O(2)-C(2)	111.7(5)		
P(1)-Pd(1)-P(1')	174.5(1)	P(1)-C(4)-C(3)	123.1(7)

156

P(1)-C(13)-P(18)	123.6(7)	P(1)-C(7)-C(8)	121.7(7)
P(1)-C(13)-P(14)	120.0(6)	P(1)-C(4)-C(5)	119.2(6)
C(19)-N(1)-C(21)	109.0(7)	C(19)-N(1)-C(19')	110.0(10)
C(20')-N(2)-C(20)	11(1)	C(20)-N(2)-C(22)	106.6(7)
C(4)-P(1)-C(7)	108.8(4)	C(7)-P(1)-C(13)	103.4(4)
C(4)-P(1)-P(13)	103.5(4)	O(2)-C(2)-C(1)	116.1(7)
O(1)-C(1)-C(6)	121.8(8)	O(1)-C(2)-C(3)	119.6(7)
O(1)-C(1)-C(2)	119.3(7)	C(2)-C(1)-C(6)	118.9(7)
O(2)-C(2)-C(3)	124.3(7)	O(1)-C(2)-C(3)	119.6(7)

(d) Countercation Exchange of [M₂L₆Pd₃Br₆]⁴⁻ Clusters [M =Ti(IV), Sn(IV)]:

To date, all alkali metal cations, NH_4^+, and $DABCO^+$ have been successfully used as countercations in the formation of $[M_2L_6Pd_3Br_6]^{4-}$ clusters. As discussed in the [133]Cs NMR studies of the $Cs_4Ti_2L_6Pd_3Br_6$ cluster, the cluster-bound cations are in fast exchange with the free cations in solution. What if there are two different countercations availble in a solution of a $[M_2L_6Pd_3Br_6]^{4-}$ cluster? The following experiments have been carried out to address this question.

A mixture of the same cluster with different countercations

If two countercations are in fast exchange, a mixture of two clusters with the same tetraanionic core will give an averaged spectrum in NMR studies. As shown in Figure 4.27, a mixture of $Cs_4Sn_2L_6Pd_3Br_6$ and $(DABCO-H)_4Sn_2L_6Pd_3Br_6$ clusters in 1:1

157
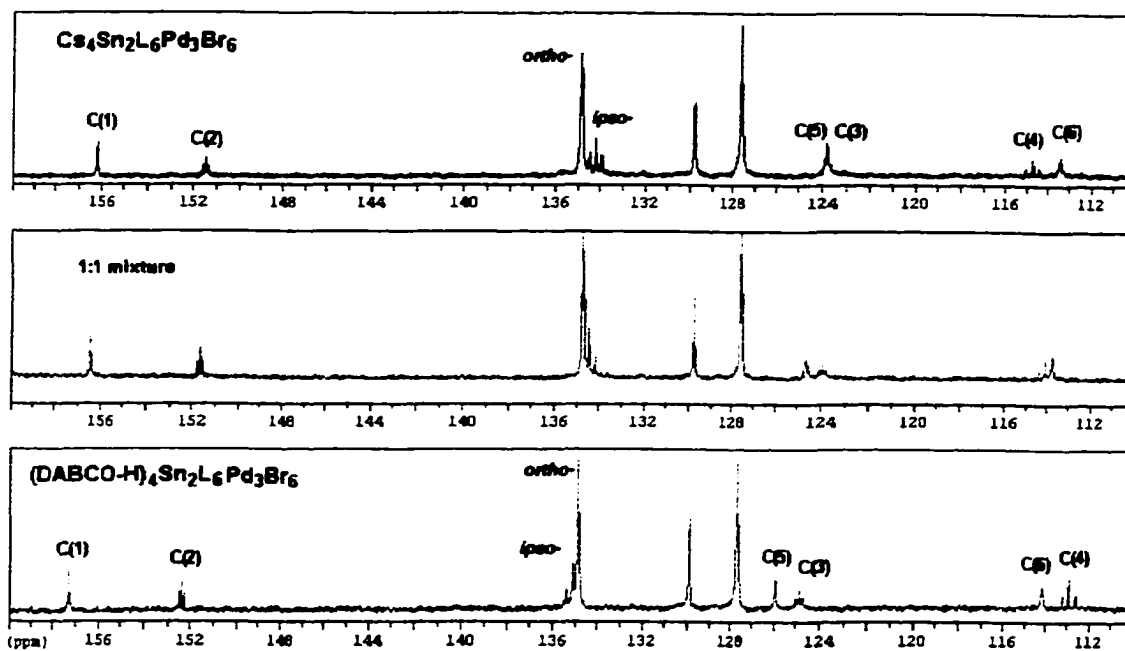
Figure 4.27 Comparative $^{13}C\{^1H\}$ NMR spectra of two clusters and their mixture in 1:1 molar ratio (DMF-d$_7$). The mixture shows an averaged spectrum.
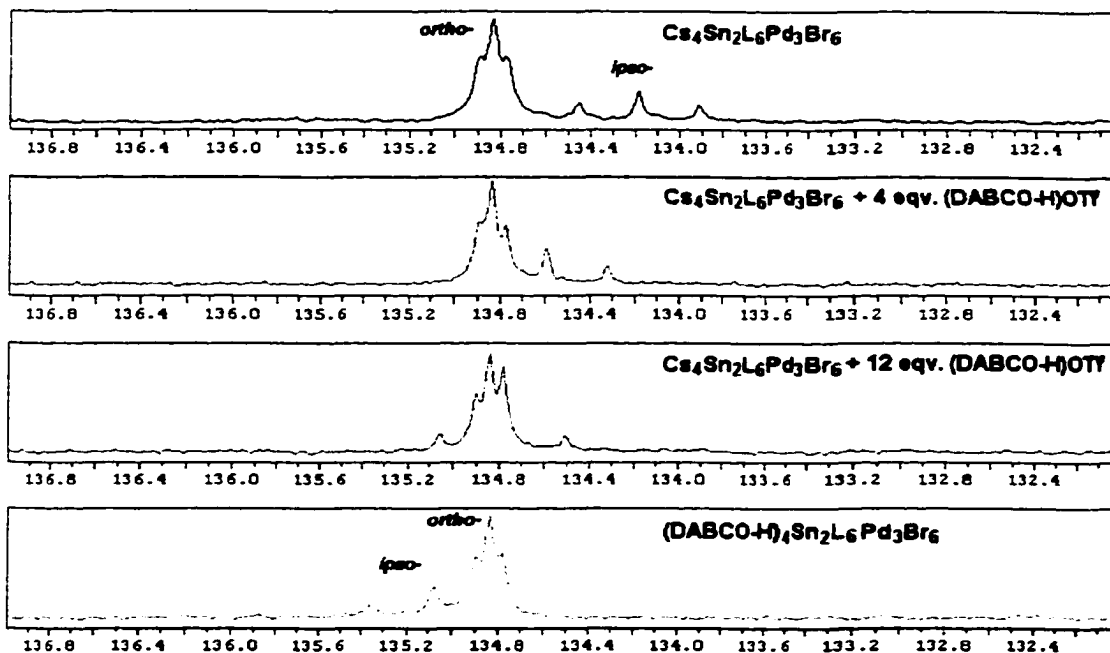
Figure 4.28 The order-switching of the *ipso-* and *ortho-*phenyl carbon virtual triplets in $^{13}C\{^1H\}$ NMR spectra upon titration of (DABCO-H)OTf into Cs$_4$Sn$_2$L$_6$Pd$_3$Br$_6$ (all *ortho-* phenyl carbon virtual triplets are anchored at δ 134.84 ppm for comparison) in DMF-d$_7$.

158

molar ratio shows one set of catecholate and phenyl carbon resonances at room temperature (Figure 4.27, middle). Furthermore, this $^{13}C\{^1H\}$ NMR spectrum is the average of the respective spectra of the two clusters (Figure 4.27, top and bottom). This observation also supports the likelihood that the cluster-bounded countercations are in fast-exchange with other free cations in solution.

Titration of a different countercation into a cluster solution

The relative positions of the *ipso-* and *ortho-*phenyl carbon virtual triplets in the series of $^{13}C\{^1H\}$ NMR titration spectra are shown in Figure 4.28. As shown in this figure, titration of (DABCO-H)OTf into $Cs_4Sn_2L_6Pd_3Br_6$ solution gradually changed the spectrum of $Cs_4Sn_2L_6Pd_3Br_6$ towards that of $(DABCO-H)_4Sn_2L_6Pd_3Br_6$. Further, four equivalents of (DABCO-H)OTf resulted in an averaged spectrum, and all chemical shift changes ($\Delta\delta$) are proportional to the amount of (DABCO-H)OTf added. These observations unambiguously demonstrate that the tetraanionic $[Sn_2L_6Pd_3Br_6]^{4-}$ cluster has no preference for either $(DABCO-H)^+$ or Cs^+. Titration of CsOTf into the (DABCO-H)$_4Sn_2L_6Pd_3Br_6$ solution gave analogous results.

(e) Self-Assembly of $[M_2L_6Pd_3Br_6]^{4-}$ Clusters [M =Ti(IV), Sn(IV)]

One-pot self-assembly of the tetraanionic $[M_2L_6Pd_3Br_6]^{4-}$ clusters was studied to see whether they can be formed spontaneously from a stoichiometric mixture of all eleven individual components. In DMF solvent, a suspension of Cs_2CO_3 with $Ti(OMe)_4$, $H_2L \cdot HBr$, and $PdBr_2 \cdot 2PhCN$ in a molar ratio 5:2:6:3 was stirred at room temperature. A brown suspension was obtained after two days. The $^{31}P\{^1H\}$ NMR spectrum of the dark-

159

red supernatant was complex with no single major peak and the solubility of this brown precipitate was very poor in any of the common solvents tried. Similar results were obtained using Rb_2CO_3 instead of Cs_2CO_3. It was suspected that the insolubility of Cs_2CO_3 in DMF could not provide a sufficiently basic condition for cluster formation. Thus NaOH and KOH in methanolic solutions were used in place of alkali metal carbonates. However, the brown insoluble precipitate was again produced within a few hours. Two relatively weak bases, DABCO and aqueous ammonia, were tried instead. Perhaps because of their DMF-solubility, the initial reaction suspension became a homogeneous solution after a few hours, and successful self-assembly was indeed achieved after four days, as monitored by $^{31}P\{^1H\}$ NMR spectroscopy. Thus, both $(NH_4)_4Ti_2L_6Pd_3Br_6$ and $(DABCO-H)_4Sn_2L_6Pd_3Br_6$ clusters were synthesized by self-assembly and isolated in excellent yields.

(f) Syntheses of the $[M_2L_6Pd_3X_6]^{4-}$ Clusters [M = Ti(IV), Sn(IV); X = Cl⁻, I⁻]

Reaction of two equivalents of Cs_2ML_3 with three equivalents of $PdCl_2 \cdot 2PhCN$ in DMF gave $Cs_4M_2L_6Pd_3Cl_6$ clusters as dark-red solids in good yields. These two clusters have been characterized by IR, ^1H, $^{13}C\{^1H\}$, $^{31}P\{^1H\}$ NMR spectroscopy, in addition to CHN elemental analyses. Their iodo analogues were prepared in quantitative yield by halide metathesis between $Cs_4M_2L_6Pd_3Br_6$ and CsI in DMF (CsI is soluble in DMF, while CsCl is insoluble). Both analytical and spectral data confirmed the formation of the iodo analogues. Spectral analyses again revealed that all of these have C_3 symmetry in solution. The chemical shifts of the $^{31}P\{^1H\}$ NMR resonances of PPh_2- groups in the

160
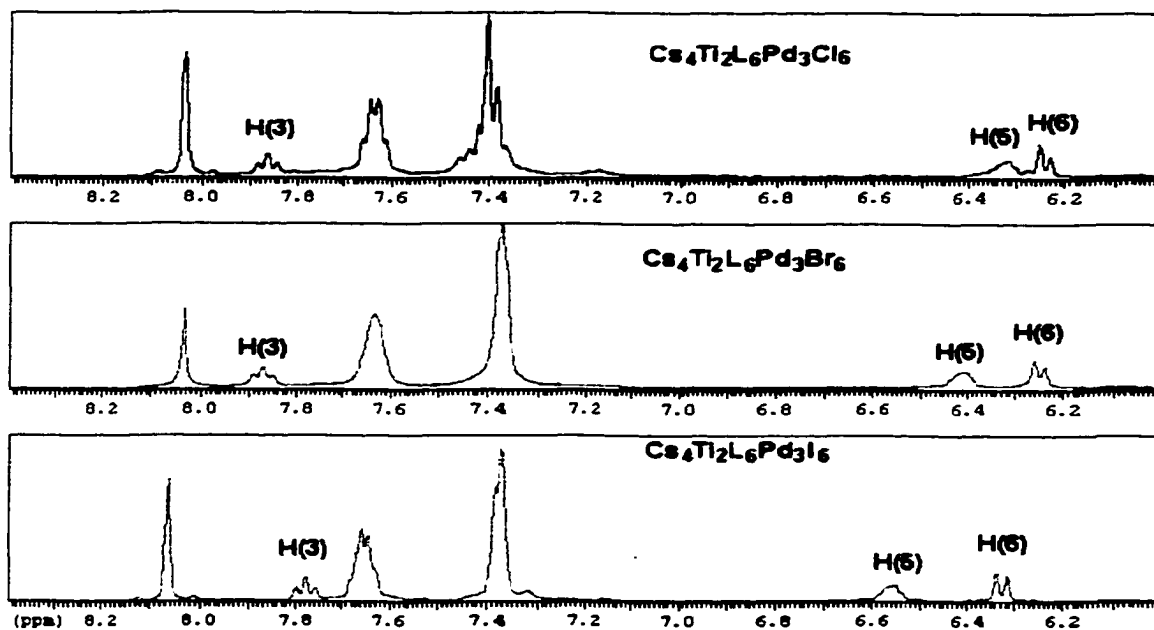
Figure 4.29 Comparative ^{1}H NMR spectra of the $Cs_4Ti_2L_6Pd_3X_6$ (X = Cl⁻, Br⁻, I⁻) clusters in DMF-d$_7$
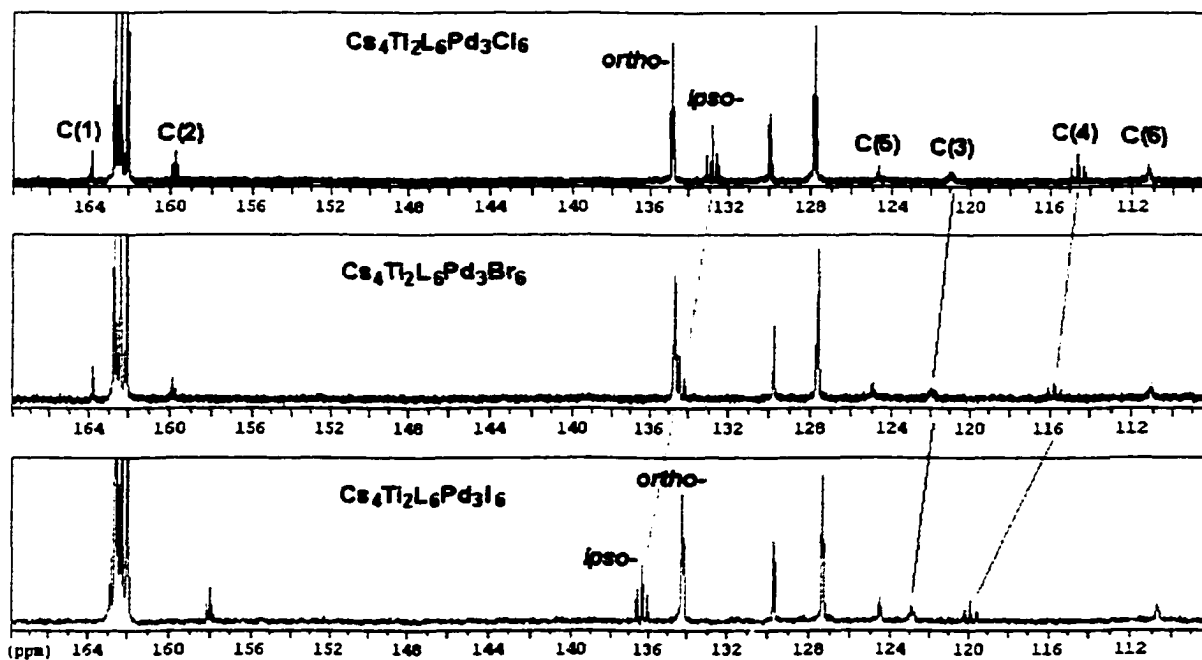
Figure 4.30 Comparative ^{13}C{^{1}H} NMR spectra of the $Cs_4Ti_2L_6Pd_3X_6$ (X = Cl⁻, Br⁻, I⁻) clusters in DMF-d$_7$

161

chloro clusters are around δ 24.0, while the iodo analogues are around δ 12.5 (*ca* δ 21.5

in bromo clusters). As shown in the comparative ^1H NMR spectra (Figure 4.29) of the

$Cs_4Ti_2L_6Pd_3X_6$ (X = Cl⁻, Br⁻, I⁻) clusters, the separation between H(5) and H(6)

resonances decrease as the halide becomes smaller [Δδ ($δ_{H(5)}$- $δ_{H(6)}$): 0.23 ppm for I⁻,

0.15 ppm for Br⁻, 0.08 ppm for Cl⁻]. The chemical shifts of H(3) in the chloro and bromo

clusters are close to each other ($δ_{H(3)}$ 7.86 for Cl⁻, $δ_{H(3)}$ 7.89 for Br⁻), while H(3) in the

iodo cluster is at 7.78 ppm.

Significant downfield ^{13}C shifts are observed for *ipso*-phenyl C (Cl⁻, δ132.8; Br⁻,

δ134.4; I⁻, δ136.3), C(3) (Cl⁻, δ121.0; Br⁻, δ121.9; I⁻, δ122.9), and C(4) (Cl⁻, δ114.6; Br⁻,

δ115.7; I⁻, δ119.9) as the halide is changed from Cl⁻ to Br⁻ to I⁻ (Figure 4.30). Whereas

C(1) and C(2) exhibit slight upfield shifts as the halide is changed from Br⁻ to I⁻. [C(1),

Δδ 0.9 ppm; C(2), Δδ 1.9 ppm]. Other carbon resonances are only slightly shifted by less

than 0.5 ppm.

2. Syntheses and Characterization of Other Mixed-Metal Clusters

Silver(I) chloride can form [AgCl(PPh₃)₂],[153] [AgCl(PPh₃)₃][154] as well as

[Ag(PPh₃)₄]⁺,[155] complexes with triphenylphosphine (PPh₃) in methylene chloride. The

[AgCl(PPh₃)₂] complex has a C_2 symmetry at the silver center, while the [AgCl(PPh₃)₃]

has a C_3 symmetry. Thus silver(I) can be used as a proper soft-metal center to provide C_2

symmetry in place of Pd(II) for cluster formation, and it may also be employed to provide

C_3 symmetry for a tetrahedral cluster formation.

In our attempts to make a tetrahedral cluster [M₄L₁₂Ag₄] from Ag(I) and Cs₂TiL₃

(or Cs₂SnL₃) precursors (in a ratio of 1:1) in DMF, no single product has been isolated.

The solution $^{31}P\{^{1}H\}$ NMR spectrum revealed that no identifiable species was formed while no Cs_2TiL_3 remained. This result was confirmed by the FAB^+ mass spectrum which was nearly a continuous band without any major peaks.

While Ag(I) could not form a tetrahedral cluster with catecholato metal complexes, it has been successfully used in place of Pd(II) for synthesizing a cluster with C_3 symmetry, $CsSn_2L_6Ag_3$.

$M(CO)_4(Piperidine)_2$ (M = W, Mo, Cr)[156] are good precursors to synthesize diphosphine Group VIB metal complexes which can be in *trans-* and *cis-*configurations. As described in the structures of $[M_2L_6Pd_3Br_6]^{4+}$ clusters, a *trans*-$M(CO)_4$ moiety is essential for the formation of $M(CO)_4$ cluster analogues. Of the three Group VIB metals, Chromium is the smallest one. Thus a *trans*-$Cr(CO)_4$ moiety should be most likely attained due to steric effects. This rationale has been confirmed by the formation of *trans*-$Cr(CO)_4(4-PPh_2-Veratrole)_2$ and not the *cis*-isomer (see page 83).

$CsSn_2L_6Ag_3$: Reaction of two equivalents of Cs_2SnL_3 with three equivalents of $AgNO_3$ (or AgOTf) in DMF gave a white solid after workup. Separation and water-washing afforded a pure product in a good yield. The IR spectrum of this cluster indicated that no nitrate or triflate remained in the composition of the cluster. CHN elemental analyses were consistent with the formula of $CsSn_2C_{108}H_{78}P_6O_{12}Ag_3$ ($CsSn_2L_6Ag_3$). This was further supported by the FAB^+ mass spectrum (Figure 4.31).
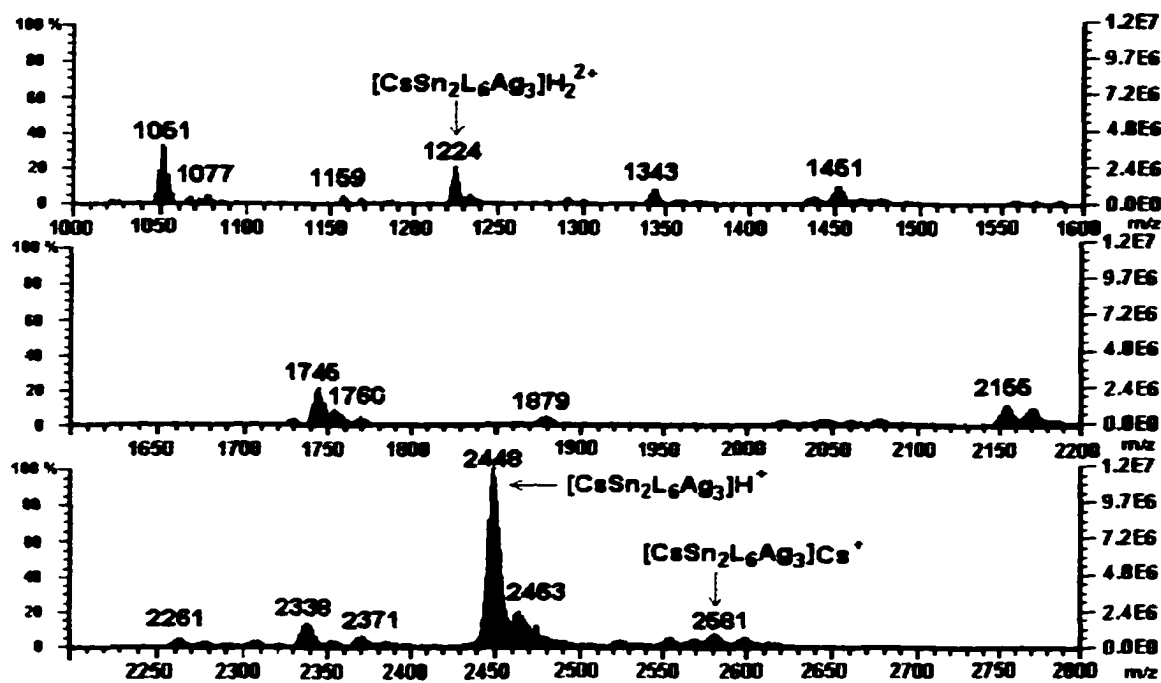
Figure 4.31 FAB$^+$ mass spectrum of the $CsSn_2L_6Ag_3$ cluster
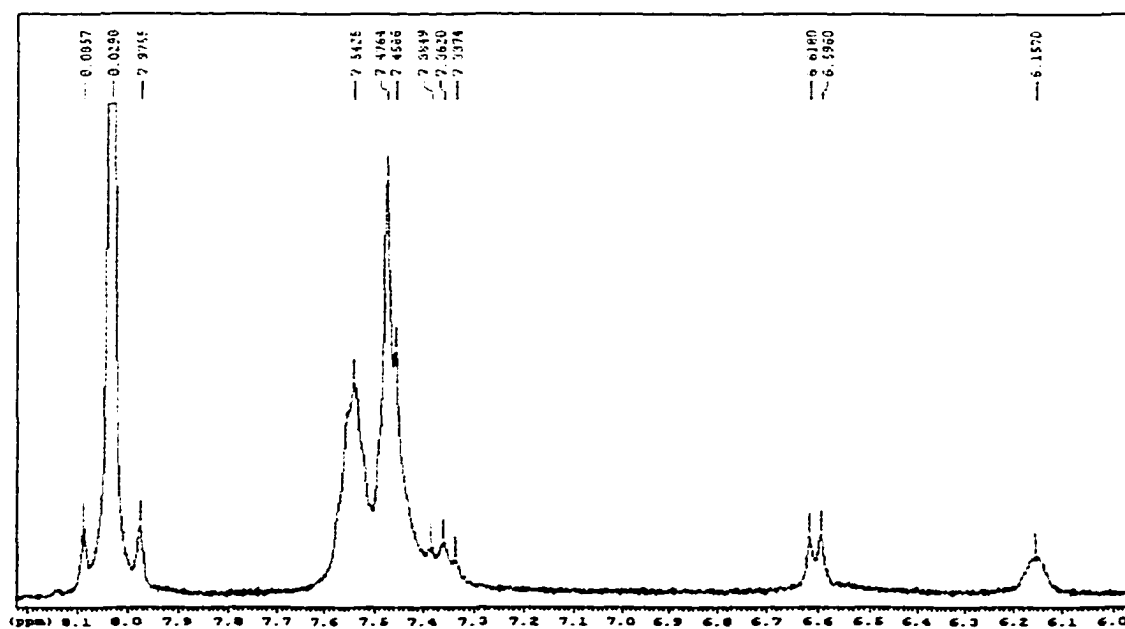
Figure 4.32 ^{1}H NMR spectrum of the $CsSn_2L_6Ag_3$ cluster in DMF-d$_7$

164

Only one set of catecholate proton resonances can be seen in the ^1H NMR spectrum of this $CsSn_2L_6Ag_3$ cluster (Figure 4.32). Compared to the Cs_2SnL_3 precursor, one catecholate-proton, H(3), shifted significantly downfield to 7.36 ppm (from ca 6.5 ppm). This observation supports that a $CsSn_2L_6Ag_3$ cluster of C_3 symmetry was formed. Due to its poor solubility, no satisfactory $^{13}C\{^1H\}$ NMR spectrum has been recorded. Its $^{31}P\{^1H\}$ NMR spectrum, however, is of special interest. As shown in Figure 4.33, the two naturally-occurring silver isotopes (^{107}Ag, I = 1/2, 51.82 %; ^{109}Ag, I = 1/2, 48.18 %) result in two doublets centered at $\delta 13.67$ with the coupling constants 496.6 Hz ($^1J_{107Ag-P}$) and 571.5 Hz ($^1J_{109Ag-P}$). The magnitude of these coupling constants confirmed that each silver atom is $trans$-coordinated by two PPh_2- groups, [131, 157] as expected for the formation of a $CsSn_2L_6Ag_3$ cluster.
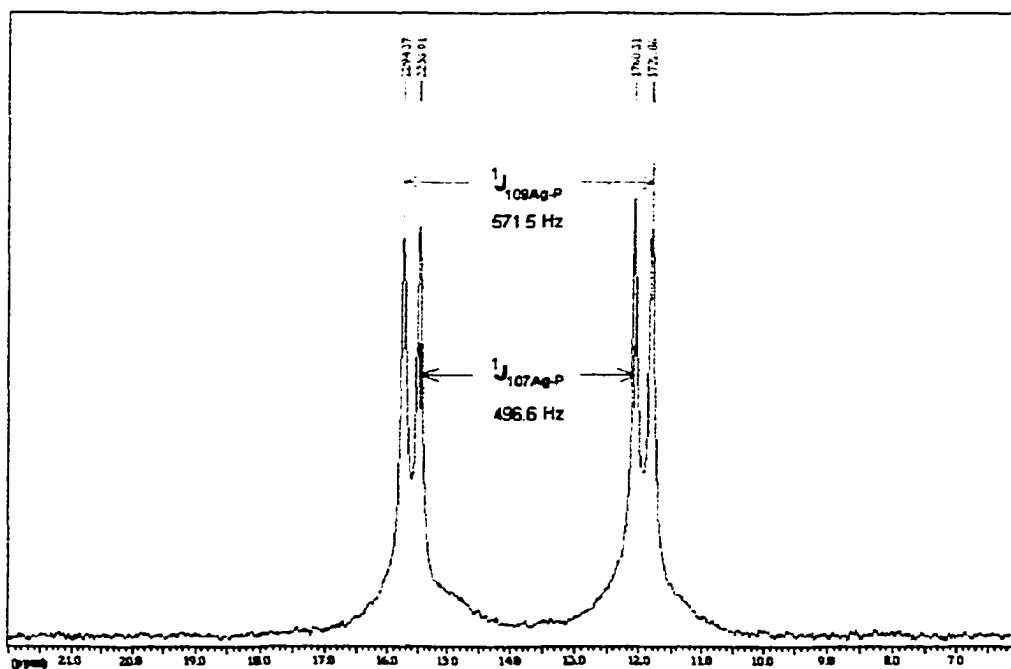
Figure 4.33 $^{31}P\{^1H\}$ NMR spectrum of the $CsSn_2L_6Ag_3$ cluster in DMF-d_7.

165

Cs$_4$M$_2$L$_6$[Cr(CO)$_4$]$_3$ [M =Ti(IV), Sn(IV)]: Reaction of two equivalents of Cs$_2$TiL$_3$ with three equivalents of Cr(CO)$_4$(Piperidine)$_2$ gave a cloudy orange solution after a week at room temperature. ^{31}P NMR analysis revealed formation of a new cluster at δ 71.92 as well as presence of unreacted Cs$_2$TiL$_3$ at δ -4.74. After workup, the desired Cs$_4$Ti$_2$L$_6$[Cr(CO)$_4$]$_3$ was successfully isolated in 66% yield. Analogously Cs$_4$Sn$_2$L$_6$[Cr(CO)$_4$]$_3$ was also synthesized in 75% yield. Both clusters have been characterized by CHN elemental analyses, IR and ^{1}H, ^{13}C{^{1}H}, and ^{31}P{^{1}H} NMR spectroscopy.

As shown in the ^{1}H NMR spectrum of the Cs$_4$Sn$_2$L$_6$[Cr(CO)$_4$]$_3$ (Figure 4.34) cluster, only one set of catecholate proton resonances is present, which indicates a three-fold symmetry. Significantly, one catecholate-proton, H(3), shifted downfield to δ 7.71 (from δ 6.5 in Cs$_2$SnL$_3$ precursor). This observation strongly supported the formation of this cluster, as previously discussed for the [M$_2$L$_6$Pd$_3$Br$_6$]$^{4+}$ clusters.

Compared to spectral data for *trans*-Cr(CO)$_4$(4-PPh$_2$-Veratrole)$_2$ in the previous chapter, the ^{13}C{^{1}H} NMR spectrum of this cluster (Figure 4.35) clearly shows that it has the same PPh$_2$- coordinated *trans*-Cr(CO)$_4$ bridging groups by the appearance of virtual triplets (see insets), although the spectrum has a low S/N level because of its limited solubility in DMF. The formation of an expected mesocate Cs$_4$Sn$_2$L$_6$[Cr(CO)$_4$]$_3$ cluster is further supported by a metal carbonyl triplet at δ 216 in this spectrum (Figure 4.36) and a characteristic strong CO stretching bond at 1855 cm^{-1} in its IR spectrum (Figure 4.37).

166
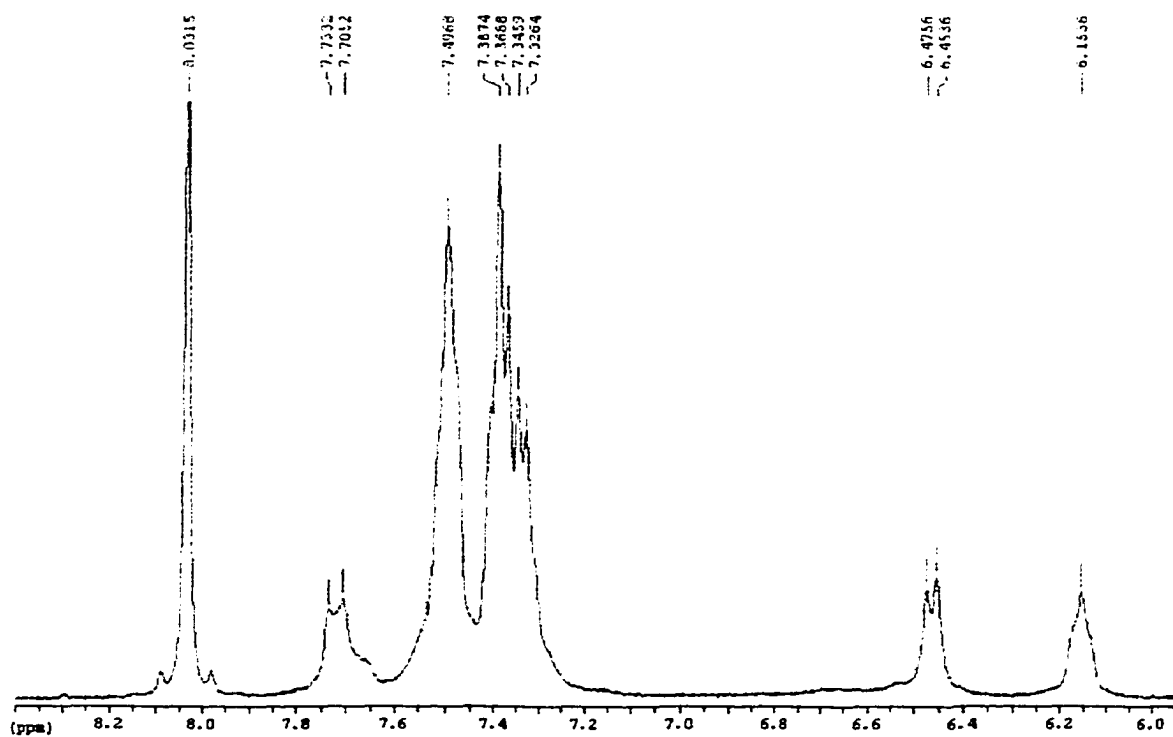
Figure 4.34 ^{1}H NMR spectrum of the $Cs_4Sn_2L_6[Cr(CO)_4]_3$ cluster in DMF-d$_7$.
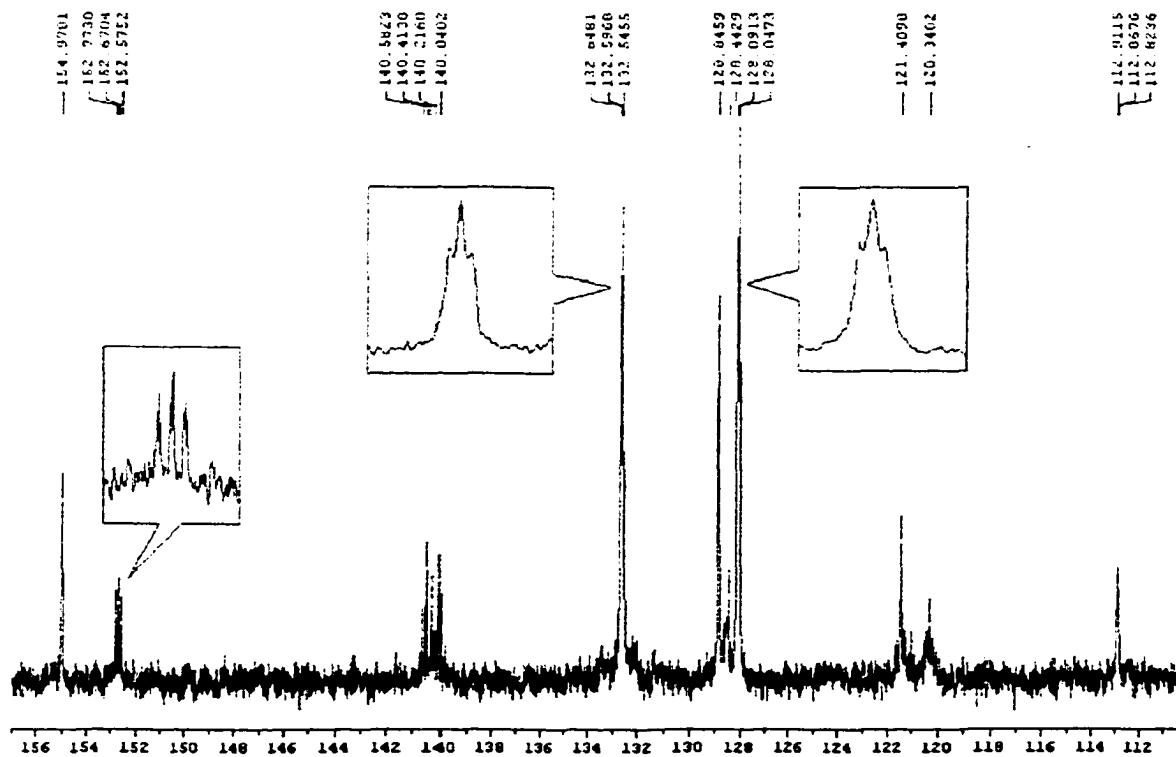
Figure 4.35 ^{13}C{^{1}H} NMR spectrum of the $Cs_4Sn_2L_6[Cr(CO)_4]_3$ cluster in DMF-d$_7$.

167
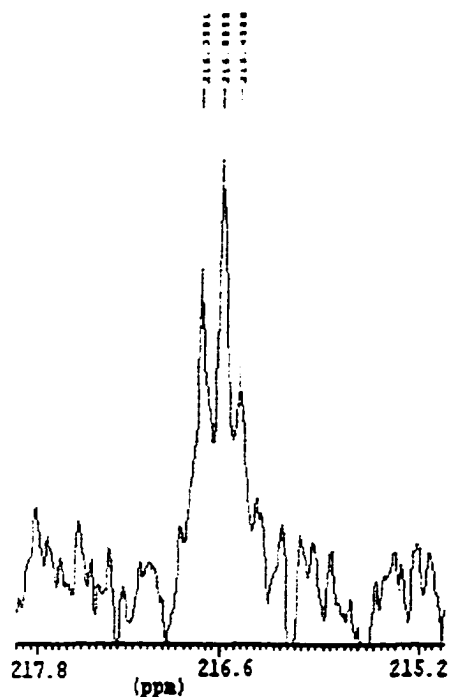
Figure 4.36 $^{13}C\{^1H\}$ NMR resonance of
The $Cr(CO)_4$ moieties in $Cs_4Sn_2L_6[Cr(CO)_4]_3$
in DMF-d_7.
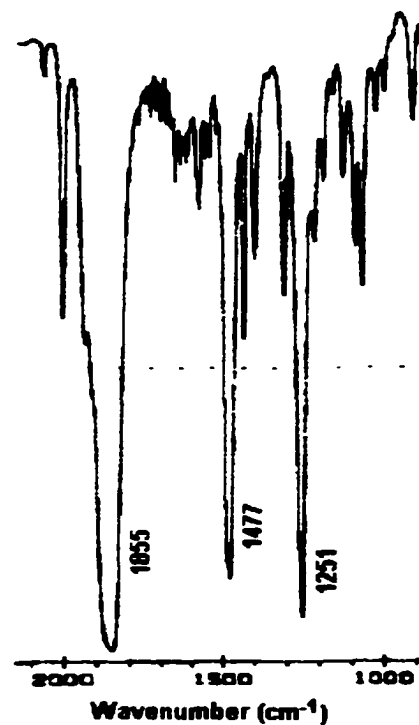
Figure 4.37 IR(KBr) spectrum
of $Cs_4Sn_2L_6[Cr(CO)_4]_3$

The $Cs_6Ga_2L_6Pd_3Br_6$ Cluster: Reaction of two equivalents of Cs_3GaL_3 with three equivalents of $PdBr_2\cdot2PhCN$ was found to give a clear, red solution which has a single $^{31}P\{^1H\}$NMR resonance at δ 22. Both of its ^1H and $^{13}C\{^1H\}$ NMR spectra revealed the expected patterns for the formation of this cluster though the signals were severely broadened, indicative of significant dynamic behavior. CHN elemental analyses also support a successful synthesis of the desired $Cs_6Ga_2L_6Pd_3Br_6$ cluster.

168

3. Attempted Syntheses of Other Clusters

(a) Attempted Syntheses of Clusters by Using H₂L (4-PPh₂-Catechol)

$Cs_4M_2L_6Pt_3Cl_6$ Clusters [M = Ti(IV), Sn (IV)]: A mixture of two equivalents of Cs_2TiL_3 and three equivalents of K_2PtCl_4 was stirred in DMF under nitrogen atmosphere for seven days, giving an orange-red cloudy solution. The supernatant gave a noisy $^{31}P\{^1H\}$ NMR spectrum which showed a major peak at δ 20.56, and an associated pair of ^{196}Pt satellites ($^1J_{Pt-P}$ = 2596 Hz). This observation is consistent with *trans*-coordination of the $PtCl_2$ linkers and formation of the $Cs_4Ti_2L_6Pt_3Cl_6$ cluster.[135] However, the pure product could not be isolated. Similarly, reaction of K_2PtCl_4 with Cs_2SnL_3 in a 3:2 molar ratio in DMF gave a cloudy golden-yellow solution whose weak $^{31}P\{^1H\}$ NMR spectrum revealed a major singlet at δ 20.09 with ^{196}Pt satellites ($^1J_{Pt-P}$ = 2582 Hz) consistent with presence of the desired $Cs_4Sn_2L_6Pt_3Cl_6$ cluster.[135] Again, isolation of a pure product was unsuccessful. This problem may be caused by the relatively high kinetic and thermodynamic stability of P-Pt bonds, which could lead to byproducts inert to the self-corrections necessary for formation of a single thermodynamic cluster.

Reaction between $ReOCl_3(PPh_3)_2$ and Cs_2TiL_3: Since *mer-trans*-$ReOCl_3(PPh_3)_2$ has C_2 symmetry, we tried to prepare its analogue of the $Cs_4Ti_2L_6Pd_3Br_6$ cluster containing three moieties of $ReOCl_3$ as linkers instead of $PdBr_2$.

Reaction of three equivalents of $ReOCl_3(PPh_3)_2$ with two equivalents of Cs_2TiL_3 in DMF at room temperature under nitrogen atmosphere gave a dark-red solution whose $^{31}P\{^1H\}$ NMR spectrum gave two peaks at -5.18 ppm (the resonance of Cs_2TiL_3) and -

169

6.26 ppm (the resonance of free PPh₃). These two peaks remained unchanged even after one month. This observation indicated that no desired reaction had occurred.

Reaction between Rh₂(OAc)₄ and Cs₂SnL₃ : It was noted by Albrecht and coworkers that a linear *bis*catechol ligand with an odd number of methylene units can yield a mesocate while an even number leads to the corresponding helicate. [38] Thus we anticipated that a corresponding helicate analogue of $[M_2L_6Pd_3Br_6]^{4-}$ clusters may form if the linear rhodium dimers, $Rh_2(OAc)_4$, would replace the bridging $PdBr_2$ moieties.

Reaction of two equivalents of Cs_2SnL_3 (or Cs_2TiL_3) with three equivalents of $Rh_2(OAc)_4$ in DMF under nitrogen atmosphere gave a dark-red solution after a few seconds (the initial color was dark-green). This solution $^{31}P\{^1H\}$ NMR spectrum gave a multiplet at δ -18.91. After a few hours, a broad lump and a singlet appeared around δ 22.3 and δ 26.4, respectively, as the multiplet disappeared. This suggested that the desired cluster was not stable, and could decompose (or oligomerize) to some unknown species even if it was formed initially.

Reaction between Re₃Cl₉ and Cs₂ML₃ [M = Ti(IV), Sn(IV)]: Re_3Cl_9 is a well-known metal cluster with C_3 symmetry, and can form a complex retaining the same symmetry with three equivalents of triphenylphosphine (Figure 4.38).[158] According to *the concept of symmetry-driven cluster formation*, it may form a tetrahedral cluster with $Cs_2(4-PPh_2-$ Catecholato)₃M with a formula of $[Cs_2(ML_3)_3]_4(Re_3Cl_9)_4$ where the Re_3Cl_9 units occupy the four faces and the four *tris*(catecholato) metal units occupy the four vertices of a tetrahedral cluster (see Page 15).

170
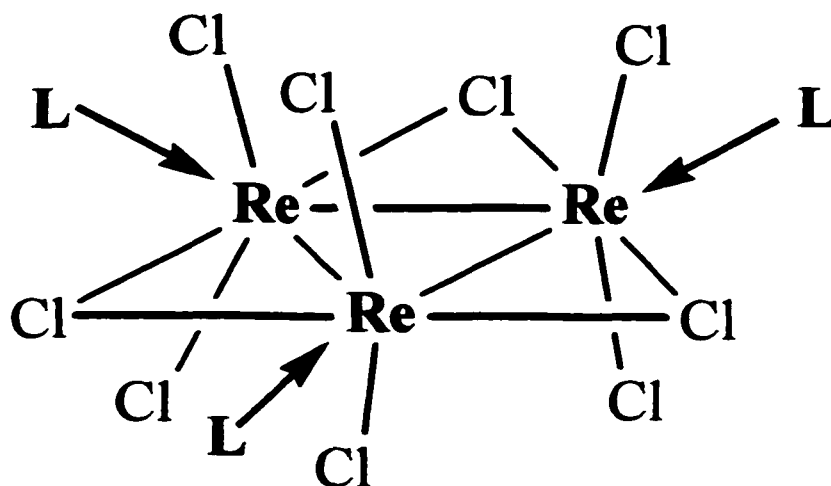
Figure 4.38 Sketch of the Re_3Cl_9 unit, which has D_{3h} symmetry. The arrows indicate the positions where the coordination of the Re_3Cl_9 unit with Cs_2ML_3 may occur.

Reaction of one equivalent of Cs_2TiL_3 (or Cs_2SnL_3) with one equivalent of Re_3Cl_9 in CH_3CN at room temperature under nitrogen atmosphere gave a dark-brown suspension whose supernatant (light brown) gave a singlet resonance at δ -6.39 in its $^{31}P\{^1H\}$ NMR spectrum. Addition of a small amount of Cs_2TiL_3 (or Cs_2SnL_3) resulted in an extra singlet at δ -5.06, which indicated that the former signal may be the desired cluster. Due to its poor solubility in CH_3CN, this product's ^1H NMR spectrum was very noisy. However, four peaks could be easily identified: δ (ppm) 7.35 (m, 6 phenyl-H), 7.26 (m, 4 phenyl-H), 6.83 (d, J = 8.3 Hz, 2 cat-H), 6.72 (m, 1 cat-H). These spectral data positively supported the formation of a cluster, although no further corroborating data have been obtained.

(b) Attempted Syntheses of Clusters by Using H₂2 (4-PH₂-Catechol)

As discussed in Chapter I, the ligand, 4-PH₂-Catechol, should be a good candidate for the formation of octahedral mixed-metal clusters. Therefore we have tried cluster syntheses (see Figure 1.50) from this ligand.

Reaction between Pd(MeCN)₄(BF₄)₂ and Cs₂Ti2₃: Precursor Pd(MeCN)₄(BF₄)₂ was chosen because it has four accessible coordination sites, and will provide a C_4 symmetry element when coordinated to four PH₂- groups. Reaction of three equivalents of Pd(MeCN)₄(BF₄)₂ with four equivalents of Cs₂Ti2₃ in degassed CH₃CN gave a brown precipitate immediately. No NMR spectra were obtainable due to the poor solubility of this product. This may indicate that an oligomerization or polymerization reaction had occurred. The absence of the characteristic stretching bands of PH₂ groups (m, 2285 cm⁻¹) in its IR spectrum further suggest that P-H cleavage side reactions may have occurred.

Reaction between RuBr₂(4-PH₂-Catechol)₄ and Ti(OMe)₄: As discussed in Chapter II, RuBr₂(H₂2)₄ is a complex with a four-fold symmetry. It may also form an octahedral cluster with Ti(IV) with a formula of Cs₁₆{[RuBr₂2₄]₆Ti₈} if a *tris*(catecholato)titanium complex of three-fold symmetry can be formed at the catechol end.

In degassed methanol, a suspension of RuBr₂(H₂2)₄ with Ti(OMe)₄ and Cs₂CO₃ in a molar ratio of 3:4:4 was stirred at room temperature. A dark-brown precipitate was formed after two days. No NMR spectra were obtainable due to the poor solubility of this product. However, its IR spectrum showed that both the PH₂- and Cat-O-Ti groups were present.

172

As seen before, the low solubility of products formed is the biggest problem in the attempted formation of octahedral clusters. In order to overcome the problem, we have modified ligand $H_2 2$ (PH_2-Catechol) to $H_2 3$ [$P(CH_2OH)_2$-Catechol], in order to improve the solubility of clusters in protic solvents.

(c) Attempted Cluster Formation using H₂3 [4-P(CH₂OH)₂-Catechol]

Reaction of Cs_2Ti3_3 with $PdX_2 \bullet 2PhCN$ in 2:3 molar ratio in DMF at room temperature yielded a brown suspension. No signal was observed in the $^{31}P\{^1H\}NMR$ spectrum of the supernatant, while the brown precipitate was insoluble in any of the common solvents. The IR spectrum of the precipitate showed a similar pattern to that of Cs_2Ti3_3 precursor, which indicated that the *tris*(catecholato)titanium complex was retained. The supernatant was slightly acidic (pH < 6), and had a positive reaction with aqueous silver nitrate solution. This observation suggests that a dehydrobromination may have occurred between the hydroxyl and $PdBr_2$ groups, giving rise to insoluble $P-CH_2-O-Pd$ bridge oligmers or polymers.

Attempts to use K_2PtCl_4, Li_2PdCl_4, $Re(O)Cl_3$ and $AgNO_3$ (or AgOTf) as C_2 linkers instead of $PdX_2 \bullet 2PhCN$ similarly failed.

Besides DMF, other solvent systems including water, CH_2Cl_2/H_2O, and DMF/H_2O were tried as the reaction medium. However, they did not give soluble products either.

Considering the possible oligomerization (or polymerization) side reactions encountered above due to the HBr loss, we speculated that using $Cr(CO)_4(Piperidine)_2$ instead would avoid this eventuality.

The reaction of Cs_2Ti3_3 with $Cr(CO)_4(Piperidine)_2$ in a molar ratio of 2:3 in CH_3CN gave a golden yellow clear solution immediately. However, after a few minutes, a substantial amount of gas evolved from this solution, while a yellow solid precipitated out. Again, this precipitate was insoluble in any of common solvents, and the absence of any strong CO stretching band in its IR spectrum suggests that the $Cr(CO)_4$ groups had decomposed. The $^{31}P\{^1H\}$ NMR spectrum of the supernatant was complex with three major resonances at δ -36.5, -49.1 and -49.4.

4. Summary

Several mixed-metal clusters of the type $[M_2L_6M'_3]$ have been successfully synthesized by both stepwise *aufbau* and self-assembly routes from the ligand H_2L (4-PPh_2-Catechol•HBr). Three of these have been crystallographically characterized by X-ray studies as triple mesocates of C_{3h} symmetry, while others most likely also adopt the same mesocate structure as suggested by solution spectral data.

So far, formation of mixed-metal clusters from ligand $H_2\mathbf{2}$ [PH_2-catechol] and ligand $H_2\mathbf{3}$ [$P(CH_2OH)_2$-Catechol] has not been realized because of possible oligomerization or polymerization side reactions and the poor solubility of intermediates (or products) that may have prevented access to the desired clusters.

5. Suggestions for Future Work

As shown in this thesis, it has proved a feasible approach to use designed hybrid ligands with two discrete and separated binding sites to synthesize mixed-metal clusters. To date, only 4-PPh$_2$-catechol (H$_2$L) has been successfully used in the formation of clusters of three-fold symmetry, while 4-PH$_2$-catechol (H$_2$2) and 4-P(CH$_2$OH)$_2$-Catechol (H$_2$3) are still under study. As discussed above, there are two major problems encountered in cluster formation from the latter two ligands: (1) poor solubility of intermediates or products, and (2) possible oligomerization or polymerization side reactions caused by the dehydrohalogenation reaction between the PH$_2$-/P(CH$_2$OH)$_2$- groups and the M-halide precursors (M = soft-metal). Considering these problems, for the ligand 4-PH$_2$-catechol (H$_2$2), the RuBr$_2$(4-PH$_2$-Catechol)$_4$ precursor may be worthy of atttention for the synthesis of possible octahedral clusters, whereby solvent and countercation effects may play important roles. As for ligand 4-P(CH$_2$OH)$_2$-Catechol (H$_2$3), pre-alkylation of the P(CH$_2$OH)$_2$- groups would be a good way to prevent possible dehydrohalogenation. How to selectively alkylate the alcohol groups while keeping the phosphine groups intact will be a challenge. Furthermore, choosing a suitable soft-metal precursor is also essential for cluster formation. For instance, both Pt(EtCN)$_4$(SO$_3$CF$_3$)$_2$ and Pd(MeCN)$_4$(BF$_4$)$_2$ can be used to provide a four-fold symmetry center, but the former should be a better precursor because it is air-stable and easily handled, [159a] while the latter one is extremely air sensitive[159b]. Other soft-metal precursors, like [Mo(NO)$_2$(CH$_3$CN)$_4$](BF$_4$)$_2$ and [W(NO)$_2$(CH$_3$CN)$_4$](BF$_4$)$_2$, may also be worth a try.[159c]

Up to now, we have not seen any evidence for helicate formation from ligand H$_2$L. Therefore, in order to realize a helicate of D_3 symmetry, we should design new

ligands, although they will not be used just for synthesizing a helicate. For example, a 4-Phosphino-Catechol (e.g. 4-PPh$_2$-CH$_2$-Catechol) with longer spacer between its two separated binding sites may be a possible ligand for a triple helicate because the longer spacer may be able to reduce the steric energy caused by helicate formation. Furthermore, the two diastereotopic methylene protons of this ligand should provide new probes for studies of the *fac/mer-* isomerization of *tris*(catecholato) metal complexes, as well as the helicate/mesocate formation.

Our well-characterized mixed-metal clusters [M$_2$L$_6$Pd$_3$Br$_6$]$^{4-}$ exhibit halide metathesis with CsI in DMF (see page 159), which implies that this type of cluster may have interesting derivative chemistry through modifying their PdBr$_2$ moieties. We may be able to introduce additional functional groups here to render them lipophilic or hydrophilic, which will lead to changed solubilities and other properties.

Prior to actual experiments, computer-modeling of desired clusters has saved much time by providing useful information which can lead experiments in the right directions. For example, through modeling we can figure out the steric energies for every potential cluster which will be very helpful in ligand design and experimental data analysis. When building a large cluster with high-symmetry, templating effects of counterions may become a major factor. Computer-modeling can also help us delineate the size and shape of the cavity inside a possible cluster for which a proper templating counterion may emerge.

176

Summary and Conclusion

4-Phosphino-Catechols combining phosphine and catechol groups have been designed for mixed-metal cluster formation by bridging two different metal centers. Three ligands 4-PPh$_2$-Catechol (H$_2$L), 4-PH$_2$-Catechol (H$_2$2) and 4-P(CH$_2$OH)$_2$-Catechol (H$_2$3) have been synthesized in excellent yields and spectrally characterized as were their precursors 4-PPh$_2$-Veratrole and 4-PH$_2$-Veratrole. Several phosphine-coordinated soft-metal [M' = Pd(II), Pt(II), Ru(II), Cr(0)] complexes have been synthesized and spectrally characterized to have 2-fold, 3-fold or 4-fold symmetry. The catecholate complexes of H$_2$L, H$_2$2 and H$_2$3 with a number of trivalent and tetravalent metal cations [M(III) = Fe, Ga; M(IV) = Ti, Sn] in the stoichiometry of 3:1 (ligand/metal) have also been prepared and characterized. Although the X-ray structure of the Cs$_2$TiL$_3$ salt revealed a C_1-*mer*-configuration in the solid-state, the room temperature and/or variable-temperature solution NMR studies of the catecholate complexes are consistent with either exclusive formation of the C_3-*fac*-isomer or very facile *fac/mer* isomerization.

Both stepwise *aufbau* and self-assembly routes have been employed to synthesize the desired mixed-metal clusters. While the attempted cluster formations from H$_2$2 and H$_2$3 failed, pentametallic [M$_2$L$_6$Pd$_3$Br$_6$]$^{4-}$ (M = Ti, Sn) clusters have been successfully synthesized and spectrally characterized to have a three-fold symmetry in solution. The solid-state structures of the Cs$_4$Ti$_2$L$_6$Pd$_3$Br$_6$, Cs$_4$Ti$_2$L$_6$Pd$_3$Br$_6$ and (DABCO-H)$_4$Ti$_2$L$_6$Pd$_3$Br$_6$ clusters have been determined from their X-ray diffraction data to be C_{3h} mesocates with Cs$^+$ or protonated 1,4-diazabicyclo[2.2.2]octane (DABCO-H$^+$) cations

177

incorporated into deep molecular clefts. Countercations have been demonstrated as playing a critical role in the formation of this type of tetraanionic clusters. While all alkali cations and protonated DABCO led to high-yield formation of the respective clusters, other cations such as tetramethylammonium (TMA^+), tetraphenylphosphonium(Ph_4P^+), and *bis*(triphenyl-phosphoranylidene)ammonium (PPN^+) give either a mixture of products or insoluble precipitates. Related pentametallic clusters $[M_2L_6Pd_3Cl_6]^{4-}$, $[M_2L_6Pd_3I_6]^{4-}$, $CsSn_2L_6Ag_3$ and $[M_2L_6Cr_3(CO)_{12}]^{4-}$ have also been synthesized via the stepwise *aufbau* route, and characterized to have a three-fold symmetry in solution.

Using the *incommensurate symmetry* requirements at two different metal centers bridged by a hybrid ligand to control desired cluster formation has been proven to be a feasible route to mixed-metal cluster formation. Extension of this methodology to other hard/soft metal as well as ligand combinations promises to be an attractive and effective entry into additional fascinating supramolecular assemblies.

.

.

Experimental Section

General Procedure. All operations and manipulations were performed in standard Schlenck glassware under a dry nitrogen atmosphere. Chemical reagents were commercial products and were used without further purification, solvents were commercial reagent grade and degassed before use. [Ruthenium trichloride hydrate(Johnson-Mattey Inc.); cobalt hexacarbonyl (Pressure Chemical Co.); potassium carbonate, acetone and acetonitrile (J. T. Baker Chemical Co.); methylene chloride (Fisher Scientific); palladium(II) chloride (Acros Chemical Co.); methanol, ethanol, veratrole, phosphorus trichloride, tin tetrachloride, 48% hydrobromide, LiAlH$_4$, potassium tetrachloroplatinate(IV), titanium(IV) methoxide, tin(IV) chloride, N,N-dimethylformamide, benzonitrile, gallium(III) nitrate hydrate, tetraphenylphosphonium chloride, bis(triphenylphosphoranylidene)ammonium chloride, tetramethylammonium hydroxide, 1,4-diazabicyclo-[2,2,2] octane (DABCO), rhenium(III) chloride, silver trifluoromethane-sulfonate, dibenzo-2,4-crown-8, piperidine, cesium carbonate, rubidium carbonate, boron tribromide and 37% formaldehyde (Aldrich Chemical Co.)]. The following reagents were prepared according to literature methods: PdBr$_2$•2PhCN, PdCl$_2$•2PhCN,[160] Cr(CO)$_4$(Piperidine)$_2$.[156] All NMR spectra were recorded on a Bruker AM360FT-NMR or a JEOL FX 90Q NMR spectrometer. Chemical shifts of ^{1}H and ^{13}C NMR spectra were referenced to (CH$_3$)$_4$Si. ^{31}P NMR spectra were referenced to external 85% H$_3$PO$_4$. ^{119}Sn NMR spectra were referenced to external (CH$_3$)$_4$Sn. [133]Cs NMR spectra were referenced to external CsOTf. Electronic spectra were measured on a Cary

179

219 spectrophotomer and EPR spectra on a Varian E-4 instrument. Infrared spectra were run on Nicolet MX-1 FT-spectrophotometer using KBr pellets. Elemental analyses were performed by the UNH Instrumentation Center on a Perkin-Elmer 2400 Elemental Analyzer. Single-crystal X-ray diffraction data were collected on a Siemens SMART diffractometer.

General X-ray Experimental: Crystal data for the three mixed-metal clusters were collected using a Siemens SMART [161] Diffractometer equipped with a CCD area detector using Mo-Kα ($\lambda = 0.71073$ Å) radiation. Data in the frames corresponding to an arbitrary hemisphere of data were integrated using SAINT.[162] Data were corrected for Lorentz and polarization effects. An empirical absorption correction based on the measurement of redundant and equivalent reflections and an ellipsoidal model for the absorption surface was applied using XPREP [163] ($Cs_4Sn_2L_6Pd_3Br_6$ structure) or SADABS [164] [structures of Cs_2TiL_3, $Cs_4Ti_2L_6Pd_3Br_6$ and $(DABCO-H)_4Sn_2L_6Pd_3Br_6$]. The structure solution and refinement for the structures of the two Sn(IV) clusters and Cs_2TiL_3 were performed using the teXsan[165] crystallographic software package (refining on F); for the structure of $Cs_4Ti_2L_6Pd_3Br_6$ cluster the initial solution was performed using teXsan but the final refinements were performed using SHELXTL (refining on F^2). [163]

4-Dichlorophosphino-Veratrole (4-PCl₂-Veratrole). A mixture of 28 mL veratrole (0.22 mol) , 56 mL of phosphorus trichloride (0.64 mol), and 4.0 mL of anhydrous stannic chloride (34 mmol) were refluxed under nitrogen atmosphere for about 20 hrs. To improve the yield, an extra 2.0 mL of anhydrous stannic chloride (17 mmol) was

added after 10 hrs. The mixture was filtered in air after it was cooled down to the room temperature. The filtrate was evaporated in vacuum to get rid of excess of phosphorus trichloride. The light-yellow residue was then distilled in vacuum. At 0.4 mmHg pressure, the desired product was collected at the temperature range of 120°C to 135°C. The purity of the product after the first distillation was about 90%. The coarse product was again redistilled, whereupon the purity of product reached nearly 100%, as measured by ^{31}P NMR spectroscopy.

4-Diphenylphosphino-Veratrole (4-PPh$_2$-Veratrole). An amount of 3.5 grams of magnesium (0.14 mol) and 80 mL of dry diethyl ether were put into a nitrogen prefilled 3-neck flask. The flask temperature was cooled down to 0°C in an ice bath. A solution of 14 mL of bromobenzene (0.13 mol) and 40 ml of dry diethyl ether was added to the flask dropwise from an addition funnel, while the mixture in the flask was stirred. After completion of addition, the mixture was heated to reflux for 1 hr, and then cooled down to 0°C using an ice bath. A solution of 7.8 grams of 4-Dichlorophosphino-Veratrole (33 mmol) and 30 mL of dry diethyl ether was added dropwise to the mixture which was stirred rigorously. While it was being added, lots of white precipitate was produced. With water condenser cooling , the mixture was heated to reflux again for 2 hrs, then cooled down to 0°C using an ice bath. A volume of 50 mL of water was added dropwise to quench the excess Grignard reagent (CAUTION! The first few drops caused a rigorous reaction producing plenty of heat). The mixture was then filtered in air, the filtrate was reduced by rotary evaporation, and then dried in vacuum, 10.2 grams of yellowish-white solid remained. Recrystallization of the yellowish-white solid from 25 mL of ethanol

gave 9.5 grams of pure white product (29 mmol) for a yield of 88%. Its CHN elemental analyses indicated that its formula is 4-PPh$_2$-Veratrole.

^{1}H NMR (360 MHz, CDCl$_3$): δ (ppm) 7.33 (m, 10 phenyl-H), 6.89 (m, 3-cat-H), 3.90 (s, -OCH$_3$), 3.77 (s, OCH$_3$); ^{13}C {^{1}H} NMR (89.9 MHz, CDCl$_3$): δ (ppm) 149.8 (s, veratrole), 149.0 (d, J$_{pc}$ = 10.0 Hz, veratrole), 137.6 (broad, phenyl), 133.5 (d, J$_{pc}$ = 18.6 Hz, phenyl), 128.6 (s, phenyl), 128.5 (d, J$_{pc}$ = 6.6 Hz, phenyl), 127.9 (broad, veratrole), 127.2 (d, J$_{pc}$ = 19.4 Hz, veratrole), 116.6 (d, J$_{pc}$ = 25.2 Hz, veratrole), 111.3 (d, J$_{pc}$ = 8.0 Hz, veratrole), 55.8 (s, OCH$_3$); ^{31}P {^{1}H} NMR (36.3 MHz, CDCl$_3$): δ (ppm) -5.35 (s). IR (KBr) ν $_{(OCH3)}$ 2957, 2833 cm^{-1}, C-H bending 1507, 1438 cm^{-1}, ν $_{(C-O-C)}$ 1254, 1235 cm^{-1}. Anal. calc'd for C$_{20}$H$_{19}$PO$_2$: C 74.52 %, H 5.94 %; found: C 74.31 %, H 5.71 %.

4-Diphenylphosphino-Catechol (4-PPh$_2$-Catechol). An amount of 5.0 grams of 4-diphenylphosphino-Veratrole (16 mmol) and 32 mL of 48% aq. hydrobromic acid (0.28 mol) were refluxed under nitrogen atmosphere for 18 hrs. On chilling, 4.7 grams (13 mmol, 81% yield) of product came out of solution. Recrystallization of this solid from 20 ml of ethanol and 2 mL of 48% aq. hydrobromic acid gave 4.1 grams (11 mmol, 70%) of a white solid. The CHN elemental analyses indicated formation of a 1:1 hydrobromide salt. ^{1}H NMR (360 MHz, DMF-d$_7$): δ (ppm) 7.40 (m, 6 phenyl-H), 7.28 (m, 4 phenyl-H), 6.93 (dd, J = 7.9 and 1.53 Hz, 1 cat-H), 6.82 (dd, J = 7.53 and 1.73 Hz, 1 cat-H), 6.71 (ddd, J = 8.23, 8.23 Hz and 1.53 Hz, 1 cat-H); ^{13}C {^{1}H} NMR (89.9 MHz, DMF-d$_7$): δ (ppm) 147.6 (s, catechol), 146.5 (d, J$_{pc}$ = 8.6 Hz, catechol), 138.8 (d, J$_{pc}$ = 11.3 Hz, phenyl), 133.4 (d, J$_{pc}$ = 19.2 Hz, phenyl), 128.9 (s, phenyl), 128.8 (d, J$_{pc}$ = 3.3 Hz,

phenyl), 126.3 (d, J_{pc} = 25.2 Hz, catechol), 125.9 (d, J_{pc} = 7.3 Hz, catechol), 121.4 (d, J_{pc} = 18.5 Hz, catechol), 116.5 (d, J_{pc} = 10.0 Hz, catechol); $^{31}P\{^{1}H\}$ NMR (36.3 MHz, DMF-d_7): δ (ppm) -6.73 (s). IR (KBr) $\nu_{(OH)}$ broad 3290 cm^{-1}, $\nu_{(aromatic-H)}$ 3077, 3049, 3029 cm^{-1}, C-H bending 1509, 1439 cm^{-1}, $\nu_{(C-OH)}$ 1291, 1266 cm^{-1}; Anal. calc'd for $C_{18}H_{16}PO_2Br$: C 57.62 %, H 4.30 %; found: C 57.37 %, H 4.38 %.

4-Dihydrophosphino-Veratrole (4-PH$_2$-Veratrole). An amount of 3.5 grams of LiAlH$_4$ cubes (92 mmol) was stirred in 60 mL of dry diethyl ether in a 3-neck flask. After the LiAlH$_4$ cubes were broken up into a gray powder, the temperature was cool down to 0°C using an ice-bath. A solution of 11 grams of 4-Dichlorophosphino-Veratrole (45 mmol), in 20 mL of dry ether was added dropwise into the flask with stirring. While it was being added, abundant white precipitate was produced. The mixture was then heated to reflux for 1 hr, and then cooled down to 0°C by an ice-bath. A volume of 30 mL of 6M aq. HCl solution was added dropwise into the mixture (CAUTION! The first few drops caused a rigorous reaction producing hydrogen gas). The mixture became two separated layers, the upper ether-layer was separated, dried and concentrated in vacuum. The product was obtained as a colorless liquid in yields of around 71%. Its ^{31}P $\{^{1}H\}$ NMR spectrum showed a singlet at -125 ppm, while its ^{1}H-coupled ^{31}P NMR spectrum gave a triplet of triplets ($^{1}J_{P-H}$ = 201.4 Hz, $^{3}J_{P-H}$ = 6.1 Hz) pattern. ^{1}H NMR (360 MHz, CDCl$_3$): δ (ppm) 6.91 (m, 1 cat-H), 6.84 (m, 1 cat-H), 6.62 (m, 1 cat-H), 3.81 (d, $^{1}J_{P-H}$ =195.4 Hz, -PH$_2$), 3.68 (s, -OCH$_3$), 3.65 (s, -OCH$_3$); ^{13}C $\{^{1}H\}$ NMR (89.9 MHz, CDCl$_3$): δ (ppm) 148.8 (s), 148.0(s), 128.6 (d, J_{pc} = 20.1 Hz), 117.9(s), 116.3 (s), 110.7 (d, J_{pc} = 6.6 Hz), 55.1 (d, J_{pc} =

7.6 Hz). IR (Nujol) $\nu_{(OCH_3)}$ 2967, 2848 cm^{-1}, $\nu_{(PH2)}$ 2368, 2302 cm^{-1} C-H bending 1588, 1519 cm^{-1}, $\nu_{(C-O-C)}$ 1269 cm^{-1}.

4-Dihydrophosphino-Catechol (4-PH$_2$-Catechol). An amount of 0.35 gram of 4-Dihydrophosphino-Veratrole (4-PH$_2$-Veratrole) (2.1 mmol) was dissolved in 15 mL CH$_2$Cl$_2$. The temperature was cooled to -78 °C with dry ice. A volume of 2.0 mL of BBr$_3$ (21 mmol) was added with a syringe. When the temperature rose to room temperature, the mixture was evaporated overnight in vacuum to remove CH$_2$Cl$_2$ and the excess BBr$_3$, then 20 mL of methanol was added dropwise to the residue (CAUTION! The first few drops caused a rigorous reaction). The resulting solution was then evaporated in vacuum, the product came out as a white solid in yields of around 57%. The CHN elemental analyses indicated a 1:1 hydrobromide salt. ^{1}H NMR (360 MHz, CD$_3$OD): δ (ppm) 6.91 (dd, J = 7.3 and 1.8 Hz, 1 cat-H), 6.82 (ddd, J = 7.8, 7.8 and 1.8 Hz, 1 cat-H), 6.69 (dd, J = 7.8 and 1.3 Hz, 1 cat-H); ^{13}C {^{1}H} NMR (89.9 MHz, CD$_3$OD): δ (ppm) 147.2 (s), 146.4 (d, J_{pc} = 8.0 Hz), 128.3 (d, J_{pc} = 19.2 Hz), 123.1 (d, J_{pc} = 15.2 Hz), 117.7 (d, J_{pc} = 2.7 Hz), 116.7 (d, J_{pc} = 8.6 Hz); ^{31}P {^{1}H} NMR (36.3 MHz, CD$_3$OD): δ (ppm) -127.2(s). IR (KBr) $\nu_{(OH)}$ broad 3346 cm^{-1}, $\nu_{(-PH2)}$ 2289 cm^{-1}, C-H bending 1512 cm^{-1}, $\nu_{(C-OH)}$ 1282 cm^{-1}; Anal. calc'd for C$_6$H$_8$O$_2$PBr: C 32.32%, H 3.62%; found C 32.18%, H 3.57%.

4-Dihydroxymethylphosphino-Catechol [4-P(CH$_2$OH)$_2$-Catechol]. Aqueous formaldehyde (37 wt%, 0.25 mL, 3.33 mmol) was added to 25 mL of oxygen-free methanol, and purged with N$_2$ gas for a half hour. A solution of 4-PH$_2$-Catechol●HBr

184

(338 mg, 1.52 mmol) in 10 mL of methanol was added dropwise to the formaldehyde solution with constant stirring at room temperature. The N_2 gas flow was kept on during the entire reaction process. The reaction was complete in 6 hrs, as monitored by ^{31}P NMR spectroscopy. Removal of the solvent in vacuum gave a white solid (401 mg) for a yield of 94%. The CHN elemental analyses indicated a 1:1 hydrobromide salt. ^1H NMR (360 MHz, D_2O): δ (ppm) 7.31 (m, 1 cat-H), 7.28 (m, 1 cat-H), 7.10 (dd, J = 8.4 and 4.1 Hz, 1 cat-H), 4.82 (s, 4H, $-CH_2OH$); ^{13}C {^1H} NMR (89.9 MHz, D_2O): δ (ppm) 154.0 (d, J_{pc} = 3.3 Hz), 148.4 (d, J_{pc} = 15.9 Hz), 129.6 (d, J_{pc} = 8.0 Hz), 122.1 (d, J_{pc} = 10.0 Hz), 120.3 (d, J_{pc} = 14.6 Hz), 104.5 (d, J_{pc} = 78.6 Hz), 54.0 (d, J_{pc} = 57.1 Hz, $-CH_2OH$); ^{31}P {^1H} NMR (36.3 MHz, D_2O): δ (ppm) 19.86 (s). IR (KBr) ν $_{(OH\ and\ CH2OH)}$ broad 3291, 3185 cm$^-$^{1}, ν $_{(CH2)}$ 2941, 2899 cm^{-1}, C-H bending 1514, 1400 cm^{-1}, ν $_{(C-OH)}$ 1303, 1295 cm^{-1}; Anal. calc'd for $C_8H_{10}O_4PBr$: C 33.95 %, H 4.27 %; found: C 34.12 %, H 4.42 %.

PdBr$_2$(4-PPh$_2$-Veratrole)$_2$: A DMF (10 mL) solution of 4-PPh$_2$-Veratrole (322 mg, 1.00 mmol) and PdBr$_2$•2PhCN (236 mg, 0.500 mmol) was stirred at room temperature for a few minutes, giving an orange-red solution. Addition of 20 mL of diethyl ether precipitated an orange-red solid, which was filtered off and dried in vacuum. Yield: 420 mg (92%). ^1H NMR (360 MHz, CDCl$_3$): δ (ppm) 7.69 (m, 2×4 phenyl-H), 7.54 (td, J = 5.8 and 1.8 Hz, 2×1 veratrole-H), 7.37 (m, 2×6 phenyl-H), 7.21 (m, 2×1 veratrole-H), 6.87 (broad d, J = 8.2 Hz, 2×1 veratrole-H), 3.90 (s, $-OCH_3$), 3.76 (s, $-OCH_3$); ^{13}C{^1H} NMR (89.9 MHz, CDCl$_3$): δ (ppm) 150.9 (s, veratrole), 148.2 (virtual t, J_{pc} = 7.0 Hz, veratrole), 134.8 (virtual t, J_{pc} = 6.3 Hz, phenyl), 131.7 (virtual t, J_{pc} = 25.2 Hz, phenyl), 130.3 (s, phenyl), 128.8 (virtual t, J_{pc} = 5.6 Hz, phenyl), 127.8 (virtual t, J_{pc} = 5.6 Hz,

veratrole), 121.4 (virtual t, J_{pc} = 26.9 Hz, veratrole), 119.1 (virtual t, J_{pc} = 8.6 Hz, veratrole), 110.5 (virtual t, J_{pc} = 6.3 Hz, veratrole), 56.0 (s, -OCH_3), 55.8 (s, -OCH_3); $^{31}P\{^1H\}$ NMR (36.3 MHz, CDCl$_3$) δ (ppm) 22.35 (s). IR (KBr) ν $_{(OCH3)}$ 2943, 2841 cm^{-1}, C-H bending 1507, 1437 cm^{-1}, ν $_{(C-O-C)}$ 1262, 1232 cm^{-1}; Anal. calc'd for PdBr$_2$P$_2$C$_{40}$H$_{38}$O$_4$: C 52.74 %, H 4.20 %; found: C 52.49 %, H 4.22 %.

PdCl$_2$(4-PPh$_2$-Veratrole)$_2$: A CH$_2$Cl$_2$ (10 mL) solution of 4-PPh$_2$-Veratrole (322 mg, 1.00 mmol) and PdCl$_2$•2PhCN (192 mg, 0.500 mmol) was stirred at room temperature for a few minutes, giving a golden-yellow solution. Evaporation of the solution yielded a yellow-solid, which was washed by three portions of diethyl ether (10 mL) and dried in vacuum. Yield: 450 mg (95%). ^{1}H NMR (360 MHz, CDCl$_3$): δ (ppm) 7.73 (m, 2×4 phenyl-H), 7.58 (td, J = 5.8 and 1.7 Hz, 2×1 veratrole-H), 7.42 (m, 2×6 phenyl-H), 7.17 (m, 2×1 veratrole-H), 6.87 (broad d, J = 8.2 Hz, 2×1 veratrole-H), 3.90 (s, -OCH_3), 3.76 (s, -OCH_3); $^{13}C\{^1H\}$ NMR (89.9 MHz, CDCl$_3$): δ (ppm) 151.0 (s, veratrole), 148.4 (virtual t, J_{pc} = 7.0 Hz, veratrole), 134.8 (virtual t, J_{pc} = 6.3 Hz, phenyl), 130.4 (s, phenyl), 130.2(virtual t, J_{pc} = 27.5 Hz, phenyl), 128.6 (virtual t, J_{pc} = 5.6 Hz, phenyl), 128.0 (virtual t, J_{pc} = 5.3 Hz, veratrole), 120.4 (virtual t, J_{pc} = 26.5 Hz, veratrole), 118.7 (virtual t, J_{pc} = 9.0 Hz, veratrole), 110.6(virtual t, J_{pc} = 6.3 Hz, veratrole), 56.0 (s, -OCH_3), 55.9 (s, -OCH_3); $^{31}P\{^1H\}$ NMR (36.3 MHz, CDCl$_3$) δ (ppm) 23.42 (s). IR (KBr) ν $_{(OCH3)}$ 2944, 2841 cm^{-1}, C-H bending 1508, 1438 cm^{-1}, ν $_{(C-O-C)}$ 1264, 1232 cm^{-1}; Anal. calc'd for PdCl$_2$P$_2$C$_{40}$H$_{38}$O$_4$: C 58.45 %, H 4.66 %; found: C 58.23 %, H 4.64 %.

186

PdI₂(4-PPh₂-Veratrole)₂: An amount of 210 mg of PdBr₂(4-PPh₂-Veratrole)₂ (0.440 mmol) was redissolved in 10 mL of DMF to give an orange-red solution, to which CsI (460 mg, 1.77 mmol) was added. The dark-red mixture was stirred overnight, and then filtered to give a dark red filtrate. Addition of 20 mL of diethyl ether precipitated a dark red solid, which was filtered off and dried in vacuum. Yield: 220 mg (95%). ^{1}H NMR (360 MHz, CDCl₃): δ (ppm) 7.66 (m, 2×4 phenyl-H), 7.45 (td, J = 6.0 and 1.8 Hz, 2×1 veratrole-H), 7.38 (m, 2×6 phenyl-H), 7.26 (m, 2×1 veratrole-H), 6.86 (broad d, J = 8.5 Hz, 2×1 veratrole-H), 3.91 (s, -OCH_3), 3.78 (s, -OCH_3); ^{13}C{^{1}H} NMR (89.9 MHz, CDCl₃): δ (ppm) 150.8 (s, veratrole), 147.9 (virtual t, J_{pc} = 7.3 Hz, veratrole), 135.0 (virtual t, J_{pc} = 25.9 Hz, phenyl), 134.8 (virtual t, J_{pc} = 3.3 Hz, phenyl), 130.1 (s, phenyl), 128.9 (virtual t, J_{pc} = 5.6 Hz, phenyl), 127.6 (virtual t, J_{pc} = 5.3 Hz, veratrole), 123.7 (virtual t, J_{pc} = 27.5 Hz, veratrole), 119.9 (virtual t, J_{pc} = 9.0 Hz, veratrole), 110.2 (virtual t, J_{pc} = 6.3 Hz, veratrole), 56.1 (s, -OCH_3), 55.9 (s, -OCH_3); ^{31}P{^{1}H} NMR (36.3 MHz, CDCl₃) δ (ppm) 13.73 (s). IR (KBr) ν $_{(OCH3)}$ 2952, 2835 cm^{-1}, C-H bending 1508, 1457 cm^{-1}, ν $_{(C-O-C)}$ 1260, 1236 cm^{-1}; Anal. calc'd for PdI₂P₂C₄₀H₃₈O₄: C 47.81 %, H 3.81 %; found: C 47.63 %, H 3.88 %.

PtCl₂(4-PPh₂-Veratrole)₂: A solution of K₂PtCl₄ (104 mg, 0.250 mmol) in 5 mL of H₂O was added to a solution of 4-PPh₂-Veratrole (161 mg, 0.500 mmol) in 10 ml of CH₂Cl₂ with constant stirring at room temperature. The biphasic mixture was stirred until the yellow color of H₂O phase became colorless. The CH₂Cl₂ phase was separated, and evaporated to *ca* 5 mL. Addition of 10 mL of diethyl ether precipitated a white solid, which was filtered off and dried in vacuum. Yield: 430 mg (94%). ^{1}H NMR (360 MHz,

CDCl$_3$): δ (ppm) 7.56 (broad t, J = 7.3 Hz, 2×4 phenyl-H), 7.32 (t, J = 3.8 Hz, 2×2 phenyl-H), 7.22 (td, J = 7.9 and 2.1 Hz, 2×4 phenyl-H), 6.97 (dd, J = 11.9 and 1.8 Hz, 2×1 veratrole-H), 6.88 (ddd, J = 11.3, 8.2 and 1.8 Hz, 2×1 veratrole-H), 6.59 (dd, J = 8.5 and 2.3 Hz, 2×1 veratrole-H), 3.85 (s, -OCH$_3$), 3.52 (s, -OCH$_3$); ^{13}C{ ^{1}H } NMR (89.9 MHz, CDCl$_3$): δ (ppm) 151.0 (s, veratrole), 147.9 (virtual t, J$_{pc}$ = 7.0 Hz, veratrole), 134.8 (virtual t, J$_{pc}$ = 5.3 Hz, phenyl), 130.8 (s, phenyl), 130.1 (dd, J$_{pc}$ = 68.3 and 2.7 Hz, phenyl), 128.5 (virtual t, J$_{pc}$ = 5.3 Hz, phenyl), 127.8 (virtual t, J$_{pc}$ = 5.6 Hz, veratrole), 120.2 (dd, J$_{pc}$ = 70.7 and 2.3 Hz, veratrole), 117.4 (virtual t, J$_{pc}$ = 7.0 Hz, veratrole), 110.1 (virtual t, J$_{pc}$ = 7.0 Hz, veratrole), 55.9 (s, -OCH$_3$), 55.7 (s, -OCH$_3$); ^{31}P{^{1}H} NMR (36.3 MHz, CDCl$_3$) δ (ppm) 14.40 (s) with two satellites (^{2}J$_{195Pt-P}$ = 3679 Hz); IR (KBr) ν $_{(OCH3)}$ 2959, 2830 cm^{-1}, C-H bending 1510, 1435 cm^{-1}, ν $_{(C-O-C)}$ 1261, 1238 cm^{-1}; Anal. calc'd for PtCl$_2$P$_2$C$_{40}$H$_{38}$O$_4$: C 52.76 %, H 4.21 %; found: C 52.78 %, H 4.18 %.

Cr(CO)$_4$(4-PPh$_2$-Veratrole)$_2$: A CH$_2$Cl$_2$ (10 mL) solution of 4-PPh$_2$-Veratrole (174 mg, 0.54 mmol) and Cr(CO)$_4$(Piperidine)$_2$ (90 mg, 0.27 mmol) was stirred overnight at room temperature, giving a light yellow-solution. Addition of diethyl ether (30 mL) to the solution afforded fluffy needle-like crystallines, which was washed by three portions of diethyl ether (10 mL) and dried in vacuum. Yield: 188 mg (86 %). ^{1}H NMR (360 MHz, CDCl$_3$): δ (ppm) 7.54 (broad, 2×4 phenyl-H), 7.34 (broad, 2×6 phenyl-H), 7.21 (broad, 2×1 veratrole-H), 7.05 (broad, 2×1 veratrole-H), 6.85 (broad d, J = 8.2 Hz, 2×1 veratrole-H), 3.88 (s, -OCH$_3$), 3.76 (s, -OCH$_3$); ^{13}C{^{1}H} NMR (89.9 MHz, CDCl$_3$): δ (ppm) 221 (t, J$_{pc}$ = 12.9 Hz, Cr(CO)$_4$), 149.8 (s, veratrole), 148.3 (virtual t, J$_{pc}$ = 6.0 Hz, veratrole), 138.2 (virtual t, J$_{pc}$ = 13.9 Hz, phenyl), 137.8 (virtual t, J$_{pc}$ = 13.3 Hz, phenyl),

132.6 (virtual t, J_{pc} = 5.3 Hz, phenyl), 129.1 (s, phenyl), 128.0 (virtual t, J_{pc} = 4.6 Hz, veratrole), 126.4 (virtual t, J_{pc} = 4.6 Hz, veratrole), 116.6 (virtual t, J_{pc} = 8.0 Hz, veratrole), 110.5 (virtual t, J_{pc} = 5.3 Hz, veratrole), 55.8 (s, $-OCH_3$), 55.7 (s, $-OCH_3$); $^{31}P\{^1H\}$ NMR (36.3 MHz, $CDCl_3$) δ (ppm) 74.1 (s). IR (KBr) $v_{(OCH3)}$ 2962, 2843 cm^{-1}, $v_{(CO)}$ 1856 cm^{-1}, C-H bending 1512, 1460 cm^{-1}, $v_{(C-O-C)}$ 1263, 1238 cm^{-1}; Anal. calc'd for $CrP_2C_{44}H_{38}O_8$: C 65.35 %, H 4.74 %; found: C 65.18 %, H 4.69 %.

RuCl₂(4-PPh₂-Veratrole)₃: A mixture of $RuCl_3 \cdot 3H_2O$ (60 mg, 0.29 mmol) and 4-PPh₂-Veratrole (280 mg, 0.87 mmol) was heated to reflux under N_2 atmosphere for 5 hours, giving a clear dark-brown solution. The solution was cooled down to room temperature to give a dark-brown precipitate, which was filtered off and dried in vacuum. Yield: 280 mg (85%). ^1H NMR (360 MHz, $CDCl_3$): δ (ppm) 7.66 (m, 3×4 phenyl-H), 7.55 (m, 3×2 phenyl-H), 7.46 (m, 3×4 phenyl-H), 7.31 (broad d, J = 12.2 Hz, 3×1 veratrole-H), 7.04 (broad dd, J = 11.0 and 8.2 Hz, 3×1 veratrole-H), 6.90 (dd, J = 8.2 and 3.0 Hz, 3×1 veratrole-H), 3.92 (s, $-OCH_3$), 3.85 (s, $-OCH_3$); $^{13}C\{^1H\}$ NMR (89.9 MHz, $CDCl_3$): δ (ppm) 152.1 (s, veratrole), 149.2 (d, J_{pc} = 14.6 Hz, veratrole), 132.8 (d, J_{pc} = 104.2 Hz, phenyl), 132.1 (d, J_{pc} = 10.0 Hz, phenyl), 131.9 (d, J_{pc} = 2.7 Hz, phenyl), 128.5 (d, J_{pc} = 11.9 Hz, phenyl), 126.0 (d, J_{pc} = 11.3 Hz, veratrole), 123.7 (d, J_{pc} = 109.5 Hz, veratrole), 114.1 (d, J_{pc} = 11.3 Hz, veratrole), 110.7(d, J_{pc} = 15.3 Hz, veratrole), 56.2 (s, $-OCH_3$), 56.0 (s, $-OCH_3$); $^{31}P\{^1H\}$ NMR (36.3 MHz, $CDCl_3$) δ (ppm) 29.72 (s); IR (KBr) $v_{(OCH3)}$ 2954, 2834 cm^{-1}, C-H bending 1510, 1434 cm^{-1}, $v_{(C-O-C)}$ 1260, 1234 cm^{-1}; Anal. calc'd for $RuCl_2P_3C_{60}H_{57}O_6$: C 63.27 %, H 5.04 %; found: C 63.45 %, H 4.95 %.

189

RuCl₂(4-PH₂-Veratrole)₄: A mixture of 4-PH₂-Veratrole (2.29 g, 13.5 mmol), and RuCl₃•3H₂O (500 mg, 1.91 mmol) in 25 mL of ethanol was heated to reflux under a N₂ atmosphere. The reaction was complete when the color of the mixture changed from dark-brown to yellow in 4 hours. After cooling down to room temperature, it was evaporated to ca 10 ml and filtered to give a yellow solid, which was dried in vacuum. Yield: 1.24 g (76%). ^{1}H NMR (360 MHz, CDCl₃): δ (ppm) 7.19 (m, 4×1 veratrole-H), 7.08(broad t, J = 8.5 Hz, 4×1 veratrole-H), 6.74 (broad, J = 8.0 Hz, 4×1 veratrole-H), 5.94 - 4.95 (second-order pattern of 4×-PH₂, AA'A"A'''X₂X₂'X₂"X₂''' , ^{1}J ₚ-ₕ = 360 Hz, ^{3}J $_{trans\text{-PH}}$ = -3 Hz, ^{3}J $_{cis\text{-PH}}$ = 6 Hz), 3.89 (s, -OCH_3), 3.77 (s, -OCH_3); ^{13}C{^{1}H} NMR (89.9 MHz, d-DMF): δ (ppm) 150.6 (s), 149.0 (s), 126.6 (s), 116.5 (s), 115.9(s), 111.0 (s), 56.2 (s), 55.2 (s); ^{31}P{^{1}H} NMR (36.3 MHz, CDCl₃) δ (ppm) -26.08 (s); proton-coupled ^{31}P NMR (36.3 MHz, CDCl₃) δ (ppm) -26.08 (second order pattern, AA'A"A'''X₂X₂'X₂"X₂''', ^{1}J ₚ-ₕ = 360 Hz, ^{2}J $_{trans\text{-P-Ru-P}}$ = 400 Hz, ^{2}J $_{cis\text{-P-Ru-P}}$ = -30 Hz, ^{3}J $_{trans\text{-PH}}$ = -3 Hz, ^{3}J $_{cis\text{-PH}}$ = 6 Hz); IR (KBr) ν $_{(OCH3)}$ 2961, 2837 cm^{-1}, ν $_{(PH2)}$ 2289, 2280 cm^{-1}, C-H bending 1507, 1451 cm^{-1}, ν $_{(C\text{-}O\text{-}C)}$ 1257, 1232 cm^{-1}; Anal. calc'd for RuCl₂P₄C₃₂H₄₄O₈: C 45.08 %, H 5.20 %; found: C 45.02 %, H 5.08 %.

RuBr₂(4-PH₂-Catechol)₄: RuCl₂(4-PH₂-Veratrole)₄ (1.20 g, 1.41 mmol) was dissolved in 20 mL of CH₂Cl₂, giving a yellow solution which was cooled down to ca -78 °C by dry-ice. BBr₃ (3.0 ml, mmol) was added to the solution via syringe with constant stirring under N₂ flow. When the solution warmed to room temperature, it was evaporated in vacuum overnight to get rid of unreacted BBr₃ and solvent. Methanol (20 mL) was added dropwise to the residue, resulting in a light yellow solution which was evaporated to give

a yellow solid. Recrystallization of the yellow solid from acetone/water gave ca. 1.0 grams of pure product in yield of 86 %. ^{1}H NMR (360 MHz, d_6-acetone): δ (ppm) 8.28, 8.23 (8× cat-OH), 7.07 (m, 4×1 cat-H), 6.90 (m, 4×1 cat-H), 6.82 (m, 4×1 cat-H), 5.94 - 4.95 (second order pattern of 4×-PH$_2$, AA'A''A'''X$_2$X$_2$'X$_2$''X$_2$''' , ^{1}J $_{P-H}$ = 360 Hz, ^{3}J $_{trans-PH}$ = -3 Hz, ^{3}J $_{cis-PH}$ = 6 Hz); ^{13}C{^{1}H} NMR (89.9 MHz, d-acetone): δ (ppm) 147.9 (s), 145.8 (s), 126.0 (s), 120.4 (s), 116.3 (s), 115.7(s); ^{31}P{^{1}H} NMR (36.3 MHz, d-acetone) δ (ppm) -26.45 (s); proton-coupled ^{31}PNMR (36.3 MHz, CDCl$_3$) δ (ppm) -26.45 (second order pattern, AA'A''A'''X$_2$X$_2$'X$_2$''X$_2$''', ^{1}J $_{P-H}$ = 360 Hz, ^{2}J $_{trans-P-Ru-P}$ = 400 Hz, ^{2}J $_{cis-P-Ru-P}$ = -30 Hz, ^{3}J $_{trans-PH}$ = -3 Hz, ^{3}J $_{cis-PH}$ = 6 Hz); IR (KBr) v $_{(catechol\ O-H)}$ 3365, 3290 cm^{-1} (broad), v $_{(PH2)}$ 2340, 2320 cm^{-1}, C-H bending 1653, 1507, 1438 cm^{-1}, v $_{(C-O-C)}$ 1280 cm^{-1}; Anal. calc'd for RuBr$_2$P$_4$C$_{24}$H$_{20}$O$_8$: C 34.76 %, H 3.40 %; found: C 34.50 %, H 3.50 %.

Cs$_2$(4-PPh$_2$-Catecholato)$_3$Ti: A mixture of Ti(OMe)$_4$ (387 mg, 2.14 mmol), 4-PPh$_2$-Catechol•HBr (2417 mg, 6.44 mmol), and Cs$_2$CO$_3$ (1757 mg, 5.40 mmol) was stirred in 60 mL of degassed methanol under nitrogen atmosphere at room temperature for 42 hours, giving an orange-red suspension. The suspension was filtered through a frit under nitrogen to give an orange-red solid, which was then washed by degassed water for at least three times and dried in vacuum overnight. The product (ca. 2.0 grams) was obtained in yields of around 78 %. ^{1}H NMR (360 MHz, d_6-acetone): δ (ppm) 7.25 (m, 3×10 phenyl-H), 6.53 (ddd, J = 9.6, 7.9 and 1.8 Hz, 3×1 cat-H), 6.39 (dd, J = 8.1 and 1.8 Hz, 3×1 cat-H), 6.35 (dd, J = 7.8 and 1.5 Hz, 3×1 cat-H); ^{13}C{^{1}H} NMR (89.9 MHz, d_6-acetone): δ (ppm) 162.5 (s, catechol), 161.8 (d, J_{pc} = 11.0 Hz, catechol), 140.8 (d, J_{pc} = 12.5 Hz, phenyl), 133.9 (d, J_{pc} = 18.8 Hz, phenyl), 129.0 (d, J_{pc} = 6.3 Hz, phenyl), 128.7

(s, phenyl), 125.9 (d, J_{pc} = 23.8 Hz, catechol), 122.7 (d, J_{pc} = 3.8 Hz, catechol), 117.2 (d,

J_{pc} = 21.9 Hz, catechol), 112.3 (d, J_{pc} = 10.9 Hz, catechol); $^{31}P\{^1H\}$ NMR (36.3 MHz, d_6-

acetone) δ (ppm) -4.88 (s); IR (KBr) ν $_{(aromatic-H)}$ 3051, 3009, 1468 cm^{-1}, ν $_{(C-O-Ti)}$ 1248

cm^{-1}. Elemental analyses: calc'd for $Cs_2TiC_{54}H_{39}P_3O_6$: C 54.50 %, H 3.30 %; found: C

54.46 %, H 3.24 %.

Rb$_2$(4-PPh$_2$-Catecholato)$_3$Ti: A mixture of Ti(OMe)$_4$ (170 mg, 0.940 mmol), 4-PPh$_2$-

Catechol•HBr (1064 mg, 2.84 mmol), and Rb$_2$CO$_3$ (547 mg, 2.37 mmol) was stirred in

30 mL of degassed methanol under nitrogen atmosphere at room temperature for two

days, giving an orange-red cloudy solution. The solution was filtered through a frit with

celite and glasswool under nitrogen to give an orange-red filtrate which was then pumped

to dryness. The orange red residue was washed by degassed water at least three times,

and was dried in vacuum overnight. The orange red product (650 mg) was obtained in a

yield of 63%. ^1H NMR (360 MHz, d_6-acetone): δ (ppm) 7.28 (m, 3×10 phenyl-H), 6.53

(ddd, J = 9.4 7.8 and 1.8 Hz, 3×1 cat-H), 6.27 (dd, J = 8.7 and 1.7 Hz, 3×1 cat-H), 6.22

(d, J = 7.6 Hz, 3×1 cat-H); $^{13}C\{^1H\}$ NMR (89.9 MHz, d_6-acetone): δ (ppm) 162.8 (s,

catechol), 161.3 (d, J_{pc} = 10.8 Hz, catechol), 141.0 (d, J_{pc} = 12.6Hz, phenyl), 133.9 (d, J_{pc}

= 18.7 Hz, phenyl), 129.0 (d, J_{pc} = 6.3 Hz, phenyl), 128.6 (s, phenyl), 125.6 (d, J_{pc} = 24.5

Hz, catechol), 122.3 (d, J_{pc} = 4.5 Hz, catechol), 117.2 (d, J_{pc} = 21.4 Hz, catechol),

112.2(d, J_{pc} = 11.3 Hz, catechol); $^{31}P\{^1H\}$ NMR (36.3 MHz, d_6-acetone) δ (ppm) -4.78

(s); IR (KBr) ν $_{(aromatic-H)}$ 3051, 1468 cm^{-1}, ν $_{(C-O-Ti)}$ 1255 cm^{-1}. Elemental analyses: calc'd

for $Rb_2TiC_{54}H_{39}P_3O_6$: C 59.20 %, H 3.59 %; found: C 59.12 %, H 3.41 %.

192

K₂(4-PPh₂-Catecholato)₃Ti: A mixture of Ti(OMe)₄ (170 mg, 0.94 mmol), 4-PPh₂-Catechol•HBr (1064 mg, 2.84 mmol), and K_2CO_3 (391 mg, 2.37 mmol) was stirred in 30 mL of degassed methanol under nitrogen atmosphere at room temperature for two days, giving an orange-red cloudy solution. The solution was filtered through a frit with celite and glasswool under nitrogen to give an orange-red filtrate, which was evaporated to dryness. The dark-red residue was washed by degassed water for at least three times, and was dried in vacuum overnight. Yield: 878 mg (93%). ^1H NMR (360 MHz, d₄-methanol): δ (ppm) 7.23 (m, 3×10 phenyl-H), 6.55 (ddd, J = 9.4, 7.8 and 1.5 Hz, 3×1 cat-H), 6.39 (dd, J = 8.1 and 1.8 Hz, 3×1 cat-H), 6.36 (dd, J =8.0 and 1.3 Hz, 3×1 cat-H); $^{13}C\{^1H\}$ NMR (89.9 MHz, d₄-methanol): δ (ppm) 161.2 (s, catechol), 159.9 (d, J_{pc} = 10.0 Hz, catechol), 140.6 (d, J_{pc} = 10.6Hz, phenyl), 134.3 (d, J_{pc} = 19.2 Hz, phenyl), 129.1 (d, J_{pc} = 6.6 Hz, phenyl), 129.0 (s, phenyl), 127.1 (d, J_{pc} = 26.6 Hz, catechol), 124.6 (d, J_{pc} = 4.0 Hz, catechol), 118.1 (d, J_{pc} = 18.6 Hz, catechol), 112.9(d, J_{pc} = 11.2 Hz, catechol); $^{31}P\{^1H\}$ NMR (36.3 MHz, d₆-acetone) δ (ppm) -4.63 (s), IR (KBr) ν (aromatic C-H) 3050 cm⁻¹, C-H bending 1471 cm⁻¹, ν (C-O-Ti) 1253 cm⁻¹. Elemental analyses: calc'd for $K_2TiC_{54}H_{39}P_3O_6$: C 64.67 %, H 3.92 %; found: C 64.40 %, H 3.63 %.

Li₂(4-PPh₂-Catecholato)₃Ti: A mixture of Ti(OMe)₄ (210 mg, 1.16 mmol), 4-PPh₂-Catechol•HBr (1314 mg, 3.50 mmol), and Li_2CO_3 (217 mg, 2.94 mmol), was stirred in 40 mL of degassed methanol under nitrogen atmosphere at room temperature for 42 hours, giving a cloudy red solution. The solution was filtered through a frit with celite and glasswool under nitrogen to give a dark-red filtrate, which was evaporated to dryness in vacuum. The solid was washed by three portions of 20 mL of degassed water , and

then dried in vacuum overnight. The product was obtained in a yield of 78 %. ^{1}H NMR

(360 MHz, d_6-acetone): δ (ppm) 7.26 (m, 3×10 phenyl-H), 6.50 (ddd, J = 9.8, 7.9 and 1.8

Hz, 3×1 cat-H), 6.23 (dd, J = 7.6 and 1.5 Hz, 3×2 cat-H); ^{13}C{^{1}H} NMR (89.9 MHz, d_6-

acetone): δ (ppm) 166.0 (s, catechol), 164.6 (d, J_{pc} = 9.3 Hz, catechol), 144.9 (d, J_{pc} =

12.5 Hz, phenyl), 138.2 (d, J_{pc} = 14.7 Hz, phenyl), 133.3 (d, J_{pc} = 3.2 Hz, phenyl), 133.1

(s, phenyl), 130.5 (d, J_{pc} = 28.1 Hz, catechol), 127.7 (d, J_{pc} = 5.7 Hz, catechol), 121.7 (d,

J_{pc} = 17.84 Hz, catechol), 116.9 (d, J_{pc} = 11.9 Hz, catechol); ^{31}P{^{1}H} NMR (36.3 MHz,

d_6-acetone) δ (ppm) -4.24 (s); IR (KBr) ν $_{(aromatic\ C-H)}$ 3050, C-H bending 1473 cm^{-1}, ν $_{(C-}$

$_{O-Ti)}$ 1252 cm^{-1}; Anal. calc'd for Li$_2$TiC$_{54}$H$_{39}$P$_3$O$_6$: C 69.10 %, H 4.19 %; found: C 68.76

%, H 4.08 %.

(HDABCO)$_2$(4-PPh$_2$-Catecholato)$_3$Ti : A mixture of Ti(OMe)$_4$ (100 mg, 0.550 mmol),

4-PPh$_2$-Catechol•HBr (626 mg, 1.67 mmol), and DABCO (3.0 g, in excess of 10

equivalents) was stirred in 20 mL of degassed methanol under nitrogen atmosphere at

room temperature for three days, giving an orange-red suspension. It was concentrated to

half volume in vacuum, and filtered through a frit under nitrogen atmosphere to give an

orange-red residue. This solid was then washed by degassed water for at least three times,

and dried in vacuum overnight. An orange-red solid (460 mg) was obtained in a yield of

73 %. ^{1}H NMR (360 MHz, d_7-DMF): δ (ppm) 7.30 (m, 3×10 phenyl-H), 6.55 (ddd, J =

10.0, 7.7 and 1.8 Hz, 3×1 cat-H), 6.26 (dd, J = 7.7 and 1.6 Hz, 3×1 cat-H), 6.12 (dd, J =

7.3 and 1.7 Hz, 3×1 cat-H), 3.22 (s, 2×12 DABCO-H); ^{13}C{^{1}H} NMR (89.9 MHz, d_7-

DMF): δ (ppm) 162.2 (s, catechol), 160.6 (d, J_{pc} = 8.0 Hz, catechol), 140.2 (d, J_{pc} = 12.5

Hz, phenyl), 133.3 (d, J_{pc} = 18.7 Hz, phenyl), 128.6 (d, J_{pc} = 6.2 Hz, phenyl), 128.3 (s,

194

phenyl), 125.5 (d, J_{pc} = 31.6 Hz, catechol), 121.6 (d, J_{pc} = 4.7 Hz, catechol), 115.9 (d, J_{pc} = 14.1 Hz, catechol), 111.2 (d, J_{pc} = 13.2 Hz, catechol), 45.1 (s); ^{31}P{^{1}H} NMR (36.3 MHz, DMF/d$_6$-Benzene) δ (ppm) -5.35 (s); IR (KBr) ν (N-H) 3431 cm^{-1}, ν (aromatic C-H) 3051, 3010 cm^{-1}, $\nu_{(-CH2CH2-)}$ 2961, 2952, 2884 cm^{-1}, C-H bending 1469 cm^{-1}, ν (C-O-Ti) 1249 cm^{-1}. Elemental analyses: calc'd for TiN$_4$C$_{66}$H$_{65}$P$_3$O$_6$: C 68.87 %, H 5.69 %, N 4.87 %; found: C 68.74 %, H 5.90 %, N 4.68 %.

(HNEt₃)₂(4-PPh₂-Catecholato)₃Ti: A mixture of Ti(OMe)$_4$ (415 mg, 2.28 mmol), 4-PPh$_2$-Catechol•HBr (2600 mg, 6.93 mmol) and 2.0 mL of NEt$_3$ (14 mmol) was stirred in degassed methanol under a nitrogen atmosphere at room temperature for three days, giving a dark-red solution. The solution was filtered through a frit with celite and glasswool (pre-purged by nitrogen) under nitrogen to give a dark-red filtrate, which was then evaporated to give an orange-red powder. This solid was washed by degassed water for several times until the supernatant had no reaction with 0.1M AgNO$_3$, and dried in vacuum. Yield: 2.40 g (93%). ^{1}H NMR (360 MHz, d$_6$-acetone): δ (ppm) 7.26 (m, 3×10 phenyl-H), 6.59 (ddd, J = 9.6, 7.7 and 1.8 Hz, 3×1 cat-H), 6.23 (dd, J = 7.0 and 1.7 Hz, 3×1 cat-H), 6.04 (dd, J = 6.7 and 1.7 Hz, 3×1 cat-H), 3.22 (q, J = 7.2 Hz, 2× 6 methylene-H), 1.16 (t, J = 7.2 Hz, 2×9 methyl-H); ^{13}C{^{1}H} NMR (89.9 MHz, d$_6$-acetone): δ (ppm) 162.2 (s, catechol), 160.7 (d, J_{pc} = 6.0 Hz, catechol), 140.9 (d, J_{pc} = 12.6 Hz, phenyl), 134.0 (d, J_{pc} = 18.8 Hz, phenyl), 129.1 (d, J_{pc} = 6.2 Hz, phenyl), 128.8 (s, phenyl), 126.6 (d, J_{pc} = 33.4 Hz, catechol), 122.9 (d, J_{pc} = 4.0 Hz, catechol), 116.6 (d, J_{pc} = 12.0 Hz, catechol), 112.0 (d, J_{pc} = 13.5 Hz, catechol), 46.8(s, -*CH₂*CH₃), 9.1(s, -CH₂*CH₃*); ^{31}P{^{1}H} NMR (36.3 MHz, d$_6$-acetone) δ (ppm) -5.11(s); IR (KBr) ν (N-H) 3434 cm^{-1}, ν (aromatic C-H)

3049, 3001 cm^{-1}, $v_{(-CH2CH3)}$ 2997, 2980, 2944 cm^{-1}, C-H bending 1469 cm^{-1}, $v_{(C-O-Ti)}$ 1244 cm^{-1}. Elemental analyses: calc'd for TiN$_2$C$_{66}$H$_{71}$P$_3$O$_6$: C 70.21 %, H 6.34 %, N 2.48%; found: C 69.92%, H 6.50%, N 2.76%.

(TMA)$_2$(4-PPh$_2$-Catecholato)$_3$Ti: Dissolving tetramethylammonium (TMA$^+$) chloride (5.0 g, 46 mmol) in 10 mL of methanol/water (v/v 3/1) gave a saturated solution, to which a solution of Li$_2$(4-PPh$_2$-Catecholato)$_3$Ti (200 mg, 0.19 mmol) in 10 mL of degassed methanol was added. A yellow precipitate was produced immediately. The precipitate was filtered off, washed with three portions of deionized water (3×10 mL), and then dried in vacuum overnight. Yield: 134 mg (67%). ^{1}H NMR (360 MHz, CD$_3$CN): δ (ppm) 7.25 (m, 3×10 phenyl-H), 6.52 (ddd, J = 9.7, 7.7 and 1.8 Hz, 3×1 cat-H), 6.15 (dd, J = 7.7 and 1.6 Hz, 3×1 cat-H), 6.07 (dd, J = 7.5 and 1.6 Hz, 3×1 cat-H), 2.90 (s, 2×N(CH$_3$)$_4$); ^{13}C{^{1}H} NMR (89.9 MHz, CD$_3$CN): δ (ppm) 163.8 (s, catechol), 162.1 (d, J_{pc} = 8.4 Hz, catechol), 141.4 (d, J_{pc} = 12.0 Hz, phenyl), 134.2 (d, J_{pc} = 18.6 Hz, phenyl), 129.6 (d, J_{pc} = 6.3 Hz, phenyl), 129.3 (s, phenyl), 126.5 (d, J_{pc} = 31.8 Hz, catechol), 122.4 (d, J_{pc} = 4.4 Hz, catechol), 116.5 (d, J_{pc} = 14.7 Hz, catechol), 111.9 (d, J_{pc} = 13.2 Hz, catechol), 56.4 (s, N(CH$_3$)$_4$); ^{31}P{^{1}H} NMR (36.3 MHz, CD$_3$CN) δ (ppm) -4.71(s); IR (KBr) $v_{(aromatic C-H)}$ 3025 cm^{-1}, $v_{(-CH3)}$ 2997, 2946 cm^{-1}, C-H bending 1465 cm^{-1}, $v_{(C-O-Ti)}$ 1247 cm^{-1}; Elemental analyses: calc'd for TiN$_2$C$_{62}$H$_{63}$P$_3$O$_6$: C 69.40 %, H 5.92 %, N 2.61 %; found: C 69.12 %, H 5.67 %, N 2.66%.

(PPN)$_2$(4-PPh$_2$-Catecholato)$_3$Ti: A mixture of 100mg of Li$_2$(4-PPh$_2$-Catecholato)$_3$Ti (0.10 mmol) and 750 mg *bis*(triphenylphosphoranylidene) ammonium (PPN$^+$) chloride

196

(1.39 mmol) was stirred in 20 mL of degassed CH_3CN under a N_2 atmosphere for an hour, giving a clear orange-red solution. Then deionized water (20 mL) was added to precipitate the product out of this solution. The yellow product was filtered off, washed with three portions of deionized water (3×10 mL), and then dried in vacuum overnight. Yield: 127 mg (68 %). ^1H NMR (360 MHz, d_6-acetone): δ (ppm) 7.72-7.48 (m, PPN^+), 7.28-7.12 (m, 3×10 phenyl-H), 6.37 (ddd, J = 11.3, 7.6 and 1.9 Hz, 3×1 cat-H), 6.07 (dd, J = 7.6 and 1.8 Hz, 3×1 cat-H), 5.95 (dd, J = 7.6 and 1.8 Hz, 3×1 cat-H); $^{13}C\{^1H\}$ NMR (89.9 MHz, CD_3CN): δ (ppm) 163.9 (s, catechol), 162.2 (d, J_{pc} = 8.8 Hz, catechol), 141.3 (d, J_{pc} = 12.0 Hz, phenyl), 134.7 (s, PPN^+), 133.9 (d, J_{pc} = 18.6 Hz, phenyl), 133.2 (m, PPN^+), 130.4 (m, PPN^+), 129.2 (d, J_{pc} = 6.3 Hz, phenyl), 128.8 (s, phenyl), 128.2(d, J_{pc} = 107.8 Hz, PPN^+), 125.9 (d, J_{pc} = 31.2 Hz, catechol), 121.2 (d, J_{pc} = 3.5 Hz, catechol), 116.1 (d, J_{pc} = 15.3 Hz, catechol), 111.4 (d, J_{pc} = 13.4 Hz, catechol); $^{31}P\{^1H\}$ NMR (36.3 MHz, CD_3CN) δ (ppm) 20.93 (s, PPN^+), -4.34(s, complex); IR (KBr) ν (aromatic C-H) 3050, 2925 cm^{-1}, C-H bending 1467 cm^{-1}, ν (C-O-Ti) 1259 cm^{-1}; Elemental analyses: calc'd for $TiN_4C_{126}H_{99}P_7O_6$: C 75.60 %, H 4.99 %, N 1.40 %; found: C 75.38 %, H 4.71 %, N 1.39%.

$(Ph_4P)_2(4$-PPh_2-Catecholato$)_3$Ti: A mixture of 200mg of $Li_2(4$-PPh_2-Catecholato$)_3$Ti (0.19 mmol) and 1000 mg tetraphenylphosphonium (Ph_4P^+) chloride (2.95 mmol) was stirred in 20 ml of degassed methanol under N_2 atmosphere for an hour, giving a clear orange-red solution. Then deionized water (20 mL) was added to precipitate the product out of this solution. The yellow product was filtered off, washed with three portions of deionized water (3×10 mL), and then dried in vacuum overnight. Yield: 232 mg (77 %).

197

^{1}H NMR (360 MHz, CD$_3$OD): δ (ppm) 7.86-7.55 (m, PPh$_4$$^+$), 7.22 (m, 3×10 phenyl-H), 6.39 (ddd, J = 10.5, 7.7 and 1.8 Hz, 3×1 cat-H), 6.03 (dd, J = 7.7 and 1.6 Hz, 3×1 cat-H), 6.00 (dd, J = 7.5 and 1.8 Hz, 3×1 cat-H); ^{13}C{^{1}H} NMR (89.9 MHz, CD$_3$CN): δ (ppm) 163.8 (s, catechol), 162.1 (d, J$_{pc}$ = 8.3 Hz, catechol), 141.3 (d, J$_{pc}$ = 12.1 Hz, phenyl), 136.4 (d, J$_{pc}$ = 3.1 Hz, PPh$_4$$^+$), 135.7 (d, J$_{pc}$ = 10.3 Hz, PPh$_4$$^+$) 133.9 (d, J$_{pc}$ = 18.6 Hz, phenyl), 131.4 (d, J$_{pc}$ = 13.Hz, PPh$_4$$^+$), 129.2 (d, J$_{pc}$ = 9.0 Hz, phenyl), 128.8 (s, phenyl), 125.9 (d, J$_{pc}$ = 31.1 Hz, catechol), 121.3 (d, J$_{pc}$ = 3.8 Hz, catechol), 119.5 (d, J$_{pc}$ = 89.6 Hz, PPh$_4$$^+$), 116.2 (d, J$_{pc}$ = 15.3 Hz, catechol), 111.5 (d, J$_{pc}$ = 13.0 Hz, catechol); ^{31}P{^{1}H} NMR (36.3 MHz, CD$_3$CN) δ (ppm) 22.92 (s, PPh$_4$$^+$), -4.38 (s, complex); Elemental analyses: calc'd for TiC$_{102}$H$_{79}$P$_5$O$_6$: C 76.35 %, H 4.97 %; found: C 76.13 %, H 4.68 %.

Cs$_2$(4-PPh$_2$-Catecholato)$_3$Sn: An amount of 295 mg of SnCl$_4$ (1.13 mmol) was weighed to a flask, 40 mL of degassed methanol was added to make a colorless solution. (CAUTION! The first few drops of methanol must be added slowly to avoid SnCl$_4$ boiling over due to the rigorous methanolysis of SnCl$_4$) Then 1275 mg of 4-PPh$_2$-Catechol•HBr (3.40 mmol) and 1660 mg of Cs$_2$CO$_3$ (5.10 mmol) were added to the solution. The mixture was stirred under a nitrogen atmosphere at room temperature for three days, giving a white suspension. This was concentrated to half volume in vacuum, and filtered off through a frit under nitrogen atmosphere to give a white solid. The solid was then washed by degassed water for at least three times, and dried in vacuum overnight. A pure white solid (898 mg) was obtained in a yield of 62 % from recrystallization of the white solid from acetone/ether. ^{1}H NMR (360 MHz, d$_6$-acetone): δ (ppm) 7.27 (m, 3×10 phenyl-H), 6.63 (dd, J = 8.7 and 1.5 Hz, 3×1 cat-H), 6.56 (dd, J =

7.7 and 1.6 Hz, 3×1 cat-H), 6.40 (dd, J = 9.4, 7.8 and 1.9 Hz, 3×1 cat-H); $^{13}C\{^1H\}$ NMR

(89.9 MHz, d_6-acetone): δ (ppm) 154.9 (s, catechol), 153.5 (d, J_{pc} = 10.6 Hz, catechol),

141.0 (d, J_{pc} = 12.5 Hz, phenyl), 134.0 (d, J_{pc} = 18.7 Hz, phenyl), 129.0 (d, J_{pc} = 6.1 Hz,

phenyl), 128.7 (s, phenyl), 124.7 (d, J_{pc} = 24.3 Hz, catechol), 121.5 (d, J_{pc} = 4.0 Hz,

catechol), 119.5 (d, J_{pc} = 21.6 Hz, catechol), 114.4 (d, J_{pc} = 10.9 Hz, catechol); $^{31}P\{^1H\}$

NMR (36.3 MHz, d_6-acetone) δ (ppm) -4.04 (s); IR (KBr) ν $_{(aromatic\ C-H)}$ 3051, 3002 cm^{-1},

C-H bending 1473 cm^{-1}, ν $_{(C-O-Ti)}$ 1246 cm^{-1}; Elemental analyses: calc'd for

$Cs_2SnC_{54}H_{39}P_3O_6$: C 51.42 %, H 3.12 %; found: C 51.32 %, H 3.16 %.

Rb₂(4-PPh₂-Catecholato)₃Sn: An amount of 176 mg of $SnCl_4$ (0.680 mmol) was

weighed to a flask, 5 mL of degassed methanol was added to make a colorless solution.

Then 4-PPh₂-Catechol•HBr (761 mg, 2.03 mmol) and Rb_2CO_3 (702 mg, 3.04 mmol)

were added to the solution. The mixture was stirred under a nitrogen atmosphere at room

temperature for three days, giving a white suspension. It was concentrated to half volume

in vacuum, and filtered through a frit under nitrogen atmosphere to give a white solid.

The solid was then washed by degassed water for at least three times, and dried in

vacuum overnight. A pure white solid (726 mg) was obtained in a yield of 89 % from

recrystallization of the white solid from acetone/ether. ^1H NMR (360 MHz, d_6-acetone):

δ (ppm) 7.26 (m, 3×4 phenyl-H), 7.24 (m, 3×6 phenyl-H), 6.58 (dd, J = 4.3 and 2.0 Hz,

3×1 cat-H), 6.49 (dd, J = 7.6 and 1.5 Hz, 3×1 cat-H), 6.38 (ddd, J = 9.6, 7.8 and 2.0 Hz,

3×1 cat-H); $^{13}C\{^1H\}$ NMR (89.9 MHz, d_6-acetone): δ (ppm) 154.6 (s, catechol), 153.2 (d,

J_{pc} = 11.3 Hz, catechol), 140.6 (d, J_{pc} = 12.6 Hz, phenyl), 133.4 (d, J_{pc} = 19.2 Hz, phenyl),

128.4 (d, J_{pc} = 6.0 Hz, phenyl), 128.1 (s, phenyl), 124.0 (d, J_{pc} = 25.2 Hz, catechol), 120.5

(d, J_{pc} = 4.0 Hz, catechol), 118.9 (d, J_{pc} = 21.2 Hz, catechol), 113.8 (d, J_{pc} = 11.3 Hz, catechol); $^{31}P\{^1H\}$ NMR (36.3 MHz, d_6-acetone) δ (ppm) −4.64 (s); IR (KBr) ν (aromatic C-H) 3051 cm^{-1}, C-H bending 1476 cm^{-1}, ν (C-O-Sn) 1247 cm^{-1}; Anal. calc'd for $Rb_2SnC_{54}H_{39}P_3O_6$: C 55.60 %, H 3.37 %; found: C 55.43 %, H 3.53 %.

$Li_2(4$-PPh_2-Catecholato)$_3$Sn: An amount of 275 mg of $SnCl_4$ (1.06 mmol) was weighed to a flask, 10 mL of degassed methanol was added to make a colorless solution (CAUTION! The first few drops of methanol must be added slowly to avoid $SnCl_4$ boiling over due to the rigorous methanolysis of $SnCl_4$). Then 4-PPh_2-Catechol•HBr (1189 mg, 3.18 mmol) and Li_2CO_3 (352 mg, 4.77 mmol) were added to the solution. The mixture was stirred under a nitrogen atmosphere at room temperature for four days, giving a slightly cloudy solution. The solution was filtered through a frit with celite and glasswool (pre-purged by nitrogen) under nitrogen to give a clear colorless filtrate, which was evaporated to give a white solid. The solid was then washed by degassed water for at least three times, and dried in vacuum for a few hours. Recrystallization of the white solid from acetone afforded a pure white product. Yield: 836 mg (78%). ^1H NMR (360 MHz, d_6-acetone): δ (ppm) 7.27 (m, 3×10 phenyl-H), 6.58 (broad d, J = 7.9 Hz, 3×1 cat-H), 6.54 (broad d, J = 6.4 Hz, 3×1 cat-H), 6.46 (broad t, J = 8.6 Hz, 3×1 cat-H); $^{13}C\{^1H\}$ NMR (89.9 MHz, d_6-acetone): δ (ppm) 154.2 (s, catechol), 152.7 (d, J_{pc} = 10.0 Hz, catechol), 140.8 (d, J_{pc} = 11.9 Hz, phenyl), 133.9 (d, J_{pc} = 19.2 Hz, phenyl), 129.0 (d, J_{pc} = 6.6 Hz, phenyl), 128.8 (s, phenyl), 125.1 (d, J_{pc} = 27.9 Hz, catechol), 122.1 (d, J_{pc} = 4.6 Hz, catechol), 119.7 (d, J_{pc} = 18.6 Hz, catechol), 114.7 (d, J_{pc} = 12.0 Hz, catechol); $^{31}P\{^1H\}$ NMR (36.3 MHz, d_6-acetone) δ (ppm) −4.76 (s); IR (KBr) ν (aromatic C-H) 3051,

200

3002 cm^{-1}, C-H bending 1467 cm^{-1}, ν $_{(C-O-Sn)}$ 1253 cm^{-1};   Anal. calc'd   for

Li$_2$SnC$_{54}$H$_{39}$P$_3$O$_6$: C 55.36 %, H 4.90 %; found: C 55.56 %, H 5.12 %.

(HDABCO)$_2$(4-PPh$_2$-Catecholato)$_3$Sn: An amount of 177 mg of SnCl$_4$ (0.680 mmol) was weighed to a flask, 30 mL of degassed methanol was added to make a colorless solution. (CAUTION! The first few drops of methanol must be added slowly to avoid SnCl$_4$ boiling over due to the rigorous methanolysis of SnCl$_4$)   Then 4-PPh$_2$-Catechol•HBr (764 mg, 2.04 mmol) and DABCO (3.5 g, in excess of 10 equivalents) were added to the solution.   The white cloudy mixture was stirred under nitrogen atmosphere at room temperature for three days, giving a white suspension. It was concentrated to half volume in vacuum, and filtered through a frit under a nitrogen atmosphere to give 680 mg of a white solid in a yield of 82 % (after washing by degassed water at least three times, and dried in vacuum overnight). ^{1}H NMR (360 MHz, d$_7$-DMF): ^{1}H NMR (360 MHz, d-DMF): δ (ppm) 7.34 (m, 3×10 phenyl-H), 6.50 (broad m, 3×3 cat-H), 3.24 (s, 2×12 DABCO-H); ^{13}C{^{1}H} NMR (89.9 MHz, d$_7$-DMF): δ (ppm) 154.8 (s, catechol), 153.1 (d, J$_{pc}$ = 8.0 Hz, catechol), 140.4 (d, J$_{pc}$ = 11.9 Hz, phenyl), 133.3 (d, J$_{pc}$ = 18.6 Hz, phenyl), 128.6 (d, J$_{pc}$ = 6.0 Hz, phenyl), 128.3 (s, phenyl), 124.3 (d, J$_{pc}$ = 31.2 Hz, catechol), 120.3 (d, J$_{pc}$ = 4.6 Hz, catechol), 118.1 (d, J$_{pc}$ = 13.3 Hz, catechol), 113.4 (d, J$_{pc}$ = 12.6 Hz, catechol), 45.0 (s, DABCO); ^{31}P{^{1}H} NMR (36.3 MHz, DMF/d$_6$-Benzene) δ (ppm) -5.32(s); IR (KBr) ν $_{(N-H)}$ 3434 cm^{-1}; ν $_{(aromatic\ C-H)}$ 3047 cm^{-1}, ν $_{(-CH2CH2-)}$ 2999, 2962 cm^{-1}, C-H bending 1473 cm^{-1}, ν $_{(C-O-Ti)}$ 1246 cm^{-1}; Elemental analyses: calc'd for SnN$_4$C$_{66}$H$_{65}$P$_3$O$_6$: C 64.88 %, H 5.36 %, N 4.59 %; found: C 64.96 %, H 5.29 %, N 4.50 %.

201

(HNEt₃)₂(4-PPh₂-Catecholato)₃Sn: A mixture of SnCl₄ (488 mg, 1.87 mmol), 4-PPh₂-Catechol•HBr (2107 mg, 5.62 mmol) and 2.4 mL of NEt₃ (17 mmol) was stirred in degassed methanol under nitrogen atmosphere at room temperature for three days, giving a colorless solution. The solution was filtered through a frit with celite and glasswool (pre-purged by nitrogen) under nitrogen to give a colorless filtrate, which was then evaporated to give a white powder. The solid was washed by degassed water for several times until the supernatant had no reaction with 0.1M AgNO₃ and dried in vacuum overnight. Yield: 1.95 g (86%). ^{1}H NMR (360 MHz, d₆-acetone): δ (ppm) 7.27 (m, 3×10 phenyl-H), 6.57 (broad, 3×2 cat-H), 6.40 (broad d, J = 6.9 Hz, 3×1 cat-H), 3.11 (q, J = 7.2 Hz, 2× 6 methylene-H), 1.10 (t, J = 7.2 Hz, 2×9 methyl-H); ^{13}C{^{1}H} NMR (89.9 MHz, d₆-acetone): δ (ppm) 154.1 (s, catechol), 152.3 (d, J_{pc} = 6.7 Hz, catechol), 140.3 (d, J_{pc} = 12.6 Hz, phenyl), 133.4 (d, J_{pc} = 18.6 Hz, phenyl), 128.5 (d, J_{pc} = 6.0 Hz, phenyl), 128.3(s, phenyl), 125.0 (d, J_{pc} = 33.8 Hz, catechol), 121.3 (d, J_{pc} = 4.0 Hz, catechol), 118.4 (d, J_{pc} = 11.3 Hz, catechol), 113.8 (d, J_{pc} = 13.3 Hz, catechol), 46.2 (s, -CH_2CH₃), 8.6 (s, -CH₂CH_3) ; ^{31}P{^{1}H} NMR (36.3 MHz, d₆-acetone) δ (ppm) -4.88 (s); IR (KBr) ν ₍N-H₎ 3438 cm⁻¹; ν ₍aromatic C-H₎ 3048 cm⁻¹, ν ₍-CH2CH3₎ 2999, 2981 cm⁻¹, C-H bending 1474 cm⁻¹, ν ₍C-O-Ti₎ 1246 cm⁻¹; Elemental analyses: calc'd for SnN₂C₆₆H₇₁P₃O₆: C 66.07 %, H 5.96 %, N 2.34 %; found: C 65.82%, H 6.14 %, N 2.57%.

(TMA)₂(4-PPh₂-Catecholato)₃Sn: An amount of 150 mg of SnCl₄ (0.580 mmol) was weighed to a flask, 30 mL of degassed methanol was added to give a colorless solution. Then 4-PPh₂-Catechol•HBr (641 mg, 1.73 mmol) and tetramethylammonium chloride

202

(939 mg, 5.18 mmol) were added to the solution, resulting in lots of white precipitate which disappeared after a few minutes. The colorless solution was stirred under nitrogen atmosphere at room temperature for two days, and then evaporated to dryness. The solid was redissolved in 20 mL of degassed acetone, giving a slightly cloudy mixture which was filtered through a frit with celite and glasswool (Pre-purged by N_2). The filtrate was then evaporated to yield a light yellow solid. Yield: 512 mg (77%). ^1H NMR (360 MHz, d_6-acetone): δ (ppm) 7.25 (m, 3×10 phenyl-H), 6.45 (broad m, 3×3 cat-H), 3.05 (s, 2×N(CH$_3$)$_4$); $^{13}C\{^1H\}$ NMR (89.9 MHz, CD$_3$CN): δ (ppm) 155.6 (s, catechol), 154.0 (d, J_{pc} = 8.0 Hz, catechol), 140.7 (d, J_{pc} = 11.9 Hz, phenyl), 133.7 (d, J_{pc} = 19.2 Hz, phenyl), 128.5 (d, J_{pc} = 6.0 Hz, phenyl), 128.2 (s, phenyl), 124.3 (d, J_{pc} = 31.2 Hz, catechol), 120.1 (d, J_{pc} = 4.0 Hz, catechol), 118.0 (d, J_{pc} = 13.9 Hz, catechol), 113.3 (d, J_{pc} = 15.2 Hz, catechol), 55.3 (s, N(CH_3)$_4$); $^{31}P\{^1H\}$ NMR (36.3 MHz, CD$_3$CN) δ (ppm) -4.93 (s). Elemental analyses: calc'd for SnN$_2$C$_{62}$H$_{63}$P$_3$O$_6$: C 65.11 %, H 5.55 %, N 2.45 %; found: C 65.23 %, H 5.78 %, N 2.48 %.

(PPN)$_2$(4-PPh$_2$-Catecholato)$_3$Sn: An amount of 460 mg of Cs$_2$Sn(4-PPh$_2$-Catecholato)$_3$ (0.36 mmol) was dissolved in 10 mL of CH$_2$Cl$_2$, giving a clear colorless solution. This solution was added to the solution of *bis*(triphenylphosphoranylidene) ammonium (PPN$^+$) chloride (400 mg, 0.70 mmol in 10 mL of CH$_2$Cl$_2$) with constant stirring under N$_2$ atmosphere. The resulted mixture was stirred for four hours, and then filtered through a frit with celite and glasswool (Pre-purged by N$_2$). The filtrate was then evaporated to yield a white solid. Yield: 730 mg (97%). ^1H NMR (360 MHz, CD$_2$Cl$_2$): δ (ppm) 7.64-7.38 (m, PPN$^+$), 7.26 (m, 3×4 phenyl-H), 7.16 (m, 3×6 phenyl-H) 6.60 (dd, J = 7.9 and

203

1.9 Hz, 3×1 cat-H), 6.52 (dd, J = 7.7 and 1.9 Hz, 3×1 cat-H), 6.41 (ddd, J = 10.2, 7.7 and 1.9 Hz, 3×1 cat-H); ^{13}C{^{1}H} NMR (89.9 MHz, CD_2Cl_2): δ (ppm) 155.6 (s, catechol), 153.9 (d, J_{pc} = 9.3 Hz, catechol), 141.1 (d, J_{pc} = 12.0 Hz, phenyl), 134.2 (s, PPN$^+$), 133.6 (d, J_{pc} = 18.6 Hz, phenyl), 132.5 (m, PPN$^+$), 129.9 (m, PPN$^+$), 128.3 (d, J_{pc} = 6.0 Hz, phenyl), 127.6 (s, phenyl), 127.3 (d, J_{pc} = 108.1 Hz, PPN$^+$), 123.9 (d, J_{pc} = 29.8 Hz, catechol), 118.9 (broad s, catechol), 118.7 (d, J_{pc} = 15.3 Hz, catechol), 113.5 (d, J_{pc} = 13.2 Hz, catechol); ^{31}P{^{1}H} NMR (36.3 MHz, CD_3CN) δ (ppm) 20.29 (s, PPN$^+$), -4.66(s, complex). Elemental analyses: calc'd for $SnN_4C_{126}H_{99}P_7O_6$: C 73.02 %, H 4.81 %, N 1.35 %; found: C 72.80 %, H 4.76 %, N 1.33 %.

Cs₃(4-PPh₂-Catecholato)₃Ga: A mixture of $Ga(NO_3)_3 \cdot 6H_2O$ (264 mg, 0.731 mmol), 4-PPh₂-Catechol•HBr (815 mg, 2.17 mmol), and Cs_2CO_3 (1063 mg, 3.26 mmol) was stirred in 30 mL of degassed methanol under nitrogen atmosphere at room temperature for three days, giving a slightly cloudy solution. The solution was filtered through a frit with celite and glasswool (pre-purged by nitrogen) under nitrogen to give a colorless clear filtrate, which was then evaporated in vacuum to give a white powder. The white solid was washed by degassed water for at least three times, and dried overnight in vacuum. Yield: 842 mg (86 %). ^{1}H NMR (360 MHz, d4-methanol): δ (ppm) 7.24 (m, 3×10 phenyl-H), 6.51 (m, 3×3 cat-H); ^{1}H NMR (360 MHz, d-DMF): δ (ppm) 7.29 (m, 3×10 phenyl-H), 6.46 (broad d, J = 8.5 Hz, 3×1 cat-H), 6.38 (broad d, J = 6.7 Hz, 3×1 cat-H), 6.27 (broad t, J = 8.5 Hz, 3×1 cat-H); ^{13}C{^{1}H} NMR (89.9 MHz, d₄-methanol): δ (ppm) 158.0 (s, catechol), 156.5 (d, J_{pc} = 10.0 Hz, catechol), 141.5 (d, J_{pc} = 10.0 Hz, phenyl), 134.3 (d, J_{pc} = 18.5 Hz, phenyl), 129.2 (d, J_{pc} = 6.3 Hz, phenyl), 129.0 (s, phenyl), 125.2 (d, J_{pc} = 27.4

204

Hz, catechol), 120.6 (s, catechol), 119.0 (d, J_{pc} = 18.4 Hz, catechol), 113.9 (d, J_{pc} = 12.4

Hz, catechol); $^{31}P\{^1H\}$ NMR (36.3 MHz, d_4-methanol) δ (ppm) -6.02 (s). Elemental

analyses: calc'd for $Cs_3GaC_{54}H_{39}P_3O_6$: C 48.21 %, H 2.92 %; found: C 48.25 %, H 3.02

%.

$Rb_3(4\text{-}PPh_2\text{-}Catecholato)_3Ga$: A mixture of $Ga(NO_3)_3 \bullet 6H_2O$ (197 mg, 0.540 mmol), 4-

PPh_2-Catechol$\bullet$HBr (610 mg, 1.62 mmol), and Rb_2CO_3 (563 mg, 2.43 mmol) was stirred

in 30 mL of degassed methanol under nitrogen atmosphere at room temperature for four

days, giving a slightly cloudy solution. The solution was filtered through a frit with celite

and glasswool (pre-purged by nitrogen) under nitrogen to give a clear colorless filtrate,

which was evaporated to give a white solid. The solid was washed with three portions of

degassed water (3×10 mL), and dried in vacuum for a few hours. Recrystallization of the

solid from acetone afforded a white solid, which was then dried in vacuum overnight.

Yield: 460 mg (71 %) . ^1H NMR (360 MHz, d_4-methanol): δ (ppm) 7.22 (m, 3×10

phenyl-H), 6.57 (broad d, J = 8.1Hz, 3×1 cat-H), 6.49 (broad d, J = 5.3 Hz, 3×1 cat-H),

6.41 (broad t, J = 8.8 Hz, 3×1 cat-H); $^{13}C\{^1H\}$ NMR (89.9 MHz, d_4-methanol): δ (ppm)

157.8 (s, catechol), 156.2 (d, J_{pc} = 10.0 Hz, catechol), 141.4 (d, J_{pc} = 9.9 Hz, phenyl),

134.2 (d, J_{pc} = 18.6 Hz, phenyl), 129.0 (d, J_{pc} = 8.0 Hz, phenyl), 128.7 (s, phenyl), 125.0

(d, J_{pc} = 27.9 Hz, catechol), 120.2 (s, catechol), 119.0 (d, J_{pc} = 17.2 Hz, catechol), 113.7

(d, J_{pc} = 12.6 Hz, catechol); $^{31}P\{^1H\}$ NMR (36.3 MHz, d_4-methanol) δ (ppm) -4.87 (s).

Elemental analyses: calc'd for $Rb_3GaC_{54}H_{39}P_3O_6$: C 53.92 %, H 3.27 %; found: C 54.20

%, H 3.18 %.

205

Li$_3$(4-PPh$_2$-Catecholato)$_3$Ga: A mixture of Ga(NO$_3$)$_3$•6H$_2$O (239 mg, 0.667 mmol), 4-PPh$_2$-Catechol•HBr (750 mg, 2.00 mmol), and Li$_2$CO$_3$ (222 mg, 3.00 mmol) was stirred in 30 mL of degassed methanol under a nitrogen atmosphere at room temperature for four days, giving a slightly cloudy solution. The solution was filtered through a frit with celite and glasswool (pre-purged by nitrogen) under nitrogen to give a clear light yellow filtrate, which was then pumped to give a light-yellow solid. The solid was washed with three portions of degassed water (3×10 mL), and dried in vacuum for a few hours. Recrystallization of the light yellow solid from acetone and diethyl ether afforded a white solid, which was then dried in vacuum overnight. Yield: 410 mg (64 %). ^{1}H NMR (360 MHz, d$_4$-methanol): δ (ppm) 7.18 (m, 3×10 phenyl-H), 6.59 (dd, J = 8.2 and 1.8 Hz, 3×1 cat-H), 6.52 (dd, J = 7.7 and 1.9 Hz, 3×1 cat-H), 6.44 (ddd, J = 9.8, 7.8 and 1.8 Hz, 3×1 cat-H); ^{13}C{^{1}H} NMR (89.9 MHz, d$_4$-methanol): δ (ppm) 157.2 (s, catechol), 155.5 (d, J$_{pc}$ = 9.4 Hz, catechol), 141.5 (d, J$_{pc}$ = 9.4 Hz, phenyl), 134.3 (d, J$_{pc}$ = 18.2 Hz, phenyl), 129.0 (d, J$_{pc}$ = 5.9 Hz, phenyl), 128.8 (s, phenyl), 125.2 (d, J$_{pc}$ = 28.9 Hz, catechol), 120.3 (s, catechol), 119.4 (d, J$_{pc}$ = 16.4 Hz, catechol), 114.2 (d, J$_{pc}$ = 12.9 Hz, catechol); ^{31}P{^{1}H} NMR (36.3 MHz, d$_4$-methanol) δ (ppm) -4.54 (s). Elemental analyses: calc'd for Li$_3$GaC$_{54}$H$_{39}$P$_3$O$_6$•4H$_2$O: C 62.40 %, H 4.56 %; found: C 62.48 %, H 4.64 %.

Cs$_2$[4-P(O)Ph$_2$-Catecholato]$_3$Sn: A volume of 2.5 mL of 30% H$_2$O$_2$ was added to a solution of Cs$_2$(4-PPh$_2$-Catecholato)$_3$Sn (290 mg, 0.230 mmol) in 20 mL of acetone with constant stirring. The orange-red solution was heated to reflux overnight. After cooling down to room temperature, it was evaporated in vacuum to give a sandy yellow powder. Yield: 290 mg (99 %). ^{1}H NMR (360 MHz, d$_6$-acetone): δ (ppm) 7.64 (m, 3×4 phenyl-

206

H), 7.45 (m, 3×6 phenyl-H), 6.80 (broad d, J = 11.9 Hz, 3×1 cat-H), 6.55 (broad d, J = 7.3

Hz, 3×2 cat-H); $^{13}C\{^1H\}$ NMR (89.9 MHz, d_6-acetone): δ (ppm) 157.0 (s, catechol),

152.9 (d, J_{pc} = 20.8 Hz, catechol), 135.3 (d, J_{pc} = 100.8 Hz, phenyl), 132.2 (d, J_{pc} = 10.0

Hz, phenyl), 131.5 (s, phenyl), 128.5 (d, J_{pc} = 11.3 Hz, phenyl), 122.2 (d, J_{pc} = 10.0 Hz,

catechol), 117.3 (d, J_{pc} = 113.4 Hz, catechol), 115.8 (d, J_{pc} = 11.3 Hz, catechol), 113.4(d,

J_{pc} = 15.9 Hz, catechol); $^{31}P\{^1H\}$ NMR (36.3 MHz, d_6-acetone) δ (ppm) 30.76 (s). IR

(KBr) C-H bending 1480 cm^{-1}, ν $_{(C-O-C)}$ 1232 cm^{-1}, ν $_{(P=O)}$ 1153 cm^{-1}; Anal. calc'd for

$Cs_2SnC_{54}H_{39}P_3O_7$: C 50.78 %, H 3.08 %; found: C 50.49 %, H 2.84 %.

{[4-P(CH₃)Ph₂-Catecholato]₃Ti }I: A volume of 2.0 mL of CH_3I (32.1 mmol) was

added to a solution of Cs_2(4-PPh₂-Catelato)₃Ti (200 mg, 0.168 mmol) in 20 mL of

CH_3CN via syringe with constant stirring under N_2 flow at room temperature. The

reaction was complete in 20 hours, as monitored by $^{31}P\{^1H\}$ NMR spectroscopy. The

solution was evaporated to give a yellow solid which was then washed by three portions

of water (10 mL), and dried in vacuum overnight. Yield: 131 mg (71%). ^1H NMR (360

MHz, CD_3CN): δ (ppm) 7.76 (m, 3×2 phenyl-H), 7.62 (m, 3×4 phenyl-H), 7.57 (m, 3×4

phenyl-H), 6.60 (ddd, J = 14.1, 8.1 and 2.1 Hz, 3×1 cat-H), 6.39 (dd, J = 9.2 and 4.1 Hz,

3×1 cat-H), 6.38 (dd, J = 15.3 and 1.8 Hz, 3×1 cat-H), 2.58 (d, J = 13.7 Hz, 3×1 P-CH_3);

$^{13}C\{^1H\}$ NMR (89.9 MHz, CD_3CN): δ (ppm) 167.2 (d, J_{pc} = 2.7 Hz, catechol), 161.4 (d,

J_{pc} = 18.5 Hz, catechol), 135.6 (d, J_{pc} = 2.8 Hz, phenyl), 134.2 (d, J_{pc} = 10.5 Hz, phenyl),

131.1 (d, J_{pc} = 12.7 Hz, phenyl), 127.0 (d, J_{pc} = 11.9 Hz , phenyl), 123.1 (d, J_{pc} = 88.8 Hz,

catechol), 114.8 (d, J_{pc} = 13.2 Hz, catechol), 114.2 (d, J_{pc} = 17.6 Hz, catechol), 104.5 (d,

J_{pc} = 96.4 Hz, catechol), 10.2(d, J_{pc} = 59.7 Hz); $^{31}P\{^1H\}$ NMR (36.3 MHz, CD_3CN) δ

207

(ppm) 20.09 (s). IR (KBr) $\nu_{(P\text{-}CH3, C\text{-}H)}$ 2963, 2891cm^{-1}, C-H bending 1479 cm^{-1}, $\nu_{(C\text{-}O\text{-}Ti)}$ 1260 cm^{-1}; Anal. calc'd for TiIC$_{57}$H$_{48}$P$_3$O$_6$: C 62.42 %, H 4.41 %; found: C 62.49 %, H 4.37%.

Cs$_2$[4-P(S)Ph$_2$-Catecholato]$_3$Ti: A mixture of Cs$_2$(4-PPh$_2$-Catecholato)$_3$Ti (200mg, 0.168 mmol), elemental sulfur powder (154 mg, 4.82 mmol) in 20 mL of CH$_3$CN was heated to reflux under a N$_2$ atmosphere. The reaction was complete in 7 days, as monitored by ^{31}P{^{1}H} NMR spectroscopy. The mixture was filtered to give a dark-red filtrate, which was evaporated in vacuum to yield an orange-red solid. Yield: 180 mg (88%). ^{1}H NMR (360 MHz, CD$_3$CN): δ (ppm) 7.66 (m, 3×4 phenyl-H), 7.49 (m, 3×2 phenyl-H), 7.41 (m, 3×4 phenyl-H), 6.85 (ddd, J = 14.3, 8.1 and 2.0 Hz, 3×1 cat-H), 6.64 (dd, J = 13.5 and 2.0 Hz, 3×1 cat-H), 6.41 (dd, J = 8.1 and 3.6 Hz, 3×1 cat-H); ^{13}C{^{1}H} NMR (89.9 MHz, CD$_3$CN): δ (ppm) 164.0 (d, J$_{pc}$ = 3.0 Hz, catechol), 159.9 (d, J$_{pc}$ = 17.8 Hz, catechol), 135.8 (d, J$_{pc}$ = 85.2 Hz, phenyl), 133.4 (d, J$_{pc}$ = 10.6, phenyl), 132.5 (s, phenyl), 129.4 (d, J$_{pc}$ = 12.4 Hz, phenyl), 125.8 (d, J$_{pc}$ = 11.9 Hz, catechol), 119.9 (d, J$_{pc}$ = 92.7 Hz, catechol), 115.8 (d, J$_{pc}$ = 12.8 Hz, catechol), 112.7(d, J$_{pc}$ = 12.7 Hz, catechol); ^{31}P{^{1}H} NMR (36.3 MHz, CD$_3$CN) δ (ppm) 42.88 (s); IR (KBr) C-H bending 1473 cm^{-1}, $\nu_{(C\text{-}O\text{-}Ti)}$ 1262 cm^{-1} , $\nu_{(P=S)}$ 712 cm^{-1}.

Cs$_3$Fe(4-PPh$_2$-Catecholato)$_3$: A mixture of Fe(NO$_3$)$_3$•9H$_2$O (135 mg, 0.333 mmol), 4-PPh$_2$-Catechol•HBr (375 mg, 1.00 mmol), and Cs$_2$CO$_3$ (490 mg, 1.50 mmol) was stirred in 20 mL of degassed methanol under a nitrogen atmosphere at room temperature for four days, giving a dark purple-red mixture. The mixture was filtered through a frit under

nitrogen, the blood-red filtrate was then evaporated in vacuum to give a dark-red residue. Three portions of 10 mL acetone were used to extract the product. Evaporation of the dark-red acetone solution in vacuum gave a dark-red solid. Yield: 112 mg (25%). No NMR spectrum for this product is available due to the paramagnetism of iron (III). EPR spectrum (1.0 mM in methanol): $g = 8.18$, 4.25, 2.34; UV/vis spectrum (methanol solution) λ_{max} 323 nm ($\varepsilon = 31,905$), λ_{max} 490 nm ($\varepsilon = 6,050$); IR (KBr) C-H bending 1474 cm^{-1}, $v_{(C-O-Fe)}$ 1254 cm^{-1}; Anal. calc'd for $Cs_3FeC_{54}H_{39}P_3O_6$: C 48.72 %, H 2.95 %; found: C 48.78 %, H 2.94 %.

$Cs_2(4\text{-}PH_2\text{-Catecholato})_3Ti$: A mixture of $Ti(OMe)_4$ (147 mg, 0.808 mmol), 4-PH_2-Catechol•HBr (545 mg, 2.41 mmol), and Cs_2CO_3 (666 mg, 2.05 mmol) was stirred in 20 mL of degassed methanol under a nitrogen atmosphere at room temperature two days. The mixture was filtered through a frit with celite and glasswool (pre-purged by nitrogen) under nitrogen, then the dark-red filtrate was evaporated in vacuum to yield a dark-red powder (496 mg, yield 84 %). ^1H NMR (360 MHz, d_4-methanol): δ (ppm) 6.67 (m, 3×1 cat-H), 6.55 (dd, J = 7.3 and 1.6 Hz, 3×1 cat-H), 6.31 (dd, J = 7.7 and 1.3 Hz, 3×1 cat-H), 3.85 (d, J_{P-H} = 196.5 Hz, 3×2 P-H, disappeared after a day); $^{13}C\{1H\}$ NMR (89.9 MHz, d_4-methanol): δ (ppm) 160.6 (s), 159.6 (d, J_{pc} = 8.0 Hz), 127.6 (d, J_{pc} = 22.6 Hz), 119.8 (d, J_{pc} = 13.7 Hz), 115.0 (s), 113.1 (d, J_{pc} = 9.3 Hz); $^{31}P\{^1H\}$ NMR (36.3 MHz, , d_4-methanol) δ (ppm) -123.8; ^{31}P NMR (36.3 MHz, d_7-DMF) δ (ppm) -123.8 (tt, J_{P-H} = 195.9 and 7.9 Hz); IR (KBr) $v_{(aromatic\ C-H)}$ 3031 cm^{-1}, C-H bending 1477 cm^{-1}, $v_{(-PH2)}$ 2285 cm^{-1}, $v_{(C-O-Ti)}$ 1246 cm^{-1}; Elemental analyses: calc'd for $Cs_2TiC_{18}H_{15}P_3O_6$: C 29.46 % H 2.06 %; found: C 29.66 %, H 2.13 %.

209

Cs$_2$[4-P(CH$_2$OH)$_2$-Catecholato]$_3$Ti: *Method A*. A mixture of Ti(OMe)$_4$ (60 mg, 0.330 mmol), 4-P(CH$_2$OH)$_2$-Catechol•HBr (291 mg, 1.00 mmol), and Cs$_2$CO$_3$ (272 mg, 0.839 mmol) was stirred in 30 mL of degassed methanol under a nitrogen atmosphere at room temperature for two days. The mixture was filtered through a frit with celite and glasswool (pre-purged by nitrogen) under nitrogen, then the orange-red filtrate was evaporated in vacuum to give a yellow powder. Yield: 230 mg (76%). *Method B.* Aqueous formaldehyde (37 wt%, 1 mL, 13.3 mmol) was added to degassed ethanol (20 mL), and this solution was purged with N$_2$ for half an hour. Then Cs$_2$(4-PH$_2$-Catecholato)$_3$Ti (734 mg, 1.00 mmol) in 20 mL of ethanol was added dropwise to this solution with constant stirring. An orange-red precipitate was formed while Cs$_2$Ti(4-PH$_2$-Catecholato)$_3$ was being added. The mixture was stirred until the reaction was complete, as monitored by ^{31}P NMR spectroscopy (product showed a singlet with δ -21.7). The precipitate was filtered off, and dried in vacuum overnight. Yield: 840 mg (92%). ^{1}H NMR (360 MHz, D$_2$O): δ (ppm) 6.89 (t, J = 8.2 Hz, 3×1 cat-H), 6.64 (d, J = 6.7 Hz, 3×1 cat-H), 6.50 (d, J = 7.9 Hz, 3×1 cat-H), 4.15 (d, J = 5.5 Hz, 3×2 PCH_2); ^{13}C{^{1}H} NMR (89.9 MHz, D$_2$O): δ (ppm) 162.0 (s), 160.3 (d, J$_{PC}$ = 8.0 Hz), 128.2 (d, J$_{PC}$ = 23.2 Hz), 123.5 (d, J$_{PC}$ = 5.3 Hz), 118.3 (d, J$_{PC}$ = 14.6 Hz), 115.5 (d, J$_{PC}$ = 10.7 Hz), 62.2 (d, J$_{PC}$ = 4.6); ^{31}P{^{1}H} NMR (36.3 MHz, D$_2$O) δ (ppm) -21.7 (s); IR (KBr) ν $_{(-OH)}$ 3388, 3177 cm^{-1}, ν $_{(CH2)}$ 2896, 2840 cm^{-1}, C-H bending 1477 cm^{-1}, ν $_{(C-O-Ti)}$ 1225 cm^{-1}; Elemental analyses: calc'd for Cs$_2$TiC$_{24}$H$_{27}$P$_3$O$_{12}$: C 31.54 % H 2.98 %; found: C 31.84 %, H 3.37 %.

Cs$_4$Ti$_2$L$_6$Pd$_3$Br$_6$: A mixture of Cs$_2$TiL$_3$ (416 mg, 0.350 mmol) and PdBr$_2$•2PhCN (248 mg, 0.525 mmol) was stirred in 20 mL of DMF under nitrogen atmosphere at room temperature for 2 hours, giving a clear orange solution. Addition of 200 mL of THF precipitated an orange-yellow solid, which was filtered off and dried in vacuum. Yield: 526 mg (95 %). Redissolving about 50 mg of this product in a mixed solvent of DMF/THF (v/v: 1/5, 10 mL) gave a clear orange-red solution. Slow diffusion of diethyl ether into this solution gave well-formed X-ray orange-red crystals. ^{1}H NMR (360 MHz, d$_7$-DMF): δ (ppm) 7.89 (t, J = 6.4 Hz, 6×1 cat-H), 7.63 (broad, 6×4 phenyl-H), 7.37 (broad, 6×6 phenyl-H), 6.40 (broad, 6×1 cat-H), 6.25 (broad d, J = 7.9 Hz, 6×1 cat-H); ^{13}C{^{1}H} NMR (89.9 MHz, d$_7$-DMF): δ (ppm) 163.8 (s, catechol), 159.9 (virtual t, J$_{PC}$ = 10.3 Hz, catechol), 134.7 (virtual t, J$_{PC}$ = 5.6Hz, phenyl), 134.4 (virtual t, J$_{PC}$ = 20.2 Hz, phenyl), 129.7 (s, phenyl), 127.6 (virtual t, J$_{PC}$ = 5.0 Hz, phenyl), 125.0 (s, catechol), 121.9 (virtual t, J$_{PC}$ = 13.9 Hz, catechol), 115.7 (virtual t, J$_{PC}$ = 28.2 Hz, catechol), 111.0(virtual t, J$_{PC}$ = 6.0 Hz, catechol); ^{31}P{^{1}H} NMR (36.3 MHz, d$_7$-DMF) δ (ppm) 22.10 (s); IR (KBr) C-H bending 1474 cm^{-1}, ν$_{(C-O-Ti)}$ 1258 cm^{-1}; Anal. calc'd for Cs$_4$Ti$_2$C$_{108}$H$_{78}$P$_6$O$_{12}$Pd$_3$Br$_6$: C 40.80 %, H 2.47 %; found: C 40.65 %, H 2.41 %. FAB$^+$ MS m/z (nitrobenzyl alcohol matrix in DMF) (◆= [Ti$_2$L$_6$Pd$_3$]$^{2+}$); Species, Observed m/z (Calculated m/z): [◆+ 6Br$^-$ + 5Cs$^+$]$^{1+}$, 3311 (3312.6), [◆+ 6Br$^-$+ 4Cs$^+$ + 1H$^+$]$^{1+}$, 3179 (3180.7), [◆+ 6Br$^-$+ 3Cs$^+$ + 2H$^+$]$^{1+}$, 3049 (3048.8), [◆+ 5Br$^-$+ 3Cs$^+$ + 1H$^+$]$^{1+}$, 2968 (2967.9), [◆+ 4Br$^-$ + 3Cs$^+$]$^{1+}$, 2886 (2887.0), [◆+ 5Br$^-$+ 2Cs$^+$ + 2H$^+$]$^{1+}$, 2835 (2836.0), [◆+ 6Br$^-$+ 1Cs$^+$ + 3H$^+$+ 1Na$^+$]$^{1+}$, 2807 (2807.0), [◆+ 4Br$^-$+ 2Cs$^+$ + 1H$^+$]$^{1+}$, 2755 (2755.1), [◆+ 6Br$^-$ + 4H$^+$+ 1Na$^+$]$^{1+}$, 2675 (2675.1).

211

Rb₄Ti₂L₆Pd₃Br₆: A mixture of Rb₂TiL₃ (191 mg, 0.174 mmol) and PdBr₂•2PhCN (124 mg, 0.263 mmol) was stirred in 10 mL of DMF under nitrogen atmosphere at room temperature for 2 hours, giving a clear orange solution. Addition of 100 mL of THF precipitated an orange-yellow solid, which was filtered off and dried in vacuum. Yield: 220 mg (84 %). Redissolving about 30 mg of the product in a mixed solvent of DMF/THF (v/v: 1/1, 10 mL) gave a clear dark-red solution. Slow diffusion of diethyl ether into this solution gave decent orange-red crystals of X-ray quality. ^{1}H NMR (360 MHz, d$_7$-DMF): δ (ppm) 8.06 (broad t, overlapped by d$_7$-DMF aldehyde proton peak, 6×1 cat-H), 7.58 (broad m, 6×4 phenyl-H), 7.34 (broad, 6×6 phenyl-H), 6.40 (m, 6×1 cat-H), 6.29 (broad d, J = 7.9 Hz, 6×1 cat-H); ^{13}C{^{1}H} NMR (89.9 MHz, d$_7$-DMF): δ (ppm) 163.8 (s, catechol), 160.5 (virtual t, J_{PC} = 10.0 Hz, catechol), 135.1 (virtual t, J_{PC} = 24.5 Hz, phenyl), 134.4 (virtual t, J_{PC} = 5.6 Hz, phenyl), 129.4 (s, phenyl), 127.4 (virtual t, J_{PC} = 5.0 Hz, phenyl), 125.7 (s, catechol), 123.0 (virtual t, J_{PC} = 13.6 Hz, catechol), 114.9 (virtual t, J_{PC} = 28.2 Hz, catechol), 111.3 (virtual t, J_{PC} = 6.0 Hz, catechol); ^{31}P{^{1}H} NMR (36.3 MHz, d$_7$-DMF) δ (ppm) 22.20 (s); IR (KBr) C-H bending 1477 cm^{-1}, ν $_{(C-O-Ti)}$ 1263 cm^{-1}; Anal. calc'd for Rb₄Ti₂C₁₀₈H₇₈P₆O₁₂Pd₃Br₆: C 43.38 %, H 2.63 %; found: C 43.42 %, H 2.59 %.

Cs₄Sn₂L₆Pd₃Br₆: A DMF (15 mL) solution of Cs₂SnL₃ (233 mg, 0.176 mmol) and PdBr₂•2PhCN (124 mg, 0.263 mmol) was stirred under nitrogen atmosphere at room temperature for 2 hours, giving a dark red solution. Addition of 200 mL of THF precipitated an orange-yellow solid, which was filtered off and dried in vacuum. Yield: 270 mg (89 %). Redissolving about 50 mg of the product in 10 mL of DMF gave a clear

orange-red solution. Slow diffusion of diethyl ether into this solution gave well-formed orange-red crystals of X-ray quality. ^{1}H NMR (360 MHz, d_7-DMF): δ (ppm) 8.15 (broad, 6×1 cat-H), 7.66 (broad, 6×4 phenyl-H), 7.39 (broad, 6×6 phenyl-H), 6.57 (bd, J = 7.6 Hz, 6×1 cat-H), 6.25 (broad, 6×1 cat-H); ^{13}C{^{1}H} NMR (89.9 MHz, d_7-DMF): δ (ppm) 156.2 (s, catechol), 151.5 (virtual t, J_{PC} = 10.0 Hz, catechol), 134.9 (virtual t, J_{PC} = 5.6 Hz, phenyl), 134.2 (virtual t, J_{PC} = 24.8 Hz, phenyl), 129.8 (s, phenyl), 127.6 (virtual t, J_{PC} = 5.0 Hz, phenyl), 123.8 (s, catechol), 120.6 (virtual t, J_{PC} = 13.4 Hz, catechol), 114.7 (virtual t, J_{PC} = 28.2 Hz, catechol), 113.4 (virtual t, J_{PC} = 4.0 Hz, catechol); ^{31}P{^{1}H} NMR (36.3 MHz, d_7-DMF) δ (ppm) 21.61 (s); IR (KBr) C-H bending 1479 cm^{-1}, ν $_{(C-O-Sn)}$ 1254 cm^{-1}; Elemental analyses: calc'd for $Cs_4Sn_2C_{108}H_{78}P_6O_{12}Pd_3Br_6$: C 39.05 %, H 2.37 %; found: C 38.91 %, H 2.29 %.

(DABCO-H)$_4$Ti$_2$L$_6$Pd$_3$Br$_6$: A DMF (15 mL) solution of (HDABCO)$_2$TiL$_3$ (101 mg, 0.09 mmol) and PdBr$_2$•2PhCN (62 mg, 0.13 mmol) was stirred under nitrogen atmosphere at room temperature. Initial turbidity disappeared to give a dark red solution in four hour. Addition of 100 mL of THF precipitated an orange-yellow solid, which was filtered off and dried in vacuum. Yield: 96 mg (71 %). Redissolving about 20 mg of the product in 5 mL of DMF gave a clear orange-red solution. Slow diffusion of diethyl ether into this solution gave well-formed orange-red crystals. ^{1}H NMR (360 MHz, d_7-DMF): δ (ppm) 10.18 (flat, 4×N-H), 7.94 (t, J = 6.0 Hz, 6×1 cat-H), 7.57 (m, 6×4 phenyl-H), 7.35 (m, 6×6 phenyl-H), 6.48 (broad, 6×1 cat-H), 6.38 (broad d, 8.0 Hz, 6×1 cat-H), 3.50 (s, 4×12 DABCO-H); ^{13}C{^{1}H} NMR (89.9 MHz, d_7-DMF): δ (ppm) 164.3 (s,

213

catechol), 159.9 (virtual t, J_{PC} = 10.3 Hz, catechol), 134.8 (virtual t, J_{PC} = 24.5 Hz, phenyl), 134.6 (virtual t, J_{PC} = 6.8 Hz, phenyl), 129.6 (s, phenyl), 127.4 (virtual t, J_{PC} = 5.0 Hz, phenyl), 126.4 (virtual t, J_{PC} = 4.8 Hz, catechol), 122.4 (m, catechol), 117.2 (m, catechol), 111.6 (virtual t, J_{PC} = 7.0 Hz, catechol), 45.4 (s, DABCO); $^{31}P\{^1H\}$ NMR (36.3 MHz, d_7-DMF) δ (ppm) 21.20 (s); IR (KBr) $v_{(N-H)}$ 3426 cm^{-1}, $v_{(aromatic\ C-H)}$ 3050, 3035, 3008 cm^{-1}; $v_{(-CH2CH2-)}$ 2953, 2885 cm^{-1}, C-H bending 1474 cm^{-1}, $v_{(C-O-Ti)}$ 1261 cm^{-1}; Elemental analyses: calc'd for $C_{132}H_{130}P_6O_{12}N_8Ti_2Pd_3Br_6$: C 51.13 %, H 4.23 %, N 3.61 %; found: C 50.87 %, H 4.19 %, N 3.73 %.

(DABCO-H)$_4$Sn$_2$L$_6$Pd$_3$Br$_6$: *Aufbau Route* A DMF (20 mL) solution of (DABCO-H)$_2$SnL$_3$ (424 mg, 0.350 mmol) and PdBr$_2$•2PhCN (248 mg, 0.525 mmol) was stirred under nitrogen atmosphere at room temperature. Initial turbidity disappeared to give a dark-red solution in four hours. Addition of 200 mL of THF precipitated an orange-yellow solid, which was filtered off and dried in vacuum. Yield: 390 mg (69 %). *Self-assembly Approach* A suspension of SnCl$_4$ with PPh$_2$-Catechol•HBr, PdBr$_2$•2PhCN and DABCO in a molar ratio of 2:6:3:18 was stirred in degassed DMF under a nitrogen atmosphere at room temperature for a week, giving a dark-red cloudy solution which was filtered through a frit with celite and glasswool to give a dark-red filtrate. The filtrate was evaporated in vacuum to give a dark-red solid in over 75 % yield.

Redissolving about 20 mg of the product in 5 mL of DMF gave a clear orange-red solution. Slow diffusion of diethyl ether into this solution gave well-formed orange-red crystals of X-ray quality. ^1H NMR (360 MHz, d_7-DMF): δ (ppm) 9.98 (flat, 4×N-H), 8.31 (dd, J = 7.6 and 1.8 Hz, 6×1 cat-H), 7.58 (broad, 6×4 phenyl-H), 7.35 (broad, 6×6

phenyl-H), 6.74 (dt, J = 8.2 and 1.6 Hz, 6×1 cat-H), 6.50 (broad m, 6×1 cat-H), 3.16 (s, 4×12 DABCO-H); $^{13}C\{^{1}H\}$ NMR (89.9 MHz, d_7-DMF): δ (ppm) 157.0 (s, catechol), 152.1 (virtual t, J_{PC} = 10.0 Hz, catechol), 134.8 (virtual t, J_{PC} = 25.9 Hz, phenyl), 134.6 (virtual t, J_{PC} = 5.3 Hz, phenyl), 129.6 (s, phenyl), 127.4 (virtual t, J_{PC} = 5.0 Hz, phenyl), 125.6 (virtual t, J_{PC} = 2.3 Hz, catechol), 124.5 (virtual t, J_{PC} = 13.9 Hz, catechol), 113.9 (virtual t, J_{PC} = 4.2 Hz, catechol), 112.6 (virtual t, J_{PC} = 27.2 Hz, catechol), 45.3 (s, DABCO); $^{31}P\{^{1}H\}$ NMR (36.3 MHz, d_7-DMF) δ (ppm) 20.73 (s); IR (KBr) $v_{(N-H)}$ 3425 cm^{-1}, $v_{(aromatic\ C-H)}$ 3051, 3006 cm^{-1}; $v_{(-CH2CH2-)}$ 2952, 2883 cm^{-1}, C-H bending 1478 cm^{-1}, $v_{(C-O-Sn)}$ 1253 cm^{-1}; Anal. calc'd for $C_{132}H_{130}P_6O_{12}N_8Sn_2Pd_3Br_6$: C 48.90 %, H 4.04 %, N 3.46 %; found: C 48.83%, H 3.96 %, N 3.49 %.

$Cs_6Ga_2L_6Pd_3Br_6$: A DMF (10 mL) solution of Cs_3GaL_3 (235 mg, 0.175 mmol) and $PdBr_2 \bullet 2PhCN$ (124 mg, 0.263 mmol) was stirred under nitrogen atmosphere at room temperature for 2 hours, giving a clear, orange red solution. Addition of 100 mL of THF precipitated an orange-red solid, which was filtered off and dried in vacuum. Yield: 287 mg (94 %). $^{31}P\{1H\}$ NMR (36.3 MHz, d_7-DMF) δ (ppm) 22.13 (s). IR (KBr) $v_{(aromatic\ C-H)}$ 3049, 3001 cm^{-1} C-H bending 1476 cm^{-1}, $v_{(C-O-Ga)}$ 1252 cm^{-1}; Elemental analyses: calc'd for $Cs_6Ga_2C_{108}H_{78}P_6O_{12}Pd_3Br_6$: C 37.18 %, H 2.25 %; found: C 36.90 %, H 2.10 %.

Reaction of $(HNEt_3)_2ML_3$ [M = Ti(IV), Sn(IV)] with $PdBr_2 \bullet 2PhCN$: A DMF solution of two equivalents of $(HNEt_3)_2ML_3$ (M = Ti(IV),) and three equivalents of $PdBr_2 \bullet 2PhCN$ was stirred under nitrogen atmosphere at room temperature for 2 hours, giving a clear, dark red solution. *(HNEt₃)₂TiL₃/ PdBr₂.2PhCN Reaction:* $^{31}P\{^{1}H\}$ NMR (36.3 MHz, d_7-

DMF) δ (ppm) 21.61, 20.66. Addition of four equivalents of CsOTf to the solution resulted in the same $^{31}P\{1H\}$, and ^1H NMR spectra of the $Cs_4Ti_2L_6Pd_3Br_6$ cluster. Dibenzo-24-crown-8 could not reverse this reaction by extracting the cesium cations from the cluster. *(HNEt₃)₂SnL₃/ PdBr₂.2PhCN Reaction:* $^{31}P\{^1H\}$ NMR (36.3 MHz, d₇-DMF) δ (ppm) 21.20, 20.23. Addition of four equivalents of CsOTf to the solution resulted in the identical $^{31}P\{^1H\}$, and ^1H NMR spectra of the $Cs_4Sn_2L_6Pd_3Br_6$ cluster. Dibenzo-24-crown-8 could not reverse this formation by extracting the cesium cations from the cluster.

CsSn₂L₆Ag₃: A mixture of AgNO₃ (25 mg, 0.15 mmol) or AgOTf (39 mg, 0.15 mmol) and Cs₂SnL₃ (126 mg, 0.10 mmol) was stirred in 20 mL of DMF in a well-wrapped flask under a nitrogen atmosphere at room temperature. Initial white turbidity disappeared to give a clear colorless solution overnight. Evaporation of this solution in vacuum yield a white solid, which was washed by acetone and water thoroughly. The product was then dried in vacuum. Yield: 105 mg (86 %). ^1H NMR (360 MHz, d₇-DMF): δ (ppm) 7.54 (broad m, 6×4 phenyl-H), 7.46 (broad m, 6×6 phenyl-H), 7.36 (broad t, 15.8 Hz, 6×1 cat-H), 6.60 (broad d, 7.9 Hz, 6×1 cat-H), 6.16 (broad m, 6×1 cat-H); $^{31}P\{^1H\}$ NMR (145.8 MHz, DMF/d₇-DMF) two doublets centered at δ (ppm) 13.67 (^1J $_{107Ag-P}$ = 495.2 Hz; ^1J $_{109Ag-P}$ = 571.5 Hz); IR (KBr) C-H bending 1474 cm⁻¹, ν $_{(C-O-Sn)}$ 1250 cm⁻¹; Elemental analyses: calc'd for $CsSn_2C_{108}H_{78}P_6O_{12}Ag_3$: C 53.00 %, H 3.21 %; found: C 52.96 %, H 2.96 %. FAB⁺ MS m/z (nitrobenzyl alcohol matrix in DMF), Species, Observed m/z (Calculated m/z): $[CsSn_2L_6Ag_3]H_2^{2+}$ 1224 (1224.8), $[CsSn_2L_6Ag_3]H^+$ 2448(2448.6), $[CsSn_2L_6Ag_3]Cs^+$ 2581 (2580.4).

216

Cs₄Ti₂L₆Pd₃Cl₆: A DMF (10 mL) solution of Cs_2TiL_3 (208 mg, 0.175 mmol) and $PdCl_2 \cdot 2PhCN$ (100 mg, 0.261 mmol) was stirred under nitrogen atmosphere at room temperature for 2 hours, giving a clear dark-red solution. Addition of 100 mL of diethyl ether precipitated a dark-red solid, which was filtered off and dried in vacuum. Yield: 220 mg (74 %). ^1H NMR (360 MHz, d_7-DMF): δ (ppm) 7.86 (broad t, J = 7.2 Hz, 6×1 cat-H), 7.63 (broad m, 6×4 phenyl-H), 7.40 (broad m, 6×6 phenyl-H), 6.32 (broad, 6×1 cat-H), 6.23 (broad m, 6×1 cat-H); $^{13}C\{^1H\}$ NMR (89.9 MHz, d_7-DMF): δ (ppm) 163.9 (s, catechol), 159.8 (virtual t, J_{PC} = 10.0 Hz, catechol), 134.8 (virtual t, J_{PC} = 6.0 Hz, phenyl), 132.8 (virtual t, J_{PC} = 24.6 Hz, phenyl), 130.0 (s, phenyl), 127.8 (virtual t, J_{PC} = 5.0 Hz, phenyl), 124.6 (s, catechol), 121.0 (m, catechol), 114.6 (virtual t, J_{PC} = 27.9 Hz, catechol), 111.2(m, catechol); $^{31}P\{^1H\}$ NMR (36.3 MHz, d_7-DMF) δ (ppm) 24.03 (s). IR (KBr) C-H bending 1475 cm^{-1}, ν $_{(C-O-Ti)}$ 1264 cm^{-1}; Anal. calcd for $Cs_4Ti_2C_{108}H_{78}P_6O_{12}Pd_3Cl_6$: C 44.53 %, H 2.70 %; found: C 44.25 %, H 2.51 %.

Cs₄Ti₂L₆Pd₃I₆: Addition of CsI (491 mg, 1.89 mmol) to 20 ml of DMF solution of $Cs_4Ti_2L_6Pd_3Br_6$ (200 mg, 0.0629 mmol) resulted in a cloudy mixture, which was stirred overnight. The mixture was filtered through a frit with celite and glasswool, giving a dark-red filtrate which was evaporated in vacuum to give a dark-red solid. Yield: 212 mg (97 %). Redissolving about 30 mg of the product in 10 mL of DMF gave a clear dark red solution. Slow diffusion of diethyl ether into this solution gave well-formed dark-red crystals. ^1H NMR (360 MHz, d_7-DMF): δ (ppm) 7.78 (broad t, J = 7.3 Hz, 6×1 cat-H),

217

7.65 (broad m, 6×4 phenyl-H), 7.38 (broad, 6×6 phenyl-H), 6.55 (broad m, 6×1 cat-H), 6.32 (broad d, J = 7.9 Hz, 6×1 cat-H); $^{13}C\{^1H\}$ NMR (89.9 MHz, d_7-DMF): δ (ppm) 162.9 (s, catechol), 158.0 (virtual t, J_{PC} = 10.0 Hz, catechol), 136.3 (virtual t, J_{PC} = 25.2 Hz, phenyl), 134.2 (virtual t, J_{PC} = 5.6 Hz, phenyl), 129.7 (s, phenyl), 127.3 (virtual t, J_{PC} = 5.0 Hz, phenyl), 124.5 (s, catechol), 122.9 (virtual t, J_{PC} = 18.9 Hz, catechol), 119.9 (virtual t, J_{PC} = 28.9 Hz, catechol), 110.7 (broad m, catechol); $^{31}P\{^1H\}$ NMR (36.3 MHz, d_7-DMF) δ (ppm) 12.89 (s). IR (KBr) C-H bending 1473 cm^{-1}, ν $_{(C-O-Ti)}$ 1253, 1264cm^{-1}; Anal. calc'd for Cs_4Ti_2 $C_{108}H_{78}P_6O_{12}Pd_3I_6$: C 37.47 %, H 2.27 %; found: C 37.40 %, H 2.18 %.

$Cs_4Sn_2L_6Pd_3Cl_6$: A DMF (20 mL) solution of Cs_2SnL_3 (264 mg, 0.208 mmol) and $PdCl_2 \bullet 2PhCN$ (115 mg, 0.300 mmol) was stirred under a nitrogen atmosphere at room temperature for 2 hours, giving a clear golden-yellow solution. After the solution was evaporated to 10 mL, a volume of 100 mL of diethyl ether was added to precipitate a yellow solid, which was filtered off and dried in vacuum. Yield: 310 mg (93 %). (< 5% impurity, which couldn't be removed, is suspected to be the helicate isomer of the product. However, the variable temperature NMR study did not provide evidence for any equilibrium between the mesocate and "helicate" isomers up to 120 °C). ^1H NMR (360 MHz, d_7-DMF): δ (ppm) 8.12 (td, J = 7.3 and 2.1 Hz, 6×1 cat-H), 7.66 (m, 6×4 phenyl-H), 7.39 (m, 6×6 phenyl-H), 6.57 (bt, J = 7.4 and 1.5 Hz, 6×1 cat-H), 6.25 (m, 6×1 cat-H); $^{13}C\{^1H\}$ NMR (89.9 MHz, d_7-DMF): δ (ppm) 156.4 (s, catechol), 151.3 (virtual t, J_{PC} = 10.0 Hz, catechol), 135.1 (virtual t, J_{PC} = 5.6 Hz, phenyl), 132.5 (virtual t, J_{PC} = 24.2 Hz, phenyl), 130.1 (s, phenyl), 127.9 (virtual t, J_{PC} = 4.6 Hz, phenyl), 123.5 (virtual

218

t, J_{PC} = 20.5 Hz, catechol), 122.9 (virtual t, J_{PC} = 12.6 Hz, catechol), 113.6 (t, J_{PC} = 6.0

Hz, catechol), 113.5 (t, J_{PC} = 28.2 Hz, catechol); $^{31}P\{^1H\}$ NMR (36.3 MHz, d_7-DMF) δ

(ppm) 21.61 (s). IR (KBr) C-H bending 1478 cm^{-1}, ν $_{(C-O-Sn)}$ 1254 cm^{-1}; Anal. calcd for

$Cs_4Sn_2C_{108}H_{78}P_6O_{12}Pd_3Cl_6$: C 42.47 %, H 2.57 %; found: C 42.20 %, H 2.59 %.

$Cs_4Sn_2L_6Pd_3I_6$: Addition of CsI (468 mg, 1.80 mmol) to 20 mL of DMF solution of

$Cs_4Sn_2L_6Pd_3Br_6$ (200 mg, 0.0602 mmol) resulted in a cloudy mixture, which was stirred

overnight. The mixture was filtered through a frit with celite and glasswool, giving a

dark-red filtrate, which was evaporated, in vacuum to give the product in quantitative

yield (216 mg). Redissolving about 30 mg of the product in 10 mL of DMF gave a clear

dark red solution. Slow diffusion of diethyl ether into this solution gave well-formed

dark-red crystals. ^1H NMR (360 MHz, d_7-DMF): δ (ppm) 8.12 (td, J = 7.6 and 1.9 Hz,

6×1 cat-H), 7.66 (m, 6×4 phenyl-H), 7.35 (m, 6×6 phenyl-H), 6.67 (Broad d, J = 7.9 Hz,

6×1 cat-H), 6.51 (broad m, 6×1 cat-H); $^{13}C\{^1H\}$ NMR (89.9 MHz, d-DMF): δ (ppm)

156.1 (s, catechol), 151.3 (virtual t, J_{PC} = 9.3 Hz, catechol), 137.4 (virtual t, J_{PC} = 25.2

Hz, phenyl), 134.6 (virtual t, J_{PC} = 5.3 Hz, phenyl), 129.6 (s, phenyl), 127.4 (virtual t, J_{PC}

= 4.6 Hz, phenyl), 125.3 (virtual t, J_{PC} = 11.3 Hz, catechol), 123.9 (s, catechol), 117.0 (m,

catechol), 113.0 (m, catechol); $^{31}P\{^1H\}$ NMR (36.3 MHz, d_7-DMF) δ (ppm) 12.25 (s). IR

(KBr) C-H bending 1474, 1487 cm^{-1}, ν $_{(C-O-Sn)}$ 1254 cm^{-1}; Anal. calc'd for

$Cs_4Sn_2C_{108}H_{78}P_6O_{12}Pd_3I_6$: C 36.00 %, H 2.18%; found: C 35.96 %, H 2.12 %.

$Rb_4Sn_2L_6Pd_3Br_6$: A DMF (12 mL) solution of Rb_2SnL_3 (243 mg, 0.206 mmol) and

PdBr$_2$•2PhCN (142 mg, 0.301 mmol) was stirred under a nitrogen atmosphere at room

temperature for 2 hours, giving a dark red solution. Addition of 100 mL of THF precipitated an orange-yellow solid, which was filtered off and dried in vacuum. Yield: 280 mg (89%). ^{1}H NMR (360 MHz, d_7-DMF): δ (ppm) 8.42 (td, J = 7.8 and 2.1 Hz, 6×1 cat-H), 7.66 (m, 6×4 phenyl-H), 7.39 (m, 6×6 phenyl-H), 6.64 (bd, J = 7.9 Hz, 6×1 cat-H), 6.25 (m, 6×1 cat-H); ^{13}C{^{1}H} NMR (89.9 MHz, d_7-DMF): δ (ppm) 156.4 (s, catechol), 152.4 (virtual t, J_{PC} = 10.0 Hz, catechol), 135.2 (virtual t, J_{PC} = 24.9 Hz, phenyl), 134.4 (virtual t, J_{PC} = 5.3 Hz, phenyl), 129.3 (s, phenyl), 127.3 (virtual t, J_{PC} = 5.0 Hz, phenyl), 125.3 (virtual t, J_{PC} = 13.6 Hz, catechol), 124.9 (s, catechol), 113.6 (virtual t, J_{PC} = 5.3 Hz, catechol), 113.1 (virtual t, J_{PC} = 28.5 Hz, catechol); ^{31}P{^{1}H} NMR (36.3 MHz, d_7-DMF) δ (ppm) 21.30 (s); IR (KBr) C-H bending 1478 cm^{-1}, v $_{(C-O-Sn)}$ 1254 cm^{-1}; Anal. calc'd for $Rb_4Sn_2\ C_{108}H_{78}P_6O_{12}Pd_3Br_6$: C 41.42 %, H 2.51 %; found: C 41.28 %, H 2.45 %.

$Li_4Ti_2L_6Pd_3Br_6$: A DMF (15 mL) solution of Li_2TiL_3 (188 mg, 0.200 mmol) and $PdBr_2\bullet2PhCN$ (142 mg, 0.301 mmol) was stirred under nitrogen atmosphere at room temperature for 2 hours, giving a dark-red solution. Addition of 100 mL of THF precipitated a dark-red solid, which was filtered off and dried in vacuum. Yield: 240 mg (90 %). Redissolving about 30 mg of the product in 10 mL of DMF gave a clear dark red solution. Slow diffusion of diethyl ether into this solution gave well-formed dark-red crystals of X-ray quality. ^{1}H NMR (360 MHz, d_7-DMF): δ (ppm) 7.81 (broad, 6×1 cat-H), 7.57 (broad, 6×4 phenyl-H), 7.34 (broad, 6×6 phenyl-H), 6.37 (broad m, 6×1 cat-H), 6.29 (broad d, J = 7.93 Hz, 6×1 cat-H); ^{13}C{ ^{1}H } NMR (89.9 MHz, d_7-DMF): δ (ppm) 162.9 (s, catechol), 161.0 (virtual t, 4.0 Hz, catechol), 135.2 (virtual t, J_{PC} = 24.54 Hz,

phenyl), 134.5 (virtual t, J_{PC} = 5.6 Hz, phenyl), 129.5 (s, phenyl), 127.4 (virtual t, J_{PC} = 5.0 Hz, phenyl), 125.3 (s, catechol), 123.0 (m, catechol), 114.7 (virtual t, J_{PC} = 28.2 Hz, catechol), 111.0 (m, catechol); $^{31}P\{^1H\}$ NMR (36.3 MHz, d_7-DMF) δ (ppm) 21.17 (s); IR (KBr) C-H bending 1477 cm^{-1}, $\nu_{(C-O-Ti)}$ 1264 cm^{-1}; Anal. calc'd for Li$_4$Ti$_2$C$_{108}$H$_{78}$P$_6$O$_{12}$Pd$_3$Br$_6$: C 48.48 %, H 2.94 %; found: C 48.24 %, H 2.73 %.

Cs$_4$Ti$_2$L$_6$[Cr(CO)$_4$]$_3$: A DMF (20 mL) solution of Cs$_2$TiL$_3$ (237 mg, 0.199 mmol) and Cr(CO)$_4$(Piperidine)$_2$ (100 mg, 299 mmol) was stirred under a nitrogen atmosphere at room temperature for 7 days, giving a clear orange red solution. Addition of 50 mL of acetone precipitated a yellow solid, which was filtered off and washed by three portions of 10 mL acetone. The yellow solid was then dried in vacuum. Yield: 210 mg (66 %). ^1H NMR (360 MHz, d_7-DMF): δ (ppm) 7.76 (broad, 6×1 cat-H), 7.49 (broad, 6×4 phenyl-H), 7.38 (broad, 6×6 phenyl-H), 7.34 (broad, 6×1 cat-H), 6.14 (broad); $^{31}P\{^1H\}$ NMR (36.3 MHz, d_7-DMF) δ (ppm) 72.09 (s); IR (KBr) $\nu_{(CO)}$ 1856 cm^{-1} C-H bending 1474 cm^{-1}, $\nu_{(C-O-Ti)}$ 1260 cm^{-1}; Anal. calcd for Cs$_4$Ti$_2$C$_{120}$H$_{78}$P$_6$O$_{24}$Cr$_3$: C 50.16 %, H 2.74 %; found: C 50.02 %, H 2.79 %.

Cs$_4$Sn$_2$L$_6$[Cr(CO)$_4$]$_3$: A DMF (20 ml) solution of Cs$_2$SnL$_3$ (251 mg, 0.199 mmol) and Cr(CO)$_4$(Piperidine)$_2$ (100 mg, 0.299 mmol) was stirred under nitrogen atmosphere at room temperature for 7 days, giving a clear orange-red solution. Addition of 50 mL of acetone precipitated a yellow solid, which was filtered off and washed by three portions of 10 ml acetone. The yellow solid was then dried in vacuum. Yield: 230 mg (74 %). ^1H NMR (360 MHz, d_7-DMF): δ (ppm) 7.71 (broad m, 6×1 cat-H), 7.50 (broad, 6×4

phenyl-H), 7.39 (broad, 6×6 phenyl-H), 6.46 (broad d, J = 4.0 Hz, 6×1 cat-H), 6.15

(broad, 6×1 cat-H); $^{13}C\{^1H\}$ NMR (89.9 MHz, d_7-DMF): δ (ppm) 155.0 (s, catechol),

152.7 (virtual t, 9.0 Hz, catechol), 140.2 (virtual t, 5.6Hz, phenyl), 132.6 (virtual t, 4.6

Hz, phenyl), 128.8 (s, phenyl), 128.4 (m, phenyl), 128.0 (virtual t, 4.0 Hz, catechol),

121.4 (m, catechol), 120.3 (m, catechol), 112.8(m, catechol); $^{31}P\{^1H\}$ NMR (36.3 MHz,

d_7-DMF) δ (ppm) 71.55 (s); IR (KBr) ν $_{(CO)}$ 1855 cm^{-1}, C-H bending 1477 cm^{-1}, ν $_{(C-O-Sn)}$

1251 cm^{-1}; Anal. calc'd for $Cs_4Ti_2C_{120}H_{78}P_6O_{24}Cr_3$: C 47.81 %, H 2.61 %; found: C

48.00 %, H 2.65 %.

Self-assembly of $(NH_4)_4Ti_2L_4Pd_3Br_6$: A suspension of $Ti(OMe)_4$ with PPh_2-

Catechol•HBr, $PdBr_2$•2PhCN and NH_4OH in a molar ratio of 2:6:3:10 was stirred in

degassed DMF under nitrogen atmosphere at room temperature for a week, giving a dark

red cloudy solution which was filtered through a frit filled with celite and glasswool to

give a dark-red filtrate. The filtrate was evaporated in vacuum to give a dark-red solid in

over 80% yield. Redissolving about 20 mg of the product in 10 mL of DMF gave a clear

dark red solution. Slow diffusion of diethyl ether into this solution gave well-formed

dark-red crystals of X-ray quality. ^1H NMR (360 MHz, d_7-DMF): δ (ppm) 8.42 (broad

m, 6×1 cat-H), 7.57 (broad, 6×4 phenyl-H), 7.34 (broad, 6×6 phenyl-H), 6.63 (broad d, J

= 7.9 Hz, 6×1 cat-H), 6.40 (broad, 6×1 cat-H); $^{13}C\{^1H\}$ NMR (89.9 MHz, d_7-DMF): δ

(ppm) 156.3 (s, catechol), 151.7 (virtual t, J_{PC} = 8.0 Hz, catechol), 135.1 (virtual t, J_{PC} =

14.6 Hz, phenyl), 134.5 (broad, phenyl), 129.4 (broad, phenyl), 128.1 (broad, phenyl),

127.4 (broad, catechol), 125.2 (m, catechol), 125.0 (m, catechol), 113.7(broad, catechol);

$^{31}P\{^1H\}$ NMR (36.3 MHz, d_7-DMF) δ (ppm) 22.10 (s); IR (KBr) ν$_{(NH4, N-H)}$ 3326 cm^{-1},

222

$\nu_{(aromatic\ C\text{-}H)}$ 3052, 3024 cm^{-1}; C-H bending 1468 cm^{-1}, $\nu_{(C\text{-}O\text{-}Ti)}$ 1259 cm^{-1}; Anal. calc'd for $Ti_2C_{108}H_{94}N_4P_6O_{12}Pd_3Br_6$ C 47.69 %, H 3.48 %, N 2.06% ; found: C 47.52 %, H 3.59 %, N 2.17%.

X-ray Structural Determination of Cs$_2$[(4-PPh$_2$-Catecholato)$_3$Ti] • 2DMF • 0.5H$_2$O:

A block red/yellow crystal having approximate dimensions of 0.30 × 0.07 × 0.07 mm was mounted on a quartz fiber using Paratone N hydrocarbon oil. All measurements were made on a Siemens SMART diffractometer with graphite monochromated Mo-K$_\alpha$ radiation. Cell constants and an orientation matrix obtained from a least-squares refinement using the measured positions of 7400 reflections, in range of $3.00 < 2\Theta < 46.5$ °, corresponded to a primitive triclinic space group P $\overline{1}$ (#2). The data were collected at a temperature of -115 ± 1 °C. a = 11.4876 (2) Å, b = 16.6820 (3) Å, c = 16.7549(4) Å, V = 3099.3(1) Å^3, Z = 2, ρ_{calc} = 1.44 g/cm^3, 2 Θ_{max} = 52.2°. Of the 17056 reflections which were collected, 10350 were unique (R_{int} = 0.040); equivalent reflections were merged. Empirical absorption correction: T_{max} = 0.801, T $_{min}$ = 0.587. All non-hydrogen atoms of the complex and coordinated DMF and water molecules were refined anisotropically, while the rest, including the atoms of the severely disordered, 1/2 occupancy DMF molecule were refined isotropically. Hydrogen atoms were included but not refined. Final R = Σ ($|F_0|-|F_c|/\Sigma|F_0|$) = 0.064 for 5852 for I > 2.00σ (I) (607 parameters, 1 restraint); for all 10350 data, R_w = [Σ w($|F_0|-|F_c|)^2/\Sigma$ wF_0^2]$^{1/2}$ = 0.083. Weighting scheme: w = 1/[$\sigma^2(F_0^2)$ + (0.0356P)^2 + 62.28P], where P = (Max(F_0^2,0) + 2F_0^2)/3.

X-ray Structural Determination of Cs$_4$Ti$_2$L$_6$Pd$_3$Br$_6$ • 9 THF • H$_2$O • 3/2 (Et$_2$O) • 3/2 DMF : A prismatic reddish-orange crystal having approximate dimensions of 0.38 × 0.30 × 0.30 mm was mounted on a quartz fiber using Paratone N hydrocarbon oil. All measurements were made on a Siemens SMART diffractometer with graphite monochromated Mo-K radiation. Cell constants and an orientation matrix obtained from a least-squares refinement using the measured positions of 8192 reflections, in range of 3.00 < 2Θ < 46.5 °, corresponded to a primitive hexagonal space group P6$_3$/m (#176). The data were collected at a temperature of -122 ± 2 °C. a = 20.4769 (1) Å, b = 20.4769 (1) Å, c = 21.9982(1) Å, V = 7988.15(7) Å^3, Z = 2, ρ_{calc} = 1.711 g/cm3, μ = 2.953 mm^{-1}, F(000) = 4082, 2 Θ$_{max}$ = 52.28°. Of the 38263 reflections which were collected, 5129 were unique (R$_{int}$ = 0.044); equivalent reflections were merged. Empirical absorption correction: T$_{max}$ = 0.429, T$_{min}$ = 0.341. One of the Cs counterions, one of the bromine atoms and much of the solvent were disordered. The non-hydrogen atoms (excluding disordered solvent molecules and mirror components of the disordered bromine) were refined anisotropically. Hydrogen atoms were included on all but the solvent molecules but not refined. Final R1 = Σ (|F$_0$|-|F$_c$|/Σ|F$_0$|) = 0.0579 for 3950 for I > 2σ (I) (207 parameters, 1 restraint); for all 5129 data, wR2 = [Σ w(F$_0$^{2}-F$_c$^{2})^2/Σ w(F$_0$^{2})^2]$^{1/2}$ = 0.1300. Weighting scheme: w = 1/[σ^2(F$_0$^{2}) + (0.0356P)^2 + 62.28P], where P = (Max(F$_0$^{2},0) + 2F$_0$^{2})/3.

224

X-ray Structural Determination of $Cs_4Sn_2L_6Pd_3Br_6$ • 5DMF • $2H_2O$ • THF • x (solvent) : A block reddish-orange crystal having approximate dimensions of $0.10 \times 0.11 \times 0.15$ mm was mounted on a quartz fiber using Paratone N hydrocarbon oil. All measurements were made on a Siemens SMART diffractometer with graphite monochromated Mo-K radiation. Cell constants and an orientation matrix obtained from a least-squares refinement using the measured positions of 6706 reflections, in range of $3.00 < 2\Theta < 46.5$ °, corresponded to a primitive triclinic space group P1 (#2). The data were collected at a temperature of -110 ± 1 °C. $a = 18.0134$ (3) Å, $b = 18.5299$ (3) Å, $c = 28.6388(1)$ Å, $\alpha = 99.494(1)$ °, $\beta = 98.315(1)$ °, $\gamma = 119.077(1)$ °, $V = 7954.9(2)$ Å^3, $Z = 2$, $\rho_{calc} = 1.59$ g/cm^3, $F(000) = 3160$, $2\Theta_{max} = 46.5$°. Of the 36575 reflections which were collected, 22133 were unique ($R_{int} = 0.068$); equivalent reflections were merged. Empirical absorption correction: $T_{max} = 0.776$, $T_{min} = 0.521$. One of the Cs counterions, one of the bromine atoms and much of the solvent were disordered. The non-hydrogen atoms (excluding disordered solvent molecules and mirror components of the disordered bromine) were refined anisotropically. Hydrogen atoms were included on all but the solvent molecules but not refined. Additionally, all phenyl rings were refined as rigid groups. Final $R = \Sigma$ ($|F_o|-|F_c|/\Sigma|F_o|$) = 0.090 for 12552 for $I > 3\sigma$ (I) (822 parameters, 18 restraint); $Rw = [\Sigma$ $w(|F_o|-|F_c|)^2/\Sigma$ $w(F_o^2)^2]^{1/2} = 0.107$. Weighting scheme: $w = 1/[\sigma^2(F_o^2) = 4F_o^2/\sigma^2(F_o^2)$.

X-ray Structural Determination of $[Sn_2L_6Pd_3Br_6]$ • $(C_6H_{12}N_2)_3$ • $3H_2O$ • x (solvent) : A triangular prismatic orange crystal having approximate dimensions of $0.42 \times 0.06 \times 0.06$ mm was mounted on a quartz fiber using Paratone N hydrocarbon oil. All

measurements were made on a Siemens SMART diffractometer with graphite monochromated Mo-K radiation. Cell constants and an orientation matrix obtained from a least-squares refinement using the measured positions of 7156 reflections, in range of $3.00 < 2\Theta < 46.5$ °, corresponded to a primitive hexagonal space group $P6_3/m$ (#176). The data were collected at a temperature of -80 ± 1 °C. a = 23.2574 (5) Å, b = 23.2574 (5) Å, c = 16.7452(4) Å, α = 90.000(1)° ; V = 7844.1(3) Å^3, Z = 2, ρ_{calc} = 1.35 g/cm^3, $2\Theta_{max}$ = 52.4°. Of the 37213 reflections which were collected, 5105 were unique (R_{int} = 0.076); equivalent reflections were merged. No decay correction was applied. Empirical absorption correction: T_{max} = 0.831, T_{min} = 0.545. All Sn, Pd, P, O and C atoms of the cluster as well as Br(1) were refined anisotropically. The non-hydrogen atoms of the DABCO and water molecule were also refined anisotropically. The two disordered Br atoms and all other atoms were refined isotropically. Hydrogen atoms were included on all appropriate atoms refined anisotropically but not refined. Final R = Σ ($|F_o|-|F_c|/\Sigma|F_o|$) = 0.055 for 215 for I > 3σ (I) (302 parameters, 1 restraint); Rw = $[\Sigma\ w(|F_o|-|F_c|)^2/\Sigma\ w(F_o^2)^2]^{1/2}$ = 0.078. Weighting scheme: w = $1/[\sigma^2(F_o^2) = 4F_o^2/\sigma^2(F_o^2)$.

226

LIST OF REFERENCES

[1]   Lehn, J.-M. *Supramolecular Chemistry, Concepts and Perspectives*, VCH, Weinheim, **1995**. See also references therein.

[2]   Banyard, S. H.; Stammers, D. K.; Harrison, P. M. *Nature (London)*, **1978,** 278, 282

[3]   Arnold, E.; Rossmann, M. G. *Acta Crystallogr., Sec. A.* **1988,** 44, 270

[4]   Caspar, D. L. D. and Klug, A. *Physical Principles in the Construction of regular Viruses, in Proceedings of Cold Spring Harbor Symposia on Quantitative Biology*, Long Island Biological Association, New York,   **1962,** vol.27

[5]   Lippard, S. J.; Berg, J. M. *Principles of Bioinorganic Chemistry*, University Science Books, Mill Valey, California, **1994**

[6]   Shultz, G. E.; Schirmer, R. H. *Principles of Protein Structure*, Springer Verlog, New York, **1979**

[7]   Lindsey, J. S. *New J. Chem.* **1991,** 15, 153

[8]   Woodward, R. B. *Pure Appl. Chem.* **1968,** 17, 519

[9]   Eschenmoser, *Quart. Rev.* **1970,** 24, 366; *Chem. Soc. Rev.* **1976,** 5, 377

[10] Olenyuk, B.; Fechlenkötter; Stang, P. J. *J. Chem. Soc., Dalton Trans.,* **1998,** 1707

[11] Stang, P. J.; Olenyuk, B. *Acc. Chem. Res.* **1997,** 30, 502

[12] Beissel, T.; Powers, R. E.; Raymond, K. N. *Angew. Chem. Int. Ed. Engl.* **1996,** 35, 1084

[13] Caulder, D. L.; Raymond, K. N. *J Chem. Soc. Dalton Trans.,* **1999,** 1185

[14] Caulder, D. L.; Raymond, K. N. *Acc. Chem. Res.* **1999,** 32, 975

[15] Harrison, P. M. and Arosio, P. *Biochim. Biophys. Acta,* **1996,** 1275, 161

[16] Proulxcurry, P. M. and Chasteen, N. D. *Coordination Chem. Rev.,* **1995,** 144, 347

[17] Stefanini, S.; Vecchini, P.; Chiancone, E. *Biochem.,* **1987,** 26, 1831

[18] Hadfield, A.; Hajdu, J.; Chapman, M. S.; Rossmann, M. G. *Acta Crystallogr., Sect. D. Biol. Crystallogr.,* **1995,** 51, 859

227

[19] Whittaker, E. J. W. *Acta Crystallogr.*, **1965**, 9, 855; 862; 865

[20] Fisher, E. *Ber. Deutsh. Chem. Ges.* **1894**, 27, 2985

[21] Werner, A. *Zeitschr. Anorg. Chem.* **1893**, 3, 267

[22] Lehn, J.-M. *Angew. Chem. Int. Ed. Engl.* **1988**, 27, 89

[23] Lehn, J.-M. *Angew. Chem. Int. Ed. Engl.* **1990**, 29, 1304

[24] Cotton, F. A.; Wilkinson, G. *Advanced inorganic Chemistry*, 5th edn., John Wiley and Sons, New York, **1988**

[25] Albrecht, M.; Kotila, S. *Angew. Chem. Int. Ed. Engl.*, **1995**, 34, 2134

[26] Albrecht, M.; Kotila, S. *Angew. Chem. Int. Ed. Engl.*, **1996**, 35, 1208

[27] Albrecht, M.; Blau, O.; Fröhlich, R. *Chem. Eur. J.* **1999**, 5, 48

[28] Albrecht, M. *Synlett*, **1996**, 565

[29] Albrecht, M.; Kotila, S. *J. Chem. Soc., Chem. Commun.*, **1996**, 2309

[30] Xu, J.; Parac, T.; Raymond, K. N. *Angew. Chem. Int. Ed. Engl.*, **1999**, 38, 2878

[31] Caulder, D. L.; Raymond, K. N. *ibid*, **1997**, 109, 1508; **1997**, 36, 1439

[32] Caulder, D. L.; Powers, R. E.; Parac, T.; Raymond, K. N. *Angew. Chem. Int. Ed. Engl.* **1998**, 37, 1840

[33] Scherer, M.; Caulder, D. L.; Johnson, D. W.; Raymond, K. N. *Angew. Chem. Int. Ed. Engl.*, **1999**, in press

[34] Carrano, C. J.; Raymond, K. N. *J. Chem. Soc., Chem. Commun.*, **1978**, 501

[35] Carrano, C. J.; Cooper, S. R.; Raymond, K. N. *J. Am. Chem. Soc.*, **1979**, 101, 599

[36] Scarrow, R. C.; White, D. L.; Raymond, K. N. *J. Am. Chem. Soc.*, **1985**, 107, 6540

[37] Albrecht, M.; Röttele, H.; Burger, P. *Chem. Eur. J.* **1996**, 2, 1264

[38] Albrecht, M.; Schneider, M.; Röttele, H. *Chem. Ber.* **1997**, 130, 615

[39] Albrecht, M.; Schneider, M.; Röttele, H. *Angew. Chem. Int. Ed. Engl.*, **1999**, 38, 557

[40] Albrecht, M.; Riether, C. *Chem. Ber.* **1996**, 129, 829

[41]   Enemark, E. J.; Stack, T. D. P. *Inorg. Chem.*, **1996**, 35, 2719

[42]   Enemark, E. J.; Stack, T. D. P. *Angew. Chem. Int. Ed. Engl.*, **1995**, 34, 996

[43]   Enemark, E. J.; Stack, T. D. P., *Angew. Chem. Int. Ed. Engl.*, **1998**, 37, 932

[44]   (a). Corbin, J. L.; Bulen, W. A. *Biochemistry*, **1969**, 8, 757; (b). Tait, G. H. *Biochem. J.*
       1975, 146, 191; (c). Ong, S. A.; Peterson, T.; Neilands, J. B. *J. Biol. Chem.* **1979**, 254,
       1860; (d). Peterson, T.; Falk, K.; Leong, S. A.; Klein, M. P.; Neilands, J. B.; *J. Am.
       Chem. Soc.* **1980**, 102, 7715; (e). Griffiths, G. L.; Sigel, S. P.; Payne, S. M.; Neilands, J.
       B. *J. Boil. Chem.* **1984**, 1, 383; (f). Yamamoto, S.; Okujo, N.; Fujita, Y.; Saito, M.;
       Yoshida, T.; Shinoda, S. *J. Biochem.* **1993**, 113, 538; (g). Telford, J. R.; Leary, J. A.;
       Tunstad, L. M. G.; Byers, B. R.; Raymond, K. N. *J. Am. Chem. Soc.* **1994**, 116, 4499;
       (h). Ehlert, G.; Taraz, K.; Budzikiewicz, H. Z. *Naturforsch.*, *C* **1994**, 49, 11

[45]   Ibers, J. A.; Holm, R. H. *Science* **1980**, 209, 223

[46]   The *trans*-influence , a thermodynamic phenomenon, concerns the ground state effects
       of ligands that are trans to each other, while the trans-effect is a kinetic phenomenon.
       See Appleton, T. G.; Clark, H. C.; Manzer, L. E. *Coord. Chem. Rev.*, **1973**, 10, 355

[47]   Piguet, C.; Bernardinelli, G.; Bocquet, B.; Schaad, O.; Williams, A. F. *Inorg. Chem.*
       1993, 33, 4112

[48]   Williams, A. F.; Piguet, C.; Bernardinelli, G. *Angew. Chem. Int. Ed. Engl.*, **1991**, 30,
       1490

[49]   Grillo, V. A.; Seddon, E. J; Grant, C. M.; Aromi, G.; Bollinger, J. C.; Folting, K.;
       Christou, G. *J. Chem. Soc., Chem. Commun.*, **1997**, 1561

[50]   Williams, A. F. *Chem. Eur. J.* **1997**, 3, 15

[51]   Piguet, C.; Bernardinelli, G.; Bocquet, B.; Quattropani, A.; Williams, A. F. *J. Am.
       Chem. Soc.* **1992**, 114, 7440

[52]   Saalfrank, R. W.; Stark, A.; Peters, K.; von Schnering, H. G. *Angew. Chem. Int. Ed.
       Engl.*, **1988**, 27, 851

[53]   Saalfrank, R. W.; Stark, A.; Bremer, M.; Hummel, H. -U. *Angew. Chem. Int. Ed. Engl.*,
       1990, 29, 311

[54]   Saalfrank, R. W.; Hörner, B.; Stalke, D.; Salbeck, J. *Angew. Chem. Int. Ed. Engl.*, **1993**,
       32, 1179

[55]   Saalfrank, R. W.; Burak, R.; Breit, A.; Stalke, D.; Herbst-Irmer, R.; Daub, J.; Porsch,
       M.; Bill, E.; Müther, M.; Trautwein, A. X. *Angew. Chem. Int. Ed. Engl.*, **1994**, 33, 1621

[56] Fleming, J. S.; Mann, K. L. V.; Carraz, C. -A.; Psillakis, E.; Jeffery, J. A.; McCleverty, J. A.; Ward, M. D. *Angew. Chem. Int. Ed. Engl.*, **1998**, <u>37</u>, 1279

[57] Amoroso, A. J.; Jeffery, J. C.; Jones, P. L.; McCleverty, J. A.; Thornton, P.; Ward, M. D. *Angew. Chem. Int. Ed. Engl.*, **1995**, <u>34</u>, 1443

[58] (a) Borgias, B. A.; Barclay, S. J.; Raymond, K. N. *J. Coord. Chem.*, **1986**, <u>15</u>, 109 (b) Borgias, B. A.; Hugi, A. D.; Raymond, K. N. *Inorg. Chem.*, **1989**, <u>28</u>, 3538 (c) Cauldle, M. T.; Crumbliss, A. L. *Inorg. Chem.*, **1994**, <u>33</u>, 4077 (d) Garrett, T. M.; Miller, P. W.; Raymond, K. N. *Inorg. Chem.* **1989**, <u>28</u>, 128 (e) Kappel, M. J.; Pecoraro, V. L.; Raymond, K. N. *Inorg. Chem.*, **1985**, <u>24</u>, 2447 (f) Karpishi, T. B.; Stack, T. D. P.; Raymond, K. N. *J. Am. Chem. Soc.*, **1993**, <u>115</u>, 6115

[59] (a) Xu, J.; Raymond, K. N. **1999**, in preparation (b) Xu, J.; Johnson, D. W.; Raymond, K. N. **1998**, unpublished results

[60] Caulder, D. L.; Raymond, K. N. *Angew. Chem. Int. Ed. Engl.*, **1997**, <u>36</u>, 1439

[61] Kersting, B.; Meyer, M.; Powers, R. E.; Raymond, K. N. *J. Am. Chem. Soc.*, **1996**, <u>118</u>, 7221

[62] Meryer, M.; Kersting, B.; Powers, R. E.; Raymond, K. N. *Inorg. Chem.*, **1997**, <u>36</u>, 5179

[63] CAChe4.0, Oxford Molecular Group, Inc., USA, **1997**

[64] Powers, R. E. The Rational Design of Supramolecular Assemblies, Ph.D. Thesis, University of California, Berkeley, CA. **1997**

[65] Parac, T. N.; Caulder, D. L.; Raymond, K. N. *J. Am. Chem. Soc.*, **1998**, <u>120</u>, 8003

[66] Borgias, B. A.; Barclay, S. J.; Raymond, K. N. *J. Coord. Chem.*, **1986**, <u>15</u>, 109

[67] Karpishin, T. B.; Stack, T. D. P.; Raymond, K. N. *J. Am. Chem. Soc.*, **1993**, <u>115</u>, 6115

[68] Kepert, D. L, *Inorganic Stereochemistry*, Springer Verlag, Heidelberg, **1982**

[69] Bruckner, C.; Powers, R. E.; Raymond, K. N. *Angew. Chem. Int. Ed. Engl.*, **1998**, <u>37</u>, 1837

[70] Johnson, D. W.; Xu, J.; Saalfrank, R. W.; Raymond, K. N. *Angew. Chem. Int. Ed. Engl.* **1999**, <u>38</u>, 2882

[71] Lam, M. H. W.; Cheung, S. T. C.; Fung, K, -M.; Wong, W. -T. *Inorg. Chem.* **1997**, <u>36</u>, 4618

[72] Colbran, S. B.; Criag, D. C.; Sembiring, S. B. *Inorg. Chim. Acta* **1990**, 176, 225

[73] Sembiring, S. B. ; Colbran, S. B. *Inorg. Chim. Acta* **1992**, 202, 67

[74] Sembiring, S. B. ; Colbran, S. B.; Craig, D. C.; Scudder, M. L. *J. Chem. Soc., Dalton Trans.* **1995**, 3731

[75] Sembiring, S. B. ; Colbran, S. B.; Craig, D. C. *J. Chem. Soc., Dalton Trans.* **1999**, 1543

[76] Ernst, S.; Hänel, P.; Jordanov, J.; Kaim, W.; Kasack, V.; Roth, E. *J. Am. Chem. Soc.* **1989**, 111, 1733

[77] (a) *The chemistry of the Quinonoid Compounds;* Rappoport, Z.; Ed.; Wiley: New York, **1988**; Vols. 1 and 2; (b) Trumpower, B. L. *Function of Quinones in Energy Conserving Systems*; Academic Press: London, **1982**; (c) Chin, D. H.; Jones, S. E.; Leon, L. E.; Bosserman, P.; Stalling, M. D.; Sawyer, D. T.; *In Biological Redox Components; ACS Symposium Series 201;* American Chemical Society: Washington, DC, **1982**; p675

[78] (a) Lubitz, W.; Abresch, E. C.; Debus, R. J.; Isaacson, R. A.; Okamura, M. Y.; Feher, G. *Biochim. Biophys. Acta* **1985**, 808, 464; (b) Deisenhofer, J.; Epp, O.; Miki, K.; Huber, R.; Michel, H. *Nature* **1995**, 318, 618; (c) Dismukes, G. C.; Frank, H. A.; Friesner, R.; Sauer, K. *Biochim. Biophys. Acta* **1984**, 764, 253.

[79] Yang, K.; Bott, S. G.; Richmond, M. G. *Organometallics 1995*, 14, 2387

[80] Lewis, J. S.; Heath, S. L.; Powell, A. K.; Zweit, J.; Blower, P. J. *J. Chem. Soc., Dalton Trans.,* **1997**, 855

[81] Lewis, J. S.; Zweit, J.; Dealing, J. L. J.; Rooney, B. C.; Blower, P. J. *Chem. Commun.* **1996**, 1093

[82] (a) Fenske, D.; Becker, H. J. *Chem. Ber.,* **1974**, 107, 117; (b) Fenske, D. *Chem. Ber.,* **1979**, 112, 363; (c) Berglund, M.; Andersson, C.; Larsson, R. *J. Organomet. Chem.* **1983**, 258, 195

[83] Duffy, N. W.; Nelson, R. S.; Richmond, M. G.; Rieger, A. L.; Rieger, P. H.; Robinson, B. H.; Tyler, D. R.; Wang, J.; Yang, K. *Inorg. Chem.* **1998**, 37, 4849

[84] (a) Mao, F.; Tyler, D. R.; Rieger, A. L.; Rieger, P. H. *J. Chem. Soc., Faraday Trans.,* **1991**, 87, 3113; (b) Mao, F.; Tyler, D. R.; Bruce, M. R.; Bruce, A. E.; Rieger, A. L.; Rieger, P. H. *J. Am. Chem. Soc.,* **1992**, 114, 6418.

[85] Shen, H.; Williams, T. J.; Bott, S. M.; Richmond, M. G. *J. Organomet. Chem.* **1995**, 505, 1

[86] (a) Braunstein, P.; Matt, D.; Fischer, J.; Ricard, L.; Mitschler, A. *Nouv. J. Chim.*, **1980**, **4**, 493; (b) Pangrac, J.; Podlahova, *Collect. Czech. Chem. Commun.*, **1981**, 46, 1222

[87] Tse, M. -C.; Cheung, K. -K; Chan, M. C.; Che, C. -M. *Chem. Commun.* **1998**, 2295

[88] Borns, S.; Kadyrov, R.; Heller, D.; Baumann, W.; Spannenberg, A.; Kempe, R.; Holz, J.; Börner, A. *Eur. J. Inorg. Chem.* **1998**, 1291

[89] Bader, A.; Linder, E. *Coord. Chem. Rev.* **1991**, 108, 27

[90] (a) Allegier, A. M; Slone, C. S.; Mirkin, C. A.; Liable-Sands, L. M.; Yap, G. P. A.; Rheingold, A. L. *J. Am. Chem. Soc.* **1997**, 119, 550; (b) Sassano, C. A.; Mirkin, C. A. *J. Am. Chem. Soc.* **1995**, 117, 11379; (c) Singewald, C. A.; Mirkin, C. A. Stern, C. L. *Angew. Chem. Int. Ed.* **1995**, 34, 1624; (d) Allegeier, A. M.; Singwald, E. T.; Mirkin, C. A.; Stern, C. L. *Organometallics* **1994**, 13, 2928.

[91] (a) Beer, P. D.; Chen, Z.; Grieve, A.; Haggitt, J. *J. Chem. Soc., Chem. Commun.* **1994**, 2413; (b) Beer, P. D.; Tite, E. L.; Ibbotson, A. *J. Chem. Soc., Dalton Trans.*, **1991**, 1691; (c) Medina, J. C.; Goodnow, T. T.; Rojas, M. T.; Atwood, J. L.; Lynn, B. C.; Kaifer, A. E.; Gokel, G. W. *J. Am. Chem. Soc.* **1992**, 114, 10583; (d) Chen, Z.; Gokel, G. W.; Echegoyen, L. *J. Org. Chem.* **1991**, 56, 3369; (e) Beer, P. D.; Keefe, A. D.; Sikanyika, H.; Blackburn, C.; McAleer, J. F. *J. Chem. Soc., Dalton Trans.*, **1990**, 3289; (f) Beer, P. D.; Nation, J. E.; Harman, M. E.; Husrthouse, M. B. *J. Organomet. Chem.* **1992**, 441, 465.

[92] Slone, C. S.; Nirkin, C. A.; Yap, G. P. A.; Guzei, I. A.; Rheingold, A. *J. Am. Chem. Soc.* **1997**, 119, 10743

[93] Allgeier, A. M.; Mirkin, C. A. *Angew. Chem. Int. Ed.* **1998**, 37, 894.

[94] Sembiring, S. B.; Colbran, S. B.; Craig, D. C. *Inorg. Chem.* **1995**, 34, 761

[95] O'Brien, I. G.; Cox, G. B.; Gibson, F. *Biochim. Biophys. Acta*, **1971**, 237, 537

[96] Scheibel, L. W.; Adler, A. *Mol. Pharm.* **1982**, 22, 140 and **1981**, 20, 218

[97] McKillop, J. H.; Wallwork, J.; Reitz, B. A.; Billingham, M. E.; Miller, R.; McDougal, I. R. *Eur. J. Nucl. Med.* **1982**, 7, 162

[98] Yano, Y.; Budinger, T. F.; Ebbe, S. N.; Mathis, C. A.; Singh, M.; Brennan, K. M.; Moyer, B. R. *J. Nucl. Med.* **1985**, 26, 1429

[99] Pierpont, C. G.; Buchanan, R. M. *Coord. Chem. Rev.* **1981**, 38, 45

[100] Pierpont, C. G.; Lange, C. W. Prog. *Inorg. Chem.* **1994**, 41, 331

232

[101] Tuck, D. G. *Coord. Chem. Rev.* **1992**, <u>112</u>, 215

[102] Anan, T. A.; Chadha, D. G.; Tuck, D. G.; Watson, K. D. *Can. J. Chem.* **1987**, <u>65</u>, 2670

[103] Anan, T. A.; McGarvey, B. R.; Ozarowski, A.; Tuck, D. G. *J. Chem. Soc. Dalton Trans.* **1989**, 439

[104] (a) Spannenberg, A.; Oberthür, M.; Noss, H.; Tillack, A.; Arndt, P.; Kempe, R. *Angew. Chem. Int. Ed.*, **1998**, <u>37</u>, 2079; (b) Li, S. -L.; Mak, T. C.; Zhang, Z. -Z. *J. Chem. Soc., Dalton Trans.*, **1996**, 3475; (c) Ara, I.; Delgado, E.; Fornies, J.; Hernandez, E.; Lalinde, E.; Mansilla, N.; Moreno, M. T. *J. Chem. Soc., Dalton Trans.*, **1996**, 3201; (d) Wlodarczyk, A.; Doyle, G. A.; Maher, J. P.; McCleverty, J. A.; Ward, M. D. *Chem. Commun.* **1997**, 769; (e) Zhang, Z. -Z.; Cheng, H.; Kuang, S. -M.; Zhou, Y. -Q.; Liu, Z. -X.; Zhang, J. -K.; Wang, H. -G. *J. Organomet. Chem.* **1996**, 516, 1; (f) Uzelmeier, C. E.; Bartley, S. L; Fourmigue, M.; Rogers, R.; Grandinetti. G.; Dunbar, K. R. *Inorg. Chem.* **1998**, <u>37</u>, 6706

[105] (a) Heinze, K.; Huttner, G.; Walter, O. *Eur. J. Inorg. Chem.*, **1999**, 593; (b) Heinze, K.; Huttner, G.; Zsolnai, L.; Jacobi, A.; Schober, P. *Chem. Eur. J.* **1997**, <u>3</u>, 732; (c) Heinze, K.; Huttner, G.; Zsolnai, L.; Schober, P. *Inorg. Chem.* **1997**, <u>36</u>, 5457; (d) Heinze, K.; Huttner, G.; Zsolnai, L. *Chem. Ber.* **1997**, <u>130</u>, 1393; (e) Beyreuther, S.; Hunger, J.; Huttner, G.; Mann, S.; Zsolnai, L. *Chem. Ber.* **1996**, <u>129</u>, 745

[106] Joss, S.; Bürgi, H. B.; Ludi, A. *Inorg. Chem.* **1985**, <u>24</u>, 949

[107] Vogler, A.; Osman, A. H.; Kunkey, H. *Coord. Chem. Rev.* **1985**, <u>64</u>, 159

[108] Hatano, K.; Ishida, Y. Bull. Chem. Soc. Japan, **1982**, <u>55</u>, 3333

[109] Lever, A. B. P.; Licoccia, S.; Ramaswamy, B. S. *Inorg. Chem. Acta*, **1982**, <u>64</u>, L87

[110] Weber, L.; Haufe, G.; Rehorek, D.; Henning, H. *J. Chem. Soc. Chem. Commum.* **1991**, 502

[111] Lorkovic, I. M.; Duff, R. R. Jr.; Wrighton, M. S. *J. Am. Chem. Soc.*, **1995**, <u>117</u>, 3617

[112] (a) Suzuki, T.; Noble, R. D.; Koval, C. A. *Inorg. Chem.* **1997**, <u>36</u>, 136; (b) Terry, P. A.; Noble, R. D.; Swanson, D.; Koval, C. A. *Am. Inst. Chem. Eng.* **1997**, <u>43</u>, 1709; (c) Terry, P. A.; Walls, H. J.; Noble, R. D.; Koval, C. A. *ibid*, **1995**, <u>41</u>, 2556.

[113] (a) Pearson, R. G. *Inorg. Chem.* **1988**, <u>27</u>, 734; *Coord. Chem. Rev.* **1990**, <u>100</u>, 403; (b) Douglas, B.; McDaniel, D.; Alexander, J. *Concepts and Models of Inorganic Chemistry*, 3rd edn. Wiley, New York, **1994**, ch.7

233

[114] McAuliffe, C. A. in *Comprehensive Coordination Chemistry*, vol.2. ed. Wilkinson, G.; Stone, F. G. A.; Abel, F. W. Pergamon, Oxford, **1987**, ch.14

[115] Levason, W. in *The Chemistry of Organophosphorus Compounds*, vol.1, ed. Hartley, F. R. Wiley, New York, **1990**, ch.16

[116] Garrett, T. M.; Miller, P. W.; Raymond, K. N. *Inorg. Chem.* **1989**, 28, 128

[117] Karpishin, T. B.; Stack, T. D. P.; Raymond, K. N. *J. Am. Chem. Soc.* **1993**, 115, 2447

[118] (a) Linton, B.; Hamilton, A. *Chem. Rev.* **1997**, 97, 1669; (b) Gellman, S. H. *Chem. Rev.* **1997**, 97, 231

[119] (a) Lehn, J. -M. *Angew. Chem. Int. Ed.* **1990**, 29, 1304; (b) Kelly, D. R. *Chem. Brit.* **1990**, 26, 24

[120] (a) Alpha, B.; Lehn, J. -M.; Mathis, G. *Angew. Chem. Int. Ed.* **1987**, 26, 266; (b) Sabbatini, N.; Guardigli, M.; Lehn, J. -M. *Coord. Chem. Rev.* **1993**, 123, 201

[121] (a) Tundo, P.; Fendler, J. H. *J. Am. Chem. Soc.* **1980**, 102, 1760; (b) Bunzli, J. -C. G.; Froidevaux, P.; Harrowfield, J. *Inorg. Chem.* **1993**, 32, 3306; (c) Deschenaux, R.; Harding, M. M.; Ruch, T. *J. Chem. Soc., Perkin Trans. 2* **1993**, 1251; (d) Campagna, S.; Denti, G.; Serroni, S.; Ciano, M.; Juris, A.; Balzani, V. *Inorg. Chem.* **1992**, 31, 2982

[122] (a) Willner, I.; Willner, B. *Topics Curr. Chem.* **1991**, 159, 153; (b) Paddon-Row, M. N. *Acc. Chem. Res.* **1994**, 27, 18; (c) Gust, D.; Moore, T. A.; Moore, A. L.; Macpherson, A. N.; Lopez, A.; DeGraziano, J. M.; Gouni, I.; Bittermann, E.; Seely, G. R.; Nieman, R. A.; Ma, X. C.; Demanche, L. J.; Hung, S. -C.; Luttrull, D. K.; Lee, S. -J.; Kerrigan, P. K. *J. Am. Chem. Soc.* **1993**, 115, 11141.

[123] Eaton, D. F.; Anderson, A. G.; Tam, W.; Mahler, W.; Wang, Y. *Mol. Cryst. Liq. Cryst.* **1992**, 211, 125

[124] (a) Pileni, M. P. *J. Phys. Chem.* **1993**, 97, 6961; (b) Ahuja, R.; Caruso, P. -L.; Paulus, W.; Ringsdorf, H.; Wildburg, G. *Angew. Chem. Int. Ed.* **1993**, 32, 1033; (c) Avnir, D.; Braun, S.; Lev, O.; Ottolenghi, M. Chem. Materials 1994, 6, 1605; (d) Heilmann, J.; Maier, W. F. *Angew. Chem. Int. Ed.* **1994**, 33, 471; (e) Wheatley, N.; Kalck, P. *Chem. Rev.* **1999**, 99, 3397

[125] (a) Daub, J.; Salbeck, J.; Knochel, T.; Fischer, C.; Kunkely, H.; Rapp, K. M. *Angew. Chem. Int. Ed.* **1989**, 28, 1494; (b) Newell, A. K.; Utley, J. H. P. *J. Chem. Soc., Chem. Commun.* **1992**, 800; (c)Achatz, J.; Fischer, C.; Salbeck, J.; Daub, J. *J. Chem. Soc., Chem. Commun.* **1991**, 504

234

[126] Miles, J. A.; Beeny, M.; Ratts, K. W. *J. Org. Chem.* **1975**, 40, 343

[127] Senear, A. E.; Valient, W.; Wirth, J. *J. Org. Chem.* **1960**, 25, 2001

[128] Wong, E. H. unpublished results

[129] Wong, E. H.; Hou, Z. unpublished data

[130] (a) Reddy, V. S.; Katti, K. V.; Barnes, C. L. *Inorg. Chim. Acta* **1995**, 240, 367; (b) Smith, C. J.; Reddy, V. S.; Karra, S. R.; Katti, K. V.; Barbour, L. J. *Inorg. Chem.* **1997**, 36, 1786; (c) Reddy, V. S.; Berning, D. E.; Katti, K. V.; Barnes, C. L.; Volkert, W. A.; Ketring, A. R. *Inorg. Chem.* **1996**, 35, 1753; (d) Reddy, V. S.; Katti, K. V.; Barnes, C. L. *J. Chem. Soc., Dalton Trans.*, **1996**, 1301; (e) Smith, C. J.; Reddy, V. S.; Katti, K. V. *J. Chem. Soc., Dalton Trans.*, **1998**, 1365

[131] Pregosin, P. S.; Kunz, R. W. *^{31}P and ^{13}C NMR of Transition Metal Phosphine Complexes*, Springer-Verlag, New York **1979**, p.89

[132] Redfield, D. A.; Cary, L. W.; Nelson, J. H.; *Inorg. Chem.* **1975**, 14, 50; *ibid*, **1976**, 15, 732; *ibid*, **1976**, 15, 1128

[133] (a) Pregosin, P. S.; Kunz, R. W.; *Helv. Chim. Acta*, **1975**, 58, 423; (b) Balimann, G.; Motschi, H.; Pregosin, P. S. *Inorg. Chim. Acta*, **1976**, 23, 191

[134] Verkade, J. G.; *Coord. Chem. Rev.* **1972/73**, 9, 1

[135] Grim, S. O.; Keiter, R. L.; McFarlane, W. *Inorg. Chem.* **1967**, 6, 1133

[136] gNMR, Version 3.6, for Macintosh, Cherwell Scientific Publishing, **1996**

[137] (a) Sofen, S. R.; Abu-Dari, K.; Freyberg, D. P.; Raymond, K. N. *J. Am. Chem. Soc.* **1978**, 100, 7882; (b) Griffith, W. P.; Pumphrey, C. A.; Rainey, T.-A. *J. Chem. Soc., Dalton Trans.* **1996**, 1125

[138] Karpishin, T. B.; Gebhard, M. S.; Solomon, E. I.; Raymond, K. N. *J. Am. Chem. Soc.* **1991**, 113, 2977

[139] Avdeef, A.; Sofen, S. R.; Bregante, T. L.; Raymond, K. N. *J. Am. Chem. Soc.* **1978**, 100, 5362

[140] (a) Gorenstein, D. G.; *Prog. NMR Spectr.* **1983**, 16, 1; (b) Quin, L. D.; Verkade, J. G. *Phosphorus-31 NMR Spectral Properties in Compound Characterization and Structural Analysis*, VCH, **1994**

[141] (a) McArdle, J. V.; Sofen, S. R.; Cooper, S. R.; Raymond, K. N. *Inorg. Chem.* **1978**, 17, 3075; (b) Llinas, M.; Wilson, D. M.; Neilands, J. B. *Biochemistry*, **1973**, 12, 3835

[142] (a) van Doorn, J. *Phosphorus and Sulfur*, **1991**, 62, 155. (b) Louattani, E.; Lledos, A.; Suades, J.; Alvarez-Larena, A.; Piniella, J. F. *Organometallics*, **1995**, 14, 1053

[143] Lamberth, C.; Machell, J. C.; Mingos, D. M. P.; Stolberg, T. L. *J. Mater. Chem.* **1991**, 1, 775

[144] A phoshino-substitution at the 4-position of a catecholate leads to a higher electron density of 0.05 e$^-$ at the 2-phenolate oxygen compared to the 1-oxygen site according to MO calculations. MO calculations were performed on $[(4-PH_2-Catecholate)_3Ti]^{2-}$ at the semi-empirical PM3(tm) and density functional theory (pBP-DN*) levels using the Spartan 5.0 programs [Wavefunction, Inc.] on a Silicon Graphics O2 workstation. At both levels, a substantially larger molecular dipole was found for the *fac*-isomer relative to the *mer*-isomer; 4.13 D versus 1.56 D from PM3(tm), and 1.12 D versus 0.54 D from DFT.

[145] Wong, C. Y.; Woollins, J. D. *Coord. Chem. Rev.* **1994**, 130, 175. (b) Denekamp, C. I. F.; Evans, D. F.; Parr, J.; Woollins, J. D. *J. Chem. Soc. Dalton Trans.*, **1993**, 1489

[146] (a) Fay, R. C.; Lindmark, A. F.; *J. Am. Chem. Soc.* **1983**, 105, 2118. (b) Fay, R. C. *Coord. Chem. Rev.* **1996**, 154, 99

[147] Mhatre, S. N.; Karweer, S. B.; Pradhan, P.; Iyer, R. K.; Moorthy, P. N. *J. Chem. Soc., Dalton Trans.* **1994**, 3711

[148] (a) Karpishin, T. B.; Stack, T. D. P.; Raymond, K. N. *J. Am. Chem. Soc.* **1993**, 115, 6115. (b) Kersting, B.; Telford, J. R.; Meryer, M.; Raymond, K. N. *J. Am. Chem. Soc.* **1996**, 118, 5712

[149] Anderson, G. K.; Lin, M. *Inorg. Syn.* **1990**, 28, 61

[150] Atwood, J. L.; Darensbourg, D. J. *Inorg. Chem.* **1977**, 16, 2314

[151] Douglas, D.; McDaniel, D.; Alexander, J. *Concepts and Models of Inorganic Chemistry, third Edition*, John Wiley & Sons, New York, **1994**

[152] Corbridge, D. E. C. *Phosphorus, and outline of its Chemistry, Biochemistry, and Technology, third Edition*, Elsevier, Amsterdam, **1985**

[153] Nomiya, K.; Tsuda, K.; Kasuga, N. C. *J. Chem. Soc., Dalton Trans.*, **1998**, 1653

[154] Sanghani, D. V.; Smith, P. J.; Allen, D. W.; Taylor, B. *Inorg. Chim. Acta*, **1982**, 59, 203

236

[155] Ardizzoia, G. A.; Monica, G. L.; Maspero, A.; Moret, M.; Masciocchi, N. *Inorg. Chem.* **1997**, 36, 2321

[156] Darensbourg, D. J.; Kump, R. L. *Inorg. Chem.* **1978**, 17, 2680

[157] (a) Muetterties, E. L.; Alegranti, C. W. *J. Am. Chem. Soc.* **1972**, 94, 6386; (b) Hollander, F. J.; Ip, Y. L.; Coucouvanis, D. *Inorg. Chem.* **1976**, 15, 2230

[158] (a) Walton, R. A. *Prog. Inorg. Chem.* **1976**, 21, 105; (b) Glicksman, H. D.; Walton, R. A. *Inorg. Chem.* **1978**, 17, 200

[159] (a) Kukushkin, V. Y.; Oskarsson, A.; Elding, L. I. *Inorg. Synth.* **1997**, 31, 281; (b) Coulson, D. R. *Inorg. Synth.* **1990**, 28, 107; (c) Thomas, R. R.; Sen, A. *Inorg. Synth.* **1990**, 28, 63

[160] (a) Doyle, J. R.; Slade, P. E.; Jonassen, H. B. *Inorg. Synth.* **1960**, 6, 218; (b) Hartley, F. R. *The Chemistry of Palladium and Platinum*, Applied Sciences, New York, **1973**, p.462; (c) Anderson, G. K.; Lin, M. *Inorg. Synth.* **1990**, 28, 61

[161] SMART, Area Detector Software Package, **1995**, Siemens Industrial Automation, Inc., Madison.

[162] SAINT, SAX Area Detector Integration Program, 4.024, 1995, Siemens Industrial Automation, Inc., Madison 1995

[163] Sheldrick, G. SHELXTL Crystal Structure Determination Software Package, 1993, Siemens Industrial Automation, Inc., Madison

[164] Sheldrick, G. SADABS, Siemens Area Detector ABSorption Correction Program, Advanced Copy, 1996

[165] TeXsan, Crystal Structure Analysis Package, 1992, Molecular Structure Corporation, The Woodlands, TX.

237